

This electronic thesis or dissertation has been downloaded from the King's Research Portal at <https://kclpure.kcl.ac.uk/portal/>



**Investigating the molecular regulation of follicle-stimulating hormone-mediated receptor oligomerisation and trafficking, and related signalling.**

Agwuegbo, Uche

*Awarding institution:*  
King's College London

The copyright of this thesis rests with the author and no quotation from it or information derived from it may be published without proper acknowledgement.

**END USER LICENCE AGREEMENT**



**Unless another licence is stated on the immediately following page** this work is licensed

under a Creative Commons Attribution-NonCommercial-NoDerivatives 4.0 International

licence. <https://creativecommons.org/licenses/by-nc-nd/4.0/>

You are free to copy, distribute and transmit the work

Under the following conditions:

- Attribution: You must attribute the work in the manner specified by the author (but not in any way that suggests that they endorse you or your use of the work).
- Non Commercial: You may not use this work for commercial purposes.
- No Derivative Works - You may not alter, transform, or build upon this work.

Any of these conditions can be waived if you receive permission from the author. Your fair dealings and other rights are in no way affected by the above.

**Take down policy**

If you believe that this document breaches copyright please contact [librarypure@kcl.ac.uk](mailto:librarypure@kcl.ac.uk) providing details, and we will remove access to the work immediately and investigate your claim.

**Investigating the molecular regulation of follicle-  
stimulating hormone-mediated receptor oligomerisation  
and trafficking, and related signalling**

A thesis submitted by

**Uchechukwu Tochukwu Agwuegbo**


for the degree of Doctor of Philosophy

King's College London University

2023

## Declaration

The experiments reported in this thesis are my own work, except where specifically indicated.

A handwritten signature in black ink, appearing to be 'U. Agwuegbo', written in a cursive style.

Uchechukwu Agwuegbo

## Acknowledgements

Firstly, I would like to express my deepest gratitude to my primary supervisor, Dr Kim Jonas, who's support and guidance throughout my studies kept me going through some of my most difficult times. I wouldn't have completed this thesis if it wasn't for her patience, dedication, and faith in me. I also want to thank my secondary supervisor, Professor Anthony Albert, for his expert advice during our meetings and his constructive feedback throughout my PhD.

Next, I would like to give a special thanks to my fellow colleagues in the Jonas' lab, Jilly, and Tom, for all their moral support over the last few years. Whenever I felt like giving up, they always uplifted me and reminded me of how resilient I am. I would also like to thank the members of the O'Byrne lab group for all their entertainment and emotional support. Our conversations were priceless.

Finally, I am eternally grateful for my family, Kamarl Sr and Kamarl Jr. You both mean the world to me and the reason why I kept persevering. Kamarl Sr, thank you for all your patience, kindness, love, and support during this difficult time. Kamarl Jr, thank you for being so understanding and independent. I hope that the successful completion of this thesis grants you many opportunities in life.

***Philippians 1:6; Being confident of this very thing, that He who has begun a good work in you will complete it until the day of Jesus Christ.***

~ Thank you, God, for finishing what you started ~



## **Covid-19 Impact Statement**

Disruptions caused by Covid-19 massively impacted my research during the crucial 2<sup>nd</sup>-3<sup>rd</sup> year transitional point, at the height of data generation, and significantly curtailed my productivity and project plans.

Prior to Covid-19, I had multiple bookings to use the Zeiss Elyra PS.1 super-resolution microscope for PD-PALM analysis. However, because the microscope was based off-site at an alternative institution, Covid-19 restrictions prevented me from using their facilities for an additional 6 months until restrictions were lifted. This meant that an important aspect of my thesis, relating to investigating FSHR oligomerisation, could not be addressed for a significant amount of time. Consequently, some profound experiments had low *n* numbers which made data interpretation difficult. To ensure we could advance my hypothesis, we sought facilities at King's for alternative microscopes, however, we anticipated great difficulty in translating new findings with previous findings from the Zeiss Elyra. Therefore, I advanced with determining other aspects of my research until normal facilities re-opened.

Advancing other aspects of my thesis was also very challenging during Covid-19. Restrictions associated with close-contact and face-to-face meetings meant that I often had to learn and optimise new techniques independently. Although independent learning is a desirable skill to attain during a PhD, together with the limited time allowed in the lab to enable staggered working, it was difficult producing valid results. This profoundly made method development and development of my analytical skills very difficult. To mitigate this, I took every opportunity to ask questions during meetings and I watched multiple

online tutorials. However, for some key techniques, such as Western blots, progression was not possible without direct assistance, despite all troubleshooting attempts. Therefore, having direct face-to-face access to colleagues and staff would have had a massive positive impact.

Part of my thesis was to look at multiple FSHR-dependent signalling pathways and FSHR trafficking and recycling. To do this, I had arranged multiple visits to other labs for a few weeks, both nationally and internationally, to learn techniques such as BRET signalling to measure FSHR and  $\beta$ -arrestin interaction, nanobody-related confocal imaging to measure FSHR trafficking dynamics, and further confocal imaging to measure FSHR co-localisation to APPL1-positive very early endosomes. However, the impact of Covid-19 massively prevented this and had detrimental effects on advancing my hypothesis. As a result, we decided to develop our own technique using nanoBiT by sub-cloning SmallBiT and LargeBiT to the FSHR and  $\beta$ -arrestin to measure their interaction. However, full development and optimisation of this technique in our cell model exceed the time length of my thesis and could not be utilised in experiments. Furthermore, since we did not have the appropriate tools and material to measure FSHR co-localisation to APPL1-positive very early endosomes, we used siRNA APPL1 to silence APPL1 and determine its role.

Moreover, in addition to the initial impact of Covid-19 on lab and facility closures, I experienced further disruption for a period of up to 9 months due to additional caring responsibilities. There were consistent school closures due to multiple Covid-19 outbreaks, meaning I had to endure multiple 10-day periods of disruption to experiments, often occurring mid-week/experiment. This made planning in advance and performing

experiments impossible at times. To overcome this, I had to home-school during the day and run experiments in the late evening. Consequently, this ended up being counterproductive, because most of my daily working hours were severely truncated, and therefore I often was not able to attend lab meetings during the working hours to receive guidance on future experiment and ideas.

Despite all the setbacks of Covid-19 I am confident that my thesis has met the quality threshold for the consideration of a PhD award. Nonetheless, I hope the examiners will consider my Covid-19 impact statement in relation to the scope and volume of my research design and execution, where effort was made or was intended, but which subsequently had to be discarded because of Covid-19.

## Abstract

Follicle-stimulating hormone (FSH), and its associated G protein-coupled receptor (GPCR), the FSH receptor (FSHR), play multiple crucial roles in female reproduction, such as folliculogenesis, dominant follicle selection and maintenance of steroidogenesis. Therefore, as key targets of assisted conception, there is therapeutic interest in identifying new modalities for modulating their functions. FSHR primarily mediates its effects via coupling to the  $G\alpha_s$ /cAMP/PKA pathway but can also activate multiple signalling pathways via various mechanisms, including mediating additional signalling platforms via internalisation and trafficking to endosomes. Nonetheless, how this signal pleiotropy is initiated remains largely unknown. Post-translational modification of FSH gives rise to two predominant glycoforms; partially glycosylated FSH (FSH<sub>21/18</sub>), which is more bioactive *in vitro* and more abundant in women in their reproductive prime, in contrast to fully glycosylated FSH (FSH<sub>24</sub>), which is less bioactive and more abundant in peri/menopausal women. As well as endogenous ligands, drug discovery programs have resulted in the production of small molecule FSHR modulators that can enhance/inhibit the actions of FSH. This may have important therapeutic benefits for enhancing FSHR activity by providing alternative routes for drug administration and a means to target reproductive pathologies associated with menopausal-related elevation of FSH. Nevertheless, how these modulators propagate their effects also remains unclear. An important modality of how GPCRs can fine-tune receptor signalling is via self-association to form dimer and oligomer complexes. The FSHR has been shown to self-associate, however, the functional role of FSHR oligomerisation, and the impact on signalling and trafficking remains elusive. Therefore, the aim of this thesis was to determine how native ligands and pharmacological FSHR modulators modulate FSHR oligomerisation, downstream signalling, and trafficking. Results showed that FSH glycoforms differentially modulate FSHR monomers,

dimers, and oligomers in a temporal- and concentration-dependent manner, correlating with the magnitude and timing of cAMP production and possible  $\beta$ -arrestin/ERK signal pathway selectivity. Furthermore, the differences in FSH glycoform-dependent cAMP-dependent signalling may be further regulated by differences in the routing of the internalised FSHR by different FSH glycoforms. Treatments with the potent FSHR agonist Compound 5 (C5) showed rapid maximal enhancement of FSHR activity that is possibly mediated by FSHR trafficking and recycling to the cell-surface. Moreover, three newly identified FSHR non-competitive antagonists, that enhance FSH binding but reduced FSH activity, may regulate these differences through changes in FSHR oligomerisation. These data suggest that different FSHR ligands and modulators display nuanced mechanisms to modulate FSHR signalling, with the potential impact on physiological outcomes to be determined. Such mechanisms may have the ability to be regulated to modulate FSHR function, with a potential to improve fertility and treat age-related reproductive pathologies.

## Publications

**UC Agwuegbo, KC Jonas (2018).** Molecular and functional insights into gonadotropin hormone receptor dimerization and oligomerization. *Minerva Ginecol.* 70(5):539-548.

GP Johnson, **U Agwuegbo, KC Jonas (2021).** New insights into the functional impact of G protein-coupled receptor oligomerization. *Current Opinion in Endocrine and Metabolic Research.* 16:43-50.

**Uchechukwu T Agwuegbo, Emily Colley, Anthony P Albert, Viktor Y Butnev, George R Bousfield, Kim C Jonas (2021).** Differential FSH Glycosylation Modulates FSHR Oligomerization and Subsequent cAMP Signaling. *Front Endocrinol.* 12:765727.

**Uchechukwu Agwuegbo, Kim Carol Jonas (2022).** Visualizing G protein-coupled receptor homomers using photoactivatable dye localization microscopy. *Methods Cell Biol.* 169:27-41.

## Abstracts

**Uche Agwuegbo, Anthony Albert, George Bousfield & Kim Jonas (2019)** Impact of a FSHR positive allosteric modulator on FSH glycosylation variant-dependent FSHR homomerisation and signal pathway activation. *Society for Endocrinology British Endocrine Society, Endocrine Abstracts (2019) 65 P348 | DOI: 10.1530/endoabs.65. P348.*

**Agwuegbo Uche**, Bousfield George, Albert Anthony, Jonas Kim (2020) The effects of FSHR positive allosteric modulator on FSH dependent FSHR homomerisation and signal pathway activation. *Fertility 2020*, SP3D.3.

**Uche Agwuegbo**, George Bousfield, Kim Jonas (2020) Differential FSH glycosylation modulates FSHR homomerisation and cAMP-dependent pathway activation. *Early Career Scientist Forum on GPCR Research*, 2020.

**Uche Agwuegbo**, Emily Colley, George Bousfield, Anthony Albert, Kim Jonas (2020) FSH glycosylation variants positively modulates re-organisation of FSHR homomer complexes and FSHR-dependent signal pathway activation. *British Pharmacology Society*, 2020.

**Uche Agwuegbo**, Emily Colley, George Bousfield, Anthony Albert, Kim Jonas (2021) Modulation of FSHR quaternary structure directs FSH-dependent signalling responses. *Fertility 2021*, SP8.3.

**Uche Agwuegbo**, Emily Colley, George Bousfield, Anthony Albert & Kim Jonas (2021) Differentially glycosylated FSHR ligands as potential modulators of FSHR quaternary complexes and FSHR-dependent signalling. *Society for Endocrinology British Endocrine Society*, Endocrine Abstracts (2021) 77 P102 | DOI: 10.1530/endoabs.77. P102.

**Uche Agwuegbo**, Emily Colley, Anthony Albert, Viktor Butnev, George Bousfield, Kim Jonas (2022) Modulation of FSHR oligomerisation by differentially glycosylated FSHR ligands regulates FSHR-dependent signalling. *Fertility 2022*, SP3C.4.

**Uchechukwu Agwuegbo**, Emily Colley, Anthony Albert, Viktor Butnev, George Bousfield, Kim Jonas (2022) Differentially glycosylated FSHR ligands as potential modulators of FSHR quaternary complexes and FSHR-dependent signalling. *European Research Network on Signal Transduction*, 2022.

**UT Agwuegbo**, R Richardson, A Albert, AC Hanyaloglu & KC Jonas (2022) FSH glycosylation variants differentially modulate FSHR trafficking. *Society for Endocrinology British Endocrine Society*.

HD Tran, **UT Agwuegbo**, GR Bousfield, A Albert & KC Jonas (2022) Identification and characterisation of novel follicle-stimulating hormone receptor antagonists. *Society for Endocrinology British Endocrine Society*.

**Uche Agwuegbo**, Rachel Richardson, George Bousfield, Anthony Albert, Aylin Hanyaloglu, Kim Jonas (2023) FSHR trafficking is modulated by differential FSH glycosylation variants. *Fertility 2023*, P118.



Hanh Duyen Tran, **Uche Agwuegbo**, Kim Jonas, Anthony Albert (2023) Identification and characterisation of novel follicle-stimulating hormone receptor antagonists. *Fertility* 2023, 2D.4.

## List of Abbreviations

---

<b>Abbreviation</b>	<b>Definition</b>
7TM	Seven-transmembrane domain receptor
aa	Amino acid
AC	Adenylyl cyclase
APPL1	Adaptor protein, phosphotyrosine interacting with PH domain and leucine zipper 1
ARC	Arcuate
ART	Assisted reproductive technology
Asn	Asparagine
ATP	Adenosine triphosphate
AVPV	Anteroventral periventricular
BRET	Bioluminescence resonance energy transfer
BMP	Bone morphogenetic protein
C5	Compound 5

cAMP	Cyclic-adenosine monophosphate
CCPs	Clathrin-coated pits
CGA	Glycoprotein hormones, $\alpha$ -polypeptide
cre	cAMP-response element
CREB	cAMP response-element binding protein
Co-IP	Co-immunoprecipitation
CRR	Cysteine-rich repeat
cryo-EM	Cryogenic electron microscopy
Cys	Cysteine
dg-eLHt	eLH $\beta$ ( $\Delta$ 121-149) combined with asparagine56-deglycosylated eLH $\alpha$
ECL	Extracellular loop
EE	Early endosome
EEA1	Early endosome antigen 1
EPAC	Exchange protein activated by cAMP

ER	Endoplasmic reticulum
FRET	Fluorescence resonance energy transfer
FSH	Follicle-stimulating hormone
FSHR	Follicle-stimulating hormone receptor
GAIP	G $\alpha$ interacting protein
GalNAc	<i>N</i> -Acetylgalactosamine
GC	Granulosa cell
GDP	Guanine diphosphate
GEF	Guanine nucleotide exchange factor
GIPC	GAIP interacting protein C-terminus
GlcNAc	<i>N</i> -Acetylglucosamine
GnRH	Gonadotrophin-releasing hormone
GnRHR	Gonadotrophin-releasing hormone receptor
GPCR	G protein-coupled receptor
GPOR	G protein-coupled oestrogen receptor 1

GpH	Glycoprotein hormone
GpHR	Glycoprotein hormones receptor
GRK	G protein-coupled receptor kinase
GTP	Guanosine triphosphate
hCG	Human chorionic gonadotrophin
HEK293	Human embryonic kidney 293
HL	Hairpin loop
HMG	Human menopausal gonadotrophin
HPO	Hypothalamus-pituitary-ovarian
ICD	Intracellular domain
ICL	Intracellular loop
IP <sub>3</sub>	Inositol trisphosphate
IVF	<i>In vitro</i> fertilisation
KISS1	Kisspeptin
KISS1R	Kisspeptin receptor

LGR	LRR-containing GPCR (LGR)
LH	Luteinising hormone
LH/CGR	LH/human chorionic gonadotrophin receptor
LRR	Leucine-rich repeats
MAPK	Mitogen-activated protein kinase
MD	Molecular dynamic
NMR	Nuclear magnetic resonance
OST	Oligosaccharyltransferase
PDs	Photoactivatable dyes
PD-PALM	Photoactivatable dye-photoactivatable localisation microscopy
PI3K	Phosphatidylinositol 3-kinase
PIP <sub>2</sub>	Phosphatidylinositol biphosphate
PK	Protein kinase
Rab5	Ras-related protein 5
RER	Rough endoplasmic reticulum

SDS-PAGE	Sodium dodecyl sulphate–polyacrylamide gel electrophoresis
siRNA	Small interfering ribonucleic acid
Smad	Small mothers against decapentaplegic
SMC	Small molecule compound
ST3Gal III	Gal $\beta$ 1,3GlcNAc $\alpha$ 2,3-sialyltransferase
ST6Gal I	Gal $\beta$ 1,4GlcNAc $\alpha$ 2,6-sialyltransferase
StAR	Steroidogenic acute regulatory protein
TGF- $\beta$	Transforming growth factor- $\beta$
TIRF-M	Total interference reflection fluorescence microscopy
TMD	Transmembrane domain
TSH	Thyroid-stimulating hormone
TSHR	Thyroid-stimulating hormone receptor
TZD	Thiazolidinone
VEE	Very early endosome
VFT	Venus Flytrap

$\alpha$	Alpha
$\beta$	Beta
$\beta_2\text{AR}$	$\beta_2$ -adrenoceptor
$\gamma$	Gamma



## Table of Contents

<b>1</b>	<b>Chapter One – General Introduction.....</b>	<b>26</b>
1.1	Overview .....	27
1.2	The hypothalamus-pituitary-ovarian axis.....	27
1.3	Ovarian physiology .....	30
1.3.1	Gonadotropin-independent folliculogenesis .....	31
1.3.2	Gonadotrophin-dependent folliculogenesis .....	31
1.3.3	Corpus luteum.....	32
1.4	Follicle-stimulating hormone .....	33
1.4.1	Transcriptional regulation of FSH subunits .....	34
1.4.2	FSH heterodimer structure .....	34
1.4.3	Post-translational modification of FSH .....	36
1.4.3.1	<i>FSH microheterogeneity</i> .....	39
1.4.3.2	<i>FSH macroheterogeneity</i> .....	40
1.5	G protein-coupled receptors .....	42
1.5.1	Class A GPCRs .....	46
1.5.2	Class B and Class C GPCRs .....	46
1.6	Glycoprotein hormone receptors .....	47
1.6.1	Leucine-rich repeats .....	47
1.6.2	Hinge region.....	49
1.6.3	Glycoprotein hormone receptor activation .....	52

1.7	Follicle-stimulating hormone receptor .....	54
1.7.1	<i>FSHR</i> regulation.....	54
1.7.2	Post-translation modification of <i>FSHR</i> and outward trafficking.....	56
1.7.3	<i>FSHR</i> localisation .....	58
1.8	Follicle-stimulating hormone receptor signalling pathways .....	60
1.8.1	<i>G<math>\alpha</math>s</i> /adenylyl cyclase signalling .....	61
1.8.2	PKA signalling crosstalk.....	64
1.8.3	Anti- and pro-apoptotic signalling .....	65
1.9	Pharmacological modulators of <i>FSHR</i> signalling .....	66
1.9.1	<i>FSHR</i> agonists .....	67
1.9.2	<i>FSHR</i> antagonists.....	68
1.10	<i>FSHR</i> inward trafficking .....	69
1.11	Follicle-stimulating hormone receptor oligomers .....	74
1.11.1	Evidence for <i>FSHR</i> oligomers .....	74
1.11.2	Structural interfaces of <i>FSHR</i> oligomers .....	75
1.11.3	Physiological role for <i>FSHR</i> oligomers .....	76
1.12	Hypothesis, aims and objectives .....	78
<b>2</b>	<b>Chapter Two: Materials and Methods.....</b>	<b>80</b>
2.1	Overview .....	81
2.2	Chemicals and reagents .....	81
2.3	Cell culture .....	84

2.3.1	Cell counting and plating .....	84
2.3.2	Transient transfection.....	84
2.3.3	Re-plating cells .....	85
2.4	Photoactivatable dye localisation microscopy .....	86
2.4.1	PD labelling of HA.11 antibody .....	86
2.4.2	Cell stimulation for PD-PALM.....	88
2.4.3	Imaging FSHR molecules via PD-PALM.....	89
2.4.4	Mapping FSHR molecules from PD-PALM.....	93
2.4.5	Selection process for FSHR density in PD-PALM.....	94
2.5	GloSensor™ cAMP assay .....	95
2.6	Dual-Luciferase® Reporter Assay system.....	96
2.7	Western blotting .....	98
2.7.1	Cell lysis and protein assay.....	98
2.7.2	SDS-PAGE .....	99
2.7.3	Transfer of protein from SDS-PAGE gel to PVDF membrane .....	99
2.7.4	PVDF membrane blocking and antibody probing .....	100
2.7.5	Quantification of protein expression.....	100
2.7.6	Primary antibody re-probing for global proteins .....	101
2.8	Immunocytochemistry immunofluorescence .....	101
2.9	siRNA approach to gene knockdown.....	103
2.10	Radioligand binding assay .....	103

2.11	Data analysis and statistics .....	104
2.11.1	Normalisation of GloSensor <sup>TM</sup> cAMP production.....	104
2.11.2	Normalisation of cre-luciferase activity.....	104
2.11.3	Normalisation of protein expression for Western blotting .....	105
2.11.4	Percentage of FSHR-positive EEA1 endosomes .....	105
2.11.5	Statistics .....	105
<b>3</b>	<b>Chapter Three: Investigating the role of FSH glycoforms on FSHR oligomerisation and correlation with cAMP-dependent signalling .....</b>	<b>107</b>
3.1	Introduction .....	108
3.2	Results .....	111
3.2.1	Concentration- and time-dependent effects of FSH glycoforms on FSHR oligomerisation .....	111
3.2.2	Effect of FSH glycoform-dependent FSHR oligomerisation on cAMP accumulation and CREB-phosphorylation .....	119
3.2.3	Effect of FSH glycoform-dependent FSHR oligomerisation on cre-luciferase activity.....	128
3.2.4	Effect of FSH glycoform-dependent FSHR oligomerisation on ERK1/2-phosphorylation.....	131
3.3	Discussion .....	133
<b>4</b>	<b>Chapter Four: Delineating how FSH glycoforms modulate FSHR trafficking and impact on cAMP-dependent signalling .....</b>	<b>139</b>
4.1	Introduction .....	140

4.2	Results .....	142
4.2.1	Effect of inhibiting FSHR internalisation on FSH glycoform-dependent FSHR cAMP production and cre-luciferase activity .....	142
4.2.2	Effect of FSH glycoforms on FSHR co-localisation to EEA1-positive endosomes.....	148
4.2.3	Effect of APPL1 silencing on FSH glycoform-dependent FSHR cAMP production and cre-luciferase activity.....	150
4.3	Discussion .....	158
<b>5</b>	<b>Chapter Five: Investigating the effect of a small positive FSHR allosteric modulator on FSHR oligomerisation and signalling .....</b>	<b>165</b>
5.1	Introduction .....	166
5.2	Results .....	168
5.2.1	Effect of C5 on FSHR oligomerisation and subsequent cAMP production ....	168
5.2.2	Effect of C5 on FSH glycoform-dependent cAMP production .....	174
5.2.3	Effect of C5 on FSH glycoform-dependent FSHR oligomerisation .....	179
5.3	Discussion .....	184
<b>6</b>	<b>Chapter Six: Screening and identification of novel FSHR inhibitors and the effect on FSH/FSHR binding, signalling and oligomerisation .....</b>	<b>190</b>
6.1	Introduction .....	191
6.2	Results .....	194
6.2.1	Screening of 84 different small molecule candidate compounds for the ability to inhibit FSH-dependent cre-luciferase activity .....	194

6.2.2	Effect of identified FSHR inhibitors on FSH/FSHR binding using radioligand binding assays .....	198
6.2.3	Concentration-dependent effects of FSH on FSHR activity when inhibited with different concentrations of different FSHR inhibitors .....	200
6.2.4	Effect of an FSHR inhibitor on FSHR oligomerisation.....	202
6.3	Discussion .....	204
<b>7</b>	<b>Chapter Seven: General Discussion .....</b>	<b>210</b>
7.1	Thesis summary.....	211
7.2	The role cell-surface FSHR oligomerisation plays in modulating FSHR signalling.....	212
7.3	What is the future for FSHR pharmacological modulators?.....	215
7.4	Limitations .....	216
7.5	Future directions.....	221
<b>8</b>	<b>References.....</b>	<b>224</b>
<b>9</b>	<b>Appendix I.....</b>	<b>246</b>
<b>10</b>	<b>Appendix II.....</b>	<b>252</b>
<b>11</b>	<b>Appendix III.....</b>	<b>257</b>

**1 Chapter One – General Introduction**

## **1.1 Overview**

An estimated 1 in 7 couples in the UK are infertile and require assisted reproductive technology (ART) to aid conception (HFEA, 2021). The UK average success rate of these techniques, such as *in vitro* fertilisation (IVF), are currently ~32% in women under 35 years, with further decreases in the success rate in women over 35 years (HFEA, 2021). As an industry predicted to be worth ~\$25.6 billion by 2026 (BioSpace, 2021), it remains important to understand the fundamentals of the mechanisms controlling fertility in women, with a view to advancing knowledge in a field that continues to rise in demand.

The heterodimeric glycoprotein hormone (GpH), follicle-stimulating hormone (FSH), and its target G protein-coupled receptor (GPCR), follicle-stimulating hormone receptor (FSHR), are essential for reproduction (Abel et al., 2000; Dierich et al., 1998; Kumar et al., 1997; Tao & Segaloff, 2009). They play essential roles in regulating follicle growth, steroidogenesis and ovulation (Messinis et al., 2014). As a result, FSH/R are main drug targets for IVF, therefore, finding alternative ways of targeting them remains key. The investigations reported in this thesis were designed to develop a better understanding of FSH/R mechanisms at a single molecule and cellular level, with the future aim of identifying alternative mechanisms to target them and improve fertility outcomes in women seeking assisted conception.

## **1.2 The hypothalamus-pituitary-ovarian axis**

Female reproduction and fertility is regulated by the hypothalamus-pituitary-ovarian (HPO) axis (Plant, 2015). In females, the axis comprises of the hypothalamus, pituitary



gland, and the ovaries, acting as a single entity to mediate the release of various hormones, including FSH, to control ovarian function and steroid hormone feedback (Figure 1.1).

Regulation of the HPO axis is thought to be initially regulated by the peptide hormone, Kisspeptin (KISS1), which is expressed in the arcuate (ARC) and anteroventral periventricular (AVPV) nucleus within the hypothalamus (Plant, 2015). Its primary target is the KISS1 receptor (KISS1R), a GPCR localised to gonadotrophin-releasing hormone (GnRH) neurones in the ARC (Plant, 2015). Pulsatile release of KISS1 mediates the pulsatile secretion of the hypothalamic decapeptide, GnRH, from GnRH neurones into the hypophyseal portal system (Dungan et al., 2006).

Within the anterior pituitary, GnRH acts on its target GPCR, the GnRH receptor (GnRHR), localised to gonadotroph cells. Gonadotroph cells synthesise and secrete FSH, and another important glycoprotein hormone called luteinising hormone (LH), which plays an essential role in ovulation. The pulse frequency and amplitude of GnRH, plus additional regulation from other transforming growth factor- $\beta$  (TGF- $\beta$ ) superfamily members, such as activin, follistatin and inhibin (Das & Kumar, 2018), together control the preferential synthesis and secretion of both FSH and LH (Clarke & Cummins, 1982; Jayes et al., 1997). During early folliculogenesis, low-frequency GnRH pulses mediate preferential FSH synthesis and secretion to enhance follicle growth. Whereas, during mid-late folliculogenesis, high-frequency GnRH pulses mediate preferential LH synthesis and secretion, leading to an LH surge and triggering ovulation (Coss, 2018; Das & Kumar, 2018; Kaiser et al., 1997; Messinis et al., 2014).

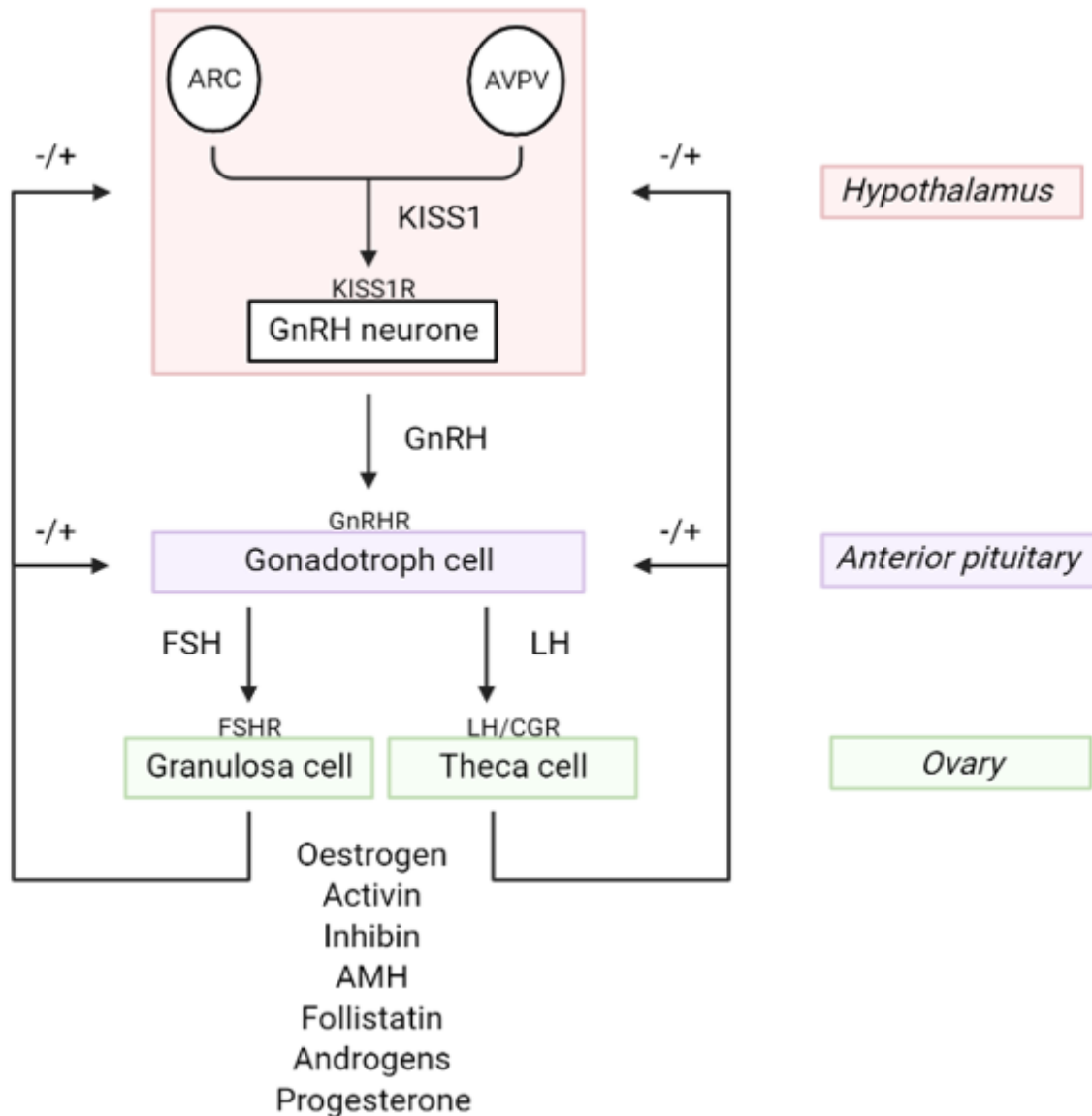


**Figure 1.1: Simplified schematic diagram of the hypothalamus-pituitary-ovarian axis.** Kisspeptin (KISS1) hormone is released from the arcuate (ARC) and the anteroventral periventricular (AVPV) nucleus in the hypothalamus and acts on KISS1 receptors (KISS1R) on gonadotrophin-releasing hormone (GnRH) neurones. GnRH secreted acts on GnRH receptors (GnRHR) located on gonadotroph cells within the anterior pituitary. Gonadotrophin hormones, follicle-stimulating hormone (FSH) and luteinising hormones (LH), are secreted and act on the FSH receptor (FSHR) on granulosa cells and LH/human chorionic gonadotrophin receptor (LH/CGR) on theca cells within the ovary. The secretion of different hormones from the ovary induces negative and positive feedback mechanisms on the hypothalamus and anterior pituitary to further regulate gonadotrophin hormone release (Plant, 2015).

Once secreted, both FSH and LH bind to their associated GPCRs expressed in the ovaries. FSH binds to the FSHR, primarily localised to granulosa cells (GCs), and LH binds to the LH/human chorionic gonadotrophin receptor (LH/CGR), primarily localised to theca cells, but is also expressed in GCs during late folliculogenesis. The actions of these glycoprotein hormones stimulate the release of oestrogen, androgens, progesterone and other TGF- $\beta$  protein hormones. They feedback on the hypothalamus and anterior pituitary to further negatively, and positively, regulate the HPO axis and reproduction (Thackray et al., 2010).

Although there are many hormones that regulate the HPO axis and female fertility, FSH and the FSHR play an imperative role within the ovaries as together they support follicular development and maturity as early as those preantral stages of follicle development (Hardy et al., 2017; Kumar et al., 1997; McGee et al., 1997; Richards & Pangas, 2010). Furthermore, as predominant drug targets in IVF, understanding their structure, function, and molecular mechanism of action is an important first step for identifying alternative mechanisms to target them and improve fertility outcomes in women seeking assisted conception.

### **1.3 Ovarian physiology**

The ovaries are comprised of oocytes surrounded by layer(s) of granulosa and theca cells (dependent on the stage of maturation), which are further surrounded by stromal cells. The FSHR is localised to GCs in early stages of folliculogenesis and the gonadotrophin hormones work in concert to regulate folliculogenesis (Richards & Pangas, 2010). Although the gonadotrophin hormones mediate many stages of folliculogenesis, the early

stages of folliculogenesis are predominantly gonadotrophin-independent (Richards & Pangas, 2010).

### 1.3.1 Gonadotropin-independent folliculogenesis

The ovarian cortex predominantly contains the resting pool of primordial follicles. The primordial follicles consist of a prophase I-arrested immature oocyte surrounded by a single layer of squamous GC cells, which are quiescent. A balanced response from stimulatory and inhibitory paracrine factors initiates the activation of a cohort of primordial follicles (Richards & Pangas, 2010). When primordial follicles are activated, the squamous GCs change their shape to cuboidal, gene transcription is initiated, GC proliferation is activated, and the follicle begins to grow in size to reach the primary stage of folliculogenesis. During this stage the FSHR expression is acquired in GCs. However, although the follicle is sensitive to FSH, with research studies showing the addition of FSH to follicle cultures accelerates mouse follicle growth *in vitro* (Hardy et al., 2017), the follicle can develop independently of FSH/FSHR activity, but development arrests thereafter (Abel et al., 2000; Kumar et al., 1997). Finally, the development of the outer layer theca cells establishes a secondary follicle, also classically known as the pre-antral stage, with theca cells forming a distinct population of cells (theca interna and externa), which are vascularised and marks the end of gonadotropin-independent folliculogenesis.

### 1.3.2 Gonadotrophin-dependent folliculogenesis

The later stage of secondary folliculogenesis marks the start of gonadotropin-dependent folliculogenesis. As the capillary network surrounding the late-stage secondary follicle continues to develop, fluid-filled cavities of serum transudate called antra, begin to form,

and further increase follicle diameter. LH/CGR that are expressed on the cell surface of theca cells are also present at this stage of follicle development. Working in concert together, LH/LHR and FSH/FSHR control androgen and oestrogen production via the two-cell two-gonadotrophin model of steroidogenesis (Adashi, 1994; Hillier et al., 1994). As theca cells respond to increased secretion of LH, cholesterol is converted to androgens. As GCs respond to increased secretion of FSH, aromatase expression is increased. Synthesised androgens are shuttled to GCs where they are converted to oestrogen via aromatase. Oestrogen then acts on the endometrium and causes proliferation, ready for potential implantation of a fertilised egg (Messinis et al., 2014).

During the mid-late stages of folliculogenesis, elevated oestrogen and inhibin negative feedback to the hypothalamus and anterior pituitary, decreases FSH production. As a result, only the most responsive follicles remain. These follicles express the LH/CGR on GCs and further mature in response to elevated LH. Other smaller follicles, that are predominantly dependent on FSH, begin the process of apoptosis and follicle atresia. This event usually produces a single dominant mature follicle. Subsequently, increased oestrogen and the switch from negative to positive oestradiol feedback, the LH surge, and together with multifaceted cascades such as inflammatory events, increased matrix metalloproteinases (MMPs), and progesterone receptor expression, all mediate the expulsion of the oocyte that goes on to ovulate (Messinis et al., 2014; Zeleznik, 2004).

### 1.3.3 Corpus luteum

The remnant cells from the ruptured follicle undergo rapid transformation into luteinised cells that respond to LH signals and form an endocrine structure called the corpus luteum.

This structure predominantly secretes the steroid hormone progesterone which acts on the endometrium to induce secretory hormones ready for potential implantation of a fertilised egg and maintenance of pregnancy. If an egg is fertilised, the homologous hormone to LH, human chorionic gonadotrophin (hCG), rescues the corpus luteum and prevents its regression into the corpus albicans. If the oocyte is not fertilised, then the natural decline in LH in the later stages of the menstrual cycle causes a breakdown of the endometrium and regression of the corpus luteum, which initiates the onset of menstruation in women (Messinis et al., 2014).

Although it's clear that both FSH and LH play an important role in ovarian physiology and ultimately ovulation and fertility in women, it is FSH and the FSHR that pioneer the early crucial stages of folliculogenesis, and therefore important structures to understand as they are predominant targets in ART.

#### **1.4 Follicle-stimulating hormone**

FSH is comprised of a non-covalently associated common  $\alpha$ -subunit and a  $\beta$ -subunit. The common  $\alpha$ -subunit is encoded by the glycoprotein hormones  $\alpha$ -polypeptide (*CGA*) gene located on chromosome 6 in humans, and is shared among other GpHs, such as LH, hCG and thyroid-stimulating hormone (TSH). The  $\beta$ -subunit is encoded by *FSH $\beta$*  gene located on chromosome 11 in humans, and is hormone-specific, conferring biological specificity at the FSHR.

#### 1.4.1 Transcriptional regulation of FSH subunits

As previously mentioned in section 1.2, synthesis of FSH is regulated by GnRH, activin, follistatin and inhibin. The transcription of *CGA* is regulated predominantly by GnRH, however, because FSH $\beta$  confers the specific biological activity of FSH dimer, the transcription of *FSH $\beta$*  is more tightly regulated by low-frequency pulses of GnRH, and therefore the rate-limiting step for the production of the biologically active FSH (Das & Kumar, 2018). *FSH $\beta$*  expression is also regulated by the activin–follistatin–inhibin loop. Activin is a gonadal peptide that positively regulates *FSH $\beta$*  expression via small mothers against decapentaplegic (Smad) 2 and Smad 3 signalling. The production of FSH then stimulates the production of the FSH gonadal antagonist peptide, inhibin, which then downregulates FSH production. Furthermore, the glycoprotein hormone follistatin also inhibits the actions of activin by directly binding to it and further down regulating *FSH $\beta$*  expression (Das & Kumar, 2018). The steroid hormones oestrogen and progesterone, that are produced in the ovaries, also regulate *FSH $\beta$*  expression through feedback loops via acting on their receptors located in the hypothalamus and anterior pituitary (Das & Kumar, 2018). Together, these hormones tightly regulate the production and formation of the FSH heterodimer.

#### 1.4.2 FSH heterodimer structure

X-ray crystallography of FSH heterodimer has shown it's comprised of a cysteine-knot motif in the centre core of each subunit, forming disulphide bridges that are essential for stabilising its structure (Fan & Hendrickson, 2005; Fox et al., 2001). Both subunits of FSH share similar topology, with each consisting of four antiparallel  $\beta$  strands connected by three hairpin loops (HL1-3) (Figure 1.2).

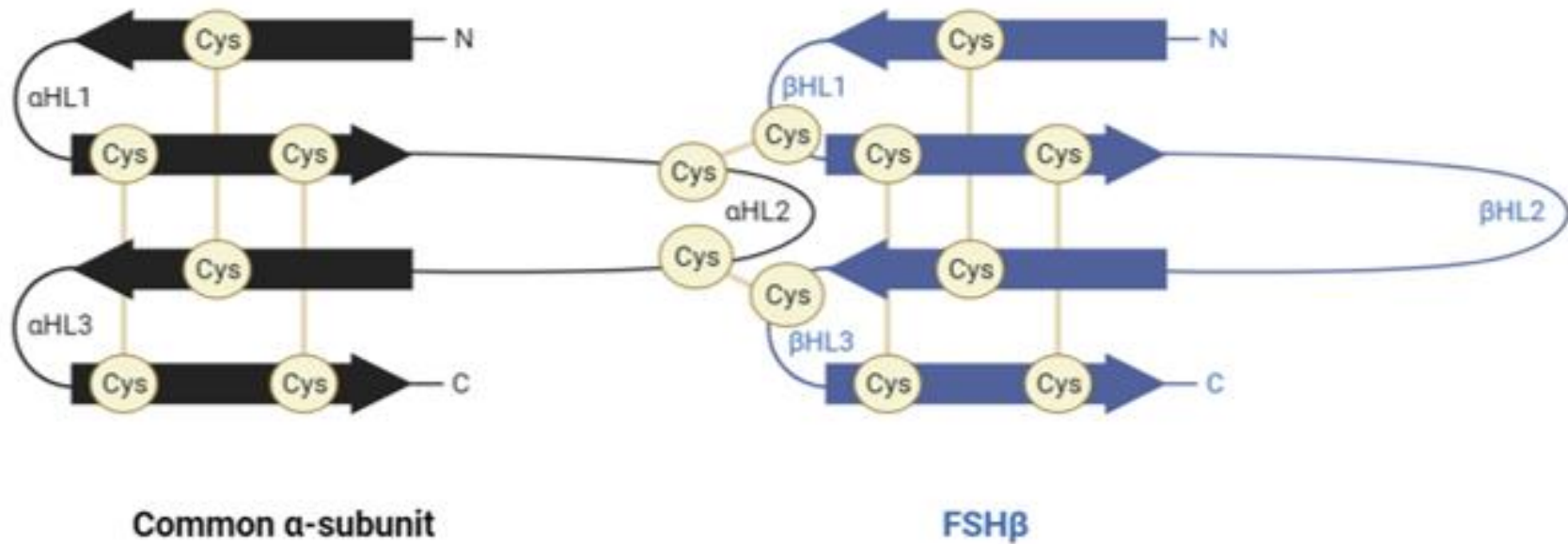


**Figure 1.2: Simplified structure of follicle-stimulating hormone.** Simplified schematic 2D structure of FSH heterodimer. The common  $\alpha$ -subunit (black) and hormone-specific FSH $\beta$  (blue) consists of four anti-parallel  $\beta$  strands (arrows) connected by three hairpin loops (HL1-3). Cysteine residues form three intramolecular disulphide bridges, to stabilise the subunits and are collectively known as the cysteine-knot motif. The heterodimer is further stabilised by intermolecular disulphide bridges (Fan & Hendrickson, 2005; Fox et al., 2001). *Figure created using BioRender.com.*



The  $\beta$  strands within each subunit are secured by the three cysteine interactions forming intramolecular disulphide bridges (Fox et al., 2001; Querat, 2021). When the two subunits form to make a heterodimer, HL1 and HL3 on one subunit forms intermolecular disulphide bridges with the HL2 on the other subunit in a head-to-tail arrangement (Querat, 2021). Once the heterodimers assemble, it is further stabilised by the ‘seatbelt’ mechanism. The ‘seatbelt’ is a region between the 10<sup>th</sup> and 12<sup>th</sup> cysteine residue of the  $\beta$ -subunit, Cys $\beta$ 93 and Cys $\beta$ 110 respectively, and directs FSH recognition and binding to FSHR (Dias et al., 1994). It involves the HL2 of the common  $\alpha$ -subunit becoming wrapped around by an intramolecular disulphide bridge ‘seatbelt’ within the FSH $\beta$ , and then buckled at the common  $\alpha$ -subunit C-terminal end by disulphide bonds (Laphorn et al., 1994; Xing et al., 2004). Once FSH heterodimer is stabilised, it is transported to the endoplasmic reticulum (ER) and Golgi for further post-translational processing.

#### 1.4.3 Post-translational modification of FSH

FSH is heavily glycosylated and has four possible asparagine (Asn)-linked glycosylation sites that are critical for heterodimer assembly and function (Baenziger & Green, 1988; Matzuk & Boime, 1989). The first two glycosylation sites are located on the common  $\alpha$ -subunit at HL2 (Asn52) and HL3 (Asn78) and are conserved across the different GpHs. They are critical for  $\alpha$ -subunit folding, stability and hormone secretion (Flack et al., 1994; Matzuk & Boime, 1988; van Zuylen et al., 1997). Flack *et al.*, investigated their role using site-directed mutagenesis in rat Sertoli cells and GCs (Flack et al., 1994). When asparagine was mutated to glutamine, to remove the glycan chains, FSH binding affinity to the FSHR was increased, whereas signal transduction was significantly reduced, suggesting glycosylation on the common  $\alpha$ -subunit is required for full FSH activity (Flack et al., 1994). The second two glycosylation sites are located on HL1 at Asn7 and Asn24 of FSH $\beta$  and

play a key role in FSH binding to the FSHR, signal transduction and FSH metabolic clearance rate (Bishop et al., 1995; Bishop et al., 1994).

Post-translational modifications of newly synthesised FSH, that gives rise to these Asn-linked glycans, first occurs within the rough ER (RER). Specific Asn-linked glycosylated precursor residues are first attached at specific Asn residues by the membrane-associated enzyme complex, oligosaccharyltransferase (OST) and glycosidases (Campo et al., 2019) (Figure 1.3, (a)). The precursor residues are further processed in the *cis*-Golgi to yield mannose-rich intermediate residues that are synthesised into various branches in the *trans*-Golgi during late processing steps (Campo et al., 2019) (Figure 1.3, (a)). The final common core structure of the Asn-glycans that are processed in the *trans*-Golgi are composed of *N*-Acetylglucosamine (GlcNAc), fucose, mannose and galactose sugar-based molecules. The branches of the Asn-glycans are further terminally decorated with variations of *N*-Acetylgalactosamine (GalNAc), sialic acid and/or sulphate (Figure 1.3, (a)). Although the Asn-glycan chains on the common  $\alpha$ -subunit are conserved across the GpHs, it has been revealed that there may be hormone-specific variation in their glycosylation pattern (Gotschall & Bousfield, 1996). Nevertheless, its differences in the FSH $\beta$  Asn-glycan residues that give rise to multiple variants of FSH.

Charged-based fractionation of FSH $\beta$  residues from various species has identified many heterogenous FSH variants with differing biological and immunological activity (Bousfield et al., 2014b; Dalpathado et al., 2006; Ulloa-Aguirre et al., 1995). These FSH variants can differ significantly and have been classified as two main levels of heterogeneity.

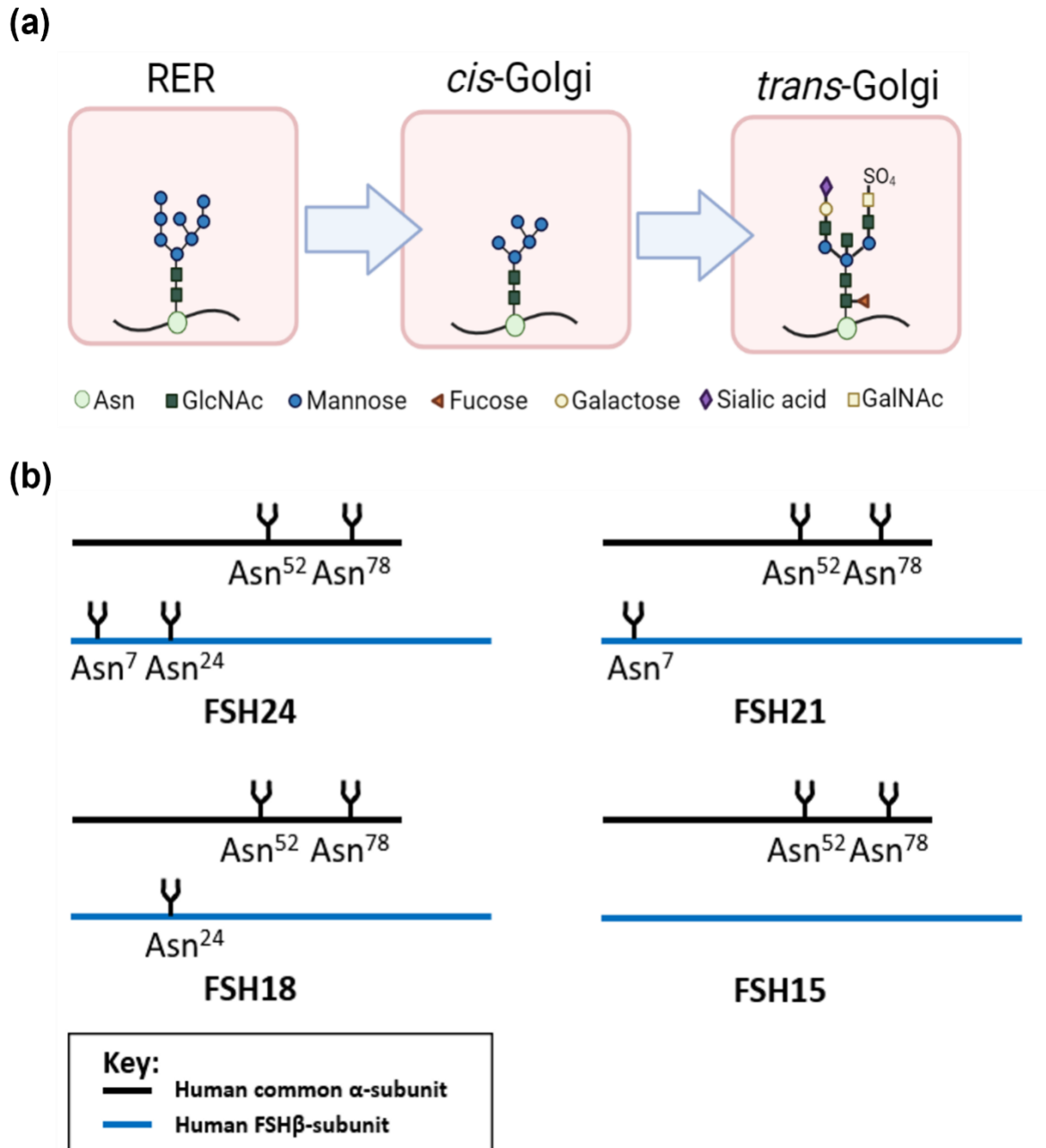


**Figure 1.3: Post-translational modification of follicle-stimulating hormone.** (a) Newly synthesised FSH is first processed in the rough endoplasmic reticulum (RER) where specific Asn-linked glycosylated precursor residues are attached. Further processing in the *cis*-Golgi yields mannose-rich intermediate residues, with final stages of processing in the *trans*-Golgi forming mature Asn-glycans terminally decorated with variations of GalNAc, sialic acid and/or sulphate. (b) The presence/absence of one or more Asn-glycan residues on FSH $\beta$  gives rise to macroheterogeneous FSH glycoforms. Fully glycosylated FSH (FSH24) possesses both Asn7 and Asn24, partially glycosylated FSH21 possesses Asn7, partially glycosylated FSH18 possesses Asn24, and deglycosylated FSH15 lacks both Asn7 and Asn24 (Campo et al., 2019). Figure created using BioRender.com.

#### 1.4.3.1 FSH microheterogeneity

Differences in the chemical composition and branching nature of either Asn7 or Asn24 gives rise to microheterogeneous versions of FSH (FSH isoforms). The difference in the chemical structure of the glycan chains predominantly reflects the presence of the negatively charged residue, sialic acid, and whether the glycan branches are bi- or tri-antennary. In the *trans*-Golgi *cisternae*, the enzymes Gal $\beta$ 1,3GlcNAc $\alpha$ 2,3-sialyltransferase (ST3Gal III) and Gal $\beta$ 1,4GlcNAc $\alpha$ 2,6-sialyltransferase (ST6Gal I) are expressed and mediate the incorporation of sialic acid onto the specific Asn-linked glycan chain (Figure 1.3, (a)). Evidence from many mammalian systems suggests that transcriptional regulation of these glycosyltransferases is predominantly regulated by steroid hormones such as oestrogen and testosterone (Ambao et al., 2009; Damián-Matsumura et al., 1999; Wide & Eriksson, 2013; Wide & Naessén, 1994).

There are an estimated population of 80-100 microheterogeneous glycan chains decorating three or four Asn-linked glycosylation sites in FSH (Bousfield et al., 2018). Charge-based fractionation procedures and nano-electrospray mass spectrometry were amongst the techniques that characterised these microheterogeneous populations of FSH (Bousfield et al., 2018; Ulloa-Aguirre et al., 1995). While the physiological relevance of FSH isoforms remain unclear, the degree of FSH glycan sialylation has been shown to alter the functional properties of FSH, changing the metabolic clearance rate and binding affinity of FSH to the FSHR (Cerpa-Poljak et al., 1993; Soudan & Pigny, 2017; Ulloa-Aguirre et al., 1999). In males, it was revealed that the more acidic FSH isoforms supported sexual maturation in rats, and puberty in humans (Ulloa-Aguirre et al., 1986; Wide, 1989). In females, FSH glycan composition has been shown to change across the different phases of the menstrual cycle, with the less acidic FSH isoforms, with more branching, secreted more during the

mid-late follicular phase, and in higher abundance than FSH isoforms in menopausal women (Creus et al., 1996; Wide & Naessén, 1994; Yding Andersen, 2002), suggesting a functional role for differential FSH isoforms in controlling the ovarian cycle and ovarian aging.

#### 1.4.3.2 FSH macroheterogeneity

The absence of Asn7 and/or Asn24 on FSH $\beta$  gives rise to macroheterogeneous versions of FSH (FSH glycoforms). Western blot analysis of human pituitary extracts identified four types of naturally occurring FSH glycoforms (Davis et al., 2014). Fully glycosylated FSH (FSH24) possess both Asn7 and Asn24 glycans, partially glycosylated FSH (FSH18 and FSH21) possess only Asn24 or Asn7, respectively, and deglycosylated FSH (FSH15) lacks both Asn7 and Asn24 glycans (Figure 1.3, (b)). The numbers associated to these glycoforms are the molecular weights (24, 21, 18 or 15kDa) resolved when using sodium dodecyl sulphate–polyacrylamide gel electrophoresis (SDS-PAGE). Although partially glycosylated FSH21/FSH18 and fully glycosylated FSH24, are all naturally secreted from the anterior pituitary, FSH21 and FSH24 remain the most abundant forms (Bousfield et al., 2007). In contrast, deglycosylated FSH15 is believed to be physiologically irrelevant because of its poor assembly with the common  $\alpha$ -subunit which mediated low FSH secretion in studies involving transgenic mice (Wang et al., 2016a).

Bousfield *et al.*, revealed that the relative abundance of FSH21 may change across the menstrual cycle. Uterine histology from four peri-menopausal women (51 years) at four different phases of the menstrual cycle showed that there was 74% FSH21 abundance during the late-follicular phase (Bousfield et al., 2014b). Furthermore, in healthy women

with regular menstrual cycles, FSH21 was shown to play a key role in natural ovarian stimulation, with peak serum levels on cycle day 5 and midcycle (Wide & Eriksson, 2018). Interestingly, data from human pituitary extracts from post-mortem women illustrated the abundance of FSH21 and FSH24 also changes with age, with FSH21 higher in females in their reproductive prime (20's) and significantly declining in peri-menopausal females (50's) (Bousfield et al., 2014b), suggesting some physiological relevance for these glycoforms.

Over the last few decades an abundance of *in vitro* and *in vivo* research has been dedicated to understanding the role of these glycoforms. Partially glycosylated FSH21 has been shown to display higher binding affinity for FSHR, is much more potent at activating canonical FSHR-dependent signalling, has more *in vitro* and *in vivo* bioactivity, and ultimately drives ovarian follicular development more than fully glycosylated FSH24 (Bousfield et al., 2014a; Hua et al., 2021; Jiang et al., 2015; Johnson et al., 2022; Wang et al., 2016b). Surprisingly, some current IVF protocols stimulate the ovaries using human menopausal gonadotrophin (HMG) harvested from post-menopausal urine, which naturally contains a higher abundance of FSH24 and, although it has not yet been investigated, may contribute to the poor success rate of IVF (Daya & Gunby, 2000). Nevertheless, how these FSH glycoforms can mediate such diverse signal responses when they engage with the FSHR remains unclear. Further understanding of FSHR physiology is required in order to begin to find alternative methods to improve fertility outcomes.

## 1.5 G protein-coupled receptors

The diverse actions of FSH are mediated through interactions with the FSHR. The FSHR is a member of the largest family of membrane-spanning receptors, GPCRs. GPCRs can respond to a diverse array of ligand subtypes, that range from odours, foods and light-sensitive compounds to peptides and proteins (Lander et al., 2001; Maudsley et al., 2005; Venkatakrishnan et al., 2013; Venter et al., 2001). In response to ligands, GPCRs can elicit diverse cellular responses, making them the largest group of proteins targeted by drugs (Brink et al., 2004; Flower, 1999; Hauser et al., 2018). They consist of seven-membrane spanning regions comprised of amino acid  $\alpha$ -helices and are also referred to as seven-transmembrane domain receptors (7TM). The transmembrane domains (TMDs) are connected by 3 intracellular loops (ICL1-3) and 3 extracellular loops (ECL1-3). The ECL contains two highly conserved cysteine residues that form disulphide bonds which stabilise the receptor structure. The hydrophilic regions of GPCRs consist of the N-terminal extracellular domain (ECD), C-terminal intracellular domain (ICD) and the C-tail. These play important roles in ligand binding, G protein coupling and signal activation.

All GPCRs, including the FSHR, are coupled to a heterotrimeric G protein, consisting of an inactive guanine diphosphate (GDP)-bound  $\alpha$  subunit, a  $\beta$ - and  $\gamma$  subunit that initiate signal transduction (Figure 1.4). Once GPCRs are activated, a conformational change within the TMD induces intrinsic guanine nucleotide exchange factor (GEF) activity, resulting in the GDP-bound  $\alpha$ -subunit conversion to an active guanosine triphosphate (GTP)-bound subunit via adenosine triphosphate (ATP). The GTP-bound  $\alpha$ -subunit then dissociates from the  $\beta$  and  $\gamma$  subunit to further affect intracellular proteins. The  $\alpha$ -subunit has four key isoforms that determine the GPCR second messenger signalling pathway activated and its

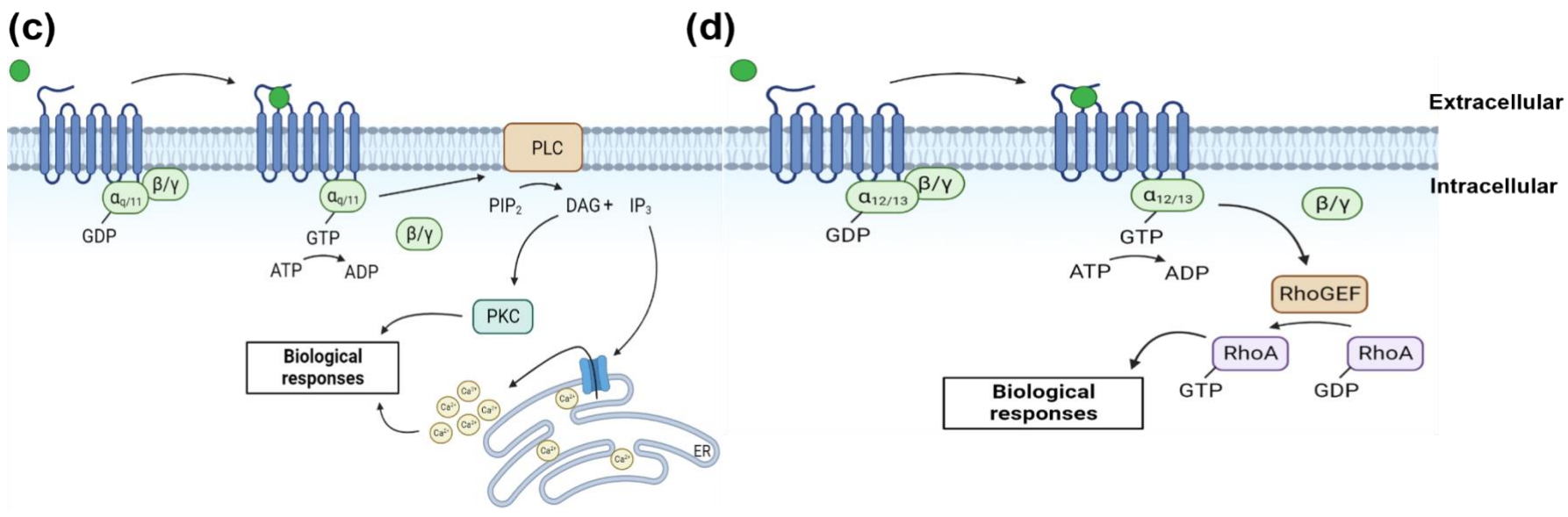
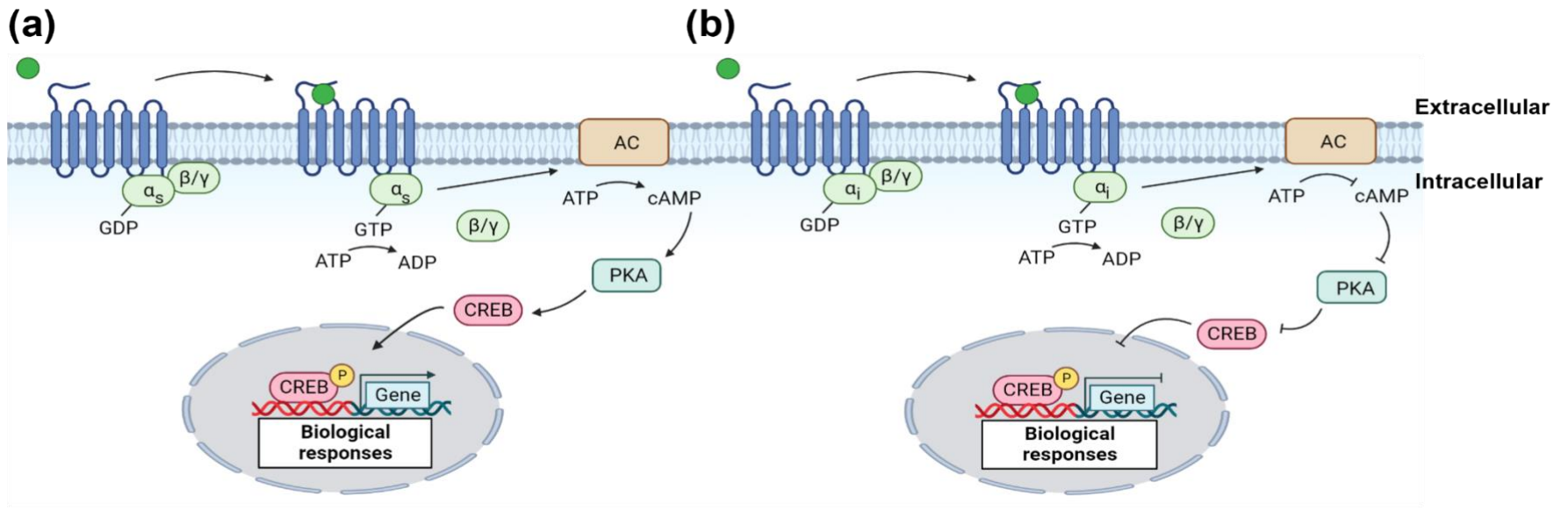




**Figure 1.4: Simplified schematic diagram of different GPCR signalling pathways. (a)**  $G\alpha_s$  signalling mediates the conversion of ATP to the second messenger cAMP via the membrane-bound enzyme adenylyl cyclase (AC). cAMP then goes on to activate other downstream signals. **(b)**  $G\alpha_i$  signalling inhibits the signalling pathway in (a) and leads to alternative biological responses. **(c)**  $G\alpha_{q/11}$  signalling mediates the conversion of  $PIP_2$  to the second messengers  $IP_3$  and DAG via the membrane-bound enzymes phospholipase C (PLC).  $IP_3$  binds to  $IP_3$  receptors (blue ion channels) located on the endoplasmic reticulum (ER) membrane to induce calcium ion release into the cytoplasm which induces a biological response. **(d)**  $G\alpha_{12/13}$  signalling mediates the conversion of inactive GDP-bound RhoA into active GTP-bound RhoA via Rho guanine nucleotide exchange factor (RhoGEF) and induces a biological response (Syrovatkina et al., 2016). *Figure created using BioRender.com.*

downstream targets. This consists of  $G\alpha_s$  and  $G\alpha_i$ /cyclic-adenosine monophosphate (cAMP)/protein kinase A (PKA) (Figure 1.4, (a-b)),  $G\alpha_q/11$ /phosphatidylinositol biphosphate ( $PIP_2$ )/inositol trisphosphate ( $IP_3$ ) (Figure 1.4, (c)), and  $G\alpha_{12/13}$ /RhoGEF/RhoA (Figure 1.4, (d)), with each pathway mediating different biological and cellular responses (Syrovatkina et al., 2016; Wettschureck & Offermanns, 2005).

Since the family of GPCRs are so large, they have been divided into different classes according to their sequence homology and structural similarities (Fredriksson et al., 2003; Stevens et al., 2013). Using phylogenetic analysis, 342 functional nonolfactory human GPCRs were sequenced, and five main families of receptors were identified (Fredriksson et al., 2003). Three of these GPCR groups, Class A (rhodopsin-like), Class B (secretin), and Class C (metabotropic glutamate), have been extensively studied and reported to have no detectable sequence homology between them (Fredriksson et al., 2003). Breakthrough in the tools used to study GPCR structure and dynamics, such as x-ray crystallography (Rasmussen et al., 2011; Rosenbaum et al., 2007), cryogenic electron microscopy (cryo-EM) (Chang et al., 2020; García-Nafría et al., 2018), atomic-level molecular dynamics (MD) (Miao & McCammon, 2016), and integrated nuclear magnetic resonance (NMR) spectroscopy (Shimada et al., 2019), has enhanced further understanding of the similarities and differences between GPCR classes. Furthermore, GPCR activation mechanisms have been shown to vary, which may be a result of several differing structure-function features (Hauser et al., 2021).

### 1.5.1 Class A GPCRs

FSHR is a member of the Class A GPCRs. These GPCRs are by far the largest and most complex class of GPCRs, and account for nearly 85% of GPCR genes (Attwood & Findlay, 1994; Fredriksson et al., 2003). They consist of a highly conserved glutamic acid/aspartic acid-arginine-tyrosine (E/DRY) motif between TMD 3 and ICL2, and has been shown to be important for stabilising the inactive-state confirmation (Vogel et al., 2008). Mutation of this motif has elucidated many different properties, such as constitutive receptor activity, increased affinity for agonist binding and retaining G protein coupling (Rovati et al., 2007). Most Class A GPCRs, except for the glycoprotein hormones receptors (GpHRs) like FSHR, have relatively short ECDs, with studies using the prototypical adenosine A(2A) receptor revealing the ligand binding site located within the TMD (Lebon et al., 2011; Ye et al., 2016). Studies on the classical  $\beta_2$ -adrenoceptor ( $\beta_2$ AR) have suggested the mode of activation of Class A GPCRs may arise from the outward movement of the intracellular region of TMD 6. It is thought that TMD 6 opens up a pocket to accommodate and activate the G protein (Dror et al., 2011; Nygaard et al., 2013; Rasmussen et al., 2011), however, this mechanism may be entirely receptor-specific.

### 1.5.2 Class B and Class C GPCRs

In contrast to Class A GPCRs, Class B and Class C GPCRs have a relatively large ECD that is almost entirely involved in ligand binding. Furthermore, the ECD contain conserved cysteine-rich repeats (CRR) residues that are likely important for GPCR stabilisation. Although the TMD and ICLs involved in receptor activation share some similarities with Class A GPCRs (Hausch, 2017), the activation mechanisms vary between the classes. For Class B GPCRs, ligand binding initiates the outward movement TMD 6, which undergoes an additional 'kink' to accommodate G proteins, G protein-coupled receptor kinases

(GRKs) and arrestins (Hollenstein et al., 2013). Moreover, Class C GPCRs form obligate dimers following ligand binding to the Venus Flytrap (VFT) ligand-binding motif within the ECD (Mao et al., 2020; Shaye et al., 2020). Interestingly, although the GpHR is a Class A GPCR, it has a uniquely large ECD that resembles the structural architect of Class C GPCRs, suggesting that these receptors function differently compared to classical Class A GPCRs.

## **1.6 Glycoprotein hormone receptors**

The GpHR is a Class A GPCR subfamily that consists of the gonadotrophin hormone receptors; FSHR and LH/CGR, which regulate reproduction in mammals, and thyroid-stimulating hormone receptor (TSHR), which regulates thyroid growth and metabolism (Jiang et al., 2014a). Unlike classical rhodopsin-like Class A GPCRs, GpHRs have a large ECD with distinct chemical and structural characteristics, such as a leucine-rich repeat (LRR) and a hinge region (Figure 1.5), believed to play a major role in hormone selectivity and specificity (Ascoli et al., 2002; Dias & Van Roey, 2001; Szkudlinski et al., 2002).

### **1.6.1 Leucine-rich repeats**

The large ECD of GpHRs, such as the FSHR, consist of a nine LRRs and belong to the LRR-containing GPCR (LGR) subgroup (Jiang et al., 2014a; Smits et al., 2003) (Figure 1.5). Distinct to other non-LGR members with short ECDs that can only bind small molecules, LGR members can bind much larger ligands with high binding affinity (Braun et al., 1991; Schmidt et al., 2001). Modelling of GpHR LRR, using the template crystal structure of porcine ribonuclease inhibitor (Kobe & Deisenhofer, 1993), revealed that

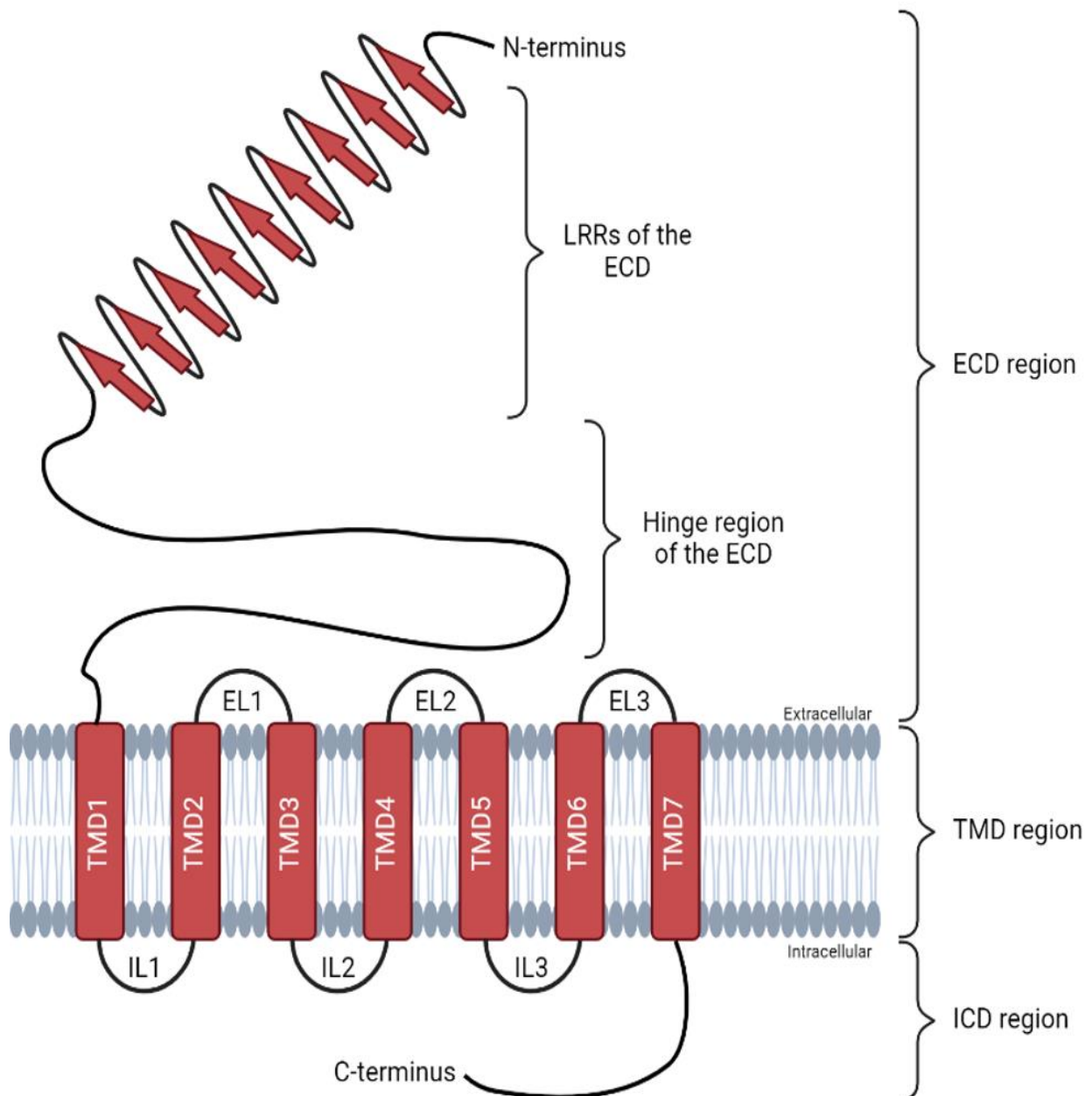


**Figure 1.5: The glycoprotein hormone receptor.** Simplified 2D schematic diagram of a GpHR. The N-terminus extracellular domain (ECD) region is uniquely large and consists of nine LRRs (red arrows), the hinge region, and three extracellular loops (ECL1-3). The ECLs link the transmembrane domain (TMD) region, consisting of seven membrane-spanning  $\alpha$ -helices (TMD1-7), with three intracellular loops (ICL1-3) and the C-terminus within the intracellular domain (ICD) region (Jiang et al., 2014a; Smits et al., 2003). *Figure created using BioRender.com.*

LRRs consist of concave  $\beta$ -strands followed by convex  $\alpha$ -helices forming a ‘horseshoe-like’ surface (Bhowmick et al., 1996; Jiang et al., 1995; Kajava et al., 1995).

The importance for LRR in ligand-binding and specificity within GpHRs was demonstrated using site-directed mutagenesis. When two amino acid residues in the LRR region within the FSHR, and eight amino acid residues in the LRR region within the TSHR, were substituted into residues from the corresponding region within the LH/CGR, a gain-of-sensitivity function was induced (Smits et al., 2003). Both mutant FSHRs and TSHRs displayed similar affinity and sensitivity to hCG as the wild type (wt) LH/CGR. Interestingly, mutated TSHRs displayed dual sensitivity to hCG and TSH hormones, and when twelve further residues were mutated, it displayed complete insensitivity to TSH (Smits et al., 2003). Furthermore, the C-terminal ends of the  $\beta$ -strands of the LRRs form an acid groove in the LH/CGR and has also been proposed to be important for hormone recognition specificity (Smits et al., 2003). Intriguingly, both FSHR and TSHR mutants, which displayed specificity to hCG, showed a comparable charge distribution within similar regions of their LRR, and it was proposed that the non-mutated residues in the wtFSHR served to prevent random recognition by hCG (Smits et al., 2003). Nevertheless, the LRR is not the only region in the ECD of GpHRs that has been proposed to contribute to hormone specificity and recognition.

### 1.6.2 Hinge region

The hinge region is another distinct, yet important, structural component of GpHRs that is unique to GpHRs, like the FSHR, as it is not found in other GPCRs. It forms part of the ECD of GpHRs and links the LRR domain to the TMD (Figure 1.5). For many years it was

unclear if the hinge region was characterised by a specific structure or whether it was a structure that was formed following ligand binding and/or signal activation (Mueller et al., 2010). This was predominantly because crystal structures of GpHRs depicted the N-terminal region of the ECD containing the LRR and not the C-terminal region where the hinge region is located (Fan & Hendrickson, 2005; Sanders et al., 2007). However, a few years later, the crystal structure of the entire ECD of the FSHR (including the hinge region) was reported (Jiang et al., 2012). Here it was described as an integral part of the ECD, and not a distinct structural unit (Jiang et al., 2012). Most information about the GpHR hinge region is based on *in vitro* and *in vivo* studies related to the TSHR, with the length and location of the hinge region widely debated. Many different groups have proposed the TSHR hinge region incorporates residues between Leu260-arginine (Arg)418 (Mueller et al., 2010). For FSHR, the hinge region has been reported to incorporate Lys260-Arg366 (Agrawal & Dighe, 2009), whereas the LH/CGR hinge region remains to be determined.

The hinge region still remains the most variable region within the primary structure of the GpHRs, with no identified conserved domain when their sequences were searched using BLAST algorithm (Altschul et al., 1997). Despite this, there has been proposed roles for the relevance of the GpHR hinge region for ligand binding and specificity. Early studies revealed naturally occurring pathogenic activation mutations in the TSHR hinge region resulted in a constitutively active receptor (Duprez et al., 1997; Grüters et al., 1998; Kopp et al., 1997). Alternatively, inactivating pathogenic mutations, arising from a missense mutation at a highly conserved cysteine residue (Cys390Trp) resulted in a loss of affinity and potency of TSH at the mutant TSHR when compared to wtTSHR (Biebermann et al., 1997). Another naturally occurring mutation in a similar region within the LH/CGR (Cys343Ser) was identified in a male patient with Leydig cell hypoplasia, which resulted

in a loss of hormone binding and subsequent signalling (Martens et al., 2002), suggesting that the undetermined LH/CGR hinge region may lie in this region. For FSHR, naturally occurring mutations of residues close to the hinge region (Asp567Asn and Thr449Ile/Ala) led to the loss of FSH selectivity, and instead, activation by CG and TSH (Montanelli et al., 2004). Nevertheless, in later studies where TSHR chimeras were generated by replacing the hinge region of the TSHR for the hinge region of the LH/CGR and FSHR, there was a strong loss of specific <sup>125</sup>I-bovine TSH binding to the TSHR chimeras (Jaeschke et al., 2011), highlighting the role the hinge region plays in GpHR hormone recognition. Additionally, the hinge region contains the tyrosine-aspartic acid/glutamic acid-tyrosine (Y-D/E-Y) motif that is conserved across GpHRs (Costagliola et al., 2002). It is suggested that post-translational sulphonation of the first tyrosine residues at Tyr385 is required for high-affinity TSH binding to the TSHR and LH binding to LH/CGR, whereas sulphonation of the second tyrosine residue at Tyr387 is important for FSH sensitivity to the FSHR (Costagliola et al., 2002), suggesting that structural differences in the hinge region of GpHRs play a key role in hormone recognition at the receptor (Bonomi et al., 2006).

In contrast, it has been proposed that the hinge region may play a more insignificant role in FSH binding within the FSHR (Agrawal & Dighe, 2009). When the entire amino acid (aa) residues within the hinge region (aa296-331) or any 10 amino acids within this region were deleted in FSHR-expressing cells, there was no effect on FSH binding to the FSHR, but instead there was loss on FSHR cAMP activation. This suggests FSHR hinge region plays a crucial role in FSHR signal transduction instead. Furthermore, a mutant FSHR lacking the LRR region failed to bind FSH, suggesting that FSH binding is more associated with the LRR region instead of the hinge region (Agrawal & Dighe, 2009).



### 1.6.3 Glycoprotein hormone receptor activation

In addition to the distinct LRR and hinge region, GpHRs activation mechanisms largely differ from other rhodopsin-like Class A GPCRs, with ligand binding predominantly occurring within the large ECD as opposed to the TMD (Cornelis et al., 2001; Remy et al., 2001; Schmidt et al., 2001). Nevertheless, most differences observed in the aa sequence between the GpHRs are located within the hinge region (Vassart et al., 2004), suggesting potentially different mechanisms of ligand binding and activation between GpHRs. Despite this, progression in understanding the mechanism of GpHR activation was slow because of the lack of structural information on the entire ECD incorporating the LRR region and the hinge region (Fan & Hendrickson, 2005).

Years later, breakthrough research depicting the crystal structure of FSH in complex with the entire ECD of the FSHR suggested FSHR interacts with FSH in a two-step manner (Jiang et al., 2012). First, by FSH recruitment to the concave site of the LRR domain in the FSHR in a hand-clasp manner, and second, by FSHR recognition of FSH from the sulphonation of a tyrosine residue (sTyr) located in the FSHR hinge region (Tyr335) (Jiang et al., 2012), further supporting previous reports (Costagliola et al., 2002). The study showed that FSH binding reshaped the FSHR ECD to form a sTyr-binding pocket that inserted into an FSH nascent pocket, thus forming hydrogen bonds between FSH and the FSHR, and ultimately leading to receptor activation (Jiang et al., 2012). By applying the new structural insights of the FSH-FSHR activation mechanisms to the homologous TSHR, a structural model of TSH in complex with the entire ECD of the TSHR was also generated to determine its activation mechanism (Krause et al., 2012). Like the FSH/FSHR complex, TSH interacted with the TSHR in a two-step manner; first, at the concave site in the LRR region of the TSHR, and second, at the corresponding sTyr385 within the hinge region of

the TSHR via a pocket in TSH. However, unlike the FSH-FSHR complex, the interaction between TSH and TSHR was described as a lever-like mechanism that displaced the hinge region by interacting with N-terminal residues (Glu297 and Cys301) and C-terminal residues (Cys390, Asp386 and sTyr385) within the hinge region (Krause et al., 2012). Furthermore, TSH interaction with the negatively charged Asp386 was previously shown to play a key role in hormone binding (Mueller et al., 2011). Additionally, other residues in the C-terminus of the hinge region were predicted to be involved in TSHR intramolecular signal transduction, such as Glu394 and Asp395 (Krause et al., 2012). Altogether, this triggered conformational changes in the TSHR ECD, thus activating an intramolecular agonist unit close to the TMD to induce receptor activation (Krause et al., 2012).

Although LH interaction with the entire ECD of the LH/CGR has not been modelled, it is likely that the mechanism of activation would be like the other GpH-GpHR complexes, such that the hormone binding first would occur in the LRR region of the LH/CGR, and then with residues within the hinge region. Moreover, key conserved residues that have been reported in both the FSHR and TSHR have also been reported in the LH/CGR, such as sTyr331 in the C-terminal hinge region in the LH/CGR (Bruysters et al., 2008; Krause et al., 2012), with important implications in hormone recognition (Costagliola et al., 2002). Additionally, similar to Asp386 found in the FSHR C-terminal hinge region, Asp330 has been found in the similar C-terminal region of the LH/CGR and was reported to be important for hormone-dependent receptor activation (Bruysters et al., 2008). Similar to the TSH-TSHR complex (Krause et al., 2012), the implications of the crystal structure of ECD of the FSHR in complex with FSH may provide new insights into LH-LH/CGR activation mechanisms (Jiang et al., 2012), as it has undoubtedly developed further understanding of the FSHR.

## 1.7 Follicle-stimulating hormone receptor

The diverse actions of FSH are facilitated through interactions with the FSHR, and so both play essential roles in female reproduction, such as regulation of folliculogenesis, dominant follicle selection, ovulation, and steroid hormone synthesis (Messinis et al., 2014). Furthermore, inactivating human mutations in the *FSHR* gene has resulted in ovarian dysgenesis with amenorrhea and infertility in females (Tao & Segaloff, 2009). Additionally, the important role of FSHR has been demonstrated in *FSHR* and *FSH $\beta$*  knock-out (KO) studies in female mice. They displayed sterility and were presented with small uteri, impaired follicular maturation and no preovulatory mature follicles or corpora lutea (Abel et al., 2000; Dierich et al., 1998; Kumar et al., 1997).

### 1.7.1 *FSHR* regulation

The human *FSHR* gene is located on chromosome 2 and consists of 10 exons. Exon 1-9 code for the ECD consisting of the LRR, while exon 10 codes for the TMD and C-terminal intracellular tail (Gromoll et al., 1996; Hermann & Heckert, 2007). Four FSHR isoforms (FSHR1-4) have also been identified, arising from differential exon splicing patterns (Sairam & Babu, 2007; Simoni et al., 2002). Furthermore, variable splicing in exons 8-10 resulted in FSHR isoforms expression in monocytes and osteoclasts (Robinson et al., 2010). Nevertheless, there is currently little understanding on their physiological relevance (Bhartiya & Patel, 2021).

Transcriptional regulation of *FSHR* is regulated in the upstream promoter region. When upstream of the first rat *FSHR* transcription start site was fused to firefly luciferase reporter gene, evidence from sequentially shorter promoter regions revealed a -100base pair (bp)

region within the promoter region was required to maintain transcriptional activity (Heckert et al., 1998). Mutations within the upstream -100bp region identified an important 14bp that included the E-box regulatory element as the main source of promoter activity. Additionally, the E-box element has been shown to bind transcription factors within the helix-loop-helix family, such as the upstream stimulatory factor 1 (Usf1) and Usf2, and play significant roles in *FSHR* transcription (Heckert et al., 1998; Heckert et al., 2000; Xing & Sairam, 2001).

It's unclear the precise mechanisms that regulate *FSHR* expression in GCs, however, primarily there is autoregulatory activity from FSH during the early stages of the ovarian cycle from feedback mechanisms from the HPO axis (see section 1.2 and 1.3). Earlier studies have identified other hormones responsible for the regulation of *FSHR* transcription and receptor expression in the ovaries, including activin and indirectly through follistatin (Nakamura et al., 1993; Sites et al., 1994; Tano et al., 1995). There has also been growing evidence that the oocyte-derived bone morphogenetic protein 15 (BMP15) and growth differentiation factor 9 (GDF9), that belong to the TGF- $\beta$  family, may play crucial roles in *FSHR* expression (Shimizu et al., 2019), as they have been previously shown to regulate follicle development (Juengel & McNatty, 2005; Persani et al., 2014). Furthermore, BMPs canonically signal via the Smad signalling pathway, with BMP15 activating Smad 1/5/8 signalling associated with epigenetic regulation of genes (Moore et al., 2003), and may play a role in the epigenetic regulation of *FSHR* expression. BMPs have also been shown to signal via the pro-apoptotic p38/mitogen-activated protein kinase (MAPK) pathway (Nöth et al., 2003; Shimizu et al., 2019), a pathway associated with Usf1 phosphorylation (Shimizu et al., 2019), and likely the upregulation of *FSHR* (Shimizu et al., 2019).

### 1.7.2 Post-translation modification of FSHR and outward trafficking

Mature human FSHR consists of 678 aa and has a molecular weight of approximately 75 kDa, and must undergo glycosylation and palmitoylation post-translational modifications in the ER and Golgi to become fully functional and trafficked to plasma membrane (Ulloa-Aguirre, Zariñán, et al., 2018). There are four possible Asn-linked glycosylation sites that have been reported on the FSHR at positions Asn174, Asn182, Asn276 and Asn301 (Davis et al., 1995; Dias et al., 2002). Western blot analysis revealed Asn174 and Asn276 were glycosylated, with glycosylation at either position sufficient for FSHR trafficking to the plasma membrane with normal binding affinity for FSH (Davis et al., 1995). A decade later, when the first crystal structure of the ECD of human FSHR was determined, structural evidence for the glycosylation at Asn174 was revealed (Fan & Hendrickson, 2005). Although Davis *et al.*, identified Asn182 as a potential glycosylation site, Fan & Hendrickson observed no carbohydrate attached to the residue (Davis et al., 1995; Fan & Hendrickson, 2005). However, glycosylated proteins have been especially difficult to study structurally because of their diverse nature, and so in x-ray crystallography these glycans are usually removed to overcome these challenges (Lee et al., 2015). Although the physiological role for these glycosylation sites is still not completely clear, it is believed that they may play a role in receptor stability and accurate protein folding, since naturally occurring mutations near these sites have resulted in inactivation of the FSHR (Simoni et al., 1997).

The FSHR also undergoes S-acylation with cysteine residues, a type of palmitoylation whereby palmitic acid is required to promote FSHR association with lipid membranes and is important for FSHR trafficking (Melo-Nava et al., 2016; Ulloa-Aguirre et al., 2013). Even though palmitoylation occurs at conserved Cys629 and Cys655, located at the C-tail

of the receptor, mutation at position Cys629 was required for the FSHR to be fully trafficked to the plasma membrane (Uribe et al., 2008).

In addition to post-translation modification, newly synthesised FSHR must be correctly folded and processed in the ER and Golgi to be trafficked to the plasma membrane. A naturally occurring inactivation mutation in the primary structure of FSHR (Ala189Val), which affected receptor folding and caused hypergonadotrophic ovarian failure (Aittomäki et al., 1995), was shown to remain intracellularly sequestered in cells expressing the mutant FSHR (Rannikko et al., 2002). Moreover, site-directed mutagenesis of the human and rat FSHR, via substitution of aa residues (9-30) with alanine which also affected FSHR folding, impaired FSHR trafficking to the plasma membrane and compromised FSH binding capability (Nechamen & Dias, 2000), indicating the significance of accurate FSHR processing in the ER and Golgi. Calnexin, calreticulin, and protein-disulphide isomerase (PDI) are chaperone proteins that play a key role in mediating accurate FSHR folding and are associated with immature forms of the GpHRs (Mizrachi & Segaloff, 2004; Rozell et al., 1998). Two loss-of-function mutations in the Hlh/CGR (Ala593Pro and Ser616Tyr), that caused intracellular retention, revealed different patterns in the chaperone proteins' association with mutant LH/CGR when compared to wtLH/CGR-chaperone protein complex (Mizrachi & Segaloff, 2004). Additionally, pharmacological chaperones have been shown to rescue intracellularly retained mutated LH/CGRs by presumably stabilising the misfolded mutant receptor (Newton et al., 2021), suggesting an important role for them in the trafficking and functioning of other GpHRs, like the FSHR.

Besides chaperone proteins, the C-tail and the ICL3 of FSHR both contain the reversed BBXXB motif (BXXBB) that has been shown to be important for receptor trafficking in other GPCRs (Timossi et al., 2004). When all three basic residues in the ICL3 were mutated to alanine, the mutant FSHR was unable to bind FSH and become activated. Interestingly, the BXXBB motif in the C-tail appeared to be more important for FSHR membrane trafficking, since individual substitutions within the motif resulted in diminished receptor expression at the plasma membrane (Timossi et al., 2004). Furthermore, the last two residues of the BXXBB motif (Arg617 and Arg618) and the preceding residue (Phe616) form the amino terminal of the highly conserved F(x)6LL motif, a motif that is important for GPCR transport from the ER to the plasma membrane (Duvernay et al., 2004; Zariñán et al., 2010), and together may all play crucial roles in FSHR trafficking and localisation at the cell surface.

### 1.7.3 FSHR localisation

In females, the FSHR is primarily expressed in GCs of follicles within the ovaries and can be detected as early as the primary stages of follicular development (Candelaria et al., 2020; Hardy et al., 2017). FSH acts via the FSHR to regulate the expression of aromatase, which is important for testosterone conversion to oestrogen, and preparing the endometrium for receptivity (Messinis et al., 2014). Nevertheless, recent literature has proposed extragonadal expression of the FSHR with distinct signal pathway activation and discrete non-gonadal physiological roles.

FSHR expression has been reported in placental vascular endothelium and human umbilical vein endothelium, with a proposed role in foetal vessel angiogenesis (Stilley et al., 2014;

Stilley & Segaloff, 2018), and was also reported in many different types of endometriotic lesion with expression at both mRNA and protein levels (Ponikwicka-Tyszko et al., 2016). However, opposing results were observed in a later study which questioned the methodology used to interrogate FSHR expression in the earlier study (Stelmaszewska et al., 2016). Furthermore, the requirement of FSHR expression for normal placental vasculature and foetal angiogenesis is contradictory, since both male and females with inactivating FSHR mutations appear to develop normally *in utero* (Tapanainen et al., 1998)

FSHR expression has also been documented in chicken adipose tissue, with a proposed role in lipid biosynthesis (Cui et al., 2012). Moreover, when a polyclonal antibody targeting FSH $\beta$  was injected into both wt- and high fat diet-induced obese mice, there was a reduction in adipose tissue and an increase in thermogenesis (Liu et al., 2017). Interestingly, the actions of FSH in regulating fat in adipocytes may be mediated via FSHR coupling to an alternative G protein (the G $\alpha_i$ ), other than its canonical G protein (G $\alpha_s$ ), and instead activating Ca<sup>2+</sup>/cAMP response-element binding protein (CREB) signalling (Liu et al., 2015).

A few studies have proposed that menopausal-related elevation in FSH is linked to bone loss, with neither FSH $\beta$ - nor FSHR-null mice inducing bone loss (Sun et al., 2006), and increases in bone mass when monoclonal FSH $\beta$  antibodies blocked the actions of FSH (Ji et al., 2018; Liu et al., 2017). Furthermore, similar to FSHR expression in adipose tissue (Liu et al., 2015), FSHR expression in osteoclasts may mediate the actions of FSH through alternative signalling pathways, such as via MEK/(extracellular-regulated kinases) ERK, NF- $\kappa$ B, and Akt signalling (Sun et al., 2006). Yet, contradictory findings were observed in



studies in female mice with pituitary-independent transgenic expression of FSH, which revealed dose-dependent increases in bone mass, with elevated tibial and vertebral trabecular bone volume (Allan et al., 2010).

Additionally, numerous studies have proposed roles for extragonadal FSHR expression within the kidneys, prostate, breasts, thyroids and brain (Chrusciel et al., 2019), with a key role in the development of Alzheimer's disease (Xiong et al., 2022). However, the idea of FSHR extragonadal expression has remained widely controversial. Most techniques utilised nested PCR to reduce non-specific amplification of DNA transcripts, which ultimately resulted in relatively low FSHR expression levels. Moreover, most immunohistochemical (IHC) studies have reported diverse findings, which was probably a result of the specificity of the antibodies used, and should have been tested on *FSHR* null mouse tissues to thoroughly validate their specificity (Kumar, 2018; Moeker et al., 2017). Nevertheless, the majority of literature has focused on FSHR localisation, structure, and function within an ovarian physiological context because of the important role the ovary plays in female reproduction and fertility. Therefore, understanding how the FSHR functions via signalling within ovaries is important in order to begin to delineate ways in which it can be regulated.

## **1.8 Follicle-stimulating hormone receptor signalling pathways**

When endogenous FSH binds and activates FSHR in the ovaries, it initiates a conformational change in the TMD. This results in a complex and diverse cascade of intracellular signalling events, that are hypothesised to mediate many different physiological responses to regulate female fertility (Messinis et al., 2014). FSHR signalling

primarily occurs via the  $G\alpha_s$ /cAMP/PKA signalling pathway, to regulate steroidogenesis (Figure 1.6). Nevertheless, the FSHR can associate with other proteins, such as  $\beta$ -arrestin and other membrane-bound receptors like the LH/CGR and the G protein-coupled oestrogen receptor 1 (GPER) (discussed further in section 1.11.3). In turn, this regulates several other signalling pathways involving many kinases, such as PKA, PKC, phosphatidylinositol 3-kinase (PI3K), PKB/Akt and ERK1/2 (Figure 1.6). The different signalling networks can be fine-tuned and regulated to promote multiple physiological effects, including GC proliferation, dominant follicle selection, and ultimately, ovulation (Casarini & Crépieux, 2019; Ulloa-Aguirre, Reiter, et al., 2018).

### 1.8.1 $G\alpha_s$ /adenylyl cyclase signalling

The canonical signalling pathway of FSHR is the  $G\alpha_s$ /cAMP/PKA (Figure 1.4, (a)). Following FSHR activation, the intrinsic GEF activity of FSHR mediates the conversion of inactive  $G\alpha_s$ -GDP to active  $G\alpha_s$ -GTP, which phosphorylates the effector protein, adenylyl cyclase (AC), and converts intracellular ATP to cAMP. PKA is a heterotetrameric protein that consists of two regulatory subunits and two catalytic subunits. cAMP activates the regulatory units of PKA, which causes activation of the PKA catalytic subunits. In turn, the activated catalytic subunits phosphorylate and activate CREB. Phosphorylated CREB translocates to the nucleus and regulates cAMP response-element (cre)-dependent genes, including the *CYP19* gene for aromatase expression (Chan & Tan, 1987; Wu et al., 1998).

FSH-dependent cAMP has multiple effects in GCs. The exchange protein activated by cAMP (EPAC) is expressed in immature rat GCs. It regulates diverse biological functions through the activation of GTPases, including Rap1 activity that activates MAPK signalling

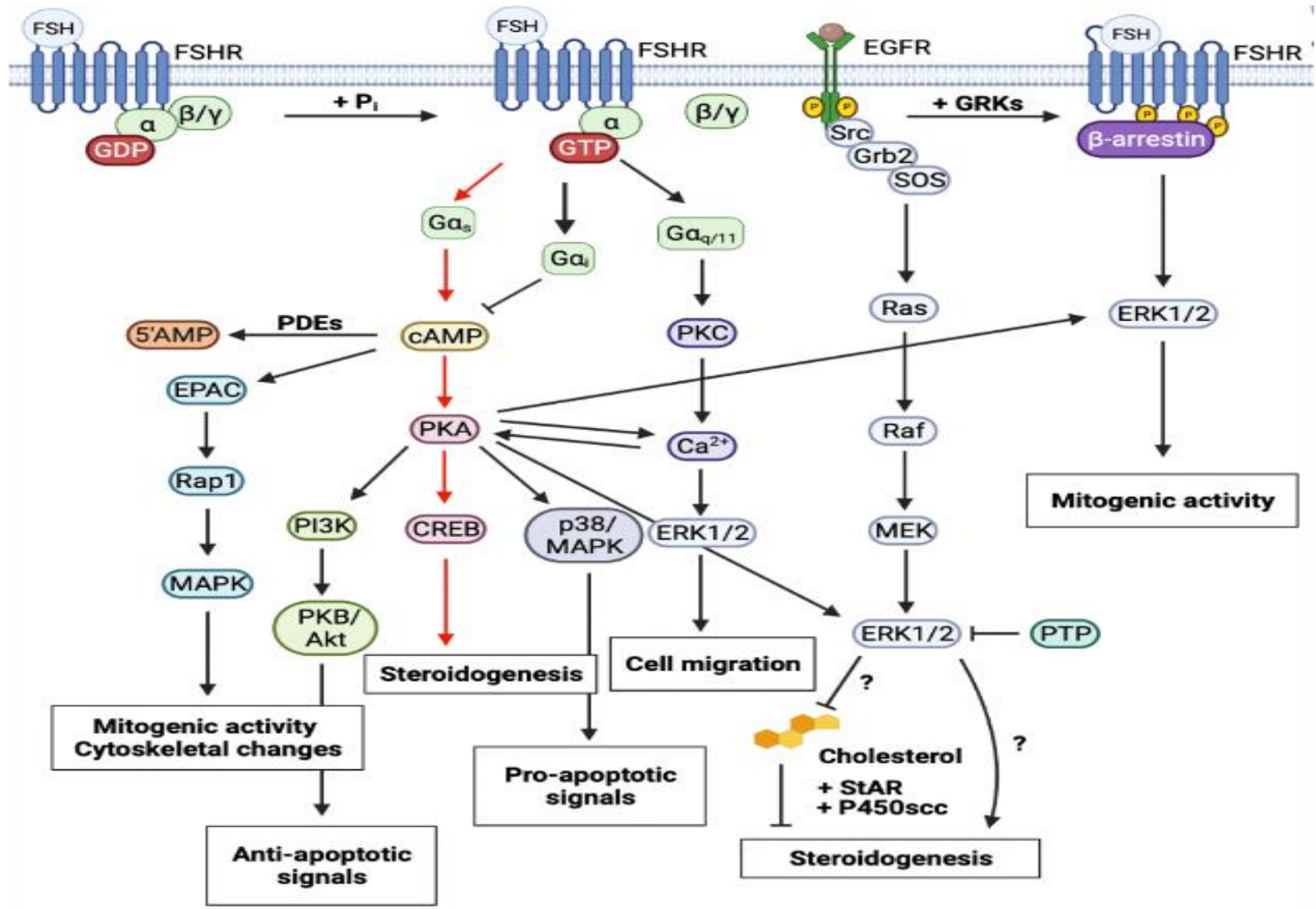


**Figure 1.6: Follicle-stimulating hormone receptor signalling.** Simplified schematic diagram of FSHR signalling. The primary signalling pathway of the FSHR is  $G\alpha_s$ /cAMP/PKA to induce steroidogenesis in granulosa cells (red arrows). PKA signalling branches out to mediate multiple signalling pathways, including ERK1/2 signal pathway crosstalk. ERK signalling induces multiple effects in granulosa cells, with different reports suggesting that it can induce and/or inhibit StAR-dependent steroidogenesis (Casarini & Crépieux, 2019). *Figure created using BioRender.com.*

1

to induce mitogenic activity and cytoskeletal changes (Schmidt et al., 2013; Wayne et al., 2007) (Figure 1.6). Furthermore, FSH-dependent cAMP upregulates steroidogenic acute regulatory protein (StAR) and cytochrome P450 cholesterol side chain cleavage (P450scc), that play key roles in the regulation of steroid hormone biosynthesis via cholesterol transfer in rat ovarian cells (Silverman et al., 1999; Stocco, 2000). Additionally, A-kinase anchoring protein (AKAP) mediates the spatial and temporal compartmentalisation of FSH-dependent cAMP, by targeting the subcellular distribution of PKA isoform type 2 (Carr et al., 1993). With phosphodiesterase (PDE) negatively controlling the level of intracellular cAMP (Conti et al., 1984), FSH-dependent cAMP signalling regulates many further downstream signal proteins, in particular PKA.

### 1.8.2 PKA signalling crosstalk

Multiple signal pathway activation branches out from PKA activity (Figure 1.6). One of the most important signal pathway crosstalk indirectly mediated by PKA is the phosphorylation of ERK-MAPK. PKA has been demonstrated to indirectly mediate ERK1/2 phosphorylation via both  $G\alpha_s$  and  $G\alpha_i$ , with roles in promoting Sertoli cells proliferation (Crépieux et al., 2001). However, in GCs, crosstalk with the epidermal growth factor receptor (EGFR) activates Raf/MEK/ERK signalling via disrupting phosphotyrosine phosphatase (PTP) inhibition to mediate GC proliferation (Cottom et al., 2003). Furthermore, there has also been a proposed role for phosphorylated-ERK1/2 in cAMP-dependent (Casarini et al., 2014) and -independent (Manna et al., 2006) steroidogenesis. However, controversial studies suggest that the ERK signalling cascade inhibits steroidogenesis by regulating the level of StAR expression (Amsterdam et al., 2002).

Signal pathway crosstalk between PKA and PKC has also been reported in isolated rat Sertoli cells by the actions of FSH (Gorczyńska et al., 1994). In the  $G\alpha_{q11}$  signalling pathway, the actions of PLC $\beta$  induce PKC activation and  $Ca^{2+}$  mobilisation and further ERK1/2 signalling to mitogenic activity. Inhibition of AC resulted in greater than 90% reduction in cytosolic  $Ca^{2+}$ , but was elevated when cAMP was supplemented, indicating the profound role of important signal pathway crosstalk (Gorczyńska et al., 1994). Cytosolic increases in  $Ca^{2+}$  was also reported in GCs when cells were treated with ovine FSH (Flores et al., 1990), and found to be partially dependent on PKA (Flores et al., 1992), with later studies confirming that both PKA and  $Ca^{2+}$  signalling work in concert with each other to mediate directional cell migration (Howe, 2011). Moreover, it has also been observed that translocated catalytic subunit of PKA to nuclear-enriched fractions, plays a role in mediating FSH mitogenic activity and GC differentiation by initiating histone H3 phosphorylation and chromatin remodelling, to induce gene activation (DeManno et al., 1999; Salvador et al., 2001)

### 1.8.3 Anti- and pro-apoptotic signalling

Activation of FSH-dependent cAMP/PKA signal pathway in GCs activates PKA-dependent anti-apoptotic signals through interactions with PI3K/PKB/Akt signalling to mediate cell survival, growth, and differentiation (Hunzicker-Dunn et al., 2012; Li et al., 2011) (Figure 1.6). Simultaneously, FSH-dependent cAMP/PKA signalling also activates pro-apoptotic signals via p38/MAPK pathway (Figure 1.6) and suggested to be the result of increases in FSHR density at the plasma membrane (Casarini et al., 2016a). Activation of either pathway is possibly dependent on the potency and the persistence of intracellular Camp (Casarini & Crépeux, 2019). In Hg15 cells permanently expressing the LH/CGR, reports have shown that LH is a key target of Akt signalling (Casarini et al., 2012), with

signalling further enhanced in the presence of FSH (Casarini et al., 2016b), and probably mediated by FSHR heterodimerisation with the LH/CGR (discussed further in section 1.11.3). This suggests that the activation of both FSH-dependent anti- and pro-apoptotic pathways may occur in pre-ovulatory follicles to facilitate dominant follicle selection by preventing follicle atresia and promoting follicle survival (Casarini & Crépieux, 2019).

### **1.9 Pharmacological modulators of FSHR signalling**

Besides the actions of FSH, there have been multiple small molecule non-peptide modulators that have been identified and shown to further amplify/diminish endogenous FSH signalling with promising therapeutic advantages. For example, current ART protocols involve the use of multiple injectables of FSH to mediate folliculogenesis and can result in low patient compliance (Anderson et al., 2018), therefore the ability to target the FSHR through oral administration is beneficial. Furthermore, recent identification of FSHR expression in extragonadal tissue have suggested an age-related role for menopausal elevated FSH and a link to ovarian cancer (Song et al., 2020), bone loss (Zhu et al., 2012), increased adiposity (Liu et al., 2015), and Alzheimer's disease (Xiong et al., 2022). Hence, the discovery and development of FSHR modulators that could diminish FSH activity would also be beneficial.

High-throughput screening techniques have been utilised to identify several small molecular allosteric modulators of the FSHR, with the use of molecular docking experiments to identify potential FSHR binding sites (Aathi et al., 2022; Anderson et al., 2018; Janovick et al., 2009). These modulators have been categorised according to their ability to alter FSHR-dependent cAMP activity.

### 1.9.1 FSHR agonists

Although many FSHR agonists have been identified (Anderson et al., 2018), it is the thiazolidinones (TZDs) that have been of recent interest because of the flexibility and versatility of their core structure, proving to be promising for future compound development (Maclean et al., 2004; Verma & Saraf, 2008). As a result, they possess three potential R groups that can be modified to produce multiple compounds with different pharmacological properties (Arey et al., 2008; Yanofsky et al., 2006).

The first reported TZDs were identified from a combinatorial library of a large collection of chemical compounds following treatment in CHO cells expressing recombinant human FSHR and a cre-luciferase reporter gene (Wrobel et al., 2006). A similar study was later conducted whereby the lead compounds, Compound 1 (C1) and C2, were shown to activate FSHR cre-luciferase reporter gene in CHO cells but exhibited low potency (Yanofsky et al., 2006). C3-C5 were further derived from parallel synthesis and shown to have higher potency and full *in vitro* efficacy than C1, but lower potency than human FSH (Yanofsky et al., 2006). Experiments using FSHR and TSHR chimeras revealed that C6 and C7, and potentially C3-C5, were bound within the TMD, independent of the FSH binding site within the N-terminus (Yanofsky et al., 2006). Furthermore, of all the small modulators, C5 was shown to be the most potent at stimulating cre-luciferase activity. It was also able to induce steroid synthesis in rat GCs with full efficacy but lower potency when compared to human FSH (Yanofsky et al., 2006). Furthermore, it was effective at increasing the binding of increasing concentrations of radiolabelled <sup>125</sup>I-FSH to the FSHR by 3-fold, with increased FSHR  $\beta$ -arrestin recruitment (Jiang et al., 2014b).



### 1.9.2 FSHR antagonists

The first reported nonpeptide FSHR antagonist was the diazonaphthylsulfonic (C1) that was shown to bind to the ECD of the FSHR and inhibit FSH-dependent cAMP production and steroid synthesis *in vitro* (Arey et al., 2002). Although high doses of C1 was shown to prevent ovulation in mature rats, the low efficacy rendered the nonpeptide unsuitable as a contraceptive (Arey et al., 2002). Modification in the core TZD ring altered its pharmacological properties and produced compounds behaving as inhibitors that activated  $G\alpha_i$  and inhibited oestradiol production, such as C3 and partially with C2 (Arey et al., 2008). A later study identified ADX61623, a small molecule inhibitor of the FSHR, that was able to significantly increase the binding affinity of  $^{125}\text{I}$ -FSH to the FSHR whilst inhibiting cAMP production and progesterone in rat GCs (Dias et al., 2011). However, the inhibitor demonstrated biased antagonism at the FSHR as it failed to reduce oestrogen production *in vitro* and was not completely effective at blocking FSH-dependent follicle maturation *in vivo*. A follow-up study was later done that aimed to identify an effective inhibitor capable of blocking cAMP production, progesterone, and oestrogen (Dias et al., 2014). Even though all signal pathways were inhibited when the new FSHR inhibitor (ADX68692) was administered *in vitro*, and there was a reduced number of oocytes recovered from female rats *in vivo*, oestrogen production was still not blocked (Dias et al., 2014).

An alternative strategy to inhibit FSHR activity is the development of blocking antibodies of FSH $\beta$ . A polyclonal antibody complimenting a 13 amino acid peptide sequence within the receptor binding domain of FSH $\beta$  was able to block FSH-dependent osteoclast formation *in vitro*, inhibited bone resorption and stimulated bone formation when injected into ovariectomised mice (Ji et al., 2018; Zhu et al., 2012). The FSH $\beta$  antibody was found

to inhibit human FSH-FSHR binding when based on FSH-FSHR crystal structure and reduced adiposity when injected into wild-type mice on a high-fat diet (Liu et al., 2017). Moreover, the first humanised FSH $\beta$  blocking antibody inhibited FSH action *in vitro* and provides the bases for further preclinical and clinical testing (Gera et al., 2020).

While there is promising therapeutic potential with FSHR allosteric modulators, these molecules possess many drawbacks. Such include toxicity, poor solubility, difficulties in chemical synthesis and low *in vivo* bioactivity (Sriraman et al., 2014), and so they are currently not commercially available. Although peptides derived from natural sequences are less controversial, they are often more susceptible to proteolytic cleavage, meaning they have a short circularity half-life, and are currently not orally active. Even though there has been some recent progress in determining the structural facets of the binding sites of small FSHR modulators (Aathi et al., 2022), advancements in identifying modulators with enhanced bioactivity and resistance to proteolytic degradation remains slow and requires further research.

### **1.10 FSHR inward trafficking**

Prolonged activation of FSHR signalling, or high concentrations of FSH exposure can be deleterious to GCs and can result in follicle atresia (Kanaya et al., 2012). To sustain normal cell physiology, there are tightly regulated conserved mechanisms to transiently desensitise FSHR signalling through the process of receptor trafficking. Previously, it was dogmatic that the role for endocytic trafficking of GPCRs was to terminate receptor signalling initiated at the plasma membrane following ligand binding. However, growing evidence from the last decade have shown that GPCR trafficking is highly integrated within the

signalling network to organise and direct receptor signalling to endosomal microdomains (Pavlos & Friedman, 2017).

Following activation of the FSHR, serine/threonine residues within the ICL2, ICL3 and the C-terminal tail are phosphorylated. Classically this is mediated by GRKs (Bhaskaran et al., 2003; Troispoux et al., 1999) (Figure 1.7), but it has also been reported to be mediated by PKA and PKC (Ulloa-Aguirre et al., 2013). There are several GRKs that can phosphorylate the FSHR which display distinct intracellular functions. GRK2 has been shown to be important for FSHR internalisation and recycling (Lazari et al., 1999; Marion et al., 2006), whereas GRK5 and GRK6 have been shown to play a role in the recruitment of the versatile adaptor protein,  $\beta$ -arrestin, from the cytoplasm (Kim et al., 2005).  $\beta$ -arrestin also plays important roles in regulating intracellular signalling, such as receptor silencing, trafficking, and signalling via several pathways like the primary MAPK signalling pathway (Krishnamurthy et al., 2003; McDonald et al., 2000; Reiter & Lefkowitz, 2006; Terrillon & Bouvier, 2004; Ulloa-Aguirre et al., 2013), which occurs later than G protein-dependent ERK signalling (Kara et al., 2006; Sayers & Hanyaloglu, 2018). Studies on other GPCRs have shown  $\beta$ -arrestin mediates GPCRs clustering and internalisation via the formation of clathrin-coated pits (CCPs) (Hanyaloglu, 2018) (Figure 1.7).  $\beta$ -arrestin can bind both GPCR and the adaptor protein 2 (AP2) associated with clathrin to form CCPs and mediate GPCR internalisation. The GTPase, dynamin, then behaves as molecular scissors to

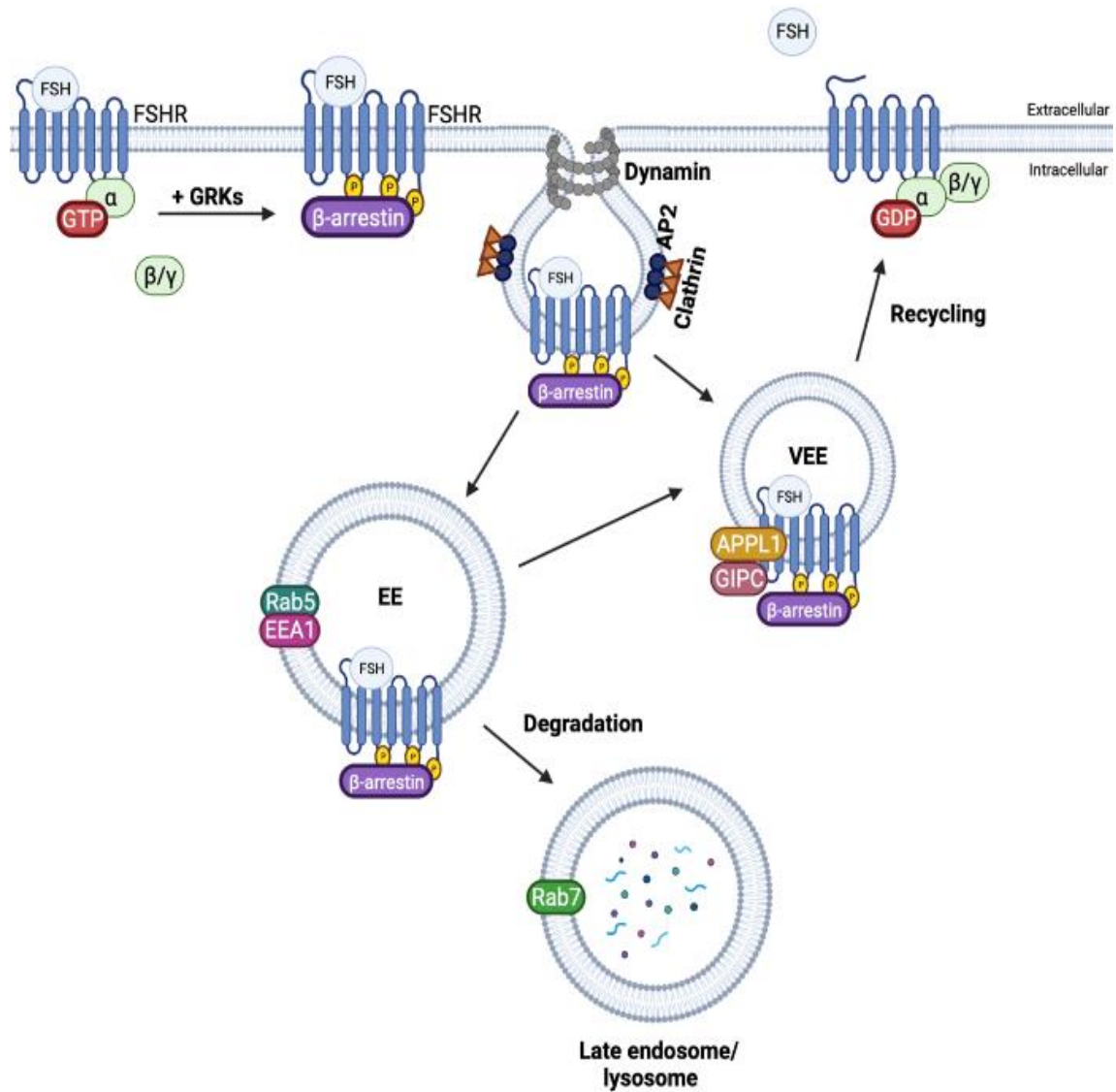


**Figure 1.7: Follicle-stimulating hormone receptor trafficking.** Simplified schematic diagram of FSHR internalisation and trafficking pathways. The intracellular domain of the activated FSHR is phosphorylated by G protein receptor kinases (GRKs) to mediate β-arrestin recruitment. FSHR-β-arrestin signalling complex is internalised into clathrin-coated pits attached to anchor protein 2 (AP2) via the GTPase, dynamin. Internalised FSHR can be routed to APPL1-positive very early endosomes (VEEs) for receptor recycling or Rab5/EEA1-positive EEs for lysosomal degradation or potential recycling (Hanyaloglu, 2018; Sayers & Hanyaloglu, 2018). *Figure created using BioRender.com.*

‘scissor-off’ the plasma membrane to form the GPCR-endosome complex (Hanyaloglu, 2018) (Figure 1.7).

Previously, it was assumed that following receptor internalisation, GPCRs, such as the FSHR, were trafficked to the early endosome (EE), that are Ras-related protein 5 (Rab5)/early endosome antigen 1 (EEA1)-positive and targeted for lysosomal degradation. Thereafter, receptors could either be recycled or routed to late endosomes that are Rab7-positive. Receptors within late endosomes form vesicles within the lumen of the EEs to form multivesicular bodies (MVBs) that fuse with lysosomes and leads to receptor degradation (Figure 1.7). However, confocal microscopy imaging of LH/CGR trafficking in live HEK293 cells revealed that the GpHRs can be routed to smaller Rab5/EEA1-negative endosomal compartments, the so called ‘very early endosomes (VEEs)’, when compared to the prototypical  $\beta_2$ AR (Jean-Alphonse et al., 2014).

Although the role of VEEs was unclear, it was shown to play an important role in LH/CGR recycling to the plasma membrane via interactions with the post synaptic density protein (PDZ) binding protein, G $\alpha$  interacting protein (GAIP)-interacting protein C-terminus (GIPC), that interacts with the PDZ binding sequence within the C-tail of most GPCRs (Hirakawa et al., 2003; Jean-Alphonse et al., 2014). Furthermore, a subpopulation of VEEs contains the adaptor protein, phosphotyrosine interacting with PH domain and leucine zipper 1 (APPL1). APPL1 plays a central role for LH/CGR recycling because knockdown of APPL1 in HEK293 cells showed an increase in the percentage of internalised LH/CGR (Sposini et al., 2017). Although FSHR is also routed to VEEs (Jean-Alphonse et al., 2014), studies have proposed that both rat and human FSHR does not recycle back to the plasma

membrane via PDZ binding proteins. Instead, it has been suggested that palmitoylation of at least three cysteine residues in the C-tail of the FSHR is required for receptor recycling to the plasma membrane (Melo-Nava et al., 2016). However, this has remained controversial as other studies have shown that the FSHR may indirectly associate with GIPC via APPL1 interactions to mediate receptor recycling (Nechamen et al., 2004; Nechamen et al., 2007; Sayers & Hanyaloglu, 2018; Thomas et al., 2011).

These intracellular endosomal compartments have been shown to represent additional signalling platforms in GPCR signalling (Pavlos & Friedman, 2017). GIPC knockdown in cells expressing the LH/CGR reduced receptor recycling to the plasma membrane and mediated changes from sustained ERK1/2 signalling to transient signalling (Jean-Alphonse et al., 2014), whereas GIPC knockdown in cells expressing the FSHR displayed reduced FSH-induced ERK signalling (Jean-Alphonse et al., 2014). Furthermore, a ‘second wave’ of sustained cAMP signalling has been observed in GPCRs routed to endosomes (Calebiro et al., 2009; Ferrandon et al., 2009; Irannejad et al., 2013; Lyga et al., 2016), that is distinct from transient cAMP signalling observed from GPCRs localised to the plasma membrane (Sposini et al., 2020).

Nevertheless, how FSH and its various glycoforms, and how small FSHR pharmacological modulators mediate the different complexities of FSHR signalling and additional signalling platforms mediated by FSHR internalisation and trafficking is still unclear. However, there must be a mechanism by which they can fine-tune FSHR signal selectivity, specificity, and amplitude.

## 1.11 Follicle-stimulating hormone receptor oligomers

One important mechanism that has been shown to fine-tune GPCR signalling is the ability for GPCRs to form dimers and oligomers by associating with themselves or with other membrane-bound receptors to form homomers or heteromers, respectively (Milligan et al., 2019; Sleno & Hébert, 2018). For Class C GPCRs, the role of dimerisation is imperative, with most receptor subtypes functioning as obligate heterodimers or homodimers, (Pin et al., 2005). Furthermore, for the prototypical Class A rhodopsin receptor there is a proposed role for dimerisation in preventing retinal degradation (Kumar et al., 2018; Zhang et al., 2016). Indeed, the FSHR has been shown to self-associate, however, the functional role of FSHR oligomers and its physiological relevance in reproductive health and disease is still widely debated.

### 1.11.1 Evidence for FSHR oligomers

Various biochemical and biophysical techniques have shown the existence of FSHR homomers (Bonomi & Persani, 2013). Co-immunoprecipitation (co-IP) of epitope-tagged FSHR C-terminal with either myc or FLAG showed FSHR initially form homodimers in the ER prior to post-translational modification, with potential FSHR oligomers at the cell surface (Thomas et al., 2007). In later studies, crystal structures of the FSHR ECD revealed that FSHR formed asymmetric trimers (Jiang et al., 2014b; Jiang et al., 2012). Live imaging of HEK293 co-expressing chimeric forms of FSHR fused to LH/CGR C-terminal and yellow fluorescent protein (YFP) (FSHR-LHRcT-YFP) and mCherry (FSHR-LHRcT-mCherry) revealed increases in fluorescence resonance energy transfer (FRET) efficiencies (Mazurkiewicz et al., 2015). Additionally, fluorescence correlation spectroscopy coupled with photon-counting histogram analysis concluded FSHR chimera proteins form homodimers that freely diffuse in the plasma membrane (Mazurkiewicz et al., 2015).

### 1.11.2 Structural interfaces of FSHR oligomers

Fan and Hendrickson's x-ray crystallography of the FSH in complex of the binding domain of FSHR (FSHR<sub>HB</sub>) revealed three-stranded  $\beta$ -sheets located on LRRs 2–4 on the outer surface of FSHR<sub>HB</sub> constituted of the dimer interfaces, with hydrophobic interactions with the conserved residue Tyr110, suggesting that similar dimer interfaces formed in homologous receptors (Fan & Hendrickson, 2005). However, when the conserved tyrosine residue was mutated to alanine (Tyr110Ala) or a glycan wedge was introduced within the region in human FSHR, there was no changes in FSHR dimerisation (Guan et al., 2010). As a result, it was proposed that the TMD and the ECD of the FSHR both contributed to the dimerisation of the full length of the FSHR but not the Tyr110 residue (Guan et al., 2010). Other reports have shown for other GPCRs, such as the dopamine D2 receptor, chemokine receptor (CCR5) and the  $\alpha$ 1B-adrenoreceptor, that TMD1 and TMD4 constitute to the dimer interface (Guo et al., 2005; Hernanz-Falcón et al., 2004; Lopez-Gimenez et al., 2007). However, when residues in TMD1 and TMD4 were mutated in the full length FSHR, dimerisation was not adversely affected, suggesting that TMD1 and TMD4 were not responsible for human FSHR dimerisation (Guan et al., 2010).

Several x-ray-resolved crystal structures for other Class A GPCRs have revealed common conserved dimer interfaces involve TMD1, TMD2 and helix 8 (Baltoumas et al., 2016; Huang et al., 2013; Zhao et al., 2019). The use of synthetic peptides to disrupt these dimers by creating aa sequences identical to the interacting TMD has helped understand the functional role for GPCR di/oligomers (Getter et al., 2019; Yang et al., 2020). However, the lack of tangible structural evidence of FSHR dimer interfaces with high resolution have made the development of disruption peptides slow. Knockout and deletion studies of the FSHR may offer some insight, but the technique does not preserve a functional single



protomer to allow investigation of the role between the interacting protomer and other protomers within the complex, and so the field overall requires further investigation.

### 1.11.3 Physiological role for FSHR oligomers

Other GpHRs exist as homo- and hetero-dimers with their functional relevance being delineated. Given the homology between the different GpHRs, it suggests physiological relevance for the existence of FSHR homomers. For LH/CGR, *in vivo* roles and roles in regulating signal strength have been suggested. The wild-type phenotype of mutant transgenic mice co-expressing binding and signal deficient LH/CGRs was rescued via mutant LH/CGR intermolecular cooperation, restoring LH/CGR function (Rivero-Müller et al., 2010). Using the modified super-resolution imaging technique, photoactivatable dye-photoactivatable localisation microscopy (PD-PALM), that was designed to visualise single molecules beyond the diffraction limit of conventional florescent-imaging techniques microscopes under high resolution (<10nm), Jonas *et al.*, was able to investigate how LH/CGR dimerisation impacted receptor function (Jonas et al., 2015). They demonstrated how altering functionally asymmetric LH/CGR protomer ratio within an oligomeric complex altered LH/CGR  $G\alpha_{q/11}$  signalling, whereby oligomerisation was sufficient for hCG-dependent  $G\alpha_{q/11}$  signalling but not for LH-dependent  $G\alpha_{q/11}$  signalling, suggesting that LH/CGR homomers may serve to fine-tune receptor signalling (Jonas et al., 2015). Although the physiological relevance for FSHR di/oligomers are not clear, the FSHR has also previously been shown to function via intermolecular cooperation. Like the previous study, mutant FSHRs that were defective in hormone binding were transactivated by signal defective hybrid FSHR (Ji et al., 2004). The FSHR ECD attached to a either glycosyl phosphatidylinositol (GPI) anchor sequence (ExoGPI) or cytoplasmic domain of CD8 of an immune receptor (ExoCD) was signal deficient and able to rescue cAMP

production when co-expressed with FSHR hormone binding FSHR mutants (Ji et al., 2004). Additionally, biased signalling has been observed from transactivation of gonadotrophin hormone receptors whereby cAMP signalling or IP signalling was generated, but not both, suggesting a functional role for FSHR homomers (Jeoung et al., 2007).

Nevertheless, the role for FSHR heteromers is clearer. In GCs the FSHR and LH/CGR are co-expressed during the mid-follicular phase of the ovarian cycle to mediate dominant follicle selection, maturation, and ovulation. Bioluminescence RET (BRET) and FRET studies have shown that FSHR and LH/CGR heterodimerise with each other when co-expressed in HEK293 cells (Feng et al., 2013; Mazurkiewicz et al., 2015). The effect of heterodimerisation between these two receptors revealed the reduction of LH/hCG- and FSH-dependent  $G\alpha_s$  signalling (Feng et al., 2013), which may mediate dominant follicle selection. Moreover, unliganded co-expressed FSHR with the LH/CGR has been shown to enhance LH/CGR-dependent  $G\alpha_{q/11}$  signalling (Jonas et al., 2018). This is important for cell proliferation and may mediate ovulation, suggesting the potential role of FSHR di/oligomerisation in regulating the multifaceted functions. Additionally, ovarian cells express both FSHR, and GPER (Wang et al., 2007), and it has been postulated that human ovarian follicle survival and dominant follicle selection is dependent on their heterodimerisation by reprogramming FSHR density-dependent pro-apoptotic death signals into anti-apoptotic signal (Casarini et al., 2020). Low FSHR membrane density is observed in the GC during early folliculogenesis and promotes anti-apoptotic proliferative FSHR-dependent signalling (Tranchant et al., 2011). Increases in FSHR density during late folliculogenesis may result in a switch to pro-apoptotic signals (Casarini et al., 2016a), but the follicle is thought to be rescued by interactions with the GPER by inhibiting cAMP/PKA signalling (Casarini et al., 2020). FSHR heteromers may also play a pivotal

role in stimulating cumulus GC differentiation via the activation of anti-apoptotic PI3K-Akt pathway. Interestingly, insulin-like growth factor 1 receptor (IGF1R) transactivation is required for FSH-dependent Akt phosphorylation (Baumgarten et al., 2014), therefore, it is no surprise that FSH and IGF-1 have also been shown to activate this pathway synergically (Hu et al., 2004; Sun et al., 2003). Nevertheless, how these FSHR dimers/oligomers formation are regulated, and their physiological role is yet to be determined.

### **1.12 Hypothesis, aims and objectives**

FSH and the FSHR are essential for reproduction and key targets in IVF protocols, therefore, understanding what modulates their function is essential for identifying alternative therapeutic treatment regimens. The FSHR displays pleiotropic signalling that mediates multiple cellular responses. How FSH glycoforms and small molecule FSHR pharmacological modulators can mediate differential FSHR signalling pathway activation remains unknown. FSHR oligomerisation and FSHR inward trafficking present a tangible means to propagate such differential regulation. Therefore, the overall aim of this thesis was to determine how different FSH glycoforms and pharmacological FSHR modulators regulate FSHR oligomerisation, downstream signalling, and trafficking. The hypothesis is that FSH glycosylation and small molecular FSHR modulators differentially impact FSHR oligomerisation, downstream signalling, and trafficking.

To address the aim, the overall objectives of this thesis were to:

1. Investigate how FSH glycoforms modulate FSHR oligomerisation and cAMP-dependent signalling.

2. Determine the effect of FSH glycoforms on FSHR trafficking.
3. Investigate the effect of a small molecule allosteric modulator on FSHR oligomerisation and signalling.
4. Screen and identify small molecular FSHR inhibitors and determine the effect on FSHR oligomerisation and signalling.

## 2 **Chapter Two: Materials and Methods**

## **2.1 Overview**

This thesis aimed to investigate the effect of different FSH glycoforms and pharmacological FSHR modulators on FSHR oligomerisation, downstream signalling, and trafficking. Therefore, to examine single FSHR molecule composition, the downstream signalling pathways arising from the FSHR molecules, and gene regulation, a range of techniques were employed. These techniques are discussed in further detail within this chapter.

A GC-derived cell line, such as the steroidogenic human ovarian tumour granulosa (KGN) cell line, would be an ideal model to investigate FSHR modulation due to the endogenous expression of FSHR. However, because GPCR antibodies are notoriously non-specific (Kumar, 2018; Moeker et al., 2017), a small epitope tag approach was used to identify N-terminal haemagglutinin (HA)-tagged FSHR (HA-FSHR). This enabled single FSHR molecules to be examined using PDs labelled to HA antibodies. Therefore, all experiments were conducted using HEK293 cells, that is a human immortalised cell line, transiently expressing HA-FSHR. This human expression cell line is widely used to study recombinant proteins because of its easy maintenance, rapid growth, and propensity for transfection. Furthermore, it expresses all the cellular proteins that were investigated in this thesis (Soto-Velasquez et al., 2018), and therefore an ideal model for the investigations within this thesis.

## **2.2 Chemicals and reagents**

HEK293 cells were obtained from American Type Culture Collection (ATCC). Purified FSH21/18, FSH24, equine FSH (eFSH), truncated eLH $\beta$  ( $\Delta$ 121-149) combined with

asparagine56-deglycosylated eLH $\alpha$  (dg-eLHt) and Compound 5 (C5) were kindly donated by Professor George Bousfield (Wichita State University, Kansas). Pituitary FSH was supplied by the National Hormone & Peptide Program (California, USA). 84 small molecule FSHR inhibitors compounds were gifted by Atomwise (Budapest, Hungary). HA-FSHR plasmid DNA was generated as previously described (Cottet et al., 2010; Jonas et al., 2018).

Dulbecco's Modified Eagle's Media (DMEM), fetal bovine serum (FBS), sodium bicarbonate, dimethyl sulfoxide (DMSO), gelatine from bovine skin, hydroxylamin hydrochloride, Dulbeccos's phosphate-buffered saline (PBS), Abberior<sup>®</sup> CAGE 552 NHS ester photoactivatable fluorophore dye, 25% (v/v) glutaraldehyde, 10X radioimmunoprecipitation assay (RIPA) lysis and extraction buffer, cOmplete<sup>™</sup> EDTA-free protease inhibitor cocktail, Bradford reagent, bovine serum albumin (BSA), skimmed milk powder, sodium dodecyl sulphate (SDS), 2-mercaptoethanol, horseradish peroxidase (HRP) substrate; Luminata Forte, Trizma<sup>®</sup>-base, tetramethylethylenediamine (TEMED), methanol and 4',6-diamidino-2-phenylindole (DAPI) were supplied by Sigma (Darmstadt, Germany).

Antibiotic-Antimycotic, Lipofectamine 2000<sup>™</sup>, low serum medium Opti-MEM<sup>™</sup>, 0.5% (v/v) Trypsin-EDTA and CO<sub>2</sub>-independent media, 8-chamber wells 1.5 borosilicate cover glass slides, 16% (w/v) formaldehyde, Carl Zeiss<sup>™</sup> Immersol<sup>™</sup> Immersion Oil 518 F, Halt<sup>™</sup> phosphatase inhibitor cocktail, NuPAGE<sup>™</sup> MOPS SDS running buffer, Novex NuPAGE<sup>™</sup> transfer buffer, Bolt<sup>™</sup> sample reducing agent, polyvinylidene fluoride (PVDF) transfer membrane, UltraPure<sup>™</sup> 0.5M EDTA pH 8.0, LDS sample buffer, UltraPure<sup>™</sup>

Tris, Sea Blue Plus 2 protein marker and small interfering ribonucleic acid (siRNA) APPL1 were supplied by Thermo Fisher Scientific (Dartford, England).

Plasmid DNA encoding GloSensor<sup>TM</sup>-20F, plasmid DNA encoding cre-luciferase reporter gene, plasmid DNA encoding *Renilla*-luciferase reporter gene, GloSensor<sup>TM</sup> cAMP reagent stock, and Dual-luciferase reporter gene assay kit (including 5X passive lysis buffer (PLB)) were purchased from Promega (Southampton, England). Sephadex G-25 Medium columns were supplied by GE Healthcare (Buckinghamshire, England). White 96-well advanced TC microplates with flat µclear<sup>®</sup> bottom were purchased from Greiner Bio-One (Stonehouse, England). Protease and phosphatase inhibitor cocktail, and Dyngo<sup>®</sup>-4a were purchased from Abcam (Cambridge, England). 30% (w/v) Protogel<sup>®</sup> was purchased from Geneflow (Lichfield, England). Tween<sup>®</sup> 20 was purchased from MP Biomedicals (Cambridge, England).



## 2.3 Cell culture

### 2.3.1 Cell counting and plating

HEK293 cells were cultured in T75 tissue culture (TC)-treated flasks in DMEM, supplemented with 10% (v/v) FBS and 1% (v/v) Antibiotic-Antimycotic (DMEM<sup>+/+</sup>). Cells were maintained and cultured at 37°C in 5% CO<sub>2</sub> in air and passaged twice weekly in sterile conditions using a class II laminar flow cabinet.

To improve cell attachment to TC plates, wells were coated in 0.1% (v/v) gelatine in sterile PBS from a 2% (w/v) stock solution made up in distilled H<sub>2</sub>O (see Appendix IA for volumes). Plates were incubated for 15 minutes at 37°C to allow the gelatine solution to completely liquefy, and then the gelatine was aspirated and discarded. Plates were dried to help cells adhere by re-incubating for a further 30 minutes - 24 hours, at 37°C before they were used for plating cells.

Once cells reached 90% confluency, they were counted using a haemocytometer, and plated in DMEM<sup>+/+</sup> into either 6-well TC plates <math>6.0 \times 10^5</math> cells/well (2mls per well), or 10cm TC dishes at  $3.5 \times 10^6$  cells/well (15mls per dish), depending on assay requirements. Cells were cultured overnight to achieve 70-80% confluency required for effective transient transfection the following day.

### 2.3.2 Transient transfection

All transient transfections were carried out using Lipofectamine 2000<sup>TM</sup> and low serum medium Opti-MEM<sup>TM</sup>. Mixtures were made up in two separate tubes containing equal

volumes of Opti-MEM™. To the first tube, Lipofectamine 2000™ was added and to the second tube, plasmid DNA(s) was added (see Appendix IB for quantities). Tubes were left to incubate for 5 minutes at room temperature (RT). Following this, the contents of both tubes were combined and gently mixed, and incubated for a further 20 minutes at RT, to ensure Lipofectamine 2000™ complexed with the plasmid DNA(s). Once the incubation was completed, the entire Lipofectamine 2000™-DNA complex was added to cells in a drop-wise fashion, gently swirled and incubated for a further 48-72 hours at 37°C before beginning any functional analysis.

### 2.3.3 Re-plating cells

Transcriptional/translational processing of GPCRs, and trafficking to the cell surface, takes 48-72 hours (Li et al., 2021). However, because the doubling time of HEK293 cells are ~36 hours, a two-stage plating process was used to ensure optimal cell confluency was reached prior to treatment and to prevent cell over-confluency. Therefore, 24 hours post-transfection, cells were re-plated into gelatine-coated wells (except for cells plated in 8-chamber wells for PD-PALM experiments which were plated onto gelatine-free cover glass slides). As different experimental procedures required different well sizes and plates (e.g., chamber slides, 6-well TC plates, 96-well TC plates, etc), this has been specified in the relevant sections within this chapter.

## 2.4 Photoactivatable dye localisation microscopy

Although there are various biochemical, biophysical, and imaging techniques that have been developed to investigate GPCR oligomerisation, such as Co-IP, Western blot, FRET/BRET, time-resolved FRET (TR-FRET), total interference reflection fluorescence microscopy (TIRF-M), and spatial intensity distribution analysis (SpIDA), these techniques either provide no spatial/temporal information on GPCR dimers oligomers and/or low resolution (Guo et al., 2017). Therefore, to investigate single FSHR molecules at the cell-surface, a super-resolution imaging technique (PD-PALM.) using TIRF-M was employed. The unique ability for stochastic photoactivation and bleaching of photoactivatable dyes allow for this technique to afford high spatial resolution of GPCR molecules beyond the light diffraction limit of standard microscopy (<10nm) (Jonas et al., 2016).

### 2.4.1 PD labelling of HA.11 antibody

Since GPCR antibodies are notoriously non-specific (Kumar, 2018; Moeker et al., 2017), a small epitope tag approach was used to identify HA-FSHR by labelling PDs directly to HA antibodies to employ PD-PALM. Furthermore, previous studies in HEK293 cells using this approach showed no effect on hormone signal activation (Jonas et al., 2016).

Monoclonal HA.11 antibody was utilised and labelled with an amino reactive NHS-ester CAGE™ 552 PD. Using Abberior's recommended labelling protocol, the PD was prepared by reconstituting in DMSO to achieve a final concentration of 10mg/ml. A previous study typically found that a 5-10 fold molar excess of dye:antibody yields a 1:1 stoichiometry (Jonas et al., 2015). To achieve a 5-fold molar excess of dye:antibody, 100µl of 1M aqueous sodium bicarbonate (pH 8.4) and 1.84µl of reconstituted CAGE 552 PD was added to 900µl

of the HA.11 antibody and magnetically stirred in the dark at RT for 2 hours. To quench the reaction, 20 $\mu$ l of 1.5M hydroxylamin (pH 8.4) was added. To resolve the CAGE 552 PD bound HA.11 population (HA.11-CAGE<sup>TM</sup> 552), the solution was filtered using gel filtration chromatography. First, Sephadex G-25 medium columns were equilibrated with 30mls of buffered PBS (pH 6.5). Next, the HA.11-CAGE<sup>TM</sup> 552 solution was loaded onto the column and eluted using PBS, with 200 $\mu$ l fractions collected in 1.5ml microfuge tubes.

The stoichiometry of dye:antibody was measured by spectrophotometric analysis, using the degree of labelling (DOL) calculation based on a derivation of the Beer-Lambert law (Equation 1). Using a spectrophotometer, the maximum absorbance ( $A_{max}$ ) for the full spectra and at absorbance at 280nm ( $A_{280}$ ) were measured for each fraction collected. This also enabled the determination of where the antibody eluted. From this the DOL for each fraction was calculated. For all PD-PALM experiments described, the HA.11-CAGE<sup>TM</sup> 552 antibody had a DOL calculated as 1.2256776.

**Equation 1: Degree of labelling of CAGE<sup>TM</sup> 552 dye to HA.11 antibody.** Calculated using a derivation of the Beer-Lambert law.  $A_{max}$  = absorbance of the dye at maximum absorbance;  $A_{280}$  = absorbance of the dye at 280nm;  $\epsilon_{max}$  is the extinction coefficient of the dye at the absorbance maximum;  $\epsilon_{280}$  is the extinction coefficient of the dye at 280nm;  $\epsilon_{Prot}$  is the extinction coefficient of the antibody at 280nm;  $A_{Prot}$  is the absorbance of the antibody at 280nm;  $C_{280}$  is the correction factor of the dye given by  $C_{280} = \epsilon_{280} / \epsilon_{max}$ .

$$DOL = \frac{A_{max} / \epsilon_{max}}{A_{Prot} / \epsilon_{Prot}} = \frac{A_{max} \cdot \epsilon_{Prot}}{(A_{280} - A_{max} \cdot C_{280}) \cdot \epsilon_{max}}$$

#### 2.4.2 Cell stimulation for PD-PALM

PD-PALM utilises TIRF-M to obtain high-contrast images of fluorophores near the plasma membrane. For optimal TIRF-M, cells must be distinct and in a monolayer. To achieve this, cells transiently expressing HA-FSHR were replated at a density  $3.5 \times 10^4$  cells per 400 $\mu$ l of DMEM<sup>+/+</sup> into each 8-chamber wells 1.5 borosilicate cover glass slides. Cells were incubated overnight at 37°C ready for treatment the following day.

Previous experience in extensively testing blocking agents found that diluting labelled antibody in DMEM<sup>+/+</sup> prevented non-specific binding of the HA.11 antibody (Jonas et al., 2016). Re-plated cells were incubated with 200 $\mu$ l of a 1.78nM concentration of HA.11-CAGE<sup>TM</sup> 552 antibody in DMEM<sup>+/+</sup> for 30 minutes at 37°C (see Appendix 1C for antibody dilutions). Cells were light-protected to minimise uncaging of fluorophores, with subsequent steps hereon performed in light-protected conditions. HA.11-CAGE<sup>TM</sup> 552 antibody was carefully removed from individual chamber wells and discarded, and cells stimulated with ligands for 0-, 2-, 5- and 15-minute time points (see specific result chapters for details). At the end of the time course, media was removed and discarded, and cells carefully washed in 250 $\mu$ l/well with sterile PBS. PBS was removed, and cells were fixed for 30 minutes at RT in 250 $\mu$ l/well with 4% (w/v) PFA containing 0.2% (v/v) glutaraldehyde. This combination of fixatives was used as the addition of glutaraldehyde has been shown to prevent lateral diffusion of transmembrane proteins when compared to fixation with PFA alone (Annibale et al., 2011a; Tanaka et al., 2010). At the end of fixation, the fixative was aspirated from cells and discarded, and cells washed twice in 250 $\mu$ l/well with sterile PBS and stored in a further fresh 250 $\mu$ l/well PBS at 4°C in a light-controlled box until imaged. Labelled cells were typically imaged within 72 hours post-labelling.

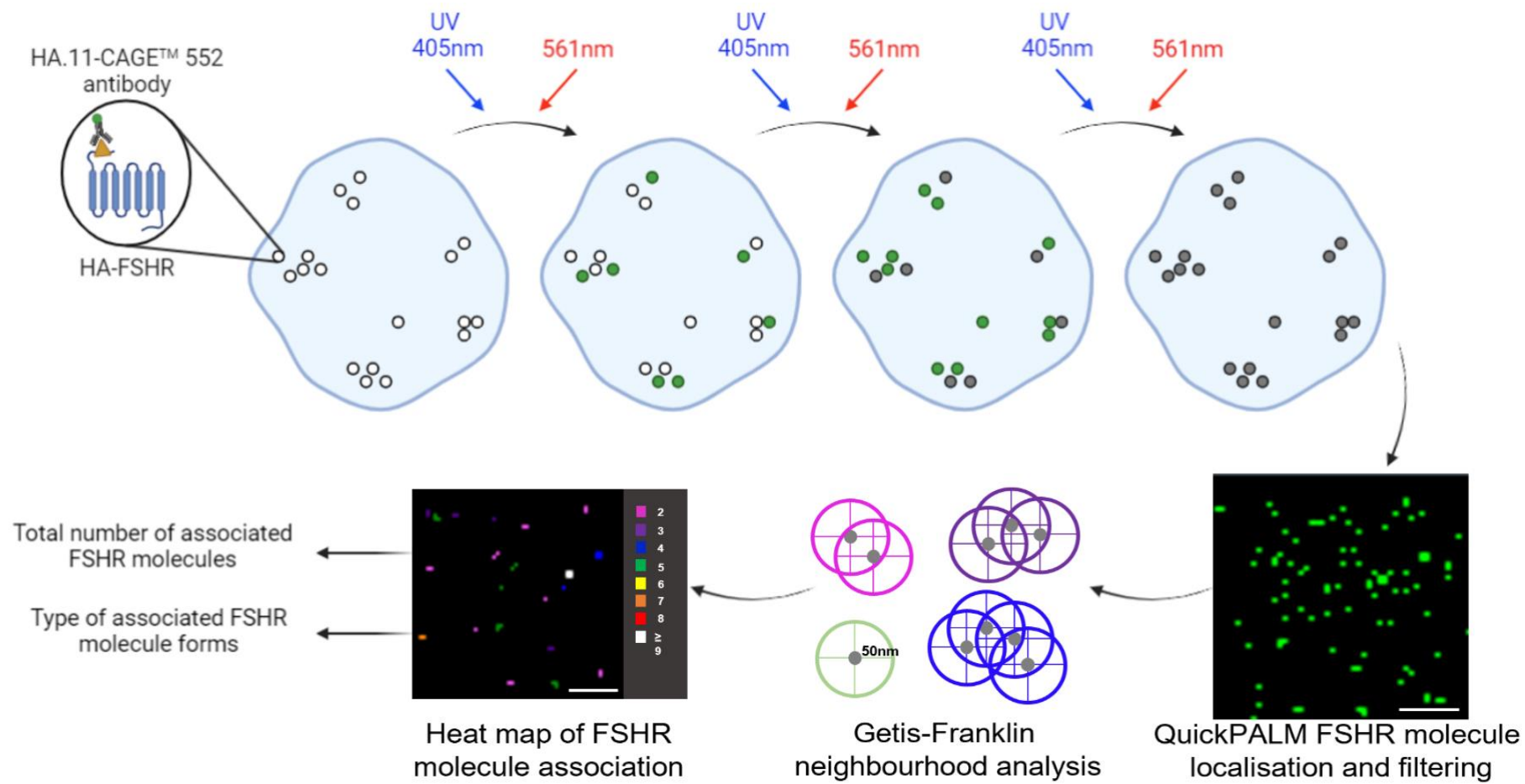
### 2.4.3 Imaging FSHR molecules via PD-PALM

The Zeiss Elyra PS.1 super resolution microscope was utilised to image the cell surface landscape of FSHR. This microscope can map single molecules of labelled proteins expressed at physiological levels (200 molecules/ $\mu\text{m}^2$ ) to a localisation precision of  $\sim 20\text{nm}$ , breaking the diffraction barrier of conventional light microscopes that have a resolution of  $\sim 200\text{nm}$ . The microscope has two cameras that allows simultaneous two-channel imaging, however, for the purpose of this thesis, only one channel was used. A cooled electron multiplying charged-coupled device camera (EM-CCD; C9100-13, Hamamatsu) was used to image cells. The microscope was equipped with 100x objective lens with a 1.45 numerical aperture (NA), resulting in better resolution and a perfect focus setup, to prevent Z-plane drift. In addition, it has multiple laser lines (405nm, 488nm, 561nm, and 642nm) depending on the fluorophore used.

For set up, lasers were typically switched on 30 minutes prior to imaging to ensure they were heated up and stabilised to ensure stability of imaging. This additionally facilitated the cooling of the EM-CCD camera to  $-70^\circ\text{C}$ . The Zeiss Elyra PS.1 was enclosed in a dark box to prevent spontaneous uncaging of PDs and to aid the regulation of the internal surrounding temperature to  $\sim 25^\circ\text{C}$ . This also helped optimise stability of imaging as excess heat generated by the lasers would have caused this to fluctuate. The microscopy was also mounted on an anti-vibration table to minimize sample drift and vibrations during imaging. These features collectively conserved the stability and integrity of imaging and ensured accurate localisation precision of data.

Before commencing imaging, the 100x 1.45 NA objective lens was cleaned using 70% (v/v) ethanol in distilled H<sub>2</sub>O and allowed to fully evaporate before placing a drop of Carl Zeiss<sup>TM</sup> Immersol<sup>TM</sup> Immersion Oil 518 F with a refractive index on 1.518. The chamber slides containing the fixed cells in PBS were then placed onto the microscope stage. The brightfield setting was utilised to ensure a section of cells within the eye piece view were in the correct focal plane before switching over to fluorescence live mode via the locate tab on the ZEN software. Once switched over to fluorescent live mode, the brightness and contrast were adjusted to visualise the selected region of cells, whilst maintaining low laser power and without switching on the 405nm laser to minimise photoactivation. The fluorescence minimum/maximum were adjusted to observe the cells while omitting background brightness/noise and optimising signal/noise. To visualise cell surface FSHR, the TIRF angle and Z-plane were adjusted to ensure imaging at an optimal TIRF-angle. Briefly, the coverslip was used to ensure the plasma membrane was located. Thereafter, a balance between minor adjustments in Z-plane and the most acute TIRF angle was implemented to ensure the cell surface was observed and fluorophores were seen activating within the cell borders, with minimal background noise.

During imaging, the laser power used determined the number of fluorophores activated and hence the degree of spatial separation. Dark state CAGE<sup>TM</sup> 552 PD fluorophores were stochastically activated/uncaged by 405nm UV laser lines, then effectively detected and photobleached by 561nm laser lines through multiple cycles (Figure 2.1). Initially, laser powers were set low to prevent mass activation/uncaging of PDs, and gradually increased during imaging experiments to ensure all fluorophores were photoactivated and sufficiently photobleached (Figure 2.1). For image acquisition, the image speed was 8 frames/second. This was selected based on previous published optimisations (Jonas et al., 2015), as



● dark state CAGE™ 552 fluorophore   ● activated CAGE™ 552 fluorophore   ● photobleached CAGE™ 552 fluorophore



**Figure 2.1: Schematic flow diagram summarising the steps required to visualise FSHR association using PD-PALM.** HEK293 cell transiently expressing HA-FSHR were pre-incubated with HA.11 mouse primary antibody directly labelled to CAGE™ 552 fluorophore dye (1:250). Cells were treated, fixed in 0.2% glutaraldehyde in 4% PFA and imaged using the Zeiss Elyra PS.1 microscope. Dark state fluorophores were stochastically activated/uncaged using 405 UV laser lines, and photobleached using 561nm laser lines through multiple cycles until all fluorophores were uncaged/activated and photobleached. Individual FSHR molecules were resolved using QuickPALM and further filtered before being quantified using Getis-Franklin nearest neighbourhood analysis. A heat map of associated FSHR molecules was generated and quantified the total number of associated FSHR molecules and the type of associated FSHR molecule forms (Jonas et al., 2015). *Scale bars*, 500nm.

imaging too fast can result in the same activated fluorophore being detected over multiple frames and cause an overestimation of FSHR oligomers, whereas imaging too slow can result in missing activated fluorophores and an underestimation of FSHR oligomers. Time-lapsed images were typically imaged over 31,500 frames to resolve all CAGE552-HA.11 bound FSHR.

#### 2.4.4 Mapping FSHR molecules from PD-PALM

To localise individual FSHR molecules, the time lapse was analysed via a free ImageJ (Fiji) software plug in - QuickPALM. To do this, CZI files were first opened on ImageJ and the brightness and contrast adjusted to visualise the cells. Since there were minor adjustments made to the Z-plane and the TIRF angle at the beginning of imaging sequence, these were removed from analysis. Following this, non-overlapping  $5\mu\text{m}^2$  sections from within the ROI were analysed using QuickPALM. To refine the stringency of the single FSHR molecules detected, the following parameters were used during analysis: with a pixel size of 100nm, only fluorophores with a signal to noise ratio (SNR)  $\geq 8$  and a full-width, half-maximum (FWHM)  $\leq 3$  pixels were detected. The x-y coordinates of each individual FSHR were mapped onto a single excel spreadsheet at the end of the analysis. To prevent overestimation of FSHR oligomers, an algorithm was utilised to filter and remove molecules that persisted for  $>1$  frame across 15 consecutive frames. This JAVA-run program typically removed  $<1\%$  of molecules. The fluorophores filtered were based on a search radius within the localisation precision of  $\sim 20\text{nm}$ .

To quantify the number of FSHRs that existed as monomers, dimers, and oligomers, a bespoke JAVA-based program, PD-interpreter ([www.superimaging.org](http://www.superimaging.org)), was employed

which used a Getis-Franklin-based nearest neighbourhood analysis (Figure 2.1). This approach identified a single FSHR molecule and recursively searched within a given radius counting further molecules within the radius until no further molecules were located. The FSHR molecules were then grouped together and the type of oligomer, e.g., trimer, tetramer, etc., was quantified. For this analysis, a search radius of 50nm was used, based on the size of the receptor (~8nm), the size of the antibody-dye label (~20nm) and the localisation precision based on the point spread function (PSF) for the PDs (~20nm). Once the search radius was set, the analysis was run, and an output cluster file was generated. The data was represented as an image displaying individual FSHR molecules plotted based on their x-y coordinates. A heat map of FSHR homomers grouped into different oligomeric complexes was also created alongside a separate excel spreadsheet quantifying the total number of resolved FSHR homomers, and the number of each FSHR homomeric subtype, which mirrored the heat map (Figure 2.1). This data was then used to determine the number of non-associated FSHR molecules (monomers) and self-associated FSHR molecules (homomers), as well as the subtype of each FSHR homomeric complex (e.g., dimers, trimers, tetramers, pentamers, 6-8 oligomers or  $\geq 9$  oligomers).

#### 2.4.5 Selection process for FSHR density in PD-PALM

GPCR plasma membrane density can impact the number of associated receptors observed (Annibale et al., 2011b). Therefore, to minimise the effect of variation in transfection efficiencies between experiments on FSHR plasma membrane density, data analysis was conducted using data files consisting of 10-40 localised FSHR molecules/ $\mu\text{m}^2$ , as this was the physiological receptor density range previously reported for the FSHR (Mazurkiewicz et al., 2015) and other native GPCRs (Herrick-Davis et al., 2015).

## 2.5 GloSensor™ cAMP assay

The canonical FSHR signal pathway is via  $G\alpha_s$ /cAMP activation (Casarini & Crépieux, 2019). Real-time assays, such as enzyme-based kinetic assays, and endpoint assays, such as enzyme-linked immunosorbent assays (ELISAs) are the two main ways to detect changes in cAMP levels. For experiments reported in this thesis, a GloSensor™ luciferase-based biosensor was utilised to detect real-time accumulation of cAMP (Wang et al., 2022). The assay worked by transfecting cells with a genetically encoded biosensor variant with a cAMP binding domain fused to firefly (*Photinus pyralis*) luciferase. Following cell pre-incubation with a cAMP substrate, intracellular increases in cAMP induced fusion to the biosensor variant and a conformational change in the biosensor which promoted large increases in light output. This technique provided more information about the total amount of cAMP produced over time and information on the magnitude of cAMP production at specific time points than an endpoint assay could.

24 hours post-transfection,  $5.0 \times 10^4$  cells transiently co-expressing HA-FSHR and GloSensor™-20F were replated in 100µl of DMEM<sup>+/+</sup> into gelatine-coated white clear-bottomed 96-well TC plates and cultured overnight. 48 hours post-transfection, the media from the cells were aspirated and discarded and cells were pre-equilibrated in 90µl of equilibrium media, consisting of 88% (v/v) CO<sub>2</sub>-independent media supplemented with 10% (v/v) FBS and 2% (v/v) GloSensor™ cAMP reagent stock, for 2 hours at 37°C in a multi-mode plate reader (PHERAstar® FS, BMG Labtech).

Prior to cell treatment, basal cAMP activity was recorded for each individual well using the multi-mode plate reader, with the setting of 100 flashes/well, as per manufacturer's

instructions. A full reading cycle was 36 seconds, which was the time it took the software to read each individual well once. The basal readings were set to record the fluorescence accumulated in each well over 10 reading cycles at 37°C. Following this, cells were then treated with a 10µl of a 10X ligand (see specific result chapters for details), producing a final volume of 100µl of 1X ligand concentration in each well of cells. cAMP accumulation was monitored using the same parameters as per the basal readings, with the exception of 50 cycles over 30 minutes at 37°C. In order to detect cAMP fluorescence, the wild type N- and C-termini of firefly luciferase was circularly permuted with a cAMP binding domain. cAMP binding led to a conformational shift in the biosensor that induced luminescence activity and was recorded over time (Wang et al., 2022).

## **2.6 Dual-Luciferase<sup>®</sup> Reporter Assay system**

Since HEK293 cells are not steroidogenic cell lines, the physiological effect of FSHR modulation on cAMP-dependent gene expression, such as *CYP19A1* that encodes aromatase for the conversion of testosterone to oestrogen, could not be determined. As an alternative, cAMP-dependent global gene expression was determined using a luciferase reporter gene subcloned to cre. The Dual-Luciferase<sup>®</sup> Reporter Assay system was an effective tool used to determine this because two distinct luciferases from firefly and *Renilla* (*Renilla reniformis*), that were subcloned to cre DNA sequence in an expression vector, were transfected into HEK293 cells. Therefore, upon the activation of FSHR and cAMP production, the activation and phosphorylation of CREB would initiate cre-binding and subsequent luciferase reporter gene activation and luminescence (see section 1.8.1). As a result, a measure on the effect of FSHR modulation on cAMP-dependent global gene expression and transcription could be determined.

Cells transiently co-expressing HA-FSHR, cre-luciferase and *Renilla*-luciferase (for transfection efficiency) were replated into gelatine-coated 96-well advanced white flat-bottom clear TC plates at a density of  $5.0 \times 10^4$  cells/well, in 100 $\mu$ l DMEM<sup>+/+</sup>. Cells were left overnight to culture and form a monolayer with approximately 70% confluency before being assayed. The following day, cells were ligand-treated using serum-free media (DMEM supplemented with 1% antibiotic-antimycotic) for 4-6 hours at 37°C. At the end of the treatment, media was aspirated from the wells and discarded. Cells were washed with 100 $\mu$ l of RT PBS and PBS aspirated and discarded. Cells were lysed using 20 $\mu$ l/well of 1X PLB made up using distilled water and placed on a vigorous rocking motor for 15 minutes at RT, as per manufacturer's instructions.

Lyophilised luciferase assay substrate was reconstituted in luciferase assay buffer II, and 100 $\mu$ l of the solution added to each well as rapidly as possible using a repeat pipette. The 96-well plate was then placed on a rocking motor to vortex the lysates for about 10 seconds before proceeding to reading luminescence of each well using the PHERAstar<sup>®</sup> FS multi-mode plate reader. A LUM Plus filter was used to measure luminescence with a gain was set at 2800. For internal control measures, *Renilla*-luciferase activity was measured. Stop & Glo<sup>®</sup> buffer was mixed with 50X Stop & Glo<sup>®</sup> substrate to produce a 1X solution and 100 $\mu$ l of the Stop & Glo<sup>®</sup> mixture was added to each individual well using a repeat pipette quickly and carefully. Lysates within the wells were vortexed using the rocking motor for approximately 10 seconds and plates were placed back onto the plate reader. *Renilla*-luciferase luminescence was measured using a LUM Plus filter with a gain set at 3600.

## 2.7 Western blotting

### 2.7.1 Cell lysis and protein assay

FSHR activation can mediate the activation via phosphorylation of multiple cellular proteins, in particular CREB and ERK1/2, that mediate steroidogenesis and cell proliferation, respectively (Casarini & Crépieux, 2019). Therefore, Western blots were performed to investigate the effect of FSHR modulation on the phosphorylation of these proteins.

Cells transiently expressing the HA-FSHR were replated into gelatine-coated 6-well TC plates ( $6.0 \times 10^5$  cells/well) in 2mls DMEM<sup>+/+</sup> and treated with ligand (see specific result chapters for details). At the end of the treatment period, cells were placed on ice and the media carefully aspirated and discarded. Cells were washed with 1ml/well of ice-cold PBS. The PBS was aspirated and discarded, and cells were lysed in 150 $\mu$ l/well of ice-cold 1X lysis buffer (see Appendix 1D for lysis buffer recipe). To aid cell lysis, cells were gently rocked on a shaking platform for 30 minutes at 4°C, and subsequently harvested via scraping into cooled 1.5ml microfuge tubes. Cell lysates were sonicated on ice for 5 seconds, centrifuged at 13,000 rpm for 10 minutes at 4°C, and supernatant removed for analysis and cell debris discarded.

Protein concentration of cell lysates was determined using a Bradford assay. Briefly, a standard curve was generated from a BSA stock solution (2mg/ml) and protein concentrations determined. From this, 30 $\mu$ g of protein was diluted and mixed with 5 $\mu$ l of 1X loading dye (see Appendix 1E for loading dye recipe) to a total volume of 20 $\mu$ l. Samples

were denatured by heating for 5 minutes at 95°C in a heated block and centrifuged at 13,000 rpm for 1 minute at RT.

### 2.7.2 SDS-PAGE

SDS-PAGE was employed to give a higher resolution of protein separation. Using the SureCast Gel Handcast System (Invitrogen), proteins were loaded onto 4% (v/v) stacking gel and separated by SDS-PAGE through a 10% (v/v) acrylamide resolving gel (see Appendix 1F for gel recipe). Molecular weight markers were loaded onto each end of the gel for determination of molecular weights of proteins probed for Western blot analysis. The running buffer utilised was 1X MOPS (20X MOPS diluted in distilled water) and run at 150 volts for ~50 minutes, or until the gel dye front reached the bottom of the gel.

### 2.7.3 Transfer of protein from SDS-PAGE gel to PVDF membrane

Transfer of protein from the gel to the PVDF membrane was preferred over nitrocellulose membrane because PVDF is more durable and has a higher protein binding. Therefore, after the electrophoresis, gels were soaked in an ice-cold 1X transfer buffer supplemented with 10% (v/v) methanol, alongside transfer cassette contents (2 sponges, 2 thick filter papers) for 15 minutes. The PVDF membrane (0.45µm pore size) was activated with methanol, and also soaked in transfer buffer for 15 minutes.

The transfer cassettes were assembled on the cathode of the Western blotter (Mini Gel Tank, Invitrogen), in the following order: sponge, filter paper, gel, PVDF membrane, filter paper, sponge. A roller was used to remove air bubbles between each layer. Once assembled, the cassettes were inserted into the transfer tank and transfer buffer used to fill



the tank. The transfer was conducted at 20 volts for 1 hour and 30 minutes, as per manufacturer's instructions.

#### 2.7.4 PVDF membrane blocking and antibody probing

Following completion of protein transfer, and confirmation of visible markers with complete transfer onto each membrane, membranes were placed into 10ml of 5% (w/v) blocking buffer (BSA in 1X tris-buffered saline tween (TBST)) (Appendix 1F) for 1 hour on a rocking platform at room temperature. Blocked membranes were incubated overnight at 4°C on a roller with 5ml of primary antibody complimentary to the phosphorylated protein of interest; either phospho-ERK1/2 mouse or phospho-CREB rabbit monoclonal antibody in blocking buffer (see Appendix 1C for specific antibody dilutions and concentrations). Following primary antibody incubation, primary antibody was removed, and membranes washed in 25ml of 1X TBST for 3 x 5 minutes on a roller. Membranes were then incubated for 1 hour at RT with HRP-conjugated secondary antibody (see Appendix 1C for specific antibody dilutions and concentrations), diluted in 5% (w/v) skimmed milk in TBST. At the end of incubation, secondary antibody was removed, and membranes washed in 25ml of 1X TBST for 3 x 5 minutes on a roller.

#### 2.7.5 Quantification of protein expression

To analyse protein expression levels, membranes were incubated for 1 minute in 1ml of premixed HRP substrate at RT. Excess HRP substrate was drained off and the membrane and the membrane imaged using a ChemiDoc™ XRS+ Imager System (Bio-RAD). Membranes were exposed every 10 seconds, typically over a 5-minute period. Images of

protein bands were collected and quantified using densitometric analysis with Image Lab version 6.0 software.

#### 2.7.6 Primary antibody re-probing for global proteins

To compare the difference between phosphorylated proteins and total proteins, membranes were stripped and re-probed for total-ERK1/2 or -CREB. A 1X stripping buffer was prepared in a fume hood and heated to 40°C (see Appendix 1H for recipe). Once heated, individual membranes were placed in a falcon tube with 50ml of 1X stripping buffer and placed a on roller for 30 minutes. Membranes were then removed from the stripping buffer and washed with 25ml of 1X TBST for 4 x 5 minutes. Following this, membranes were ready to be incubated overnight at 4°C with the total protein primary antibody in blocking buffer, followed by the appropriate HRP-conjugated to the secondary antibody in 5% (w/v) skimmed milk in TBST and then imaged (see Appendix 1C for specific antibody dilutions and concentrations).

### **2.8 Immunocytochemistry immunofluorescence**

Although Western blots are a useful technique to investigate protein expression, it provides no information about protein spatial localisation. Therefore, immunocytochemistry immunofluorescence was performed to determine percentage of internalised FSHRs that were routed to endosomes.

EEA1 is an intermediate marker for the EE formation and prerequisite for GPCR degradation via lysosomes (Kaur & Lakkaraju, 2018). To investigate the effect of FSH glycoforms on FSHR trafficking to EEA1-positive endosomes, HEK293 cells transiently

expressing N-terminally FLAG-tagged FSHR were re-plated onto 1X Poly-D-Lysine-coated coverslips within 24-well plates ( $1.5 \times 10^5$  cells/coverslip/well). 48-hour post-transfection (40-80% cell confluency) the media was removed, and cells were incubated with  $8\mu\text{g/ml}$  of mouse anti-FLAG primary antibody in serum-free DMEM supplemented with 0.1% (v/v) BSA for 15 minutes at  $37^\circ\text{C}$ .

With the antibody still present, cells were stimulated with  $\pm 30\text{ng/ml}$  of pituitary FSH (positive control), FSH21/18 or FSH24 for 0-, 5- or 15- minutes, using a reverse time-course. Following treatment, media from cells was discarded and cells were washed twice with 1ml of cold PBS supplemented with  $\text{Ca}^{2+}$  because the M1-FLAG antibody binding is  $\text{Ca}^{2+}$ -dependent). The remaining FLAG antibodies were stripped from plasma-membrane-bound FSHRs to ensure only internalised FSHRs were assessed by quickly washing cells four times with 0.04% (v/v) EDTA in PBS without  $\text{Ca}^{2+}$ . Cells were then fixed in 4% (v/v) PFA for 20 minutes at room temperature. The PFA was discarded, cells were quickly washed with PBS (+  $\text{Ca}^{2+}$ ) four times and blocked using blocking buffer (PBS +  $\text{Ca}^{2+}$  + 2% (v/v) FCS) for 20 minutes at RT.

Subsequently, blocked cells were permeabilised with 0.2% (v/v) Triton-X in blocking buffer for 15 minutes at RT to enable the large antibodies to pass through the plasma membrane. Next,  $88\text{ng/ml}$  of rabbit anti-EEA1 primary antibody in blocking buffer was added to all cells and left for 2 hours at RT. Once the primary antibody was discarded, cells were washed with blocking buffer three times before  $2\mu\text{g/ml}$  of goat anti-mouse AlexaFluor 488 and  $2\mu\text{g/ml}$  of anti-rabbit AlexaFluor 555 secondary antibodies in blocking buffer was added to cells and further incubated at room temperature for 30 minutes (light-protected).

Finally, once the secondary antibody was discarded, cells were washed twice in PBS + 2% (v/v) FCS, incubated in 300nM DAPI for 5 minutes and then mounted onto slides using Fluoromount G, ready to be imaged. 7-8 cells were imaged per condition using a TCS-SP5 confocal microscope (Leica) with a 63 x 1.4 numerical aperture objective and Leica LAS AF image acquisition.

## **2.9 siRNA approach to gene knockdown**

RNA interference is a tool that has been widely used to knockdown/silence the expression of individual genes to study cellular function in biology (Han, 2018). The approach works by introducing a messenger RNA (mRNA) sequence, via transfection, that compliments the mRNA sequence corresponding to the gene of interest. With siRNA bound to the mRNA of interest, translation of the gene is prevented. Therefore, an siRNA approach to silent APPL1 was conducted to investigate the role of the adaptor protein APPL1 in FSH glycoform-dependent FSHR signalling.

To achieve this, cells were transfected with  $\pm 0.8\mu\text{M}$  siAPPL1 mediated by Lipofectamine 2000<sup>®</sup> (see chapter 2.3.2 for details) and cultured for 96 hours prior to treatment. 24-hours post-siAPPL1 transfection, cells were further transfected with FSHR and cultured for the remaining 72 hours prior to treatment for either GloSensor<sup>™</sup> cAMP assays (see chapter 2.5 for details) or cre-luciferase reporter assays (see chapter 2.6 for details).

## **2.10 Radioligand binding assay**

To determine the effect of different ligands on FSHR binding affinity, collaborators carried out radioligand binding assays (Professor George Bousfield and Dr Viktor Butnev, Wichita

State University, Kansas). 250,000 EpiHEK293 cells were transiently transfected with hFSHR. Cold tracer  $^{125}\text{I}$ -hFSH preparations were made (0.1-1000ng/tube). 100 $\mu\text{M}$  of SMC 48, 74 or 80 was prepared by adding 100 $\mu\text{l}$  of a 0.5mM stock to each assay tube, making a final volume of 500 $\mu\text{l}$ . The same FSH dilutions were added to control and inhibitor-containing tubes. Cells were incubated for 3 hours at 37°C before the counts per minute (cpm) of  $^{125}\text{I}$ -FSH was determined.

## **2.11 Data analysis and statistics**

### 2.11.1 Normalisation of GloSensor™ cAMP production

To determine the amount of cAMP produced during experiments, the average baseline fluorescence reading (prior to treatment) in each well was subtracted from each fluorescence reading recorded within the same well following ligand stimulation. The total amount of cAMP accumulation was determined by measuring the area under the curve (AUC). The maximal cAMP response was determined by recording the highest cAMP fluorescence reading.

### 2.11.2 Normalisation of cre-luciferase activity

Possible differences due to variation in transfection efficiency were minimised by measuring the ratio for cre-luciferase luminescence reading over *Renilla*-luciferase luminescence reading for each individual well.

### 2.11.3 Normalisation of protein expression for Western blotting

To account for any variation due to errors in loading or protein transfer,  $\beta$ -tubulin, a constitutively expressed protein that does not vary between treatment groups, was used as a housekeeping control to normalise the relative expression of the protein of interest.

### 2.11.4 Percentage of FSHR-positive EEA1 endosomes

To determine the percentage of FSHRs co-localised to EEA1-positive endosome, subsequent raw-image files were analysed using ImageJ software. The total number of FSHR-positive endosomes were recorded based on the shape and size of the AlexaFluor 488 dye in the green channel. When the channels were switched to red AlexaFluor 555 to locate EEA1-positive endosomes, the number of FSHRs that were co-localised were also recorded, and the percentage of FSHR-positive EEA1 endosomes were measured and recorded as percentage.

### 2.11.5 Statistics

All experimental data was represented as the mean  $\pm$  SEM. A minimum of 3 independent experiments were conducted, unless stated otherwise. GloSensor<sup>TM</sup> and cre-luciferase assays were conducted in triplicates for technical replicates. All statistical analysis was performed using GraphPad Prism version 9.0 software.

Comparison between one independent variable with three or more groups affecting a dependent variable was measured using ordinary one-way ANOVA. This was followed by either a Dunnett's multiple comparisons test when comparison of the mean between a number of treatments and a single control was measured, or a Tukey's multiple

comparisons test when comparison of multiple means across all treatments was measured. Comparison between two independent variables with three or more groups affecting a dependent variable were measured using two-way ANOVA. This was followed by either a Dunnett's multiple comparisons test when comparison of the mean between a number of treatments and a single control was measured, or a Šidák's multiple comparisons test when comparison of multiple means across all treatments was measured. Comparison between two groups of cells with different transfection efficiencies was measured using Student's unpaired t-test, followed by Holm-Šidák's multiple comparisons test.

Ligand concentration-response curves were generated by fitting data to a non-linear regression model with three parameters. From this the half maximal effective concentration ( $EC_{50}$ ) were determined which represented the concentration of the ligand that was able to induce half of the cAMP/cre-luciferase maximal response and gave an indication on the potency of the ligand. The  $EC_{50}$  was calculated using GraphPad Prism version 9.0 software, and alternatively could be calculated by dividing the difference between the maximal response and the baseline of a curve and dividing the value by 2. The output value of  $f(y)$  can then be used to interpolate the value of  $f(x)$ .

Statistical significance was determined as a probability value of  $p < 0.05$ .

**3 Chapter Three: Investigating the role of FSH glycoforms on FSHR oligomerisation and correlation with cAMP-dependent signalling**



### 3.1 Introduction

To begin to delineate the molecular regulation of FSH-mediated receptor oligomerisation and trafficking, and related signalling, in order to identify alternative mechanisms to target them and improve fertility outcomes, the first step was to investigate how endogenous FSH glycoforms mediate differential FSHR signalling pathway activation. As outlined in chapter 1.4.3.2, post-translational modification of FSH gives rise to the predominant macroheterogeneous FSH glycoforms, partially glycosylated FSH<sub>21/18</sub> and fully glycosylated FSH<sub>24</sub>. FSH<sub>21/18</sub> displays higher binding affinity and faster binding kinetics at the FSHR, induces higher  $G\alpha_s$ /cAMP/PKA signalling and more predominant in reproductive prime women. In contrast, FSH<sub>24</sub> displays lower binding affinity and slower binding kinetics at the FSHR, induces lower  $G\alpha_s$ /cAMP/PKA signalling and more predominant in peri-menopausal women (Bousfield et al., 2014a; Hua et al., 2021; Jiang et al., 2015; Landomiel et al., 2019; Wang et al., 2016b; Zariñán et al., 2020). Yet how FSH glycoforms modulate these differences in FSHR signalling remain unclear.

One way to modulate GPCR signal specificity, selectivity and amplitude is via receptor di/oligomerisation. FSHR has been demonstrated to self-associate to form homomers (see chapter 1.11), with one of the first biochemical evidence for their existence obtained using co-IP. Differentially tagged myc- and FLAG-tagged FSHR were demonstrated to form homodimers in the ER during early biosynthesis prior to post-translational modification (Thomas et al., 2007). These findings were further corroborated in later studies using BRET in living HEK293 cells (Guan et al., 2010). Furthermore, FSHR chimeras formed from FSHR fused to fluorescent tagged C-terminus LH/CGRs produced high FRET efficiencies and revealed FSHR as a freely diffusing homodimer in the plasma membrane (Mazurkiewicz et al., 2015). Interestingly, crystal structure analysis of FSHR superimposed

onto a predetermined complex structure showed FSHR formed constitutive trimers (Jiang et al., 2014b). Although the functional role for FSHR oligomers is unclear, research on FSHR heteromerisation with the LH/CGR suggests it may modulate signal selectivity, specificity, and amplitude. When the FSHR and LH/CGR were co-expressed in HEK293 cells, increased BRET efficiencies revealed these receptors formed heterodimers. In addition, when these receptors were expressed at different ratios, the magnitude of cAMP production was altered (Feng et al., 2013). Moreover, when FSHR-LH/CGR heteromers were exposed to LH,  $G\alpha_s$ -dependent cAMP signalling was attenuated and  $G\alpha_{q/11}$ -dependent  $Ca^{2+}$  signalling was enhanced and sustained (Jonas et al., 2018). This demonstrates the capability for FSHR di/oligomers to mediate signal selectivity.

Besides RET techniques, detection of GPCR di/oligomers at a molecular level also utilised single molecule imaging techniques, such as TIRF-M with post-acquisition extrapolation of intensity data to resolve the GPCR molecules (Calebiro et al., 2013; Hern et al., 2010; Kasai et al., 2011). However, such techniques lack the ability to spatially separate and localise the resolved GPCR molecules beyond the diffraction limit of standard fluorescent imaging techniques. The advancements in the single molecule imaging technique, PD-PALM, has enabled the detection and spatial organisation of GPCR molecules at a resolution of <10nm, and provides a new mechanism to investigate how FSH glycoforms specify the differences observed in the kinetics and amplitude of cAMP signalling, with single molecule precision, and at physiological levels of receptor density (Jonas et al., 2015; Jonas & Hanyaloglu, 2019). Therefore, the aim of this chapter was to investigate the role of different FSH glycoforms on FSHR oligomerisation and the  $G\alpha_s$ /cAMP/PKA signalling pathway; from second messenger to transcription factor to cre-responses. The objectives set out to address the aim were to:

1. Determine the concentration- and time-dependent effects of FSH glycoforms on FSHR oligomer formation at the plasma membrane in HEK293 cells expressing FSHR.
2. Investigate the correlation between the effect of FSH glycoforms on FSHR oligomer formation and cAMP accumulation and CREB-phosphorylation in a time-dependent manner in HEK293 cells expressing FSHR.
3. Determine correlation between the effect of FSH glycoforms of FSHR oligomer formation and cre-luciferase activity in HEK293 cells expressing FSHR.
4. Investigate the correlation between FSH glycoforms on FSHR oligomer formation and ERK1/2-phosphorylation in HEK293 cells expressing FSHR.

## 3.2 Results

### 3.2.1 Concentration- and time-dependent effects of FSH glycoforms on FSHR oligomerisation

To assess FSHR monomer, dimer, and oligomer populations at the plasma membrane, cells transiently expressing HA-FSHR were cultured for PD-PALM experiments (see chapter 2.4 for details). Based on differential cAMP production evoked by FSH21/18 and FSH24 (Jiang et al., 2015), cells were treated with either 0- (control), 1-, 30-, or 100ng/ml of different FSH glycoforms. Alongside FSH21/18 and FSH24, a potent FSHR stimulator-equine FSH (eFSH) was used as a positive control. Additionally, an FSHR  $\beta$ -arrestin biased agonist with diminished ability to activate cAMP- truncated eLH $\beta$  ( $\Delta$ 121-149) combined with asparagine56-deglycosylated eLH $\alpha$  (dg-eLHt) (Butnev et al., 2002; Wehbi et al., 2010) was used as a negative control. Cells were then washed, fixed, and imaged (see chapter 2.3 for details).

Analysis of the basal number of associated FSHR showed that  $30.2 \pm 1.8\%$  of FSHR were associated as dimers and oligomers, with  $\sim 70\%$  as FSHR monomers (Figure 3.1). When the basal composition of associated cell surface FSHR was assessed, results showed  $15.5 \pm 0.8\%$  resided as dimers and  $5.5 \pm 0.5\%$  as trimers (Figure 3.1), suggesting that the majority of FSHR reside as lower order homomers and monomers. Acute 2-minute treatment with 30ng/ml eFSH or FSH21/18 significantly decreased the overall percentage of associated FSHR, with  $20.0 \pm 1.3\%$  and  $17.5 \pm 1.6\%$  associated as homomers, respectively (Figure 3.1, (b)). A decrease was observed in almost all FSHR homomeric

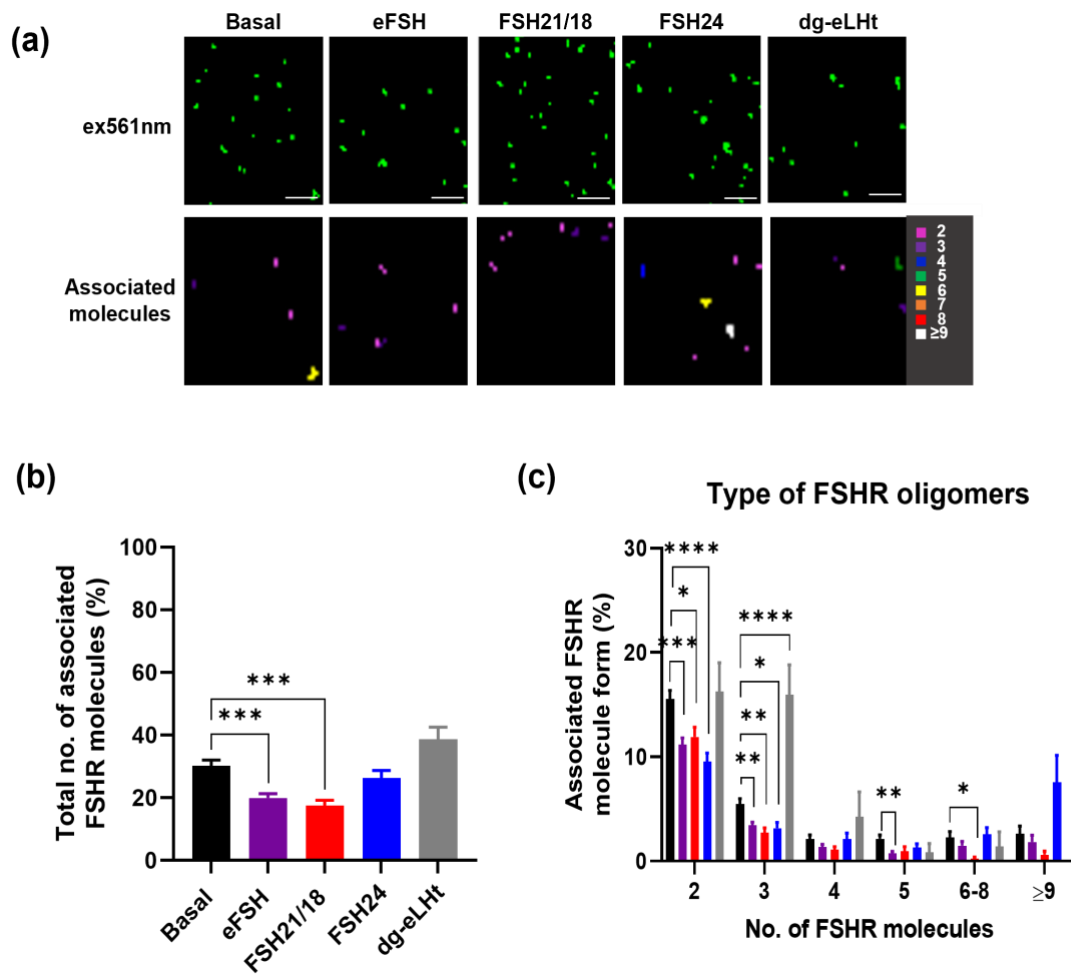


**Figure 3.1: Effect of 2-minute treatment with 30ng/ml of FSH glycoforms on FSHR oligomerisation.** HEK293 cells transiently expressing HA-tagged FSHR were pre-incubated for 30 minutes with CAGE 552-HA antibody and treated with  $\pm$  30ng/ml of eFSH, FSH21/18, FSH24 or dg-eLHt for 2 minutes, fixed for 30 minutes and imaged via PD-PALM. **(a)** Representative x-y coordinate plots of resolved FSHR molecules (upper panels) and reconstructed heat map of FSHR molecules following treatment (lower panels). Images are  $2\mu\text{m}^2$  from a  $5\mu\text{m}^2$  area. Scale bars, 500nm. **(b)** Percentage of the total number of associated FSHR molecules; data analysed using ordinary one-way ANOVA, followed by Tukey's multiple comparisons' test. **(c)** Percentage of associated FSHR molecule form; 2 (dimer), 3 (trimer), 4 (tetramer), 5 (pentamer), 6-8,  $\geq 9$ , with data analysed using multiple unpaired t-tests. All data represent mean  $\pm$  SEM of  $n \geq 3$  independent experiments and  $n \geq 9$  cells analysed per experiment. \*,  $p < 0.05$ ; \*\*,  $p < 0.01$ ; \*\*\*,  $p < 0.001$ ; \*\*\*\*,  $p < 0.0001$ .

subtypes (dimers, trimers, pentamers and 6-8 oligomers) (Figure 3.1, (c)). In contrast, treatment with FSH24 had no effect on the total percentage of associated FSHR, however modulation in the type of FSHR homomeric complexes was observed with a modest increase in  $\geq 9$  complexes and a decrease in dimers. Surprisingly, 2-minute treatment with dg-eLHt showed a trend for increasing FSHR association with  $38.7 \pm 3.8\%$  of FSHR molecules associated (Figure 3.1, (b)), and  $15.9 \pm 2.9\%$  of these FSHRs as trimers (Figure 3.1, (c)).

5-minute stimulation with eFSH treatment showed the percentage of FSHR association to resemble basal (Figure 3.2, (ai)), suggesting a rapid re-organisation of dissociated FSHRs into FSHR homomers. However, FSH21/18 maintained a sustained reduction in the number of FSHR homomers observed (Figure 3.2, (ai)). 5-minute treatment with FSH24 resulted in dissociation of FSHR (Figure 3.2, (ai)), with a decrease in dimeric and trimeric FSHR homomers observed ( $p < 0.001$ ) (Figure 3.2, (aii)), suggesting that FSH24 has slower kinetics and takes longer to engage with the FSHR. 5-minute dg-eLHt treatment significantly increased FSHR association (Figure 3.2, (ai)), suggesting that different FSH ligands have distinct effects on FSHR oligomerisation at the plasma membrane. A more chronic 15-minute treatment with either eFSH, FSH21/18 or FSH24 resulted in FSHR total homomeric complex percentages resembling those of basal levels (Figure 3.2, (bi)), implying that by this time point FSHRs have dissociated and re-associated in response to FSH. However, dg-eLHt-treated cells continued to show increased FSHR association ( $49.7 \pm 6.4\%$ ) with increases observed in trimers, tetramers to  $\geq 9$  complexes (Figure 3.2, (bii)), further supporting the proposition that different FSH ligands can differentially modulate FSHR association.

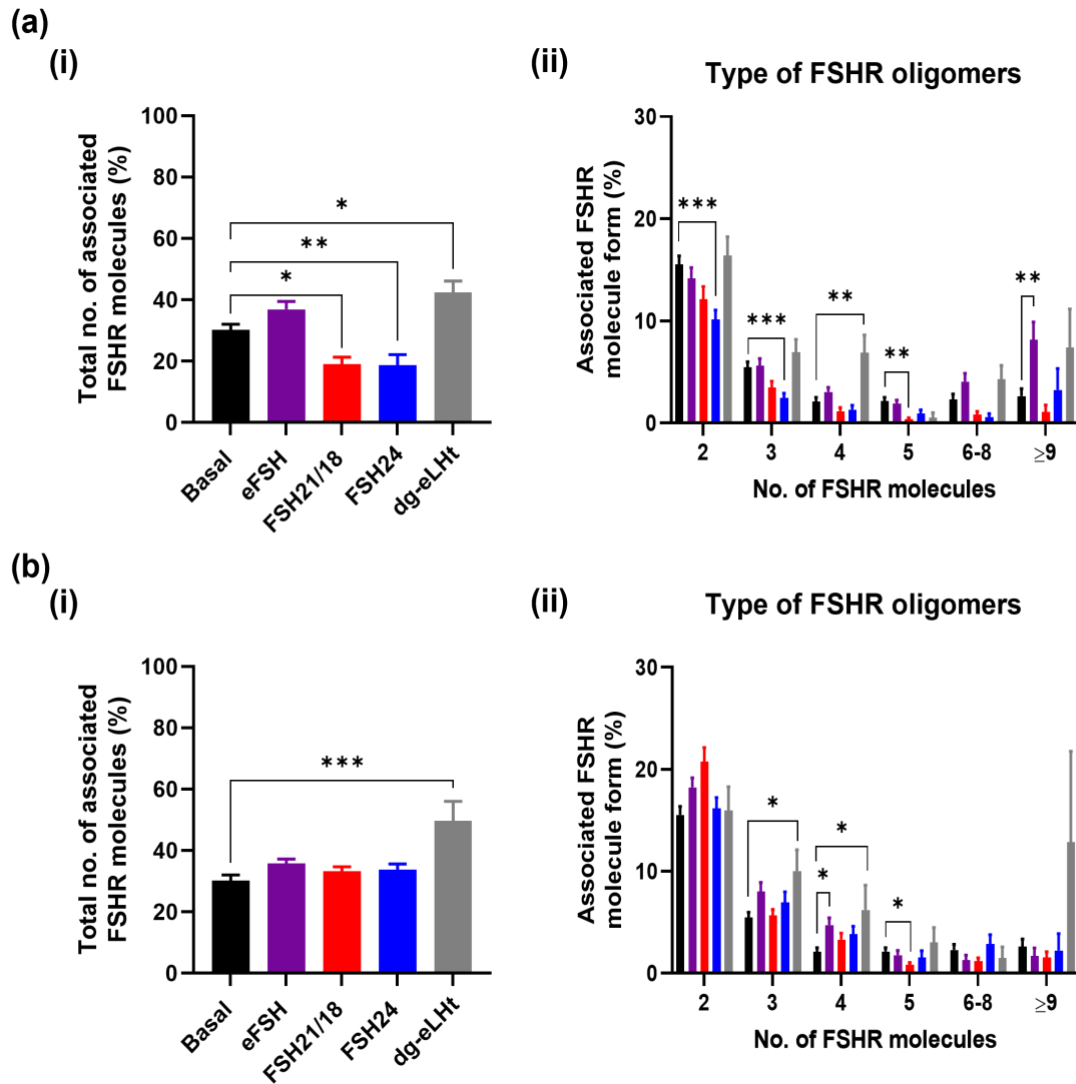


**Figure 3.2: Effect of 5- and 15-minute treatment with 30ng/ml of FSH glycoforms on FSHR oligomerisation.** HEK293 cells transiently expressing HA-tagged FSHR were pre-incubated for 30 minutes with CAGE 552-HA antibody and treated with  $\pm$  30ng/ml of eFSH, FSH21/18, FSH24 or dg-eLHt for **(a)** 5 minutes or **(b)** 15 minutes, fixed for 30 minutes and imaged via PD-PALM. **(i)** Percentage of the total number of associated FSHR molecules; data analysed using ordinary one-way ANOVA, followed by Tukey's multiple comparisons' test. **(ii)** Percentage of associated FSHR molecule form; 2 (dimer), 3 (trimer), 4 (tetramer), 5 (pentamer), 6-8,  $\geq$ 9, with data analysed using multiple unpaired t-tests. All data represent mean  $\pm$  SEM of  $n \geq 3$  independent experiments and  $n \geq 9$  cells analysed per experiment. \*,  $p < 0.05$ ; \*\*,  $p < 0.01$ ; \*\*\*,  $p < 0.001$ .

Since FSH concentrations and glycosylation patterns are differentially regulated across the menstrual cycle (Wide & Eriksson, 2018), and have also been shown to change with age (Bousfield et al., 2014b), the next steps were to determine the effects of FSH ligand concentration on FSHR association. As previously described, cells expressing HA-FSHR were treated  $\pm$  eFSH, FSH21/18, FSH24 or dg-eLHt for 2-, 5- or 15-minutes, but instead with either 1- or 100ng/ml of each FSHR ligand. Assessment of FSHR association following 2-minute treatment with 1ng/ml of all ligands revealed no significant changes in the total percentage of FSHR homomers (Figure 3.3, (b)), nor the type of FSHR homomeric complexes observed (Figure 3.3, (c)), suggesting that lower concentrations of FSHR ligands has little effect on FSHR association at this acute time-point. Similarly, 5-minute treatment with 1ng/ml eFSH, FSH21/18 and dg-eLHt had no effect on FSHR association (Figure 3.4, (ai)). FSH24 induced a significant increase in FSHR association, with an increase in the formation of pentamers ( $6.1 \pm 2.6\%$ ) (Figure 3.4, (aii)), contrasting to the dissociation of FSHR homomers observed with 30ng/ml FSH24 shown previously. 15-minute treatment with FSH21/18 also induced FSHR association (Figure 3.4, (bi)), with an increase in FSHR tetramers ( $9.0 \pm 1.8\%$ ) and  $\geq 9$  oligomers ( $18.2 \pm 4.1\%$ ) (Figure 3.4, (bii)). FSH24-treated cells appeared to show FSHR return to basal configuration (Figure 3.4, (b)).

When cells were treated with 100ng/ml of either FSH21/18 or FSH24 for 15 minutes, FSHR molecules at the plasma membrane were incapable of localisation and analysis via PD-PALM. Instead, it appeared that the FSHR molecules may have formed clusters at the plasma membrane or internalised and routed to endosomes during the imaging process (Figure 3.5). Taken together, these data suggest that different FSHR ligands specify distinct



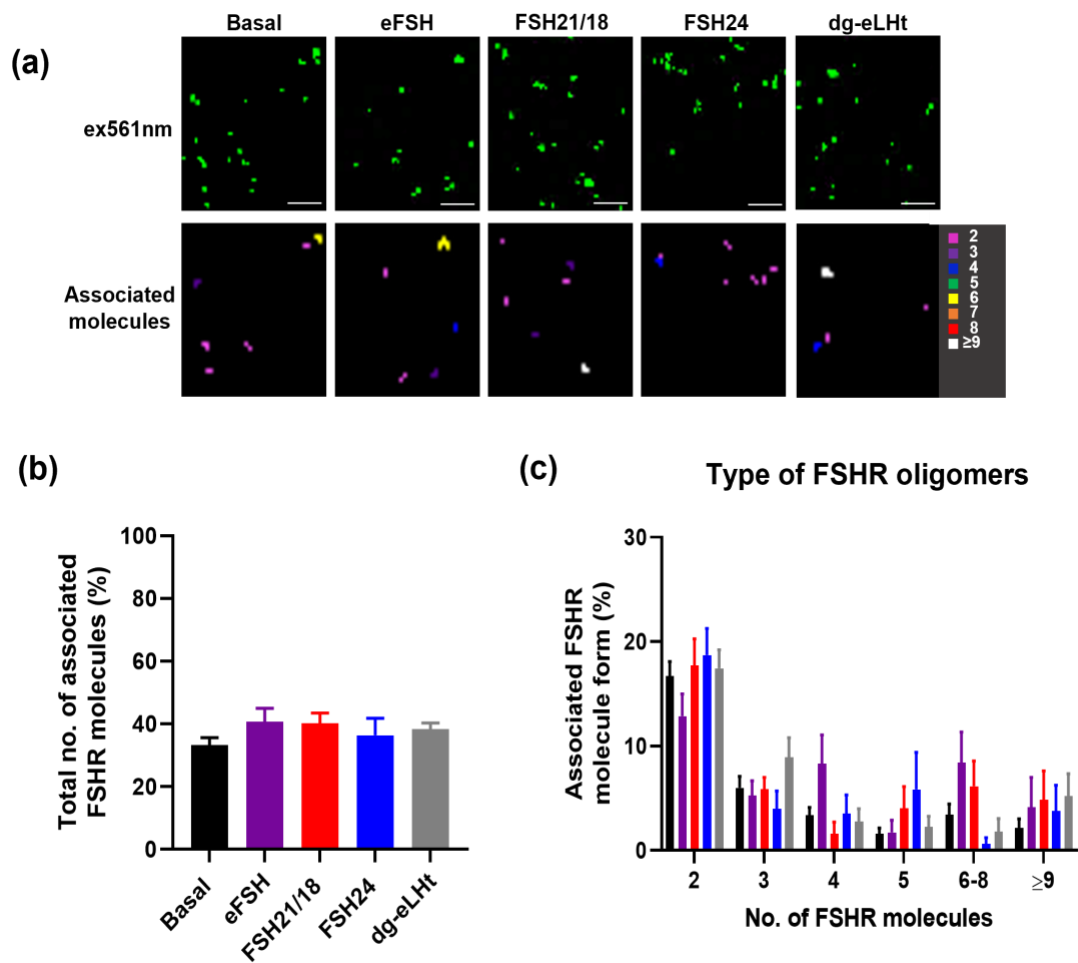


**Figure 3.3: Effect of 2-minute treatment with 1ng/ml of FSH glycoforms on FSHR oligomerisation.** HEK293 cells expressing HA-tagged FSHR, labelled with CAGE 552-HA antibody and treated with  $\pm$  1ng/ml of eFSH, FSH21/18, FSH24 or dg-eLHt 2 minutes. Cells were fixed and imaged via PD-PALM. **(a)** Representative resolved localised FSHR molecules following treatment (upper panels) and heat map showing associated FSHR molecules (lower panels). Images are  $2\mu\text{m}^2$  from a  $5\mu\text{m}^2$  area. *Scale bars*, 500nm. **(b)** Percentage of the total number of associated FSHR molecules; data analysed using ordinary one-way ANOVA, followed by Tukey's multiple comparisons' test. **(c)** Percentage of associated FSHR molecule form; 2 (dimer), 3 (trimer), 4 (tetramer), 5 (pentamer), 6-8,  $\geq 9$ ; data analysed using multiple unpaired t-tests. All data represent mean  $\pm$  SEM of  $n \geq 3$  independent experiments and  $n \geq 9$  cells analysed per experiment.

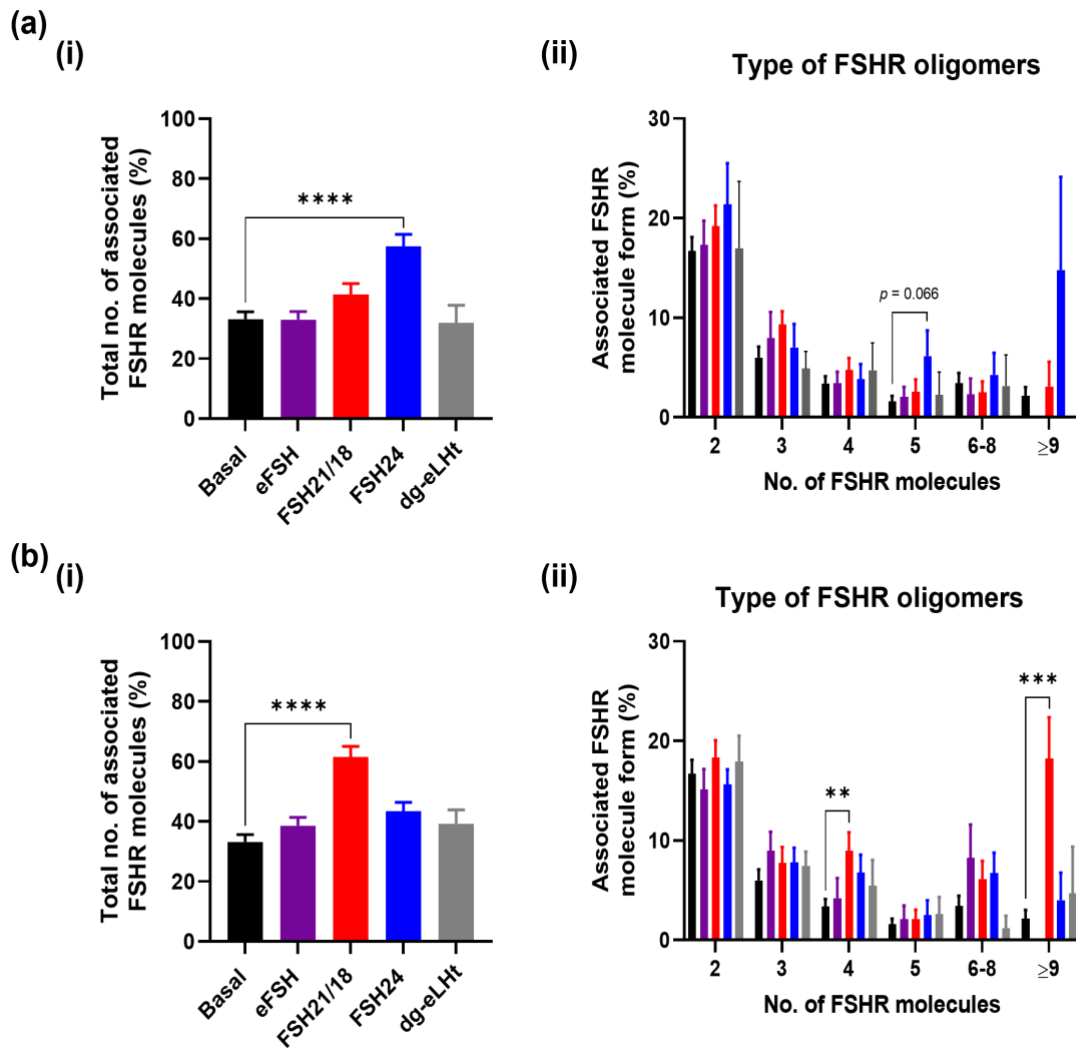


**Figure 3.4: Effect of 5- and 15-minute treatment with 1ng/ml of FSH glycoforms on FSHR oligomerisation.** HEK293 cells expressing HA-tagged FSHR, labelled with CAGE 552-HA antibody and treated with  $\pm$  1ng/ml of eFSH, FSH21/18, FSH24 or dg-eLHt for **(a)** 5 minutes or **(b)** 15 minutes. Cells were fixed and imaged via PD-PALM. **(i)** Percentage of the total number of associated FSHR molecules; data analysed using ordinary one-way ANOVA, followed by Tukey's multiple comparisons' test. **(ii)** Percentage of associated FSHR molecule form; 2 (dimer), 3 (trimer), 4 (tetramer), 5 (pentamer), 6-8,  $\geq$ 9; data analysed using multiple unpaired t-tests. All data represent mean  $\pm$  SEM of  $n \geq 3$  independent experiments and  $n \geq 9$  cells analysed per experiment. \*\*,  $p < 0.01$ ; \*\*\*,  $p < 0.001$ ; \*\*\*\*,  $p < 0.0001$ .

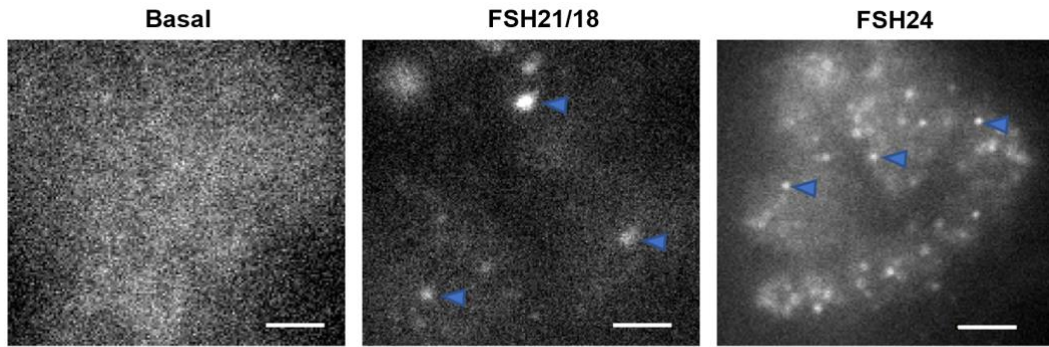


**Figure 3.5: Effect of 15-minute treatment with 100ng/ml of FSH glycoforms on FSHR oligomerisation.** PD-PALM images of HEK293 cells transiently expressing HA-tagged FSHR. Cells were pre-incubated for 30 minutes with CAGE 552-HA antibody and treated with  $\pm$  100ng/ml of FSH21/18 or FSH24 for 15 minutes, fixed for 30 minutes and imaged via PD-PALM. Treatment with FSH glycoforms appears to show FSHR molecules clustered within endosomes, indicated by the blue triangles. *Scale bars*, 2.5 $\mu$ m.

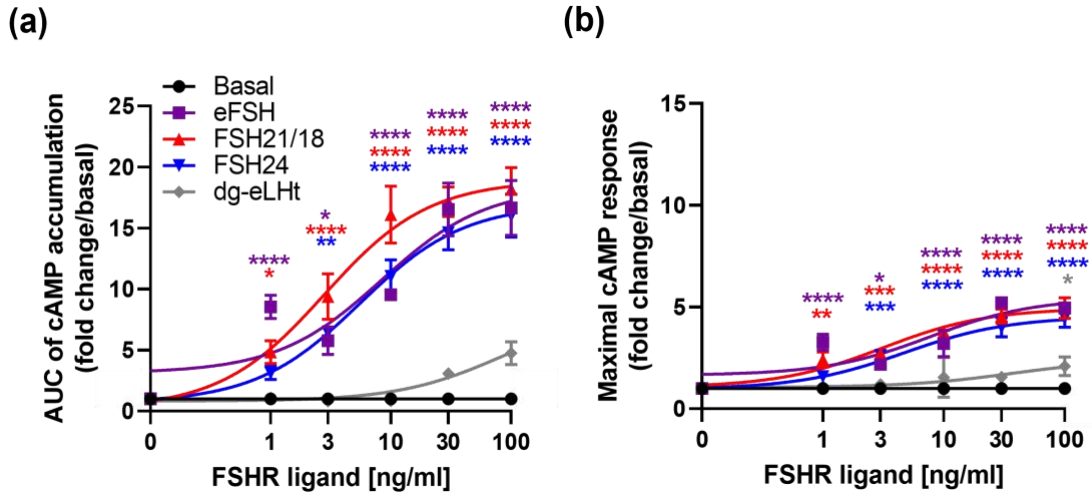
re-organisation of FSHR monomer, dimer, and oligomer populations in both a time- and concentration-dependent manner.

### 3.2.2 Effect of FSH glycoform-dependent FSHR oligomerisation on cAMP accumulation and CREB-phosphorylation

Given that the canonical FSHR signalling pathway is  $G\alpha_s$ /cAMP/PKA/CREB, the next step was to investigate if changes in FSHR monomers, dimers and oligomers observed at the plasma membrane correlated with modulation in cAMP signals. For this, GloSensor™ cAMP assays were performed to record real-time intracellular cAMP accumulation. Following transient transfection, cells were replated and pre-equilibrated for 2 hours prior to treatment (see chapter 2.5 for details). Cells were treated for up to 30 minutes at 37°C with increasing concentrations of either eFSH, FSH21/18, FSH24 or dg-eLHt (0-100ng/ml) and real-time cAMP fluorescence was measured using a multi-mode plate reader.

Following 30-minute treatment with different concentrations of different FSH glycoforms, full cAMP concentration-response curves showing the AUC of cAMP accumulation and the maximal cAMP response were generated (Figure 3.6). As anticipated, all FSH glycoforms, apart from dg-eLHt, were able to induce significant increases in the total cAMP production (Figure 3.6, (a)) and cAMP maximal response (Figure 3.6, (b)). The glycosylation status of FSH appeared to have little effect on cAMP production, even though  $EC_{50}$  values for FSH21/18 were the lowest for both the AUC (2.8ng/ml) and maximal response (3.14ng/ml) data (Figure 3.6, (c)). This suggests that by this time point all glycoforms of FSH are able to induce similar total amounts of cAMP.

To investigate kinetics of the FSH glycoforms, their effect on cAMP production was measured at earlier time points. The AUC and maximal response were measured at 2-, 5- and 15-minutes from the 30-minute data (Figure 3.7). At 2 minutes, a concentration- and



(c)

	EC <sub>50</sub> (ng/ml)	
	AUC	Maximal response
eFSH	8.37	7.77
FSH21/18	2.80	3.14
FSH24	5.54	4.70
dg-eLHt	84.14	36.33

**Figure 3.6: Concentration-dependent effects of FSH glycoforms on cAMP accumulation during 30-minute stimulation.** HEK293 cells transiently co-expressing the HA-tagged FSHR and pGloSensor™-20F plasmid were pre-equilibrated for 2 hours at 37°C and then treated for 30 minutes with increasing concentrations (0-100ng/ml) of eFSH, FSH21, FSH24 or dg-eLHt. **(a)** AUC of cAMP accumulation, which indicates the total amount of cAMP accumulation. **(b)** Maximal cAMP response. **(c)** EC<sub>50</sub> values. Data represented as fold change/basal and analysed using ordinary two-way ANOVA, followed by Dunnett's multiple comparisons test. All data represent mean ± SEM of n=3-5 independent experiments conducted in triplicate. \*, *p*<0.05; \*\*, *p*<0.01; \*\*\*, *p*<0.001; \*\*\*\*, *p*<0.0001. Asterisks colours represent comparisons between a specific treatment group and basal.

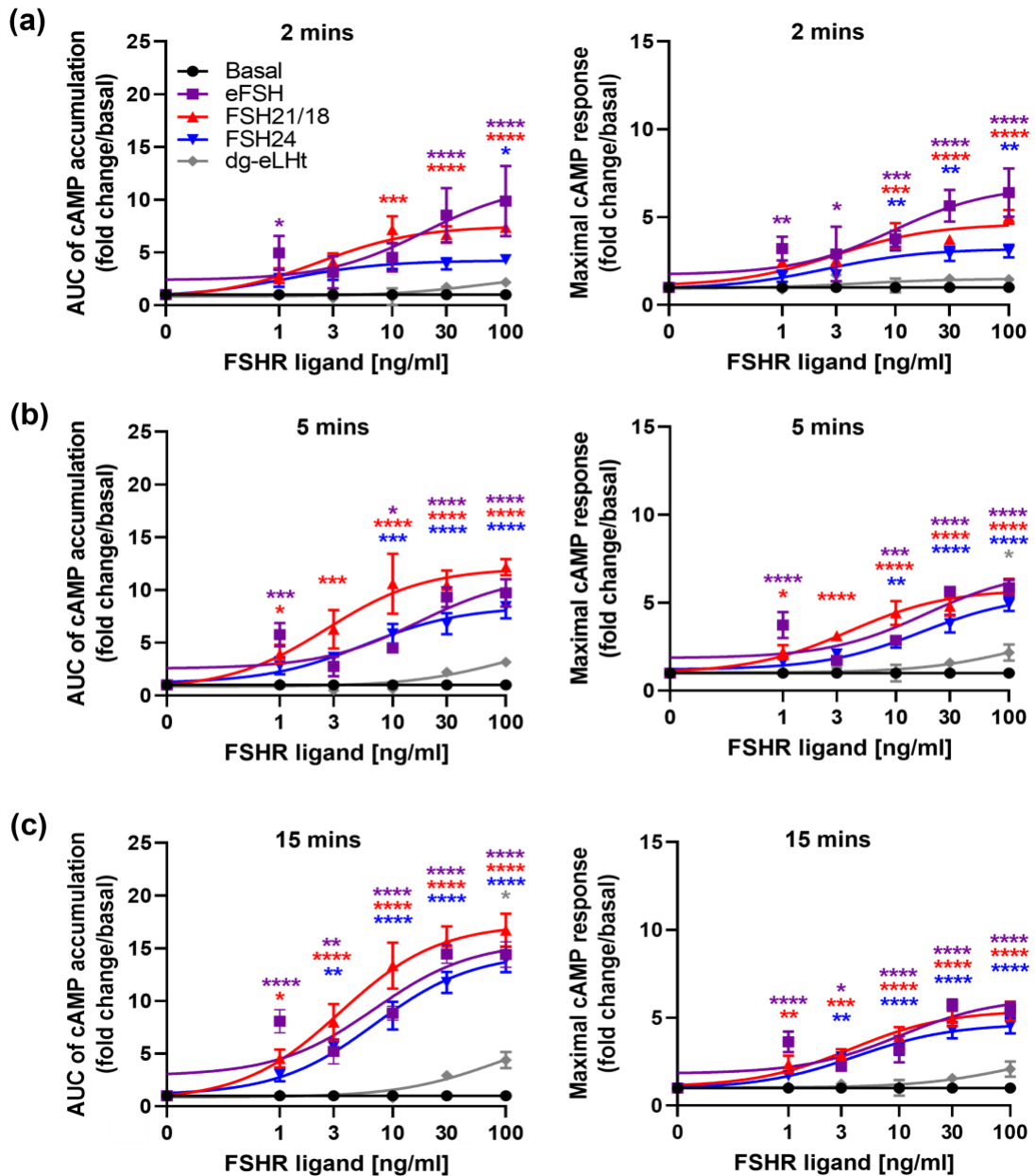


**Figure 3.7: Concentration-dependent effects of FSH glycoforms on total cAMP accumulation during 2-, 5- and 15-minute stimulation.** HEK293 cells transiently co-expressing the HA-tagged FSHR and pGloSensor™-20F plasmid were pre-equilibrated for 2 hours at 37°C and then treated for up to 30 minutes with increasing concentrations (0-100ng/ml) of eFSH, FSH21, FSH24 or dg-eLHt. The AUC of cAMP accumulation and maximal cAMP response was measured at **(a)** 2 minutes, **(b)** 5 minutes, and **(c)** 15 minutes. Data represented as fold change/basal and analysed using ordinary two-way ANOVA, followed by Dunnett's multiple comparisons test. All data represent mean  $\pm$  SEM of n=3-5 independent experiments conducted in triplicate. \*,  $p < 0.05$ ; \*\*,  $p < 0.01$ ; \*\*\*,  $p < 0.001$ ; \*\*\*\*,  $p < 0.0001$ . Asterisks colours represent comparisons between a specific treatment group and basal.

ligand- dependent difference in the total amount of cAMP accumulated and maximal response was observed (Figure 3.7, (a)). FSH21/18 induced a higher fold-increase in cAMP production in contrast to FSH24. By 5-minute stimulation, cAMP production continued to increase for all FSH glycoform treatments, apart from dg-eLHt, with FSH21/18 evoking the highest AUC for cAMP accumulation (Figure 3.7, (b)). The maximal cAMP response appeared to remain similar with less differences between the different FSH glycoforms, suggesting that the highest amount of cAMP is produced very rapidly after stimulation. Similar to the 30-minute data, by 15 minutes, FSH glycoform-dependent differences in the AUC of cAMP accumulation and maximal response became less apparent (Figure 3.7, (c)). This suggests that the ability for FSH glycoforms to differentially stimulate cAMP production is less effective as early as 15 minutes following stimulation in HEK293 cells. As expected, dg-eLHt displayed the lowest efficacy and potency, with increases in total cAMP accumulation emerging at concentrations above 10ng/ml for all time points (Figure 3.7). Which further supports reports that show dg-eLHt behaving as a  $\beta$ -arrestin biased agonist at low concentrations (Butnev et al., 2002; Wehbi et al., 2010).

To understand how cAMP production correlated with the PD-PALM data, data from cells treated with 30ng/ml of FSH glycoforms was extrapolated and further analysed at 2-, 5-, and 15-minute time points (Figure 3.8). The mean cAMP accumulated over 30 minutes following a 30ng/ml treatment with all ligands were plotted (Figure 3.8, (a)). A 2-minute treatment with either eFSH and FSH21/18 induced a significant increase in cAMP production of  $8.6 \pm 2.6$ - and  $6.7 \pm 0.8$ -fold change/basal, respectively (Figure 3.8, (b)). There were no significant effects of either FSH24 or dg-eLHt, on cAMP production at this time point (Figure 3.8, (b)). When compared and correlated with PD-PALM data, a trend was observed at 2-minute treatment whereby 30ng/ml of eFSH and FSH21/18 promoted

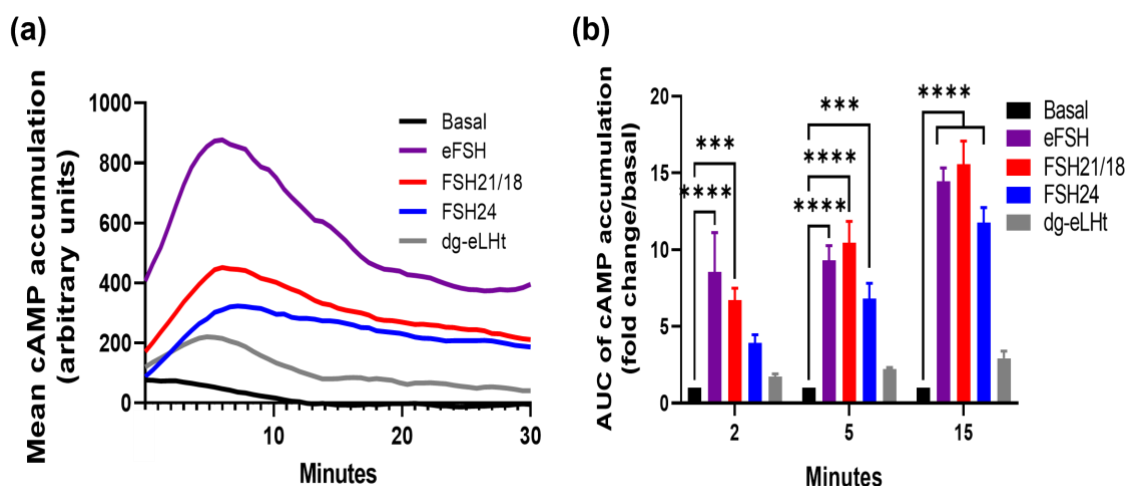


**Figure 3.8: 30ng/ml of FSH glycoforms differentially modulate cAMP production in a temporal manner.** HEK293 cells expressing the HA-tagged FSHR and pGloSensor™-20F plasmid to assess live GloSensor™ cAMP kinetics. Following treatment with 0-100ng/ml of eFSH, FSH21/18, FSH24 or dg-eLHt, 30ng/ml data was extrapolated and analysed. **(a)** Smoothened curve of the mean cAMP accumulation following treatment over 30 minutes (no error bars). **(b)** AUC of the mean ligand-dependent cAMP accumulation at 2-, 5- and 15 minutes. AUC data was baseline subtracted and represented as fold change/basal. Data analysed using two-way ANOVA, followed by Dunnett's multiple comparisons test. All data represent mean  $\pm$  SEM of n=3-5 independent experiments, measured in triplicate. \*\*\*,  $p < 0.001$ ; \*\*\*\*,  $p < 0.0001$ .

dissociation of FSHR homomers into predominantly monomers (Figure 3.1, (b-c)), suggesting that dissociation of FSHR oligomers into monomers and re-organisation of FSHR oligomeric complexes may, at least in part, promote acute cAMP production. Moreover, that no change or enhancement of FSHR oligomerisation may facilitate low level production of cAMP.

Treatment for 5-minutes with FSH24 significantly increased cAMP (Figure 3.8, (b)). When compared to observations with PD-PALM data, a decrease in FSHR association at 5-minute



treatment with FSH24 was observed (Figure 3.2, (a)). This provided further support that FSHR dissociation into monomers may promote cAMP production. Predominantly eFSH- and FSH21/18-dependent pentamer dissociation was observed with acute 2- (Figure 3.1, (c)) and 5-minute treatment (Figure 3.2, (aii)) compared to FSH24-dependent FSHR dimer and trimer dissociation (Figure 3.2, (aii)). The dg-eLHt preparation failed to significantly stimulate cAMP production (Figure 3.8, (b)), as compared to PD-PALM data, which showed increased FSHR oligomerisation (Figure 3.1). 15-minute stimulation with either eFSH, FSH21/18 or FSH24 continued to significantly increase cAMP production (Figure 3.8, (b)). At this time point, FSHR homomer arrangements predominantly resembled basal conditions in all treatment groups (Figure 3.2, (b)), suggesting that this receptor configuration may be important in initiating FSHR signal activation, with other mechanisms such as receptor internalisation important in maintaining cAMP production thereafter. As anticipated, dg-eLHt was unable to induce significant cAMP production at any time point analysed (Figure 3.8, (b)). PD-PALM data at the corresponding time point showed preferential re-arrangement of FSHR into higher order oligomers (Figure 3.2, (b)), suggesting that low level cAMP production (and potential  $\beta$ -arrestin recruitment and subsequent signalling) may be mediated, at least in part, by FSHR oligomer formation.

Next, to determine the correlation between cAMP production and PD-PALM data from cells treated with 1ng/ml of FSH glycoforms, data from cells treated with 1ng/ml of FSH glycoforms was extrapolated and further analysed at 2-, 5- and 15-minutes time points (Figure 3.9). An acute, 2-minute treatment with all ligands, except eFSH, showed minimal increases in cAMP production in comparison to basal (Figure 3.9, (b)). When compared to

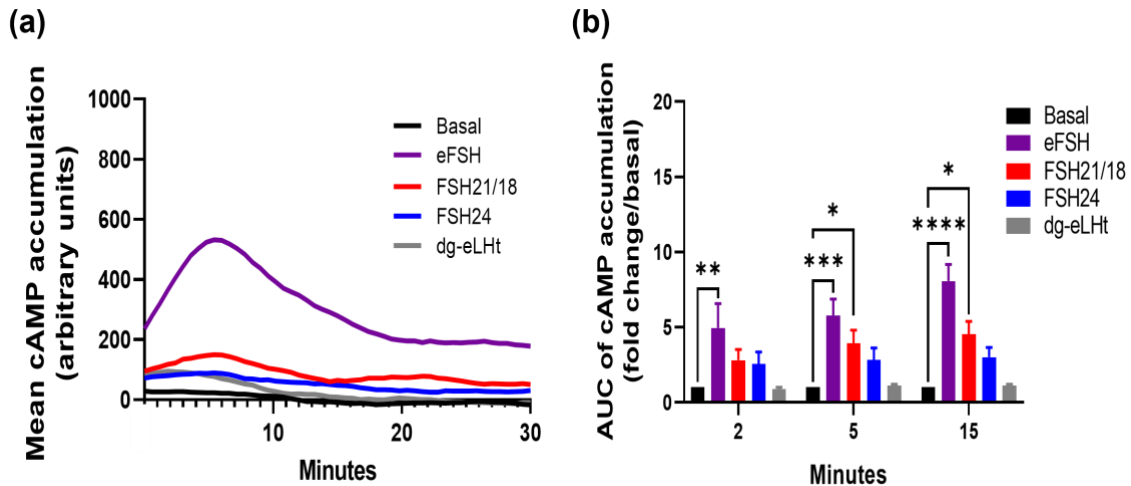


**Figure 3.9: 1ng/ml of FSH glycoforms differentially modulate cAMP production in a temporal manner.** HEK293 cells expressing the HA-tagged FSHR and pGloSensor<sup>TM</sup>-20F plasmid to assess live GloSensor<sup>TM</sup> cAMP kinetics. Following treatment with 0-100ng/ml of eFSH, FSH21/18, FSH24 or dg-eLHt, 1ng/ml data was extrapolated and analysed. **(a)** Smoothened curve of the mean cAMP accumulation following treatment over 30 minutes (no error bars). **(b)** AUC of the mean ligand-dependent cAMP accumulation at 2-, 5- and 15 minutes. AUC data was baseline subtracted and represented as fold change/basal. Data analysed using two-way ANOVA, followed by Dunnett's multiple comparisons test. All data represent mean  $\pm$  SEM of n=3-5 independent experiments, measured in triplicate. \*,  $p < 0.05$ ; \*\*,  $p < 0.01$ ; \*\*\*,  $p < 0.001$ ; \*\*\*\*,  $p < 0.0001$ .

the PD-PALM data (Figure 3.1), these data correlated with a lack of effect on FSHR oligomerisation at 2 minutes, following 1ng/ml treatment with any FSH glycoform (Figure 3.3, (b-c)). At 5- and 15 minutes, although an eFSH-dependent increase in cAMP production of  $5.8 \pm 1.1$ - and  $8.1 \pm 1.1$ -fold was observed, respectively (Figure 3.9, (b)), when correlated to the PD-PALM data at these time points, no changes in the total percentage of FSHR homomers at the plasma membrane were observed (Figure 3.4). This suggests that there may be a dose-dependent threshold for different FSH glycosylated ligands to modulate FSHR homomerisation. Small changes were observed in FSHR homomer subtypes, which may be important for modulating the magnitude of cAMP

signalling, however this remains to be demonstrated. In contrast, FSH24 treatment at 5- and 15-minutes had no significant effect on cAMP production (Figure 3.9, (b)). When correlating PD-PALM analysis, an increase in FSHR oligomerisation was observed, predominately from enhanced formation of pentamers (Figure 3.4, (a)), which may indicate that low level cAMP production may favour FSHR association. Moreover, there was increases in the total percentage of FSHR homomers with FSH21/18 treatment at 15 minutes (Figure 3.4, (bi)), correlating with low level cAMP production at the same time (Figure 3.9, (b)). As anticipated, no significant changes in cAMP were observed following 2-, 5-, or 15-minute treatment with dg-eLHt (Figure 3.9, (b)).

To explore the correlation between the effect of FSH glycoform-dependent FSHR oligomerisation on CREB-phosphorylation, cultured cells were treated with  $\pm$  30ng/ml of either FSH21/18 or FSH24 for 0-, 2-, 5-, 15 or 30 minutes and lysates were prepped for membrane blotting and primary antibody incubation (see chapter 2.7 for details). Blots showed a triphasic trend in FSH21/18-dependent CREB-phosphorylation (Figure 3.10, (a)). CREB-phosphorylation was increased by 2-minute treatment, then decreased by 5- and 15-minutes, and finally increased again by 30-minutes (see Appendix II for full uncropped blots). Densitometric analysis of the blots revealed a  $3.4 \pm 0.7$ -fold increase/basal in FSH21/18-dependent CREB-phosphorylation by 2-minute treatment when compared basal levels ( $p < 0.01$ ) (Figure 3.10, (b)). When cells were treated with 30ng/ml of FSH24, blots revealed a gradual decrease in CREB-phosphorylation after 5-minutes treatment (Figure 3.10, (a)). Densitometric analysis of the blots further confirmed a decreasing trend of  $86 \pm 4.6\%$  in FSH24-dependent CREB-phosphorylation by 15-minute treatment ( $p = 0.301$ ) (Figure 3.10, (b)), suggesting that FSH24 may mediate alternative FSHR

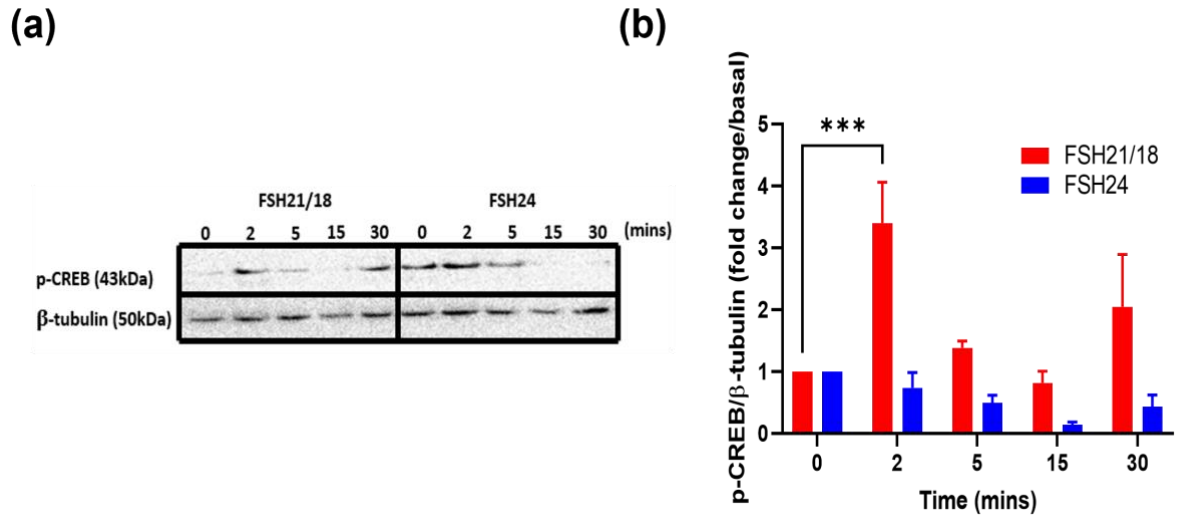


**Figure 3.10: Different FSH glycoforms stimulate differential CREB-phosphorylation.** HEK293 cells were transiently expressing HA-tagged FSHR. Following treatment with  $\pm$  30ng/ml with either FSH21/18 or FSH24, cells were lysed, and lysates probed for p-CREB. **(a)** Representative Western blots of FSH21/18 and FSH24-dependent p-CREB. **(b)** Densitometric analysis of (a). Each p-CREB was normalised to  $\beta$ -tubulin internal loading control and expressed as fold change/basal CREB-phosphorylation. Data was analysed using ordinary two-way ANOVA, followed by Dunnett's multiple comparisons test. Each data point represents mean  $\pm$  SEM for  $n=3$  independent experiments. \*\*\*,  $p < 0.001$ .

downstream signalling pathways. Increases in FSH21/18-dependent CREB-phosphorylation at 2-minute treatment correlated with FSHR dissociation in monomers during PD-PALM experiments (Figure 3.1) and increases in cAMP production (Figure 3.8, (b)) at the same time point, further suggesting a role for FSHR oligomers in mediating  $G\alpha_s$ /cAMP/PKA/CREB signalling.

### 3.2.3 Effect of FSH glycoform-dependent FSHR oligomerisation on cre-luciferase activity

Next, to investigate the correlation between FSH glycoform-dependent FSHR oligomerisation on the effect of cre-luciferase activity, cultured cells were stimulated with increasing concentrations (0-100ng/ml) of eFSH, FSH21/18, FSH24 or dg-eLHt for 4-6 hours at 37°C (Figure 3.11, (a)) (see chapter 2.6 for details). eFSH and FSH21/18 induced similar cre-luciferase activity at all concentrations with a maximal  $22.5 \pm 3.3$ - and  $19.17 \pm 0.9$ -fold increase in cre-luciferase activity at 100ng/ml, respectively (Figure 3.11, (a)). FSH24-treated cells induced less cre-luciferase activity than FSH21/18 at higher concentrations, inducing a maximal  $15.1 \pm 1.4$ -fold increase in cre-luciferase activity at 100ng/ml (Figure 3.11, (a)). This suggests that FSH24 displays less efficacy at inducing cre-luciferase activity when it engages with the FSHR. As anticipated, dg-eLHt failed to induce any changes in cre-luciferase activity at concentrations  $\leq 10$ ng/ml when compared to basal activity. However, at the higher concentrations of  $\geq 10$ ng/ml, dg-eLHt appeared to act as a weak activator of cre-luciferase activity (Figure 3.11, (a)), which was also observed in the cAMP GloSensor™ data (Figure 3.6-3.7) and corroborates with previous reports when cAMP accumulation was assessed (Wehbi et al., 2010).

Comparison of 30ng/ml treatments with FSH glycoforms, which correlated with PD-PALM, GloSensor™ cAMP and Western blot experiments, showed ligand-dependent significant increases in cre-luciferase activity by  $>10$ -fold when compared to basal ( $p < 0.0001$ ) (Figure 3.11, (b)). FSH21/18 induced higher cre-luciferase activity ( $17.8 \pm 0.7$ -fold) than FSH24 ( $11.8 \pm 0.8$ ), which correlated with the GloSensor™ cAMP data (Figure 3.8), and further suggests that the changes observed in FSHR complexes at the plasma

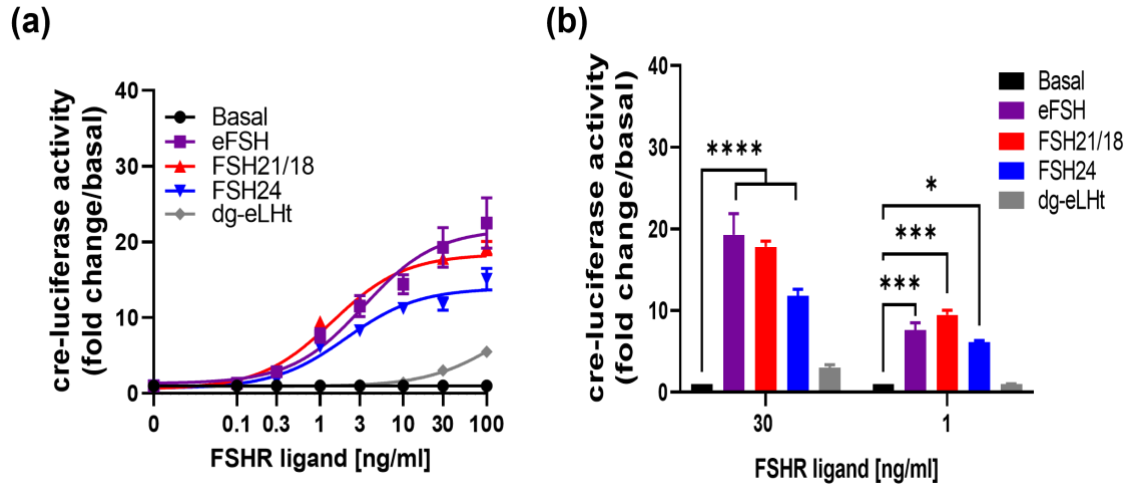


**Figure 3.11: Different concentration of FSH glycoforms stimulate differential cre-luciferase activity.** HEK293 cells were co-transfected with cre-luciferase and *Renilla*-luciferase plasmids. Cells were treated in serum-free media for 4-6 hours with increasing concentrations (0-100ng/ml) of eFSH, FSH21/18, FSH24 or dg-eLHt. **(a)** Concentration-dependent effects of FSHR ligands on cre-luciferase activity. **(b)** Extrapolation of data from (a) to measure the effect of  $\pm$  30- and 1ng/ml of eFSH, FSH21/18, FSH24 or dg-eLHt on cre-luciferase activity. Each cre-luciferase reading was normalised to *Renilla*-luciferase readings for transfection efficiency control. Data represented as fold change/basal and analysed using ordinary two-way ANOVA, followed by Dunnett's multiple comparisons test. Each data point represents mean  $\pm$  SEM for n=3-5 independent experiments, measured in triplicate. \*,  $p < 0.05$ ; \*\*\*,  $p < 0.001$ ; \*\*\*\*,  $p < 0.0001$ .

membrane may contribute to modulating the magnitude of cre-responsive gene activation. 30ng/ml of dg-eLHt was unable to induce changes in cre-luciferase activity, which may be mediated by the increases in FSHR oligomer formation observed at the plasma membrane (Figure 3.2). Comparison of cre-luciferase responses following 1ng/ml treatment with eFSH, FSH21/18, FSH24 and dg-eLHt revealed both eFSH and FSH21/18 induced a  $7.6 \pm 0.9$ - and  $9.5 \pm 0.6$ -fold increase in cre-luciferase activation, respectively ( $p < 0.001$ ) (Figure 3.11, (b)), with FSH24 inducing a  $6.1 \pm 0.2$ -fold increase in cre-luciferase activity ( $p < 0.05$ ) (Figure 3.11, (b)). This suggests there may be a correlation, as differential regulation of FSHR homomeric forms and cAMP production was observed at this concentration. As predicted, dg-eLHt failed to significantly induce any increase in cre-luciferase activity (Figure 3.11, (b)), further supporting its  $\beta$ -arrestin biased agonist activity.

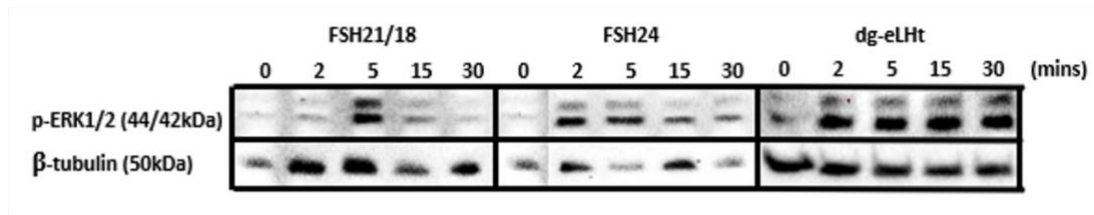
### 3.2.4 Effect of FSH glycoform-dependent FSHR oligomerisation on ERK1/2-phosphorylation

FSH glycoforms have been shown to mediate  $\beta$ -arrestin-dependent ERK signalling (Zariñán et al., 2020). Therefore, to understand the correlation between FSHR oligomerisation and ERK1/2 activation, cells were treated with 30ng/ml of FSH21/18, FSH24 or dg-eLHt for 0-, 2-, 5-, 15- or 30 minutes and phosphorylated-ERK1/2 protein abundance was determined from Western blot analysis (see chapter 2.7 for details). Blots showed FSH21/18 increased ERK1/2-phosphorylation by 5-minutes, and decreased thereafter, whereas FSH24 appeared to induce increases in ERK1/2-phosphorylation as early as 2-minutes (Figure 3.12, (a)). Furthermore, dg-eLHt-treated cells displayed increasing trends in ERK1/2-phosphorylation for all time points (Figure 3.12, (a)), supporting its role as a  $\beta$ -arrestin biased agonist as  $\beta$ -arrestin scaffolding has been shown to induce ERK signalling (Ulloa-Aguirre et al., 2013) (see Appendix II for full uncropped blots).

Densitometric analysis of blots further revealed FSH21/18 induced  $1.7 \pm 0.5$ -fold increase and FSH24 a  $2.7 \pm 0.1$ -fold increase in ERK1/2-phosphorylation at 5-minute treatment, whereas dg-eLHt induced  $2.1 \pm 0.4$ -fold increase in ERK1/2-phosphorylation at 30-minute treatment (Figure 3.12, (b)), although significant was not determined due to low  $n$  numbers ( $n=2-3$ ). PD-PALM data at the corresponding time points show potentially opposing results. FSH24-dependent decreases in FSHR association at 5-minute treatment correlated with potential increases in ERK1/2-phosphorylation compared to increases in dg-eLHt-dependent increases in FSHR association at 5-minute treatment and a potential lack of corresponding ERK1/2-phosphorylation. These data may suggest  $\beta$ -arrestin-dependent



(a)



(b)

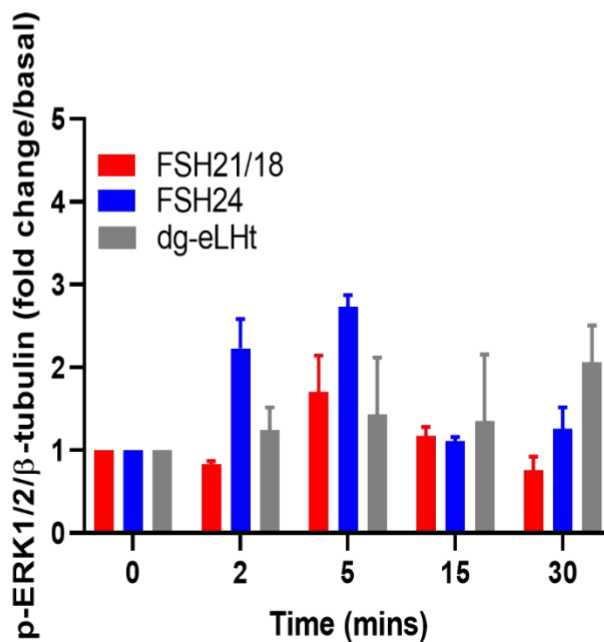


**Figure 3.12: Differential FSH glycoforms may stimulate differential ERK1/2-phosphorylation.** HEK293 cells transiently expressing HA-tagged FSHR were treated with  $\pm$  30ng/ml with either FSH21/18, FSH24 or dg-eLHt for 0-30 minutes. Cells were lysed and lysate probed for p-ERK1/2. **(a)** Representative Western blots of FSH21/18, FSH24 and dg-eLHt-dependent p-ERK1/2. **(b)** Densitometric analysis of (a). Each p-ERK1/2 was normalised to  $\beta$ -tubulin internal loading control and expressed as fold change/basal ERK1/2-phosphorylation. Each data point represents mean  $\pm$  SEM for n=2-3 independent experiments.

ERK1/2 signalling may be mediated, in part, by alternative mechanisms other than FSHR oligomerisation.

### 3.3 Discussion

FSH glycosylation variants have been previously shown to display differences in the magnitude of signal activation and specificity of pathways activated (Bousfield et al., 2018; Jiang et al., 2015; Wang et al., 2016b; Zariñán et al., 2020). Yet how FSHR decodes and propagates such signal diversity and differences in signal amplitude and duration remains unknown. GPCR homomerisation is a well-recognised mechanism for modulating functional diversity and specifying signal responses (Milligan et al., 2019; Sleno & Hébert, 2018). These findings support a mechanism for cAMP-mediated pathways and a potential for ERK-phosphorylation.

These data have shown that pituitary FSH glycoforms regulate FSHR homomerisation in a time- and concentration-dependent manner. At higher physiological concentrations, eFSH and FSH21/18 rapidly dissociated FSHR homomers predominantly into monomers, correlating with significant increases in eFSH and FSH21/18-dependent cAMP production and cre-luciferase activity. Interestingly, FSH24 displayed slower temporal kinetics in modulating FSHR homomerisation but dissociated FSHR homomers into predominantly monomers at time points when cAMP production was significantly increased. These data are in concordance with early studies of the related glycoprotein hormone receptor, TSHR, where FRET and co-immunoprecipitation analysis revealed less active dimer and oligomer conformations dissociated into monomers upon TSH stimulation (Latif et al., 2002). Conversely, at high concentrations of the  $\beta$ -arrestin biased agonist, dg-eLHt, a rapid increase in FSHR homomerisation was observed. This suggests dg-eLHt displays functional selectivity at the FSHR, which corroborates previous reports (Wehbi et al., 2010), and has been previously documented for FSH glycoforms (Timossi et al., 1998; Timossi et al., 2000) and other ligands of the FSHR (Arey et al., 2008).

The glycoprotein hormone receptors have been previously reported to display inherent negative cooperativity, or functional asymmetry (Urizar et al., 2005). This has been described for homomers for many GPCRs (Ha & Ferrell, 2016; Rivero-Müller et al., 2013) and has been proposed as a mechanism for mediating more graded responses. It has additionally been suggested that negative cooperativity may play an important role in many biological responses as it can cause marked threshold and ultra-sensitivity, allowing a biological system to filter out small stimuli and respond decisively to suprathreshold stimuli (Ha & Ferrell, 2016). Moreover, within the FSHR, Jiang *et al.* predicted FSHR dissociation into monomers would enhance FSH binding and FSHR signalling activities by 3-fold (Jiang et al., 2014b). The study further suggested, via mutagenesis, that FSHR homomers was an inherent way to prevent additional FSH binding and constitutive receptor activation. These ideas are further supported by the findings within this chapter. FSHR dissociation following 30ng/ml stimulation, and FSHR association/no change following 1ng/ml stimulation, with FSH glycoforms may decode a concentration-dependent ligand threshold to regulate signal activation. In a physiological context within the ovary, such regulation may help prevent mass activation of FSHR, and fine-tune FSHR function during the fluctuations in FSH concentrations that are observed in different phases of folliculogenesis such as follicle recruitment, dominant follicle selection, and ovulation (Driancourt, 2001; Gougeon, 2010; Son et al., 2011).

Differences in binding affinity and the number of FSHR sites occupied by FSH21/18 and FSH24 have previously been reported, with FSH21/18 displaying a higher binding affinity to FSHR and occupying more FSHR (Butnev et al., 2015; Davis et al., 2014). Additionally, competition binding assays have shown that unlabelled eFSH and FSH21/18 were more efficacious at displacing <sup>125</sup>I-FSH24 and <sup>125</sup>I-FSH21/18 at lower concentrations than

unlabelled FSH24 (Bousfield et al., 2014a), supporting the differences in FSHR binding affinities. In the context of the findings in this chapter, it is possible that these reported differences in the binding properties of the FSH glycoforms may have implications for the temporal differences observed in FSHR oligomer re-arrangement and dissociation into monomers observed with eFSH and FSH21/18 versus FSH24. However, future studies are required to determine how FSH glycoform-dependent differences in FSHR binding affinity and kinetics may drive changes in FSHR oligomerisation.

When PD-PALM experiments were conducted using 100ng/ml of FSH21/18 and FSH24, FSHR molecules appeared to form clusters, possibly within endosomes. Nevertheless, this observation was speculative, since HEK293 cell endosomes were not characterised in this study. FSHR internalisation is a process that has been shown to be mediated by the molecular scaffold  $\beta$ -arrestin, and has long been established with roles in ERK-phosphorylation (De Pascali & Reiter, 2018; Gloaguen et al., 2011; Kara et al., 2006; Landomiel et al., 2019; Lefkowitz & Shenoy, 2005; Ulloa-Aguirre et al., 2013). Interestingly, a recent study has suggested FSH glycoform-specific differences in the dependency of  $\beta$ -arrestin for ERK activation (Zariñán et al., 2020). With the recently reported roles of ligand-dependent differences in regulatory ‘phosphorylation barcodes’ for other Class A GPCRs (Dwivedi-Agnihotri et al., 2020), it may be that FSH ligands generate differential phosphorylation barcodes resulting in ligand-specific modulation of FSHR trafficking and signal propagation. Recent reports have suggested that internalisation of FSHR is required for initiation of FSH-dependent cAMP production (Sposini et al., 2020). This study showed that low molecular weight FSHR agonists differentially modulate FSHR endocytosis (Sposini et al., 2020), and may explain the differential profiles observed in this chapter for activating cAMP. Although the PD-PALM data suggests FSHR oligomers

localised at the plasma membrane mediate cAMP signalling, these subset of FSHRs may be inactive and represent a snapshot of what happens at the plasma membrane. How FSH glycoforms direct FSHR internalisation and trafficking, remains to be determined. However, the use of single molecule imaging and single particle tracking presents exciting opportunities to determine the spatial-temporal regulation of these processes and uncover how/if different FSHR complexes that are both active and inactive are routed through the endosomal machinery to modulate FSH ligand-dependent signalling.

Biased signalling with FSH21/18 and FSH24 has been observed from this data as FSH21/18 induced CREB-phosphorylation more rapidly, in contrast to FSH24 that potentially induced ERK1/2-phosphorylation more rapidly. These results may contradict another study in HEK293 cells stably expressing the FSHR whereby FSH21/18 induced higher percentages of p-ERK1/2 (Zariñán et al., 2020). However, this study used higher concentrations of FSH (50ng/ml), demonstrating a possible threshold for FSH24-dependent p-ERK1/2 activation in HEK293 cells. Furthermore, previous *in vivo* studies that injected mice with FSH21/18 or FSH24 and performed Western blots on ovarian extracts at more chronic time points showed differing results (Hua et al., 2021; Wang et al., 2016b), suggesting that higher concentrations, prolonged treatment times and/or endocrine factors from *in vivo* models may induce opposing results and therefore play important roles on the actions of FSH glycoforms. Alternatively, these results may propose FSH24-dependent ERK1/2-phosphorylation via  $\beta$ -arrestin signalling in HEK293 cells, as other studies have suggested a link (Zariñán et al., 2020). However, caution is needed when interpreting results reported in this chapter due to low *n* numbers ( $n=2-3$ ). It would also be interesting to see what role FSHR oligomers play in  $\beta$ -arrestin recruitment at the FSHR when

stimulated by different FSH glycoforms using PD-PALM, however this remains to be determined.

This study utilised the FSHR biased agonist, dg-eLHt, with known preferential  $\beta$ -arrestin signalling at lower concentrations ( $\leq 1\text{nM}$ ) and weak cAMP activation (Wehbi et al., 2010). Higher concentrations of dg-eLHt enhanced FSHR oligomerisation in a temporal manner, which may have correlated with trend increases in ERK1/2-phosphorylation observed in the Western blot results and suggests FSHR oligomerisation could potentiate ERK signalling. Furthermore, Western blot results have shown the biased signalling displayed by dg-eLHt with its inability to induce CREB-phosphorylation at physiological concentrations, supporting its role as a  $\beta$ -arrestin biased agonist. However, results need to be treated with caution as the data represented  $n=2-3$ . For other GPCRs, agonist-dependent induction of homomerisation has also been observed, including the dopamine D2 receptor homodimers (Tabor et al., 2016). As dg-eLHt is a preferentially recruits  $\beta$ -arrestin, which has well established roles in receptor desensitisation and internalisation, we cannot rule out the induction of FSHR clustering, rather than FSHR oligomerisation, for initiation of FSHR internalisation. This is particularly important at high ligand concentrations, such as 100ng/ml, as FSHRs molecules appeared to be clustered within endosomes. Indeed, interesting next steps will be to explore the effects of FSH glycoforms on the desensitisation, internalisation, and trafficking of FSHR. It will be interesting to unpick how these observed differences in FSHR organisation at the plasma membrane may direct FSHR internalisation and trafficking, and to understand the relationship between canonical  $G\alpha_s$  coupling and  $\beta$ -arrestin recruitment and signalling.

Although eFSH has been reported as a very potent form of FSH, here it was shown that FSH21/18 exhibited the highest potency, displayed by having the lowest EC<sub>50</sub> values following 30-minute treatment during GloSensor™ experiments. It is possible that this may have been the result of technical limitations from the technique used. FSH-induced FSHR-cAMP production is a rapid process and the delay between stimulating cells and recording cAMP readings resulted in high basal cAMP levels for eFSH- and FSH21/18- stimulated cells, therefore underestimating their potency.

In conclusion, it has been demonstrated that differential FSHR glycoforms modulate FSHR homomerisation in a concentration and time-dependent manner. These data suggest that modulation of FSHR homomerisation may provide a mechanism to fine-tune signal specificity and amplitude. This may be important means to decode the occurring cyclical and age-dependent changes in FSH concentration and glycosylation patterns in both a physiological and pathophysiological context. Considering that current IVF protocols involve stimulating ovaries with predominantly FSH24, it raises important questions to consider when treating women for infertility-related issues. Moreover, modulation of FSHR homomerisation may provide potential novel therapeutic avenues for targeting FSHR to improve IVF outcomes.

4 **Chapter Four: Delineating how FSH glycoforms modulate FSHR trafficking and impact on cAMP-dependent signalling**



## 4.1 Introduction

The previous chapter revealed that FSH glycoforms mediate differential FSHR cAMP-dependent signalling, at least in part, by FSHR oligomer rearrangement. However, important mechanism by which the FSHR has been shown to modulate cAMP-dependent signalling is through membrane trafficking (Sposini et al., 2020), whereby intracellular compartments represent additional signalling platforms to mediate spatial encrypted signalling (Pavlos & Friedman, 2017; Sayers & Hanyaloglu, 2018). The internalised FSHR has been shown to traffic to two main distinct endosomal compartments; the classical EEA1/Rab5-positive EEs that is the precursor to the degradative Rab7-positive late endosome pathway, and the smaller APPL1-positive VEEs that plays a key role in GpHR recycling to the cell-surface (Sposini et al., 2020; Sposini et al., 2017).

Given that partially glycosylated FSH21/18 and fully glycosylated FSH24 display different *in vivo* bioactivities, activating cAMP differently (Bousfield et al., 2018), it suggests that they may activate different FSHR internalisation pathways by targeting the FSHR to distinct intracellular signalling compartments. Furthermore, with age-related differences in the abundance of FSH glycoforms previously reported (Bousfield et al., 2014b), and therefore a possible role in ovarian aging, understanding how FSH glycoforms regulate FSHR trafficking, and related signalling may identify alternative ways to further target the FSHR. This may have beneficial therapeutic implications for improving fertility outcomes. Therefore, the aim of this chapter was to determine the effect of FSH glycoforms on FSHR trafficking and impact on signal activation. The objectives to address this aim were to:

1. Determine the effect of inhibiting FSHR internalisation on FSH glycoform-dependent FSHR cAMP production and cre-luciferase activity in HEK293 cells.

2. Investigate the effect of FSH glycoforms on FSHR co-localisation to EEA1-positive endosomes in HEK293 cells.
3. Determine the effect of APPL1 silencing on FSH glycoform-dependent FSHR cAMP production and cre-luciferase activity in HEK293 cells.

## 4.2 Results

### 4.2.1 Effect of inhibiting FSHR internalisation on FSH glycoform-dependent FSHR cAMP production and cre-luciferase activity

Firstly, to determine the impact of FSHR internalisation on FSH glycoform-dependent FSHR cAMP production, transfected cells were cultured for GloSensor™ cAMP assay analysis (see chapter 2.5 for details). To inhibit endocytosis-dependent FSHR internalisation, cells were pre-treated with  $\pm 50\mu\text{M}$  of Dyngo®-4a, a potent dynamin GTPase inhibitor (McCluskey et al., 2013), for 30 minutes. Then cells were stimulated with  $\pm 10\text{ng/ml}$  of purified pituitary FSH (positive control), FSH21/18 or FSH24 for 30 minutes and live cAMP fluorescence measured to determine the AUC and maximal cAMP response (see chapter 2.5 for details).

When cells were stimulated with different FSH glycoforms, there was an increase in cAMP response for all treatments when compared to basal levels (Figure 4.1, (a)). When FSHR internalisation was inhibited in the presence of Dyngo®-4a, there appeared to be almost complete abrogation of FSH glycoform-dependent cAMP response (Figure 4.1, (b)), which corroborates with previous publications (Sposini et al., 2020). Furthermore, Dyngo®-4a inhibited all FSH glycoform-dependent total cAMP accumulation (Figure 4.2) and the maximal cAMP response (Figure 4.3) at all time points measured ( $p < 0.01$ ), suggesting that rapid endocytosis-dependent FSHR internalisation is required for FSH-dependent FSHR cAMP production.

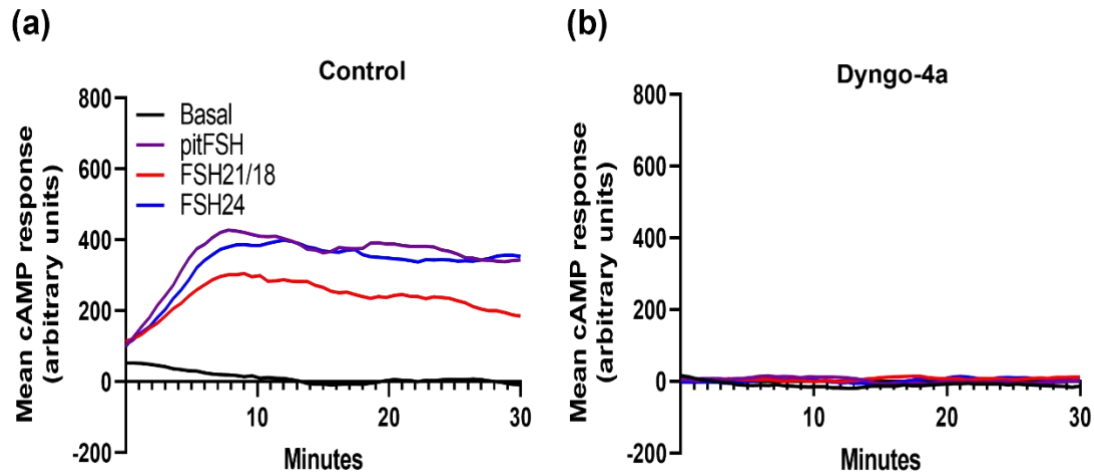


**Figure 4.1: Effect of Dyngo<sup>®</sup>-4a on FSH glycoform-dependent cAMP production.** HEK293 cells expressing HA-tagged FSHR were pre-treated for 30 minutes with  $\pm 50\mu\text{M}$  of Dyngo<sup>®</sup>-4a and then treated with  $\pm 10\text{ng/ml}$  of pituitary FSH, FSH21/18 or FSH24 for 30 minutes. **(a)** Cells stimulated with FSH glycoform in the absence of Dyngo<sup>®</sup>-4a. **(b)** Cells stimulated with FSH glycoform in the presence of Dyngo<sup>®</sup>-4a. Data shows smoothed curve of the mean cAMP accumulation following treatment over 30 minutes from  $n=3$  independent experiments measured in triplicate (no error bars).

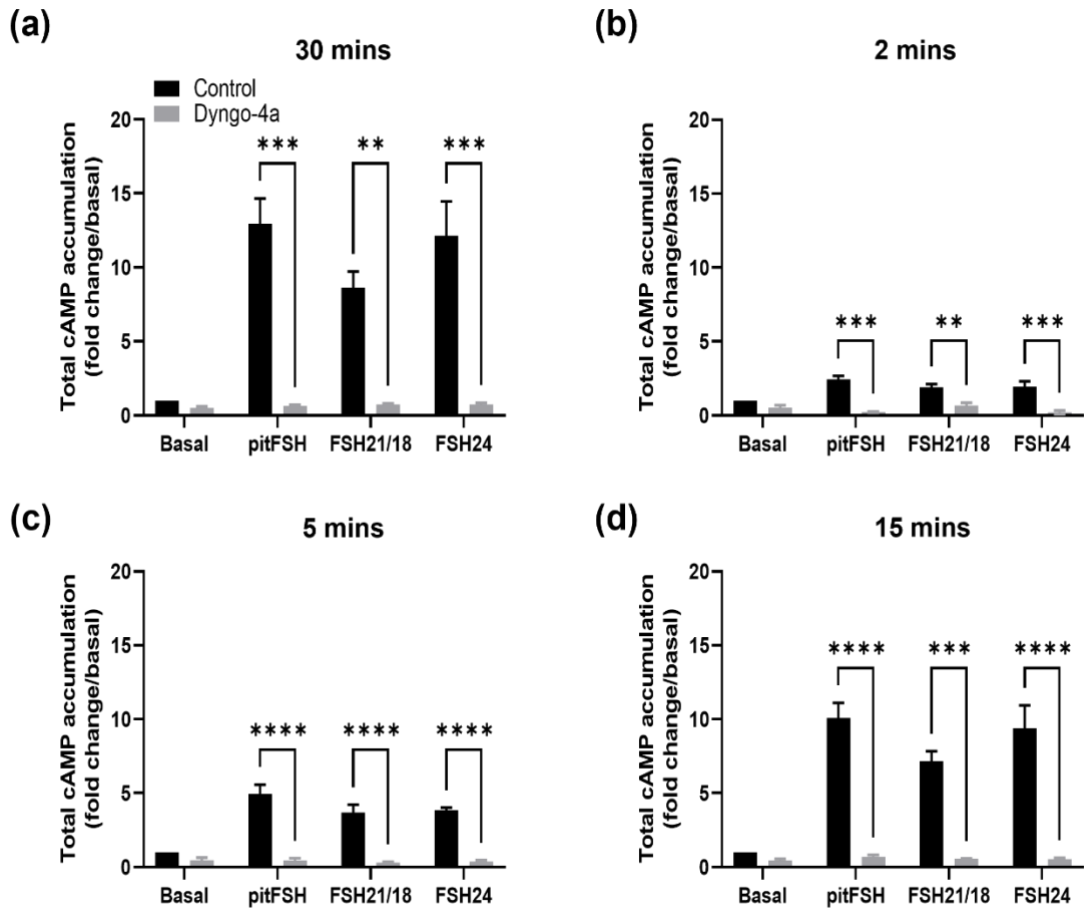


**Figure 4.2: Effect of Dyngo<sup>®</sup>-4a on FSH glycoform-dependent FSHR-dependent total cAMP accumulation.** HEK293 cells transiently expressing the HA-tagged FSHR were pre-treated for 30 minutes with  $\pm$  50 $\mu$ M of Dyngo<sup>®</sup>-4a and then treated with  $\pm$  10ng/ml of pituitary FSH, FSH21/18 or FSH24 for 30 minutes. The AUC of total cAMP accumulation was determined at (a) 30-, (b) 2-, (c) 5-, and (d) 15-minute time points. Data represented as fold change/basal. Data analysed using 2-way AVOVA, followed by Šidák's multiple comparison's test. \*\*,  $p < 0.01$ ; \*\*\*,  $p < 0.001$ ; \*\*\*\*,  $p < 0.0001$ .

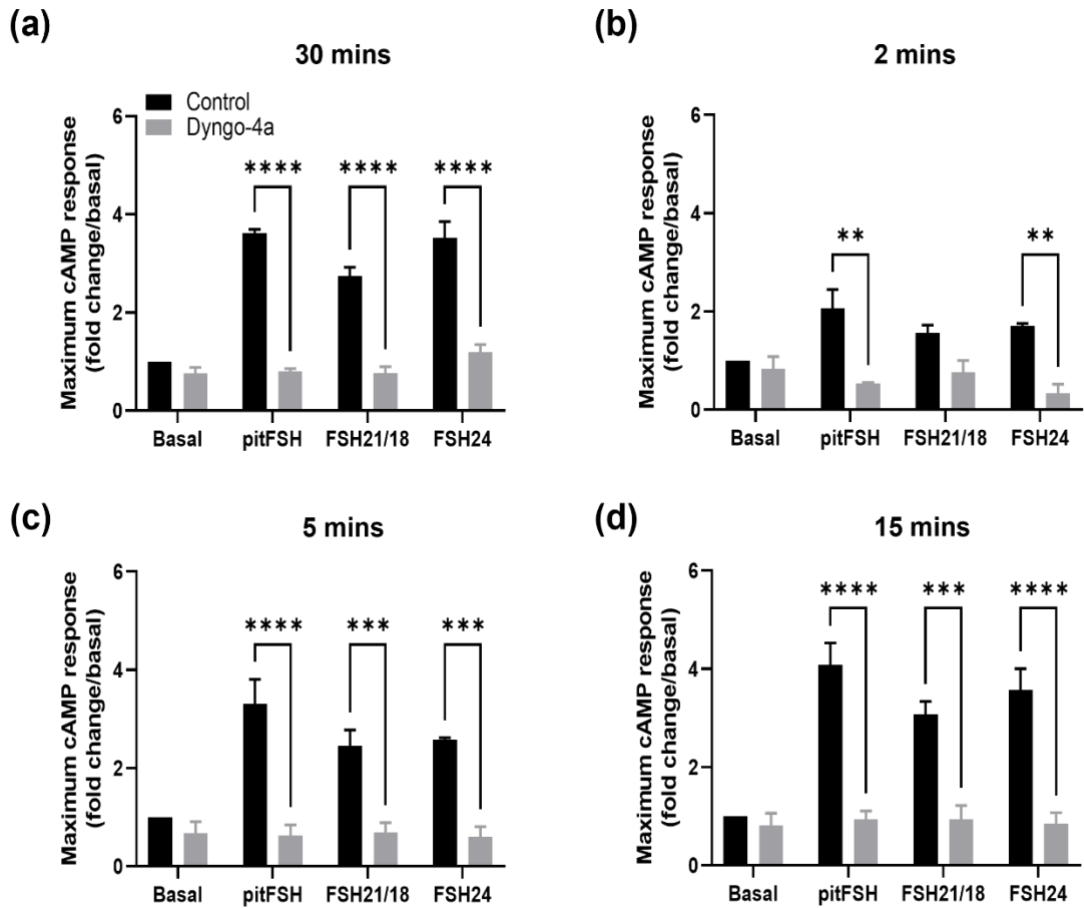


**Figure 4.3: Effect of Dyngo<sup>®</sup>-4a on FSH glycoform-dependent FSHR-dependent maximal cAMP response.** HEK293 cells transiently expressing the HA-tagged FSHR were pre-treated for 30 minutes with  $\pm$  50 $\mu$ M of Dyngo<sup>®</sup>-4a and then treated with  $\pm$  10ng/ml of pituitary FSH, FSH21/18 or FSH24 for 30 minutes. The maximal cAMP response was determined at **(a)** 30-, **(b)** 2-, **(c)** 5-, and **(d)** 15-minute time points. Data represented as fold change/basal. Data analysed using 2-way AVOVA, followed by Šidák's multiple comparison's test. \*\*,  $p < 0.01$ ; \*\*\*,  $p < 0.001$ ; \*\*\*\*,  $p < 0.0001$ .

Unlike previous results, FSH21/18 was less potent than FSH24 at stimulating cAMP production as FSH21/18-dependent cAMP production was less apparent (Figure 4.1, (a)). Following 30-minute stimulation, FSH21/18 stimulated an  $8.6 \pm 1.1$ -fold increase in total cAMP accumulation compared to an FSH24-dependent  $12.2 \pm 2.3$ -fold increase in cAMP accumulation when compared to basal (Figure 4.2, (a)). However, these observations may be due to differences in the preparation and purification of a new batch of FSH glycoforms.

To assess how the impact of Dyngo<sup>®</sup>-4a on FSH-glycoform FSHR-dependent cAMP accumulation related to downstream cre-luciferase activity, cultured cells, that were pre-treated in  $\pm 50\mu\text{M}$  of Dyngo<sup>®</sup>-4a, were stimulated with increasing concentrations of either pituitary FSH, FSH21/18 or FSH24 (0-100ng/ml) (Figure 4.4). Like the GloSensor<sup>™</sup> cAMP data, Dyngo<sup>®</sup>-4a completely inhibited all FSH glycoform-dependent cre-luciferase activity (Figure 4.4). However, at higher concentrations of FSH21/18 ( $>3\text{ng/ml}$ ), Dyngo<sup>®</sup>-4a's ability to inhibit cre-luciferase activity was reduced, as increases in cre-luciferase activity began to emerge (Figure 4.4, (b)). Similar results were observed in FSH24-treated cells at even higher concentrations ( $>10\text{ng/ml}$ ) (Figure 4.4, (c)), and may be because FSH24 is less potent than FSH21/18. These results suggest that further downstream FSHR signalling pathway the effects of Dyngo<sup>®</sup>-4a is reduced.

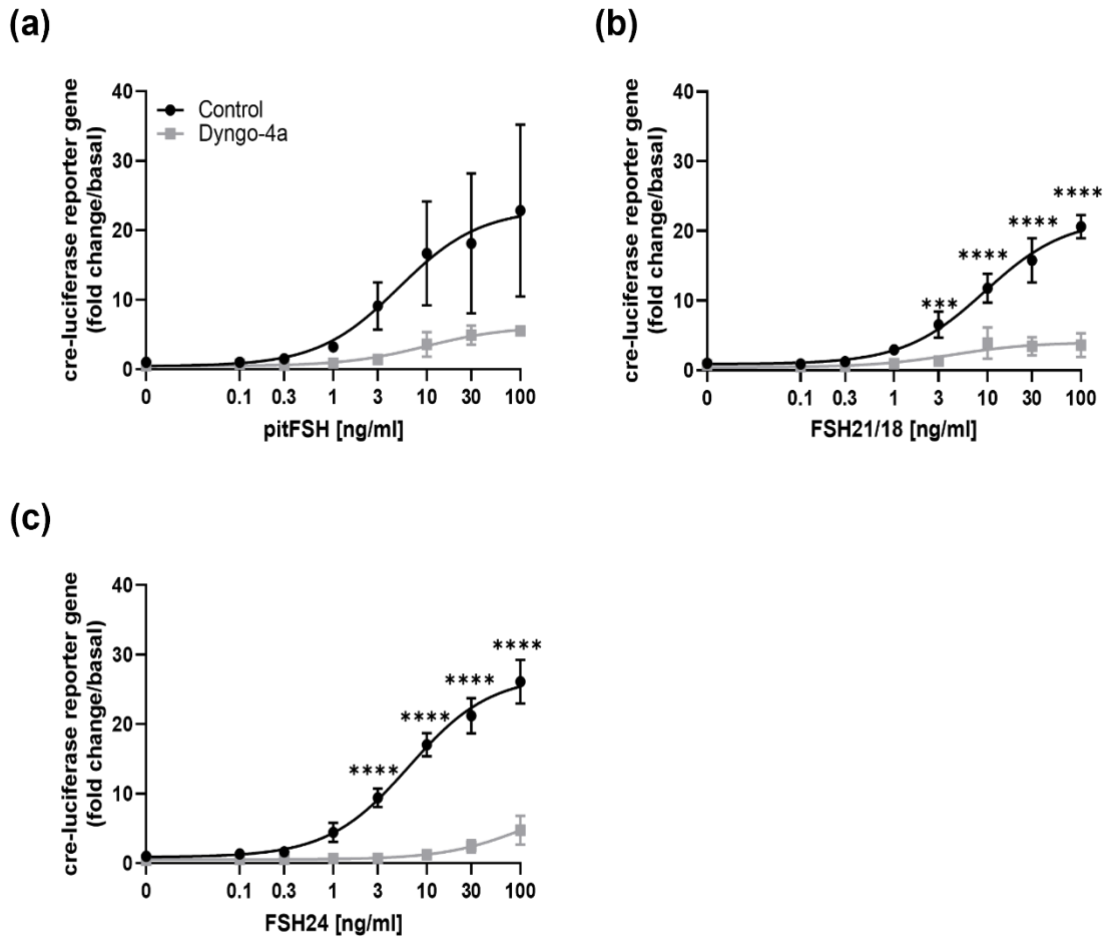


**Figure 4.4: Effect of Dyngo<sup>®</sup>-4a on FSH glycoform-dependent FSHR-dependent cre-luciferase activity.** HEK293 transiently co-expressing HA-tagged FSHR, and cre-luciferase and *Renilla*-luciferase were pre-treated in serum-free media with  $\pm$  50 $\mu$ M of Dyngo<sup>®</sup>-4a for 30 minutes. Cells were then treated for 4-6 hours with increasing concentrations (0-100ng/ml) of **(a)** pituitary FSH (n=2), **(b)** FSH21/18 (n=3), or **(c)** FSH24 (n=3). All data points were normalised to *Renilla*-luciferase for transfection efficiency and represented as fold change/basal. Data analysed using 2-way ANOVA, followed by Šidák's multiple comparison's test. Each data point represents mean  $\pm$  SEM for n=2-3 independent experiments, measured in triplicate. \*\*\*,  $p < 0.001$ ; \*\*\*\*,  $p < 0.0001$ .



#### 4.2.2 Effect of FSH glycoforms on FSHR co-localisation to EEA1-positive endosomes

FSHR co-localisation with EEA1-positive endosomes was analysed to delineate the endosomal compartment internalised FSHRs were routed to in the presence of different FSH glycoforms. EEA1 is an intermediate marker for EE formation and a prerequisite for GPCR degradation via lysosomes. To achieve this, cells transiently expressing FLAG-FSHR were cultured for immunocytochemistry immunofluorescence analysis via confocal microscopy (see chapter 2.8 for details).

Following stimulation with  $\pm$  30ng/ml of pituitary FSH (positive control), FSH21/18 or FSH24, cell membranes were stripped of FLAG antibody bound to plasma membrane FSHR. This was to aid visualisation of internalised FSHR rather than membrane bound FSHR. following ligand stimulation (Figure 4.5, (a)). At basal level, the majority of internalised FSHR were not co-localised to EEA1-positive endosomes (Figure 4.5, (bi and ci), with only  $18.8 \pm 2.2\%$  of FSHR targeted to EEA1-positive endosomes (Figure 4.5, (bii and cii)). 5-minute stimulation with pituitary FSH resulted in a small increase in FSHR-positive EEA1 endosomes ( $28.5 \pm 2.5\%$ ) (Figure 4.5, (bii)), However, in FSH21/18- or FSH24-stimulated cells, 5-minute treatment resulted in no changes in the percentage of FSHR co-localisation to EEA1-positive endosomes when compared to basal level (Figure 4.5, (bii)). 15-minute treatment with FSH21/18 appeared to induce an increase in the percentage of FSHRs co-localised to EEA1-positive endosomes ( $34.0 \pm 4.0\%$ ), whereas FSH24 induced no changes when compared to basal level (Figure 4.5, (cii)). This suggests the majority of FSHRs are routed to alternative endosomal compartments that regulate the differential cAMP signalling display by FSH glycoforms.

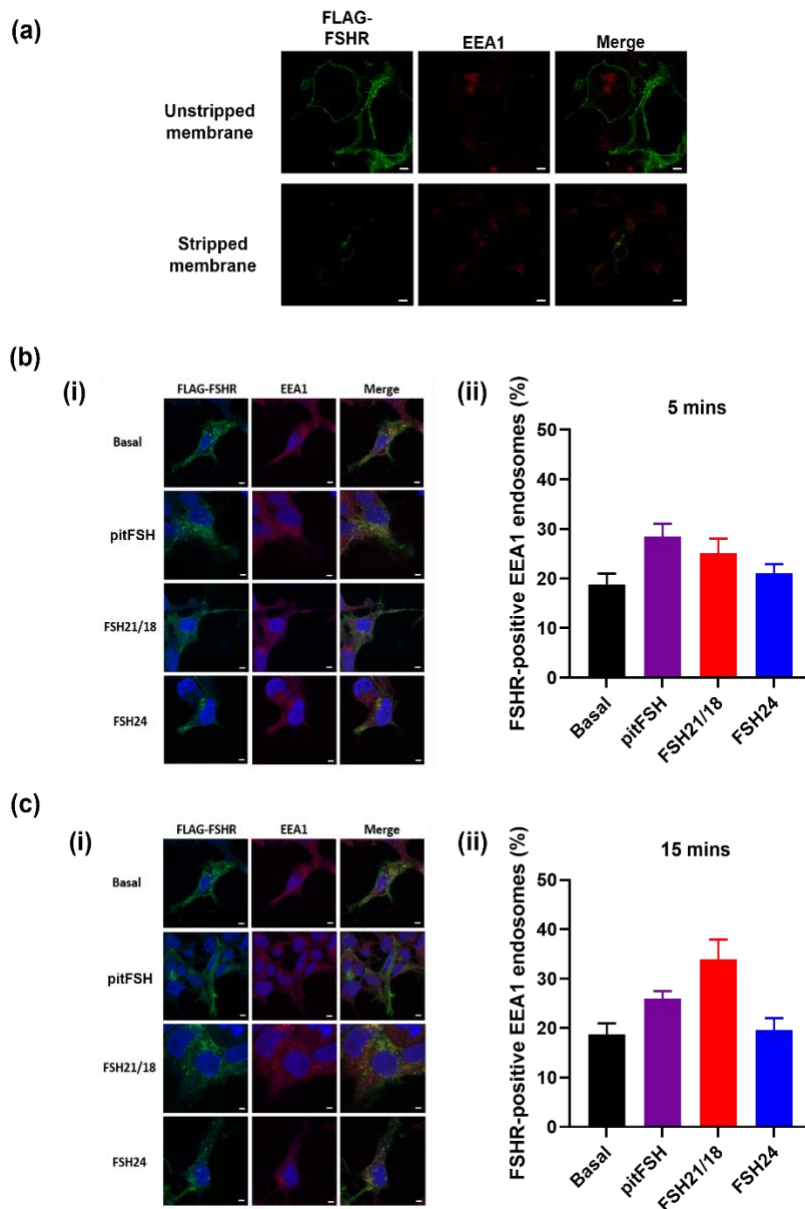


**Figure 4.5: Effect of different FSH glycoforms on FSHR targeted to EEA1-positive endosomes.** HEK293 transiently expressing FLAG-tagged FSHR were incubated with mouse anti-FLAG primary antibody (1:500). Following treatment with  $\pm$  30ng/ml of pituitary FSH, FSH21/18 or FSH24, cells were washed in cold PBS (+  $\text{Ca}^{2+}$ ) and treated with  $\pm$  0.04% EDTA in PBS (-  $\text{Ca}^{2+}$ ) to strip the remaining antibodies from the plasma membrane and assess internalised FSHRs. Cells were fixed in 4% (v/v) PFA, permeabilised with 0.2% (v/v) Triton-X and incubated with rabbit anti-EEA1 primary antibody (1:500). Cells were subsequently blocked and incubated in goat anti-mouse AlexaFluor 488 and goat anti-rabbit AlexaFluor 555 secondary antibodies before being mounted on slides and imaged. **(a)** Effect of FLAG antibody stripping on visualising FSHR localised to plasma membrane. Following **(b)** 5- or **(c)** 15-minute treatment, **(i)** representative confocal images of FLAG-FSHR (green), EEA1 (red) and DAPI (blue) were generated. **(ii)** Quantification of FSHR-positive EEA1 endosomes from (i). Each data point represents mean  $\pm$  SEM for  $n = 7-8$  cells per condition collected from  $n=1$  independent experiment. *Scale bars*, 5 $\mu\text{m}$ .

#### 4.2.3 Effect of APPL1 silencing on FSH glycoform-dependent FSHR cAMP production and cre-luciferase activity

Since a small percentage of FSHRs were shown to co-localise with EEA1-positive endosomes, it suggested that the majority of FSHRs are targeted to alternative endosomal signalling compartments. APPL1 is an adapter protein that is localised to the distinct VEEs and plays an essential role in regulation FSHR cAMP signalling (Sposini et al., 2020). Therefore, siRNA APPL1 (siAPPL1) was transfected into cells to silence APPL1 protein and determine its effect on FSH glycoform-dependent FSHR cAMP production and cre-luciferase activity (see chapter 2.9 for details).

APPL1 silencing appeared to enhance both FSH21/18-dependent (Figure 4.6, (ai)) and FSH24-dependent (Figure 4.6, (aii)) cAMP production when compared to control cells. Quantitative analysis of the AUC of cAMP accumulated over 30-minute stimulation with 30ng/ml of FSH showed that APPL1 silencing induced a further  $10.9 \pm 6.6$ - and 12.8-fold increase in FSH21/18- and FSH24-treated cells, respectively (Figure 4.7, (a)). When the data was analysed at more acute time points, it was shown that by 2 minutes APPL1 silencing had very little effect on FSH glycoform-dependent cAMP accumulation (Figure 4.7, (b)). However, by 5- and 15 minutes, an increase in both FSH glycoform-dependent cAMP accumulation began emerging in the absence of APPL1 (Figure 4.7, c-d)). APPL1 silencing enhanced both FSH21/18- and FSH24-dependent maximal cAMP by 30 minutes (Figure 4.8, (a)), with increases in FSH21/18- and FSH24-dependent maximal cAMP accumulation emerging as early as 2- ( $p < 0.05$ ) (Figure 4.8, (b)) and 15-minutes ( $p = 0.054$ ) (Figure 4.8, (d)), respectively.

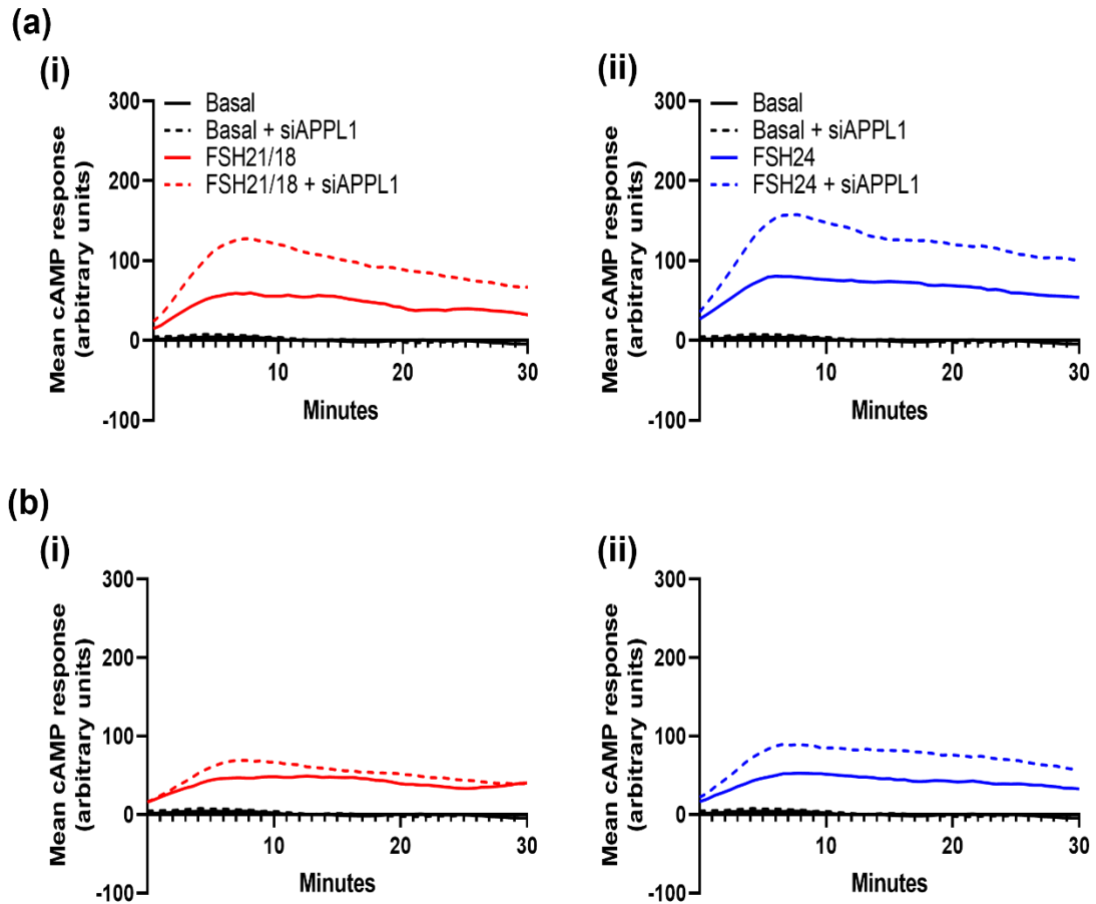


**Figure 4.6: Effect of APPL1 silencing on FSH glycoform-dependent FSHR-dependent cAMP production.** HEK293 cells expressing the FSHR were transfected with  $\pm$  siAPPL1 to knockdown APPL1 protein. Cells were then stimulated with **(a)**  $\pm$  30- or **(b)**  $\pm$  1ng/ml of **(i)** FSH21/18 or **(ii)** FSH24 for 30 minutes. Data shows smoothed curve of the mean cAMP accumulation from  $n=3$  independent experiments measured in triplicate (no error bars).

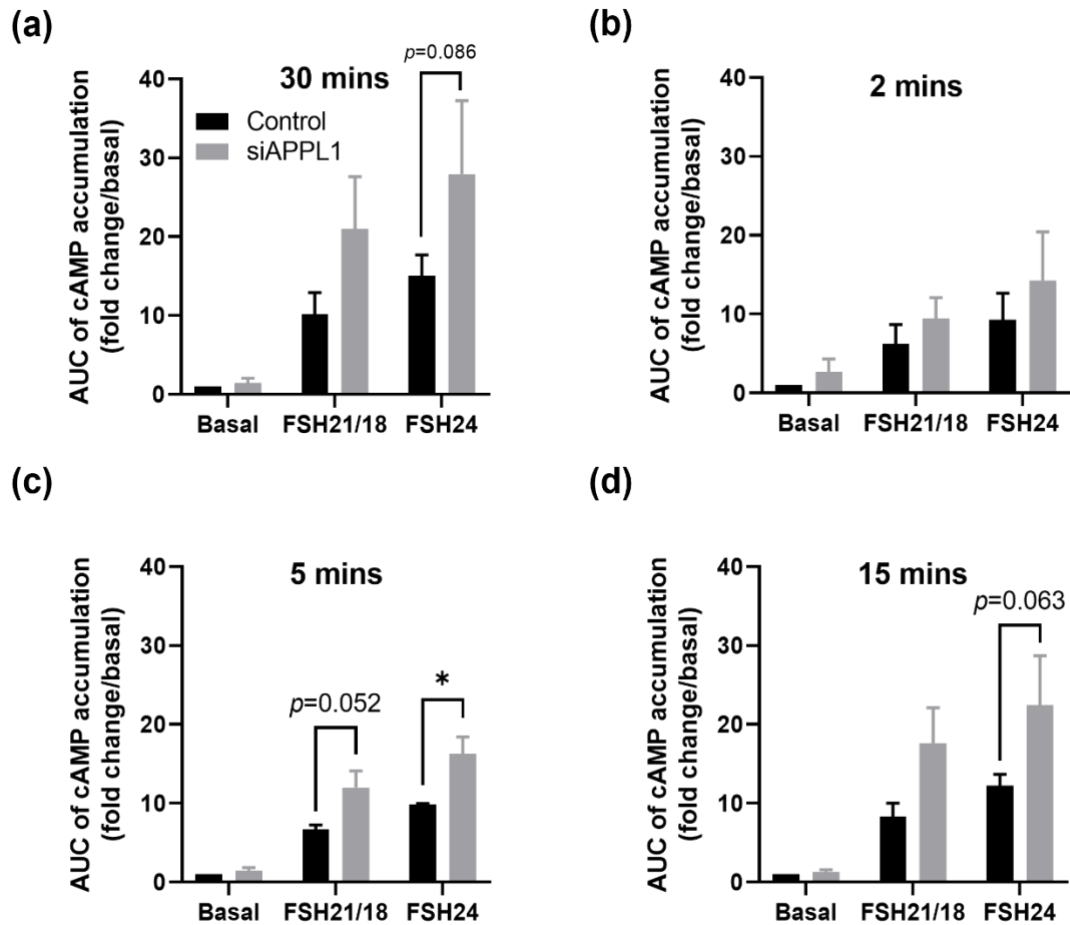


**Figure 4.7: Effect of APPL1 silencing on FSH glycoform-dependent cAMP accumulation using 30ng/ml of.** Data from cells stimulated with 30ng/ml was extrapolated from Figure 4.6. The AUC of cAMP accumulation was determined at (a) 30-, (b) 2-, (c) 5-, and (d) 15-minute time points. Data represented as fold change/basal. Data analysed using 2-way AVOVA, followed by Šidák's multiple comparison's test. All data represent mean  $\pm$  SEM of  $n=3$  independent experiments conducted in triplicate. \*,  $p<0.05$ .

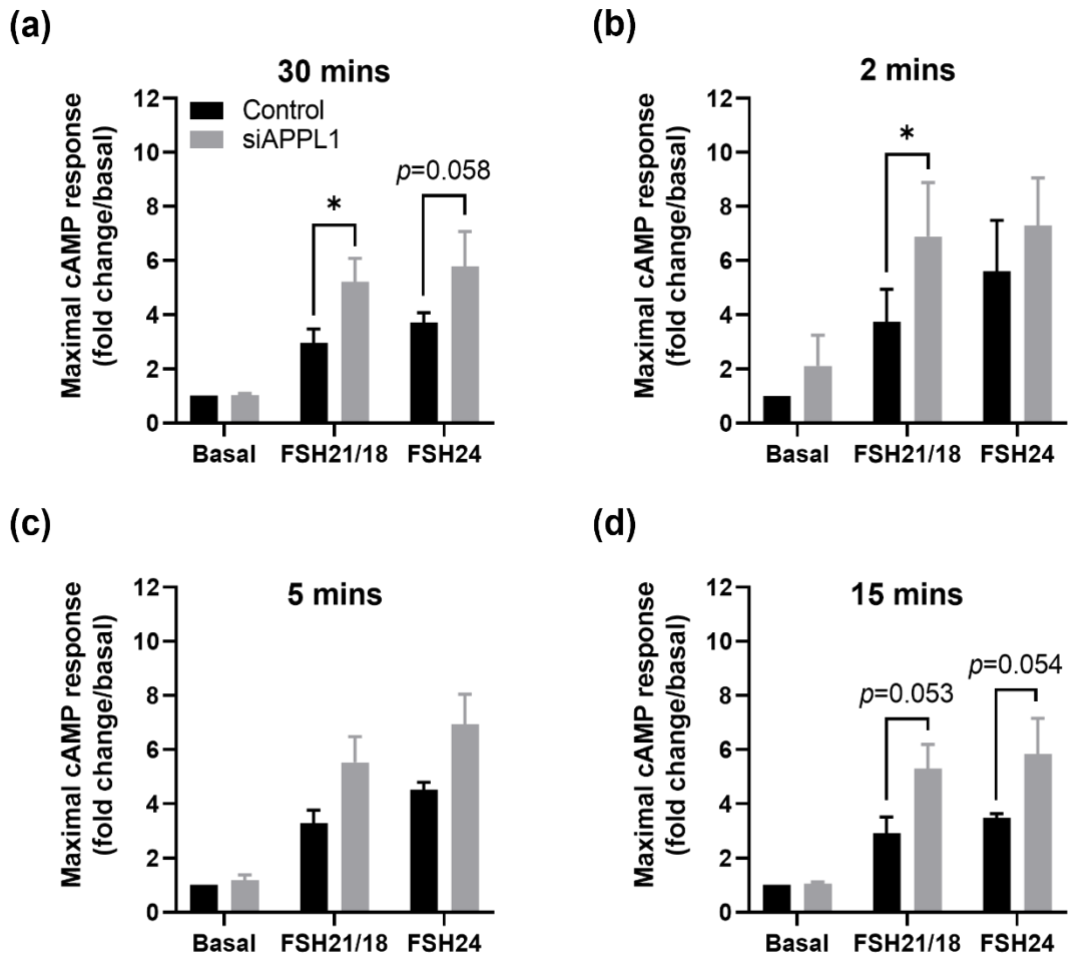


**Figure 4.8: Effect of APPL1 silencing on maximal cAMP response using 30ng/ml of FSH glycoforms.** Data from cells stimulated with 30ng/ml was extrapolated from Figure 4.6. The maximal cAMP response was determined at (a) 30-, (b) 2-, (c) 5-, and (d) 15-minute time points. Data represented as fold change/basal. Data analysed using 2-way AVOVA, followed by Šidák's multiple comparison's test. All data represent mean  $\pm$  SEM of  $n=3$  independent experiments conducted in triplicate. \*,  $p<0.05$ .

To assess the effect of APPL1 silencing on lower concentrations of FSH glycoform on cAMP production, cells were stimulated with 1ng/ml of both FSH21/18 and FSH24 for 30 minutes (Figure 4.6, (b)). At lower concentrations of FSH, APPL1 silencing appeared to enhance cAMP production in FSH24-treated cells (Figure 4.6, (b)). Quantitative analysis revealed that APPL1 silencing significantly enhanced a  $7.4 \pm 4.3$ -fold increase in FSH24-dependent cAMP accumulation ( $p < 0.05$ ), with significant increases observed as early as 5 minutes (Figure 4.9, (c)). Additionally, APPL1 silencing significantly enhanced FSH24-dependent maximal cAMP response as early as 15 minutes ( $p < 0.01$ ) (Figure 4.10). APPL1 silencing had little effect on cAMP accumulation when lower concentrations of FSH21/18 were used at all time points (Figure 4.9), but enhanced maximal cAMP responses at later time points ( $p < 0.05$ ) (Figure 4.10). These data suggests that APPL1 silencing potentiates FSH glycoform-dependent cAMP accumulation in a temporal- and concentration-dependent manner. Furthermore, it proposes that APPL1 negatively regulates FSH glycoform-dependent cAMP production in HEK293 cells.

To determine how the effect of APPL1 silencing on FSH-glycoform FSHR-dependent cAMP production related to downstream cre-luciferase activity, cells transfected with  $\pm$  siAPPL1 were stimulated with increasing concentrations of FSH glycoforms (0-100ng/ml) and cre-luciferase activity was measured. APPL1 silencing had no effect on FSH21/18-dependent cre-luciferase activity at all concentrations used (Figure 4.11, (a)), suggesting that APPL1 does not regulate FSH21/18-dependent cre-luciferase activity. To the contrary, APPL1 silencing appeared to enhance FSH24-dependent cre-luciferase to similar levels elicited by control cells treated with FSH21/18 (Figure 4.11, (b)). This suggests that APPL1 negatively regulate FSH24-dependent FSHR cre-luciferase activity in HEK293 cells, and that inhibiting APPL1 may stimulate FSH21/18-like FSHR signalling.

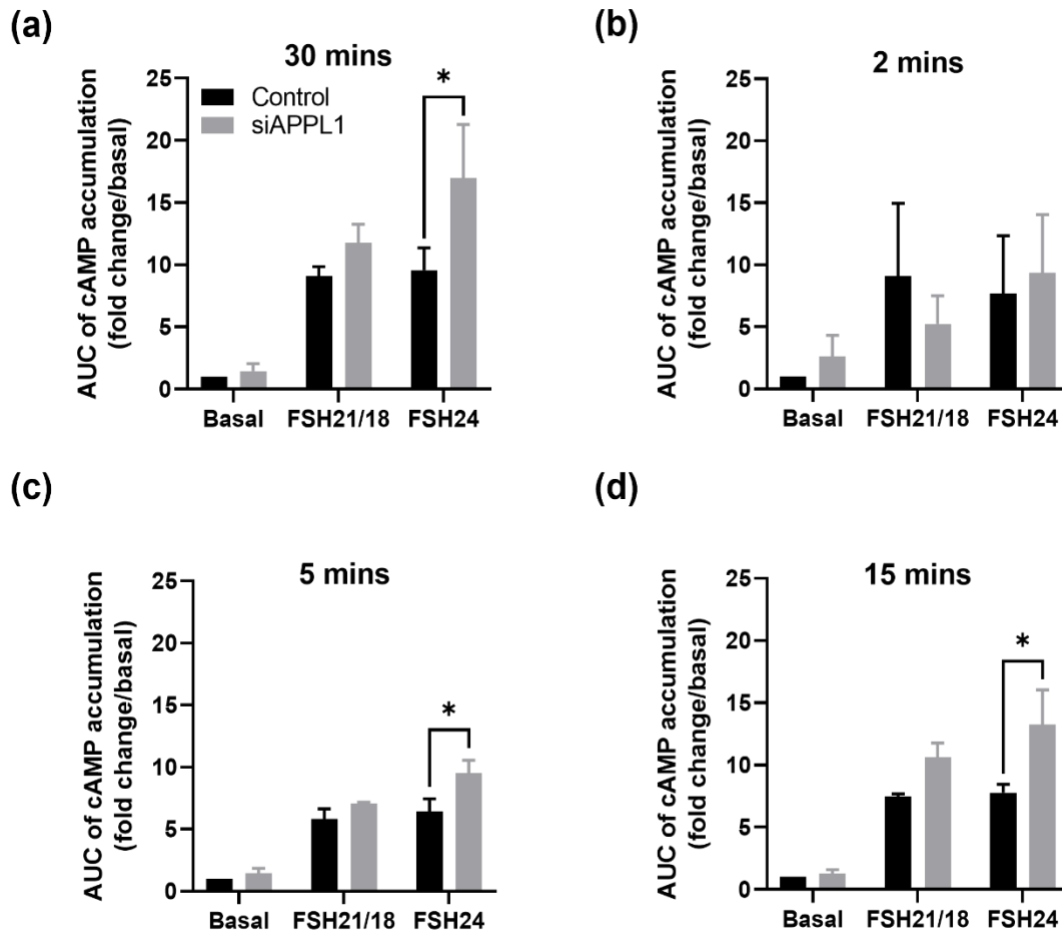


**Figure 4.9: Effect of APPL1 silencing on total cAMP accumulation using 1ng/ml of FSH glycoforms.** Data from cells stimulated with 1ng/ml was extrapolated from Figure 4.6. The AUC of cAMP accumulation was determined at (a) 30-, (b) 2-, (c) 5-, and (d) 15-minute time points. Data represented as fold change/basal. Data analysed using 2-way AVOVA, followed by Šidák's multiple comparison's test. All data represent mean  $\pm$  SEM of n=3 independent experiments conducted in triplicate. \*,  $p < 0.05$ .



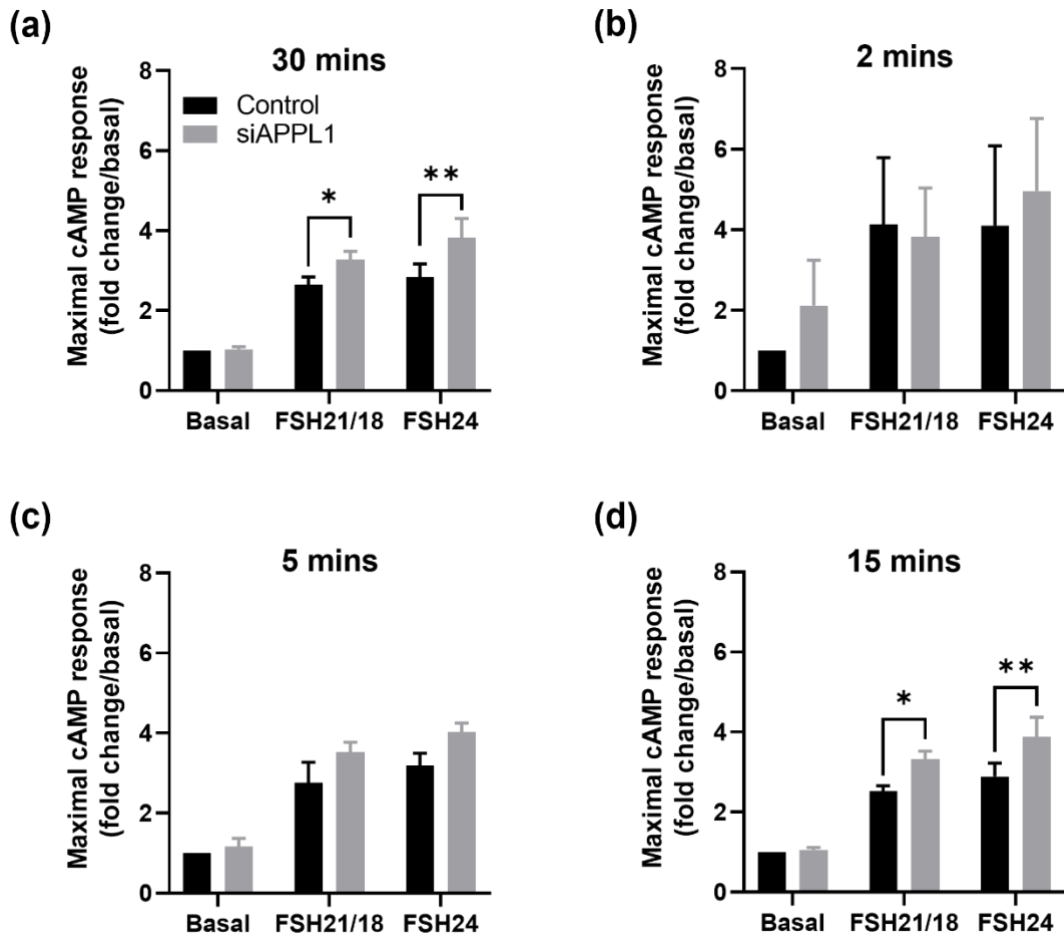


**Figure 4.10: Effect of APPL1 silencing on maximal cAMP response using 1ng/ml of FSH glycoforms.** Data from cells stimulated with 1ng/ml was extrapolated from Figure 4.6. The maximal cAMP response was determined at (a) 30-, (b) 2-, (c) 5-, and (d) 15-minute time points. Data represented as fold change/basal. Data analysed using 2-way AVOVA, followed by Šidák's multiple comparison's test. All data represent mean  $\pm$  SEM of n=3 independent experiments conducted in triplicate. \*,  $p < 0.05$ ; \*\*,  $p < 0.01$ .

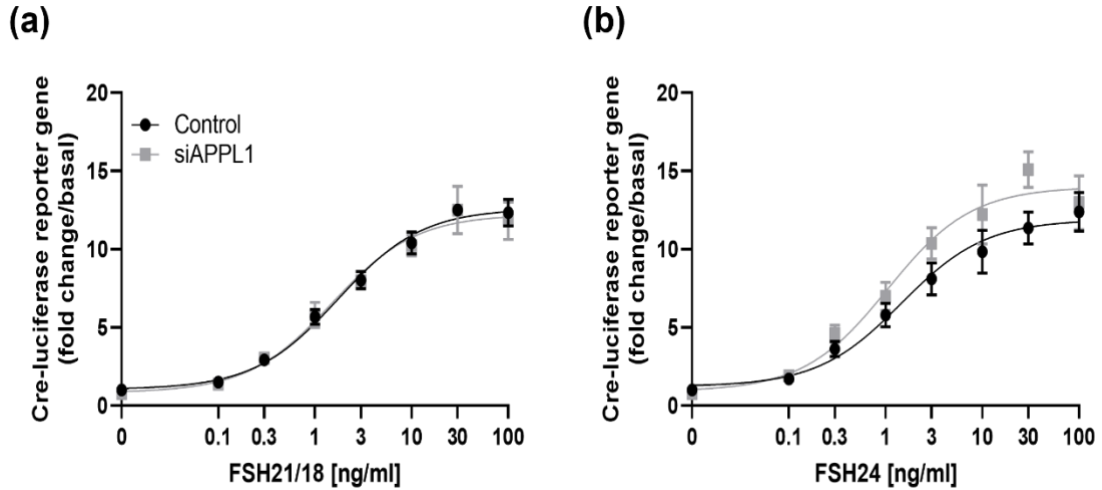


**Figure 4.11: Effect of APPL1 silencing on FSH glycoform-dependent cre-luciferase activity.** HEK293 cells expressing the FSHR, cre-luciferase and *Renilla*-luciferase were transfected with  $\pm$  siAPPL1 to knockdown APPL1 protein. Cells were then stimulated with increasing concentrations (0-100ng/ml) of **(a)** FSH21/18 or **(b)** FSH24 for 4-6 hours. All data points were normalised to *Renilla*-luciferase for transfection efficiency and represented as fold change/basal. Data analysed using 2-way AVOVA, followed by Šidák's multiple comparison's test. Each data point represents mean  $\pm$  SEM for n=3 independent experiments, measured in triplicate.

### 4.3 Discussion

This study aimed to determine how differential FSH glycoforms modulate FSHR trafficking and signalling. The findings suggest that FSHR-dependent cAMP signalling predominantly occurred within endosomal compartments of HEK293 cells. It was also shown that FSHR routing to EEA1-positive endosomes for sorting may be FSH glycoform-dependent. In this study it was also revealed that APPL1 silencing potentiates FSH glycoform-dependent cAMP production and FSH<sub>24</sub>-dependent cre-luciferase activity, therefore APPL1 has a role in regulating their magnitude.

GPCR endocytosis has previously been associated with the attenuation of receptor signalling. Therefore, when FSHR internalisation was pharmacologically inhibited, it was surprising that FSH glycoform-dependent cAMP production and cre-luciferase activity was attenuated. This suggests that FSHR signalling predominantly occurs within endosomal compartments and requires dynamin-mediated endocytosis of FSHR for full cAMP signalling. Other GPCRs, such as the related glycoprotein hormone receptors, LH/CGR (Lyga et al., 2016) and TSHR (Calebiro et al., 2009), as well as PTHR (Ferrandon et al., 2009), and the  $\beta_2$ AR (Irannejad et al., 2013) have been reported to also signal from endosomes, but as a 'second wave' of sustained cAMP signalling distinct from transient signals activated at the plasma membrane (Sposini et al., 2020). Additionally, in a similar study where FSHR internalisation was inhibited in HEK293 cells, ~25% of cAMP signalling was still observed when cells were pre-treated with 30 $\mu$ M of Dyngo<sup>®</sup>-4a (Sposini et al., 2020). Furthermore, other studies on the  $\beta_2$ AR and FSHR that utilised 30 $\mu$ M of Dyngo<sup>®</sup>-4a were also able to visualise receptor-mediated cAMP signalling at the plasma membrane (Irannejad et al., 2013; Sposini et al., 2020). It could be that the concentration

of Dyngo<sup>®</sup>-4a used in this was too high, or that the enhanced cre-luciferase activity observed at higher concentrations of FSH glycoforms suggests a lack of total blockade of cAMP signalling. Interestingly, the glycosylation status of FSH appeared to have no impact on FSHR internalisation. This would make sense if FSHR signalling predominantly occurred within endosomes as FSH glycoforms would need to initiate FSHR internalisation to activate signalling pathways. However, to begin to fully delineate the role that FSH glycosylation has on FSHR internalisation, it would be interesting to understand whether deglycosylated FSH $\alpha$  at asparagine-52 (N<sup>52</sup>dg- $\alpha$ )-FSHR complex, that is able to bind to the FSHR but not activate adenylate cyclase (Butnev et al., 2002), is retained at the plasma membrane. Also, if FSH glycoforms could be differentially labelled with AlexaFluor, then the FSHR trafficking pathway to different endosomal compartments could potentially be determined.

In this study, it was shown that FSH21/18 possibly mediated a minority of FSHRs to EEA1-positive endosomes pre-targeted for potential receptor degradation and signal termination, with the majority of FSHR EEA1-negative endosomes. Interestingly, the  $\beta_2$ AR is primarily routed to the EEA1-positive EEs yet is still recycled to the cell-surface (Jean-Alphonse et al., 2014; Sposini et al., 2017). This raises the important questions about the fate of these subpopulation of FSHRs routed to EEA1-positive endosomes and why they are differentially routed by FSH glycoforms to different endosomal compartments. Although FSH24 did not mediate any difference in FSHR routing to EEA1-positive endosomes, it is possible that FSH24 induces similar/higher percentages of FSHRs targeted to EEA1-positive endosomes than FSH21/18 at later time points than what was conducted in this study. This is because FSH24 engages with the FSHR slower and displays slower kinetics

than FSH21/18 (Bousfield et al., 2014a), therefore future experiments would need to be extended to later time points to investigate this further.

In this chapter, APPL1 silencing enhanced FSH21/18- and FSH24-dependent cAMP production at both higher and lower concentrations with some temporal regulation of cAMP signals observed. Although the significance of these findings is not clear, if APPL1-positive endosomes could be targeted, then there may be therapeutic implications for younger women that naturally have lower circulating levels of FSH24, and who may be presented with reproductive pathologies such as premature ovarian failure, in which ovaries produce low amounts of oestrogen (Bousfield et al., 2014b). cAMP-dependent signalling within the GCs of these cohort of women could be enhanced and potential improve fertility (Casarini & Crépieux, 2019; Messinis et al., 2014). However, this would need further investigation to be determined, and whether there may be other detrimental effects of APPL1 silencing *in vivo*.

The data in this chapter suggests a role for APPL1 in modulating the magnitude of cAMP signalling and signal termination. Although it's not clear from this study whether the FSHR is targeted to APPL1-positive endosomes for receptor recycling, a recent similar study showed that ~40% of the FSHR were routed to APPL1-positive endosomes and APPL1 KD reducing >50% of FSHR recycling (Sposini et al., 2020). Furthermore, another earlier study on the homologous LH/CGR showed similar results (Sposini et al., 2017). Sposini *et al.* revealed that the LH-LH/CGR complex, when internalised, co-localised to APPL1-positive endosomes, and APPL1 KD by siAPPL1 increased the percentage of LH-LH/CGR internalisation (Sposini et al., 2017). The study proposed that APPL1 regulated LH/CGR

recycling to the plasma membrane via APPL1-phosphorylation from PKA. Furthermore, Sposini *et al.* showed that LH/CGR-dependent cAMP production was also enhanced (by 100%) as a result of APPL1 knockdown, showing that APPL1 negatively regulates GpHR cAMP production, possibly by forming an autoregulatory loop with cAMP, PKA and APPL1 (Sposini et al., 2017), and may be a similar mechanism adopted by the FSHR within this study.

When the effect of APPL1 on cre-responsive genes was assessed, it was surprising to observe that APPL1 silencing had no effect on FSH21/18-dependent cre-luciferase activity, despite enhanced cAMP activity previously observed. Instead, APPL1 silencing appeared to enhance higher concentrations of FSH24-dependent cre-luciferase activity. Since APPL1 inhibits FSHR-dependent cAMP signalling and mediates FSHR recycling (Sposini et al., 2020), possibly as a result of cAMP inhibition (Sposini et al., 2017), it is possible that FSH24 routes the FSHR to APPL1-positive VEEs where cAMP signalling is inhibited, thus leading to FSHR recycling to the cell-surface where FSHRs are predominantly inactive. Alternatively, since results indicated that FSH21/8 may target FSHR to EEA1-positive endosomes, it is possible that this mechanism supports increased cAMP signalling as the FSH21/18-FSHR-cAMP signalling complex is retained in the EE compartment.

It is tempting to suggest that targeting APPL1-positive endosomes in older women, who have higher concentrations of circulating FSH24 (Bousfield et al., 2014b), may enhance their cre-responsive gene levels to similar levels displayed by FSH21/18. Nevertheless, it remains important to consider that the difference in the length of stimulation with FSH24 between GloSensor™ and cre-luciferase assays may play a significant role. Chronic 4-6-

hour stimulation with FSH24 may enhance cre-luciferase activity because of FSH24's slower binding kinetics to the FSHR, this means it may have fully engaged with the FSHR by the time the cells were lysed. In contrast, FSH21/18's faster binding kinetics to the FSHR may have meant that possible increases in cre-luciferase activity, following APPL1 silencing, may have been missed, therefore shorter treatments time may be required to see the effects. This idea is further supported by the fact that acute increases in cAMP production was observed following APPL1 silencing during GloSensor™ assays when cells were stimulated with FSH21/18, in which a similar trend with cre-luciferase activity would be expected considering it is downstream of the cAMP/PKA signalling pathway.

One key limitation in this study was the difference in the bioactivity of the different FSH glycoform preparations. In the previous chapter (chapter 3), and from literature, partially glycosylated FSH21/18 induces higher FSHR-dependent cAMP signalling than fully glycosylated FSH24 (Jiang et al., 2015; Liang et al., 2020; Wang et al., 2016b; Zariñán et al., 2020). However, the results in this chapter did not show these distinct signalling profiles. It's important to note that the new preparation of FSH21/18 used in this study, may have had FSH24 contamination. The ratio of FSH24:FSH21 in these preps may have been higher than usual. Both FSH21/18 and FSH24 are purified from the same preparation, therefore there is an increased batch-to-batch variability in potency. The original batch of FSH glycoforms utilised in the experiments within chapter 3 had at least a 5-fold difference between FSH21/18- and FSH24-dependent FSHR signalling, whereas the difference in FSHR signalling in this chapter was down to 3-fold. A recent study has shown that increases in FSH24:FSH21/18 decreases follicle growth and survival (Johnson et al., 2022), demonstrating the impact of FSH glycoform ratio on FSHR signalling. Given this, the

effect of FSH21/18 on FSHR trafficking and signalling cannot be fully concluded, and results should be interpreted with caution.

Another limitation to this chapter was the possibility of cell toxicity from Dyngo<sup>®</sup>-4a experiments likely arising from the transfection reagent that would need to be considered and could be the cause of the significant reduction in cellular signalling. Furthermore, dynamin inhibition has been associated with cell death in some cell types (von Beek et al., 2021). On the other hand, in other cell types Dyngo<sup>®</sup>-4a was reported as non-toxic and did not affect cell viability (McCluskey et al., 2013). Therefore, future experiments to determine the tolerance of different concentrations of Dyngo<sup>®</sup>-4a over different incubation periods in HEK293 cells would need to be conducted to confirm this in the current cell model. Examples of these assays could include trypan blue staining or measuring caspase or ATP levels.

The validity of the interpretation of the immunocytochemical staining would also need to be considered in this chapter. Appropriate negative controls are required to accurately interpret findings and to reproduce results. To accurately report that the staining in this study correspond to FSHR and EEA1, future studies would need to compare the specificity of the antibodies used. This could be done by comparing HEK293-FLAG-tagged FSHR-positive cells with untransfected cells or cells expressing untagged FSHR. Alternatively, the specificity of the antibodies could be indirectly determined by comparing cells where the primary antibodies are omitted to determine if the secondary antibody is also specific.



Finally, it is important to consider the validity of the siAPPL1 experiments in this chapter in the absence of important non-targeting controls and confirmation of target knockdown. Although targeted knockdown has been previously confirmed in earlier studies by comparing non-targeting scrambled RNA, and confirming APPL1 knockdown via Western blot (Sposini et al., 2020; Sposini et al., 2017), such controls would need to be performed in current experiments to ensure robustness.

In conclusion, FSHR-dependent cAMP-related signalling predominantly occurs from within endosomes of HEK293 cells. FSH glycoforms may play a role in routing the FSHR to distinct signalling compartments following internalisation, with few FSHRs targeted EEA1-positive endosomes. Moreover, APPL1 silencing differentially regulates FSH glycoform dependent FSHR-dependent cAMP responses and enhances FSH24-dependent cre-luciferase activity. These data suggests that FSHR trafficking pathway could be targeted to modulate FSHR signalling. This may have age-related implications for women with different circulating levels of FSH glycoforms that are poor responders to IVF. Such patients may be presented with higher serum levels of FSH24, therefore by targeting APPL1 in GCs, as a means to silencing it, may enhance FSHR-dependent cAMP signalling and physiological responses, thus enhancing fertility. Nevertheless, further experiments are required to conclude this.

**5 Chapter Five: Investigating the effect of a small positive FSHR allosteric modulator  
on FSHR oligomerisation and signalling**

## 5.1 Introduction

Besides the endogenous actions of FSH, there have been multiple small molecule non-peptide modulators that have been identified and shown to further amplify FSHR signalling with promising therapeutic advantages (Aathi et al., 2022). Current IVF protocols utilise multiple injectable recombinant and purified FSH preparations to stimulate the ovaries and can result in poor patient compliance (Anderson et al., 2018). Therefore, identifying small molecule non-peptide FSHR agonists, that have the potential to be administered orally, may be a competitive alternative to IVF to improve fertility.

Although a number of FSHR agonists have been screened and identified (Anderson et al., 2018), the TZD-derived C5 FSHR PAM had promising therapeutic potential (see chapter 1.9.1). C5 was more potent ( $EC_{50} = 2\text{nM}$ ) at inducing cre-luciferase activity when compared to other TZD-derived small molecular compounds treated in CHO cells, with the ability to fully induce oestradiol in rat GCs and progesterone in mouse adrenal Y1 cells (Yanofsky et al., 2006). Binding studies have shown C5 can increase the binding of radiolabelled  $^{125}\text{I}$ -FSH to the FSHR by 3-fold (Jiang et al., 2014b). Moreover, personal communication with George Bousfield has shown C5 can increase the binding of  $^{125}\text{I}$ -hFSH24 to the human FSHR by 4-fold. With an age-related decline in the success rate of IVF, together with the increased abundance of less bioactive circulatory FSH24 in older women (Bousfield et al., 2014b; HFEA, 2021), the potential to enhance FSH24 engagement with the FSHR via may be of therapeutic advantage in these increasing cohort of patients. However, the effects of C5 on FSH glycoform-dependent signalling and how it may correlate with FSHR oligomerisation remains unknown. Therefore, the aim of this chapter was to investigate the effect of C5 on FSHR-mediated signalling and oligomerisation. To fulfil this aim, the objectives were to:

1. Understand the effect of C5 on FSHR cAMP dependent signalling and the correlation to FSHR oligomerisation in HEK293 cells expressing the FSHR.
2. Investigate the effects of C5 on FSH glycoform-dependent cAMP pathway activation in HEK293 cells expressing FSHR.
3. Determine the effect of C5 on FSH glycoform-dependent FSHR oligomerisation in HEK293 cells expressing FSHR.

## 5.2 Results

### 5.2.1 Effect of C5 on FSHR oligomerisation and subsequent cAMP production

Since C5 was previously shown to behave as an FSHR agonist and activate cAMP-dependent signalling in CHO, GCs and adrenal Y1 cells (Yanofsky et al., 2006), the first step was to recapitulate these findings in HEK293 cells transiently expressing FSHR. Cells transfected and cultured for GloSensor™ cAMP analysis were stimulated with increasing concentrations of C5 (0-10 $\mu$ M) for 30 minutes and live cAMP fluorescence was measured (see chapter 2.5 for details). Results revealed all concentrations of C5 were able to induce cAMP with similar efficacy and potency (Figure 5.1, (a)). When the AUC was measured, to determine the total amount of cAMP, the data showed that even the lowest concentration of C5 (0.1 $\mu$ M) was able to induce a  $10.8 \pm 1.0$ -fold increase in total cAMP when compared to basal, with an  $EC_{50} = 30$ nM (Figure 5.1, (b)). Similarly, when maximal cAMP response was measured to determine the magnitude of cAMP, the data showed all concentrations of C5 were able to induce a  $\sim 4$ -fold increase in maximal cAMP with an  $EC_{50} = 35$ nM (Figure 5.1, (c)). This suggests C5 behaves as a potent FSHR agonist in HEK293 cells.

To determine whether the C5-dependent FSHR cAMP signalling was mediated by FSHR oligomerisation, transfected cells were stimulated with  $\pm 1\mu$ M of C5 for 30 minutes then fixed and imaged for PD-PALM analysis (see chapter 2.4 for details). Results demonstrated C5 induced a 4-fold significant increase in the number of FSHR molecules localised at the plasma membrane ( $p < 0.0001$ ) (Figure 5.2, (a)). Interestingly, the increase in FSHR density did not affect the number of associated FSHR molecules (Figure 5.2, (b)), nor the type of associated FSHR molecule complexes (Figure 5.2, (c)). This suggests that C5 may mediate increased FSHR cAMP signalling by increasing FSHR density on the plasma membrane and not via FSHR oligomerisation.

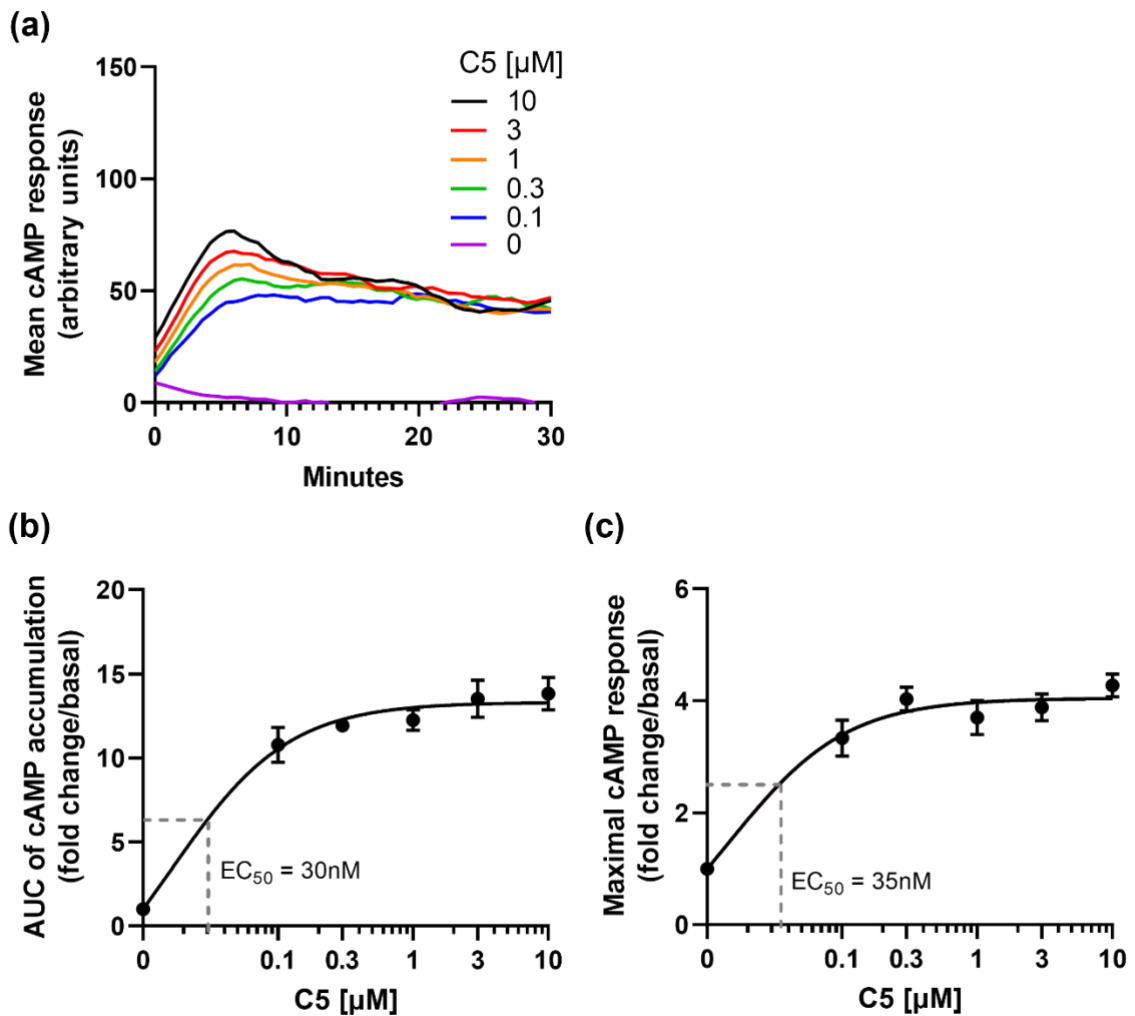


**Figure 5.1: Effect of Compound 5 on FSHR-dependent cAMP production.** HEK293 cells transiently co-expressing the HA-tagged FSHR and pGloSensor™-20F plasmid were treated for 30 minutes with 0-10 $\mu\text{M}$  of Compound 5 (C5) and GloSensor™ cAMP fluorescence was measured. **(a)** Smoothened curve of the mean cAMP accumulation following treatment, (no error bars). **(b)** AUC of total cAMP accumulation and **(c)** maximal cAMP response was measured. Data represented as fold change/basal. All data represent mean  $\pm$  SEM of n=3 independent experiments conducted in triplicate.

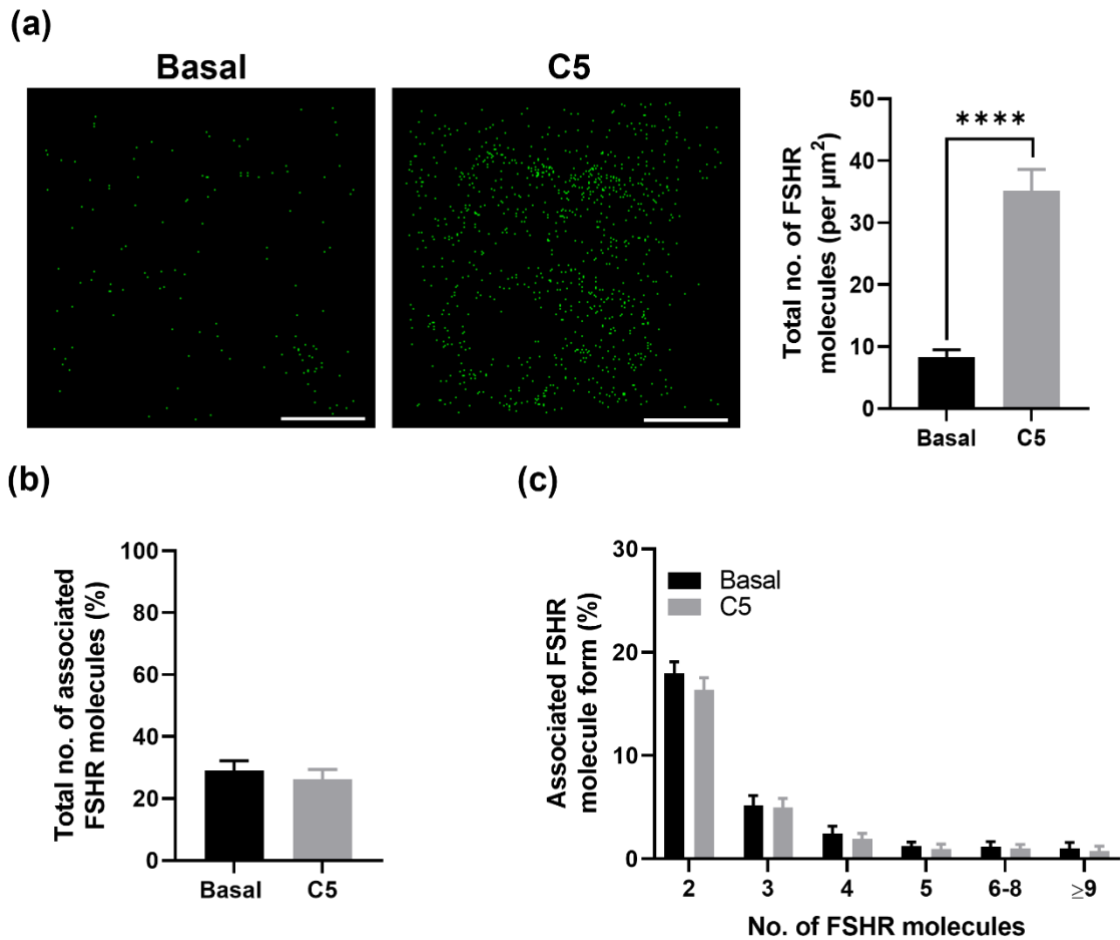


**Figure 5.2: Effect of Compound 5 on FSHR oligomerisation.** HEK293 cells transiently expressing HA-tagged FSHR were pre-incubated for 30 minutes with CAGE 552-HA antibody and treated  $\pm 1\mu\text{M}$  of Compound 5 (C5). Cells were fixed and imaged via PD-PALM. **(a)** The total number of FSHR molecules at the cell membrane. *Scale bars*,  $6.2\mu\text{m}$ . **(b)** The percentage of the total number of associated FSHR molecules following pre-treatment; data analysed using unpaired t test. **(c)** The percentage of associated FSHR molecule form; 2 (dimer), 3 (trimer), 4 (tetramer), 5 (pentamer), 6-8,  $\geq 9$ ; data analysed using multiple unpaired t-tests. All data represent mean  $\pm$  SEM of  $n \geq 3$  independent experiments. \*\*\*\*,  $p < 0.0001$ .

The previous chapter (chapter 4) suggested that FSHR-dependent cAMP signalling was dependent on FSHR internalisation; a process that can also regulate FSHR plasma membrane density via receptor recycling. To ascertain the cellular localisation of C5-mediated FSHR signalling, and whether C5-mediated signalling was a result of FSHR internalisation/recycling processes, cells cultured for GloSensor™ cAMP assays were pre-treated with  $\pm 50\mu\text{M}$  of the potent dynamin inhibitor (Dyngo®-4a) to prevent FSHR endocytosis (McCluskey et al., 2013), and stimulated with increasing concentrations of C5 (0-10 $\mu\text{M}$ ) for 30 minutes. Pre-treatment with Dyngo®-4a reduced C5-dependent FSHR-dependent cAMP production by  $\sim 50\%$  (Figure 5.3, (a-b)), with significant reduction in the total amount of cAMP accumulation for all concentrations of C5 ( $p < 0.05$ ) (Figure 5.3, (c)). This suggests that C5-dependent FSHR cAMP signalling is partially mediated via endocytosed FSHR, with implications on receptor recycling leading to increased FSHR density, as inhibiting FSHR endocytosis abrogates cAMP signalling. When cells were pre-treated with 50 $\mu\text{M}$  of Dyngo®-4a and stimulated with increasing concentrations of C5 there was complete inhibition of C5-dependent FSHR-dependent cre-luciferase activity (Figure 5.4). This may suggest that the effect of Dyngo®-4a on C5-dependent FSHR signalling is amplified at the gene expression level.



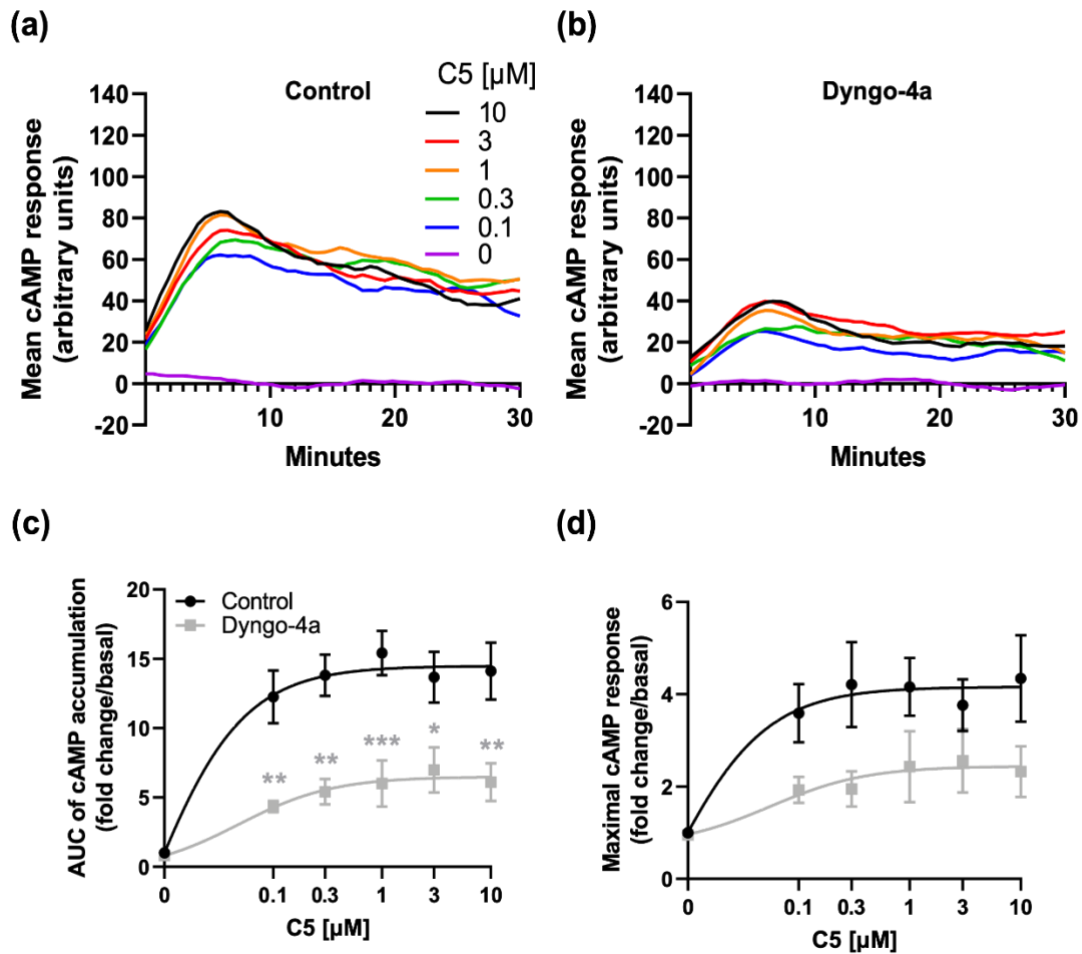


**Figure 5.3: Effect of Dyngo-4a on Compound 5-dependent FSHR cAMP production.** HEK293 cells co-expressing HA-tagged FSHR and pGloSensor<sup>TM</sup>-20F plasmids were pre-treated with either DMSO or 50 $\mu\text{M}$  of Dyngo<sup>®</sup>-4a and then stimulated with increasing concentrations of Compound 5 (C5) (0-10 $\mu\text{M}$ ) for 30 minutes. Smoothened curve of the mean cAMP accumulation was generated from **(a)** DMSO-pre-treated cells or **(b)** Dyngo<sup>®</sup>-4a-pre-treated cells, (no error bars). **(c)** AUC of total cAMP accumulation and **(d)** maximal cAMP response after 30-minute treatment. Data represented as fold change/basal and analysed using ordinary two-way ANOVA, followed by Šidák's multiple comparisons test. All data represent mean  $\pm$  SEM of  $n=3$  independent experiments conducted in triplicate. \*,  $p<0.05$ ; \*\*,  $p<0.01$ ; \*\*\*,  $p<0.001$ .

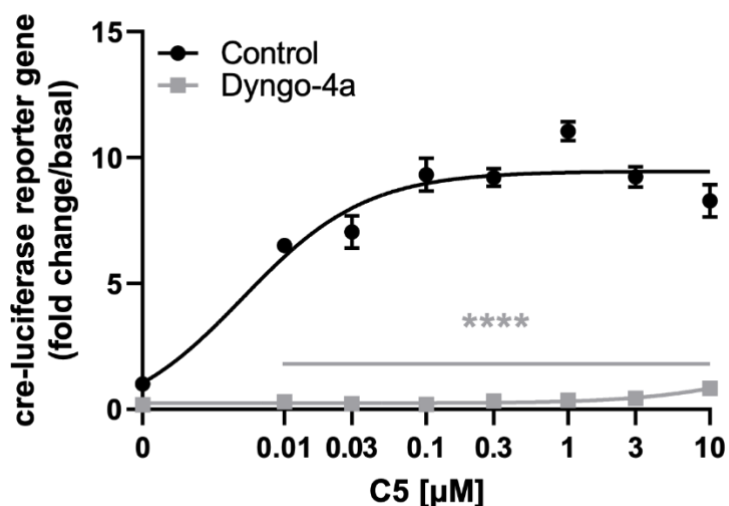


**Figure 5.4: Effect of Dyngo-4a on Compound 5-dependent FSHR cre-luciferase activity.** HEK293 transiently co-expressing HA-tagged FSHR and cre-luciferase and *Renilla*-luciferase plasmids were pre-treated in serum-free media with  $\pm 50\mu\text{M}$  of Dyngo<sup>®</sup>-4a for 30 minutes. Cells were then stimulated for 4-6 hours with increasing concentrations of Compound 5 (C5) (0-10 $\mu\text{M}$ ). All data points were normalised to *Renilla*-luciferase for transfection efficiency. Concentration-dependent effects of C5 on cre-luciferase activity were measured and represented as fold change/basal and analysed using ordinary two-way ANOVA, followed by Šidák's multiple comparisons test. Each data point represents mean  $\pm$  SEM for n=3 independent experiments, measured in triplicate. \*\*\*\*,  $p < 0.0001$ .

### 5.2.2 Effect of C5 on FSH glycoform-dependent cAMP production

Since C5 has been shown to enhance  $^{125}\text{I}$ -FSH binding to the FSHR (Jiang et al., 2014b), with increased binding shown for  $^{125}\text{I}$ -FSH24 (personal communication with George Bousfield), the next step was to establish the effect of C5 on FSH glycoform-dependent cAMP production. Transfected cells were cultured and replated for GloSensor<sup>TM</sup> cAMP analysis (see chapter 2.5 for details). Cells were co-treated with  $\pm 1\mu\text{M}$  C5 and increasing concentrations of either FSH24, eFSH, or FSH21/18 (0-100ng/ml) for 30 minutes, and live cAMP fluorescence accumulation was assessed. In the presence of C5, FSH24-treated cells stimulated increases in cAMP response at lower concentrations (Figure 5.5, (a-b)). This suggests there is a loss of FSH24 concentration-responsiveness, with basal C5-treated cells eliciting equivalent total cAMP accumulation (Figure 5.5, (c)) and maximal cAMP responses (Figure 5.5, (d)) as cells stimulated with the lowest and highest concentration of FSH24 in the presence of C5. Similar findings were observed when cells were co-treated with positive control eFSH (Figure 5.6) and FSH21/18 (Figure 5.7), further corroborating reports of C5 as a potent FSHR agonist.

To determine whether the actions of C5 on FSH glycoform-dependent FSHR signalling were amplified at a gene expression level, cre-luciferase reporter gene assays were performed on cultured and transfected cells (see chapter 2.6 for details). Cells were co-treated with  $\pm 1\mu\text{M}$  of C5 and increasing concentrations of either FSH24, eFSH or FSH21/18 (0-100ng/ml) for 4-6 hours before being lysed and assessed for cre-luciferase activity (see chapter 2.6 for details). Results showed that C5 alone maximally enhanced cre-luciferase activity with no further effects observed from the addition of any of the FSH glycoforms (Figure 5.8).

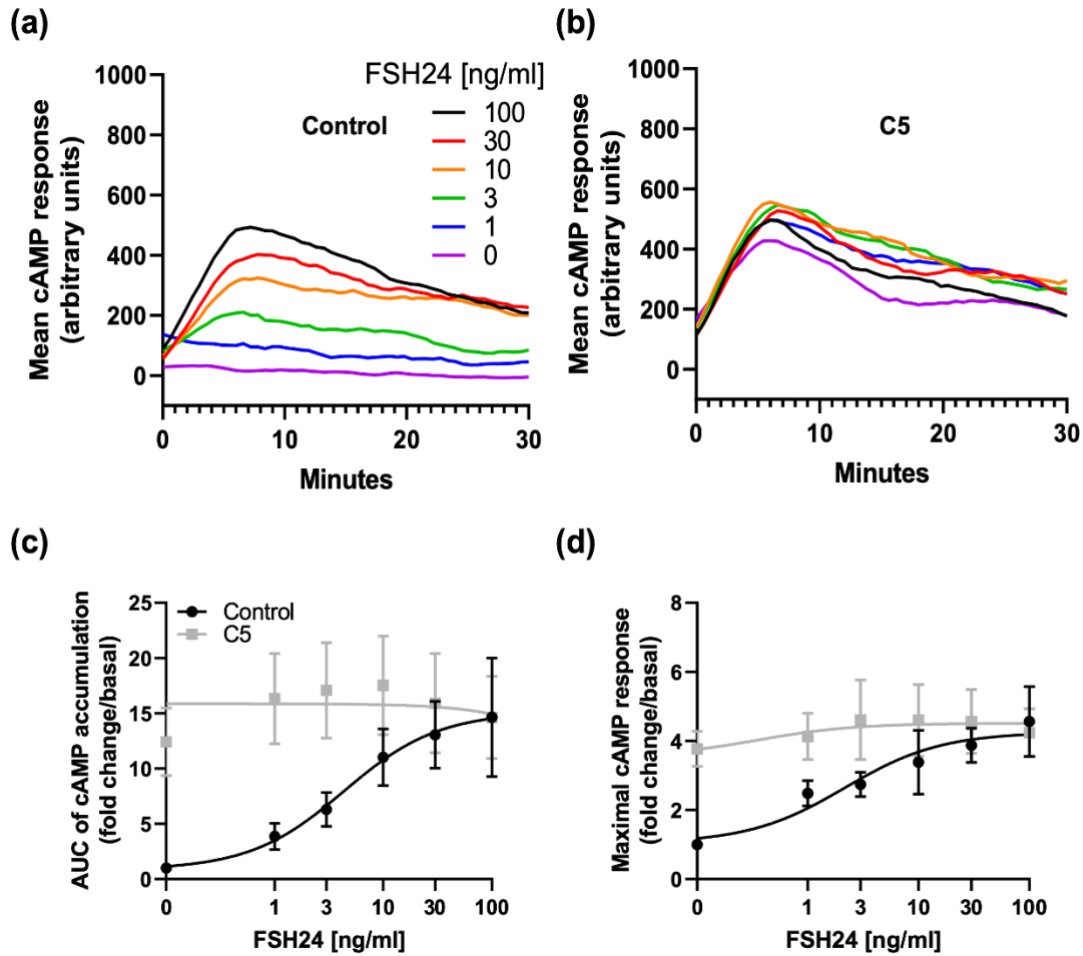


**Figure 5.5: Effect of Compound 5 on FSH24-dependent FSHR-dependent production.** HEK293 cells transiently co-expressing the HA-tagged FSHR and pGloSensor<sup>TM</sup>-20F plasmid were co-treated with  $\pm 1\mu\text{M}$  of Compound 5 (C5) and increasing concentrations of FSH24 (0-100ng/ml) for 30 minutes and GloSensor<sup>TM</sup> cAMP fluorescence was measured. Smoothened curves of the mean cAMP accumulation were generated following treatment with **(a)** cell pre-treated with DMSO and **(b)** cell pre-treated with C5. **(c)** AUC of total cAMP accumulation and **(d)** maximal cAMP response was measured. Data represented as fold change/basal and analysed using ordinary two-way ANOVA, followed by Šidák's multiple comparisons test. All data represent mean  $\pm$  SEM of  $n=3$  independent experiments conducted in triplicate.

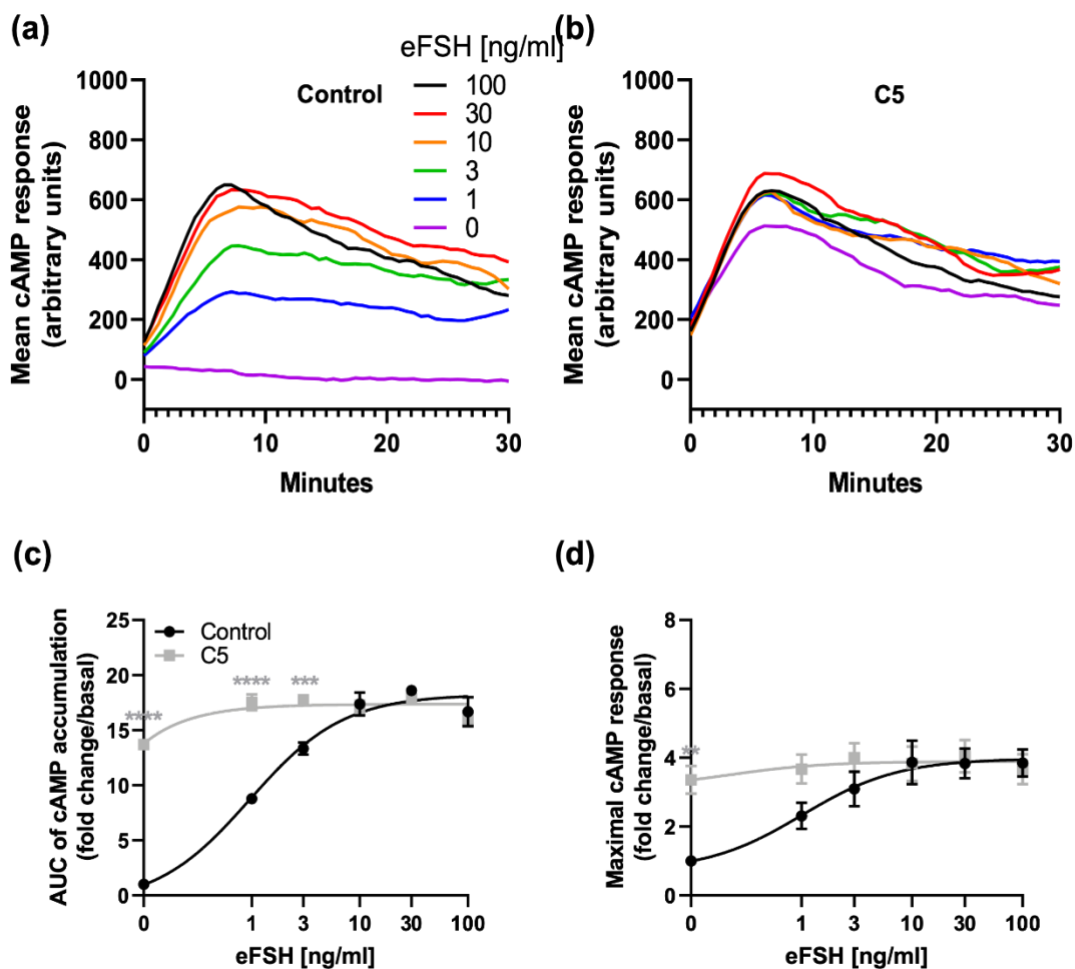


**Figure 5.6: Effect of Compound 5 on eFSH-dependent FSHR-dependent production.** HEK293 cells transiently co-expressing the HA-tagged FSHR and pGloSensor™-20F plasmid were co-treated with  $\pm 1\mu\text{M}$  of Compound 5 (C5) and increasing concentrations of eFSH (0-100ng/ml) for 30 minutes and GloSensor™ cAMP fluorescence was measured. Smoothened curves of the mean cAMP accumulation were generated following treatment with **(a)** cell pre-treated with DMSO and **(b)** cell pre-treated with C5. **(c)** AUC of total cAMP accumulation and **(d)** maximal cAMP response was measured. Data represented as fold change/basal and analysed using ordinary two-way ANOVA, followed by Šidák's multiple comparisons test. All data represent mean  $\pm$  SEM of  $n=3$  independent experiments conducted in triplicate. \*\*\*,  $p<0.001$ ; \*\*\*\*,  $p<0.0001$ .

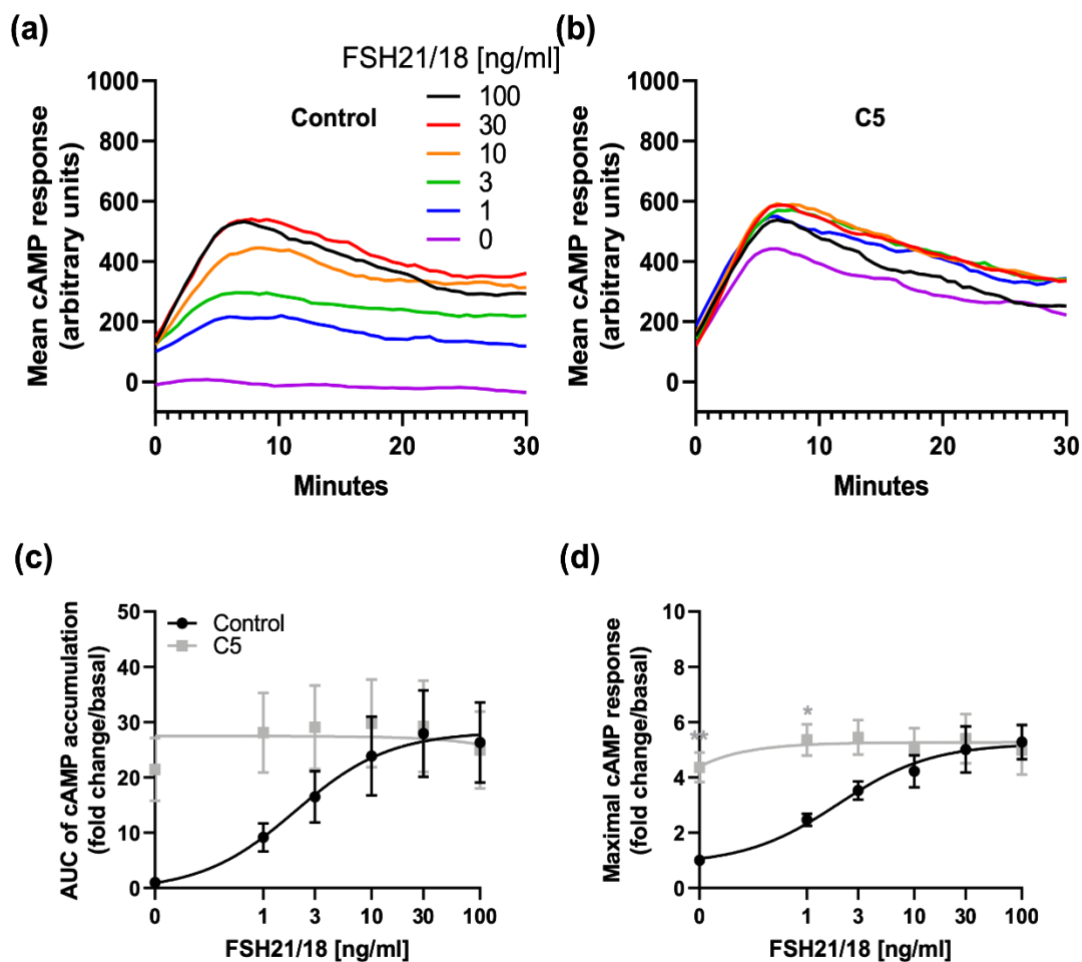


**Figure 5.7: Effect of Compound 5 on FSH21/18-dependent FSHR-dependent production.** HEK293 cells transiently co-expressing the HA-tagged FSHR and pGloSensor<sup>TM</sup>-20F plasmid were co-treated with  $\pm 1\mu\text{M}$  of Compound 5 (C5) and increasing concentrations of FSH21/18 (0-100ng/ml) for 30 minutes and GloSensor<sup>TM</sup> cAMP fluorescence was measured. Smoothened curves of the mean cAMP accumulation were generated following treatment with **(a)** cell pre-treated with DMSO and **(b)** cell pre-treated with C5. **(c)** AUC of total cAMP accumulation and **(d)** maximal cAMP response was measured. Data represented as fold change/basal and analysed using ordinary two-way ANOVA, followed by Šidák's multiple comparisons test. All data represent mean  $\pm$  SEM of n=4 independent experiments conducted in triplicate.

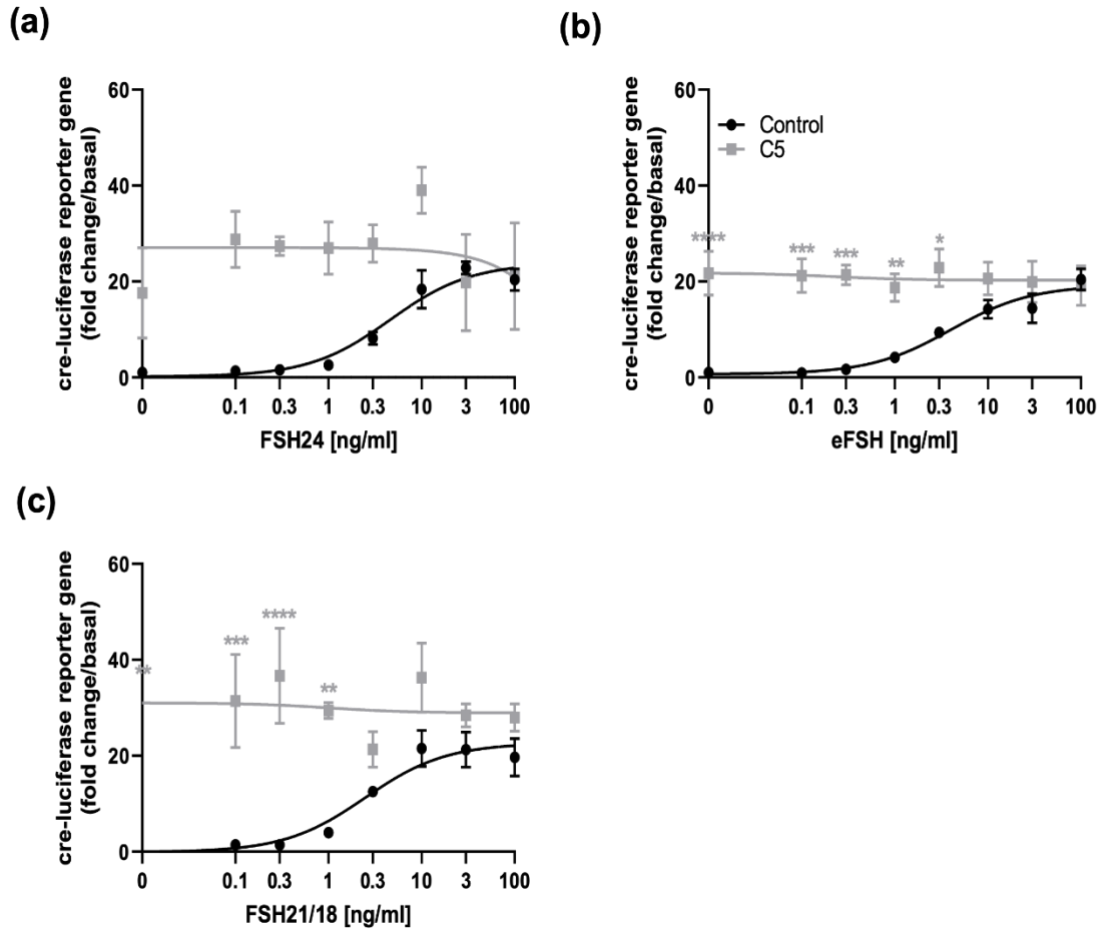


**Figure 5.8: Effect of Compound 5 on FSH glycoform-dependent FSHR-dependent cre-luciferase activity.** HEK293 cells were transiently co-expressing HA-tagged FSHR, cre-luciferase and *Renilla*-luciferase plasmids were co-treated in serum-free media with  $\pm 1\mu\text{M}$  of Compound 5 (C5) and increasing concentrations (0-100ng/ml) of **(a)** FSH24 ( $n=2-4$ ), **(b)** eFSH, or **(c)** FSH21/18, for 4-6 hours. All data points were normalised to *Renilla*-luciferase for transfection efficiency. Concentration-dependent effects of FSH glycoforms on cre-luciferase activity were measured and represented as fold change/basal and analysed using ordinary two-way ANOVA, followed by Šidák's multiple comparisons test. Each data point represents mean  $\pm$  SEM for  $n=3-5$  independent experiments, measured in triplicate. \*,  $p<0.05$ ; \*\*,  $p<0.01$ ; \*\*\*,  $p<0.001$ ; \*\*\*\*,  $p<0.0001$ .

### 5.2.3 Effect of C5 on FSH glycoform-dependent FSHR oligomerisation

Although figure 5.2 showed no changes in FSHR oligomerisation when cells were stimulated with 1 $\mu$ M of C5, previous results showed FSH glycoforms may mediate increases in FSHR-dependent cAMP signalling via FSHR oligomerisation (see chapter 3). To establish whether C5-dependent increases in cAMP in the presence of FSH glycoforms could be mediated by FSH glycoform-dependent FSHR oligomerisation, cells transiently expressing HA-FSHR were cultured, pre-treated with  $\pm$  1 $\mu$ M of C5 for 30 minutes and then stimulated with  $\pm$  30ng/ml of FSH glycoforms, and imaged for PD-PALM analysis (see chapter 2.4 for details).

Interestingly, the basal level of associated FSHR were higher than previous observation, with  $44.4 \pm 3.3\%$  of FSHR molecules associated as dimers and oligomers at the plasma membrane (Figure 5.9, (a)). As anticipated, 30-minute pre-treatment with C5 alone had no effect on either the total percentage of FSHR association, nor the percentage of associated FSHR subtypes observed (Figure 5.9, (a)). Co-treatment of C5 with FSH24 had no effect on the percentage of the total number of associated FSHR molecules at 2- and 5-minute treatment. However, at 15 minutes, C5 co-treatment decreased the total number of associated FSHR molecules from  $52.1 \pm 2.7\%$  to  $35.0 \pm 3.4\%$  ( $p < 0.05$ ) (Figure 5.9, (a)). Moreover, this appeared to be from dissociation of FSHR pentameric and 6-8 molecule forms (Figure 5.9, (biii)), suggesting that C5-dependent increases in cAMP in the presence of FSH24 may be mediated by changes in FSHR oligomerisation.

Unlike earlier chapters (see chapter 3), decreases in FSHR association was not observed by 5-minute treatment in cells stimulated with FSH24 alone (Figure 5.9, (a)).



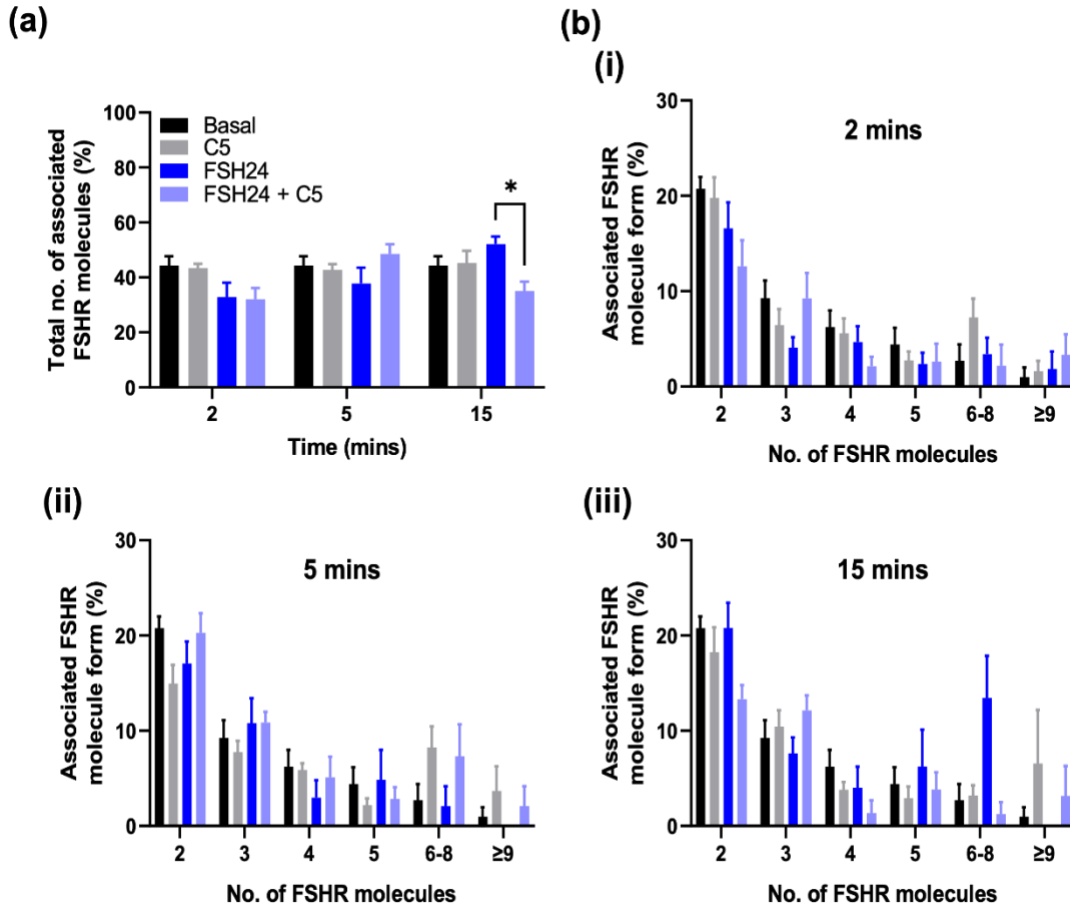


**Figure 5.9: Effect of Compound 5 on FSH24-dependent FSHR oligomerisation.** HEK293 cells transiently expressing HA-tagged FSHR were pre-incubated for 30 minutes with CAGE 552-HA antibody and co-treated with  $\pm 1\mu\text{M}$  of Compound 5 (C5) and 30ng/ml of FSH24, fixed and imaged via PD-PALM. **(a)** The percentage of the total number of associated FSHR molecules at either 2-, 5- or 15 minutes treatment; data analysed using ordinary two-way ANOVA, followed by Tukey's multiple comparisons test. **(b)** The percentage of associated FSHR molecule form; 2 (dimer), 3 (trimer), 4 (tetramer), 5 (pentamer), 6-8,  $\geq 9$ , at **(i)** 2 minutes, **(ii)** 5 minutes, and **(iii)** 15 minutes. Data analysed using multiple unpaired t-tests. All data represent mean  $\pm$  SEM of  $n \geq 3$  independent experiments and  $n \geq 9$  cells analysed per experiment. \*,  $p < 0.05$ .

Similar results were observed in cells co-treated with C5 and positive control eFSH (Figure 5.10), whereby C5 did not have any effect on FSH-dependent modulation of FSHR association at 2-, and 5-minute treatment (Figure 5.10, (a-bii)). Instead, decreases in FSHR association were only observed by 15-minute treatment (Figure 5.10, (a)), which appeared to arise from FSHR pentamer rearrangements (Figure 5.10, (biii)). Furthermore, decreases in FSHR association was not observed by 2-minute treatment in cells stimulated with eFSH alone in contrast to previous data (Figure 5.10, (a)). When cells were co-treated with C5 and FSH21/18 for 15 minutes, there was a significant increase in the percentage of FSHR association from  $32.4 \pm 3.8\%$  to  $50.1 \pm 4.5\%$  ( $p < 0.01$ ) (Figure 5.11, (a)), with FSHR monomers appearing to predominantly form  $\geq 9$  FSHR oligomers (Figure 5.11, (biii)). This suggests that in the presence of C5, FSHR oligomerisation is differentially modulated by different FSHR glycoforms. Nevertheless, like the FSH24- and eFSH data, there was no observed decrease in FSHR association in FSH21/18-treated cells by 2 minutes (Figure 5.11, (a)), unlike previous results (see chapter 3), and perhaps the result of utilising different FSH glycoform preparations.

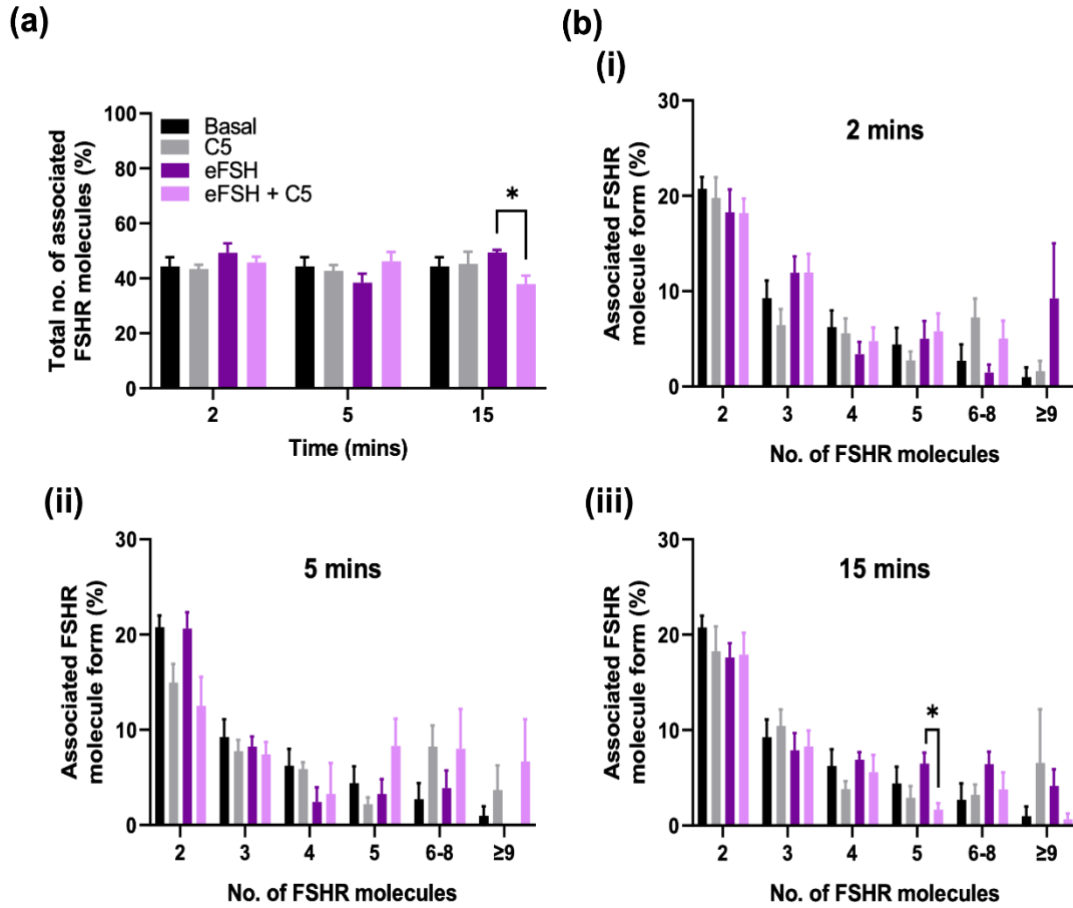


**Figure 5.10: Effect of Compound 5 on eFSH-dependent FSHR oligomerisation.** HEK293 cells transiently expressing HA-tagged FSHR were pre-incubated for 30 minutes with CAGE 552-HA antibody and co-treated with  $\pm 1\mu\text{M}$  of Compound 5 (C5) and 30ng/ml of eFSH, fixed and imaged via PD-PALM. **(a)** The percentage of the total number of associated FSHR molecules at either 2-, 5- or 15 minutes treatment; data analysed using ordinary two-way ANOVA, followed by Tukey's multiple comparisons test. **(b)** The percentage of associated FSHR molecule form; 2 (dimer), 3 (trimer), 4 (tetramer), 5 (pentamer), 6-8,  $\geq 9$ , at **(i)** 2 minutes, **(ii)** 5 minutes, and **(iii)** 15 minutes. Data analysed using multiple unpaired t-tests. All data represent mean  $\pm$  SEM of  $n \geq 3$  independent experiments and  $n \geq 9$  cells analysed per experiment. \*,  $p < 0.05$ .

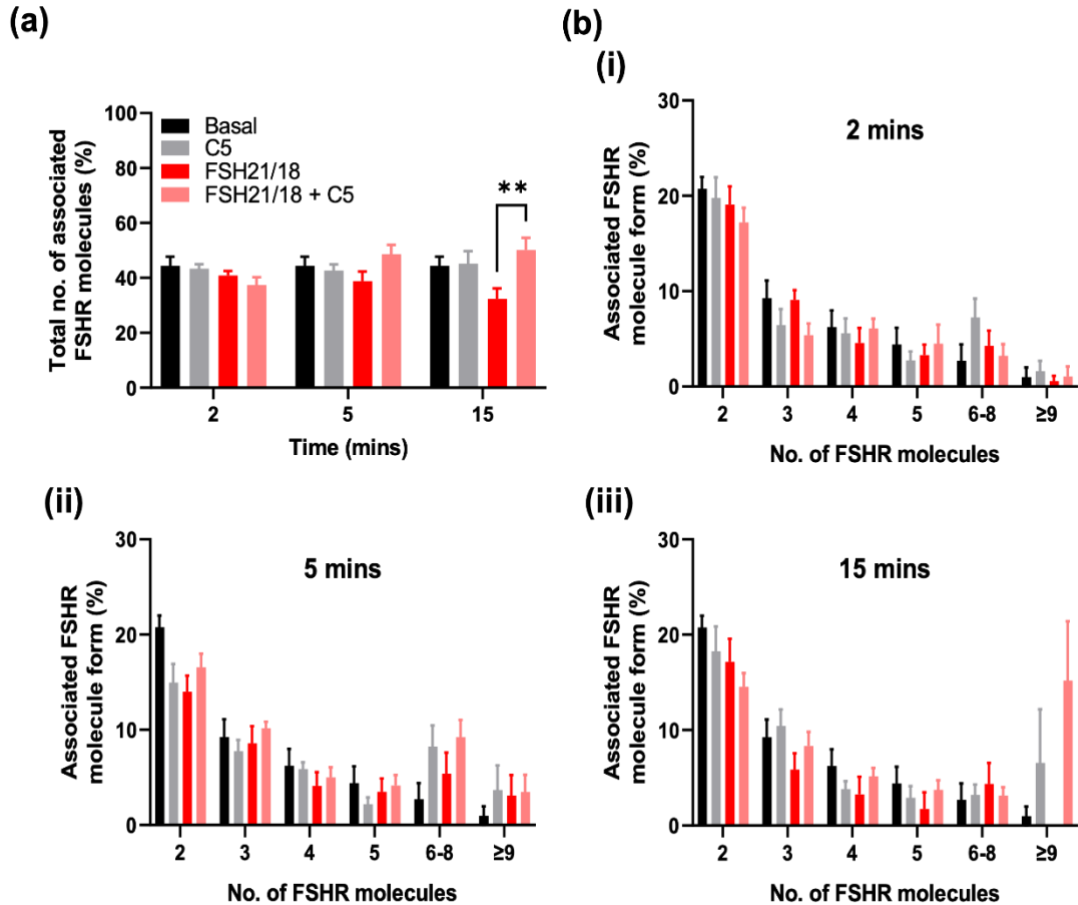


**Figure 5.11: Effect of Compound 5 on FSH21\18-dependent FSHR oligomerisation.** HEK293 cells transiently expressing HA-tagged FSHR were pre-incubated for 30 minutes with CAGE 552-HA antibody and co-treated with  $\pm 1\mu\text{M}$  of Compound 5 (C5) and 30ng/ml of FSH21/18, fixed and imaged via PD-PALM. **(a)** The percentage of the total number of associated FSHR molecules at either 2-, 5- or 15 minutes treatment; data analysed using ordinary two-way ANOVA, followed by Tukey's multiple comparisons test. **(b)** The percentage of associated FSHR molecule form; 2 (dimer), 3 (trimer), 4 (tetramer), 5 (pentamer), 6-8,  $\geq 9$ , at **(i)** 2 minutes, **(ii)** 5 minutes, and **(iii)** 15 minutes. Data analysed using multiple unpaired t-tests. All data represent mean  $\pm$  SEM of  $n \geq 3$  independent experiments and  $n \geq 9$  cells analysed per experiment. \*\*,  $p < 0.01$ .

### 5.3 Discussion

The small molecular FSHR agonist, C5, has been previously shown to behave as a potent FSHR agonist (Yanofsky et al., 2006) and has also been shown to enhance FSH24 binding to the FSHR (personal communication with George Bousfield). This has made C5 an attractive oral therapeutic target to bypass the use of FSH injectables during IVF, together with a potential role for enhancing endogenous action of FSH24 in older reproductive women. However, the effects of C5 on FSH glycoform-dependent signalling and how it may correlate with FSHR oligomerisation were not clear. Therefore, the aim of this chapter was to investigate the effect of C5 on FSHR-mediated signalling and oligomerisation. Results revealed C5 behaved as a potent FSHR agonist, inducing FSHR endocytosis-dependent cAMP accumulation and cre-luciferase activity, and increases in FSHR density in HEK293 cells. Furthermore, FSH glycoform-dependant cAMP production were ineffective in the presence of C5 and may have been partially mediated by changes in FSHR oligomerisation.

Results in this chapter have further corroborated that C5 behaves as a potent FSHR agonist by modulated basal FSHR activity and significantly increasing cAMP and cre-luciferase activity. Several other studies also demonstrated FSHR signal activation when C5 was administered in the absence of FSH (Arey et al., 2008; Yanofsky et al., 2006). In one recent study, where C5 was referred to as T1, C5 demonstrated the ability to mediate FSHR coupling to G $\alpha$ s and G $\alpha$ i with greater efficacy than FSH (De Pascali et al., 2021). Therefore, not only does C5 increase the potency of FSH at lower concentrations, as the data has shown, but C5 can induce FSHR signalling independent of FSH. This offers potential therapeutical use as an alternative to current FSH injectables if C5 could be administered orally to enhance the action of endogenous circulating FSH glycoforms

especially amongst poor responders such as older women with higher circulating less bioactive FSH24 (Bousfield et al., 2014b). Besides, oral administration preference has already been successful in treating patients for rheumatoid arthritis (Hansen & Kavanaugh, 2014; Lundquist et al., 2014) and multiple sclerosis (Safavi et al., 2015). Furthermore, administration of C5 may treat reproductive pathologies related to low/insufficient FSH, such as hypogonadism, provided that the FSHR is functional in these patients.

Remarkably, PD-PALM data in this chapter revealed that C5 increased FSHR density at the plasma membrane. Although the mechanism governing this observation was not investigated, it was suggested that FSHR density may be mediated by FSHR internalisation/recycling processes. Sposini *et al* showed that C5 increased the number of FSHRs targeted to endosomes, and mediated FSHR recycling back to the plasma membrane via the adaptor protein, APPL1 (Sposini et al., 2020). Another study on mutant LH/CGRs, that were intracellularly retained within the cytoplasm, were rescued, and trafficked to the cell surface by another GPCR allosteric agonist (Org 42599) (Newton et al., 2011). Furthermore, another similar LH/CGR agonist (Org 41841), that behaved as an FSHR allosteric modulator, was shown to behave as a pharmacochaperone drug by increasing the expression of mutant and WT FSHRs to the plasma membrane without increasing FSHR mRNA (Janovick et al., 2009). It is possible that C5 may behave in this way with the FSHR, increasing the number of newly synthesised FSHR routing to the plasma membrane, and may play a predominant role in FSHR recycling. In addition, it is important to consider that C5-dependent FSHR membrane density may affect the balance between distinct signal transduction pathways (Tranchant et al., 2011), therefore, it would be interesting to explore  $\beta$ -arrestin-dependent ERK1/2-phosphorylation within the HEK293 cell model.

Even though C5 has been shown to enhance <sup>125</sup>I-FSH24 binding to the FSHR (personal communication with George Bousfield), in this study C5 alone maximally enhanced cAMP production with very little effect of FSH glycoform co-treatment. This suggests that C5 may induce minimal adverse side effects in the presence of higher concentrations of FSH glycoforms. This may be of therapeutic advantage, especially within the cohort of older reproductive women who have higher circulating serum levels of FSH24, but also amongst younger reproductive prime women who have higher circulating serum levels of FSH21/18 (Bousfield et al., 2014b). The enhanced FSHR signalling activity observed in the presence of C5 may be mediated by FSHR oligomerisation, as PD-PALM results revealed significant decreases in FSH glycoform-dependent FSHR association into more active monomer at later time points, which may have implications on increased receptor activity through receptor negative cooperativity (Urizar et al., 2005). Alternatively, C5 may mediate the magnitude of FSHR-dependent cAMP signalling through other distinct mechanisms independent of FSHR oligomerisation. One study using transgenic mice ubiquitously expressing a cAMP sensor recorded sustained cAMP signalling triggered by internalisation of the TSHR (Calebiro et al., 2009). Moreover, during the experiments undertaken in this chapter it was reported that internalisation of the FSHR mediated sustained cAMP signalling (Sposini et al., 2020), giving further insight into alternative mechanisms of FSHR signalling.

In this study, C5 appeared to increase FSH21/18-dependent FSHR association by 15-minute treatment, suggesting that in the presence of C5, FSH glycoforms differentially mediate FSHR oligomerisation. The site of action of C5 has been previously mapped to the TMD using an FSHR/TSHR chimera (F/T III) generated by replacing the TSHR with a proportion of the FSHR sequence corresponding to TMD1, ICL1, TMD2 and ECL2

(Yanofsky et al., 2006), suggesting that C5 interact with FSHR in an allosteric manner. Interestingly, the proposed interaction site of C5 is near the conserved dimerisation interface of other Class A GPCRs (Baltoumas et al., 2016; Huang et al., 2013; Zhao et al., 2019) and possibly the FSHR (Guan et al., 2010). Given that different FSH glycoforms possess a different number of Asn-linked glycan chains on their  $\beta$ -subunit (see chapter 1.4.3.2), the glycoform-dependent differences in FSHR oligomerisation observed in the presence of C5 could be influenced by differences in interactions between the FSH glycan chains and C5, and ultimately the FSHR dimerisation interface. Indeed, both eFSH and FSH24 possess a total of four Asn-linked glycan chains and an increase in FSHR oligomerisation was observed in these treatment groups in the presence of C5. In contrast, FSH21/18 possesses a total of three Asn-linked glycan chains and a decrease in FSHR oligomerisation was observed in this treatment group. However, structure-based techniques such as x-ray crystallography and cryo-EM would need to be applied to investigate this concept further.

The basal level of associated FSHR were higher than previous observations (see chapter 3), with ~44.4% of FSHR molecules associated as dimers and oligomers and could have contributed to the lack of FSH glycoform effects on FSHR oligomer rearrangement. Although this observation may have been modulated, in part, by FSHR density (Annibale et al., 2011b), it is possible that differences in FSH glycoform preparation may have also played a role. The batch of FSH glycoforms used in this chapter were different from the FSH glycoforms used in the previous chapters. inter-batch variability from newly synthesised FSH glycoform preparations, arising from differences in their microheterogeneity (see chapter 1.4.3.1), may have affected the efficacy and biological activity when the FSH glycoforms engaged with the FSHR (Ulloa-Aguirre et al., 1999).



Additionally, differences in the kinetics of the FSH glycoforms were reported in various other research groups utilising the same FSH glycoform preparations, and so results in this chapter must be interpreted with caution.

Similar to the limitations discussed in chapter 4, a key limitation in this chapter, which may affect the interpretation of the results reported here, was the possibility of cell toxicity from Dyngo<sup>®</sup>-4a experiments. Since dynamin inhibition has been associated with cell death in some cell types (von Beek et al., 2021), it is possible that the reduction in FSHR-dependent cAMP in cells pre-treated Dyngo<sup>®</sup>-4a could be the result of cell death. Nevertheless, Dyngo<sup>®</sup>-4a has been reported to be non-toxic in other cell lines, not affecting cell viability (McCluskey et al., 2013), which could suggest that the data reported in this chapter are valid. To ascertain this possibility, future experiments would need to include a Dyngo<sup>®</sup>-4a tolerance test. This would involve subjecting HEK293 cells to different concentrations of Dyngo<sup>®</sup>-4a over different incubation periods. A cell viability test could then determine the status of cells by measuring live cell number via trypan blue staining or by measuring caspase or ATP levels.

While there is promising therapeutic potential with C5, FSHR agonists are currently not commercially available as they possess many drawbacks. There is a risk of potential off-target effects of C5, as extragonadal expression of the FSHR has been proposed (Cui et al., 2012; Ponikwicka-Tyszko et al., 2016; Robinson et al., 2010; Stilley et al., 2014; Stilley & Segaloff, 2018; Sun et al., 2006). Additionally, FSHR agonists display inherent toxicity, poor solubility, difficulties in chemical synthesis and low *in vivo* bioactivity (Sriraman et al., 2014), all of which was not assessed in this chapter. Although there has been some

recent progress in determining the structural facets of the binding sites of small FSHR modulators (Aathi et al., 2022), advancements in identifying modulators with enhanced bioactivity and resistance to proteolytic degradation remains slow and requires further research.

In conclusion, it has been demonstrated that the potent FSHR agonist, C5, can enhance both FSH glycoform-dependent and -independent FSHR signalling. The mechanism by which C5 mediate this is thought to be via both FSHR oligomerisation and trafficking and recycling of the FSHR to the plasma membrane. This may become an important way to target the FSHR and improve fertility outcomes for older women undergoing IVF or for poor responders by orally enhancing the actions of endogenous FSH and FSHR activity, however this would need to be explored further.

**6 Chapter Six: Screening and identification of novel FSHR inhibitors and the effect on FSH/FSHR binding, signalling and oligomerisation**

## 6.1 Introduction

Similar to FSHR agonists, there have been multiple small molecule non-peptide modulators that have been identified and shown to further diminish FSHR signalling with promising therapeutic advantages (Aathi et al., 2022). Currently there have been several age-related extragonadal roles of FSH/FSHR that have been proposed, with menopausal-dependent elevation in FSH linked to bone loss (Ji et al., 2018; Sun et al., 2006; Zhu et al., 2012), increased adiposity (Abildgaard et al., 2021; Liu et al., 2017) ovarian cancer (Song et al., 2020) and Alzheimer's disease (Xiong et al., 2022). Moreover, current contraception's are predominantly steroid hormone-based and associated with rare, but major, health risks such as venous and arterial thrombosis (Sech & Mishell, 2015) and cardiovascular disease (Sitruk-Ware & Nath, 2011). Therefore, finding targeted ways to inhibit FSHR activity is an appealing approach to combat these issues.

Suramin was the first known FSHR inhibitor that was previously used as a treatment for metastatic cancer (Stein et al., 1989). It has been shown to decrease plasma testosterone levels in male human and rat Leydig cells (Danesi et al., 1996), however, there were reports of many associated side effects such as nephrotoxicity, hypersensitivity reactions, dermatitis, anaemia, peripheral neuropathy, and bone marrow toxicity (Wiedemar et al., 2020). Indeed, other non-peptide FSHR inhibitors have been identified and shown to inhibit FSH-dependent cAMP production and steroid synthesis in *in vitro* and prevent ovulation in mature rats (Arey et al., 2002). Nevertheless, they displayed low efficacy and were concluded as unsuitable for contraception. This was due to mice developing chronic ovarian inflammation, with eosinophilic foreign material observed at the peritoneal surface as a result from high doses (100mg/kg) administered via IP injections (Arey et al., 2002).

Later studies identified the tetrahydroquinoline derivative, Compound 10, as a non-competitive FSH-dependent cAMP inhibitor in CHO cells expressing human FSHR (van Straten et al., 2005), and oestradiol and progesterone in rat GCs (referred to as ADX49626) (Dias et al., 2011). In the same study, high throughput screening identified a non-steroidal Addex compound, ADX61623, as a biased FSHR inhibitor capable of inhibiting FSH-dependent intracellular cAMP and progesterone, but not oestradiol production (Dias et al., 2011). Although this provided promising avenues for the development of highly specific drugs to target key branches of FSHR signalling pathways, ADX61623 was unable to decrease oocyte development when rats were treated with maximum doses of 50mg/kg, and was unsuitable for non-steroidal contraceptive purposes (Dias et al., 2011). A follow up study identified two additional non-steroidal compounds, ADX68692 and ADX68693 (Dias et al., 2014). ADX68692 displayed relatively good oral availability and was able to inhibit cAMP, progesterone, oestradiol production, and disrupt the oestrus cycle in mature female rats at low doses (up to 25mg/kg). However, further examinations were required to determine whether complete inhibition could be achieved at higher doses (Dias et al., 2014). In contrast, ADX68693, displayed even better oral availability but was unable to inhibit oestrogen, nor decrease the number of oocytes ovulated in rats (Dias et al., 2014).

Although many small molecule FSHR inhibitors have been previously identified, none are commercially available. By partnering with Atomwise, a drug discovery company who used artificial intelligence (AI) to produce 84 small molecule potential FSHR inhibitors, the aim of this chapter was to screen and identify potential FSHR inhibitors and determine their effect on FSH/FSHR-dependent binding, cAMP-dependent signalling and FSHR oligomerisation, with a view to find a potential FSHR inhibitor for commercial use. The objectives set out to address this aim were to:

1. Screen the 84 compounds for ability to inhibit FSH-dependent cre-luciferase activity in HEK293 cells expressing FSHR.
2. Determine the effect of identified FSHR inhibitors on FSH/FSHR binding using radioligand binding assays in EpiHEK293 cells expressing the FSHR.
3. Determine the concentration-dependent effects of identified FSHR inhibitors on FSH-dependent cre-luciferase activity in HEK293 cells expressing FSHR.
4. Investigate the effect of an FSHR inhibitor on FSHR oligomerisation in HEK293 cells expressing FSHR.

## 6.2 Results

### 6.2.1 Screening of 84 different small molecule candidate compounds for the ability to inhibit FSH-dependent cre-luciferase activity

First, to explore the ability for the 84 different small molecule compounds (SMCs) to inhibit FSH-dependent FSHR activity, HEK293 cells transiently expressing the FSHR were cultured for cre-luciferase activity analysis (see chapter 2.5 for details). Cells were pre-treated in serum free media with  $\pm 100\mu\text{M}$  of each 84 SMC (single-shot screening) for 30 minutes at  $37^{\circ}\text{C}$  and stimulated with  $100\text{ng/ml}$  of pituitary FSH (FSH) for 4-6 hours before lysates were analysed for cre-luciferase activity (see chapter 2.6 for details).

When cells were pre-treated with  $100\mu\text{M}$  of the individual SMCs alone, the compounds displayed distinct effects on basal FSHR cre-luciferase activity, with some compounds decreasing (SMC 16-22, 24, 27-28, 30, 48, 50, 59-60, 62, 64-65, 68-75, 77-81, 83-84), some increasing (SMC 1-5, 7-15, 32, 37, 39, 44-45 and 53) and some having no effect (SMC 6, 23, 25-26, 29, 31, 33-36, 38, 41-43, 46-47, 49, 51-52, 56-58, 61, 63, 66-67, 76 and 82) on basal cre-luciferase activity (Figure 6.1), suggesting some of the compounds may behave as partial agonists or antagonists. When cells were stimulated with  $100\text{ng/ml}$  of FSH, a similar trend was observed, inducing, or reducing further cre-luciferase activity, respectively (Figure 6.1).

To identify potential FSH inhibitors from the catalogue of 84 SMCs, the percentage of inhibition of FSH-dependent cre-luciferase activity was measured, of which 4 SMCs (SMC 48, -74, -80 and -84) were found capable of lowering FSH activity by  $>90\%$  (Figure 6.2).

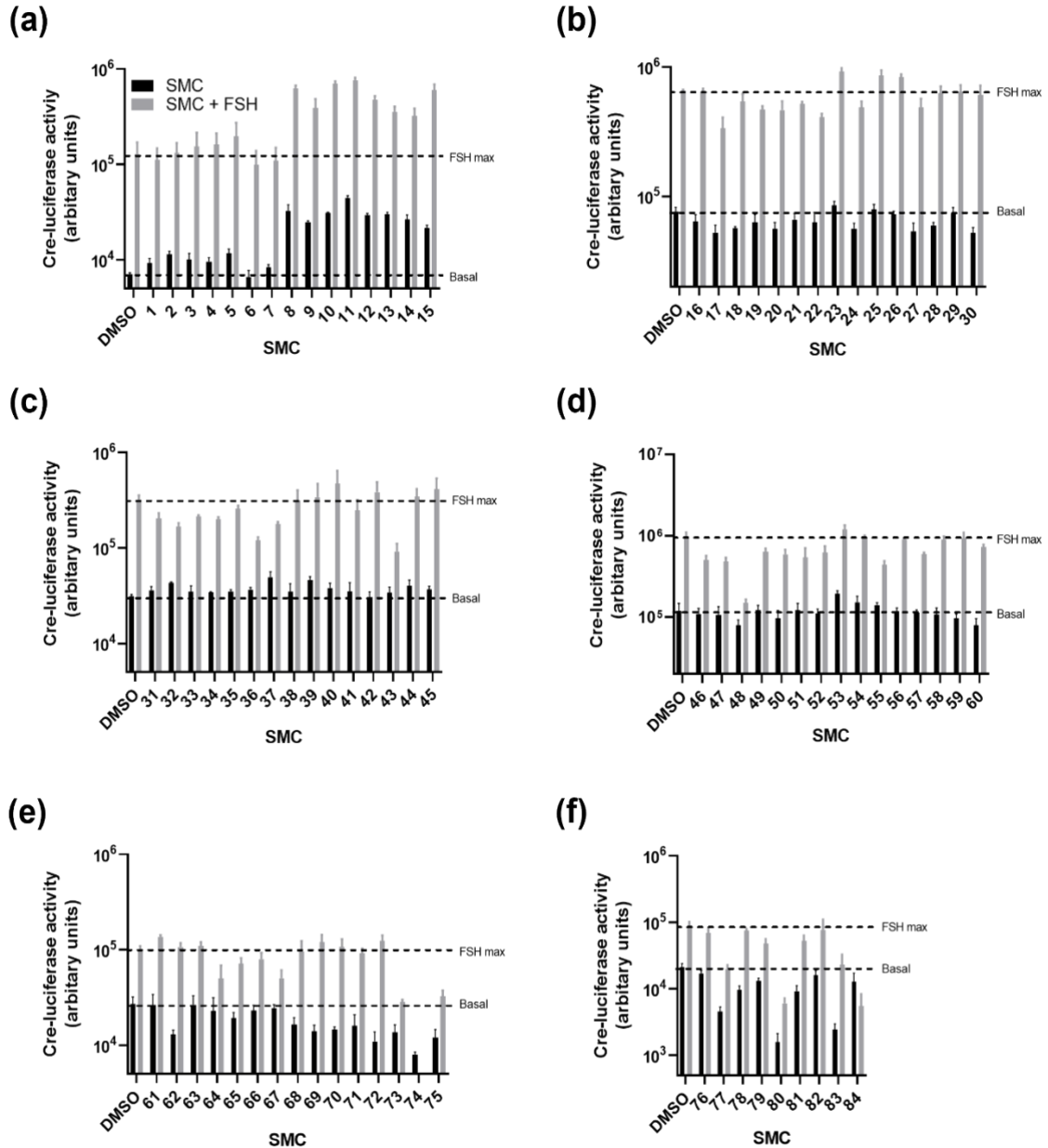


**Figure 6.1: Screening of potential FSHR inhibitors for effect on basal and FSH-dependent cre-luciferase activity.** HEK293 cells transiently co-expressing HA-tagged FSHR, and cre-luciferase and *Renilla*-luciferase plasmids were pre-treated  $\pm$  100 $\mu$ M of (a) small molecule compound (SMC) 1-15, (b) SMC 16-30, (c) SMC 31-45, (d) SMC 46-60, (e) SMC 61-75 or (f) SMC 76-84 for 30 minutes, and subsequently stimulated with 100ng/ml FSH for 4-6 hours. Cre-luciferase and *Renilla*-luciferase activities were measured, and cre-luciferase activity normalised to individual *Renilla*-luciferase activity as a transfection efficiency control. Each data point represents the mean  $\pm$  SEM from n=1 independent experiment, measured in triplicate.



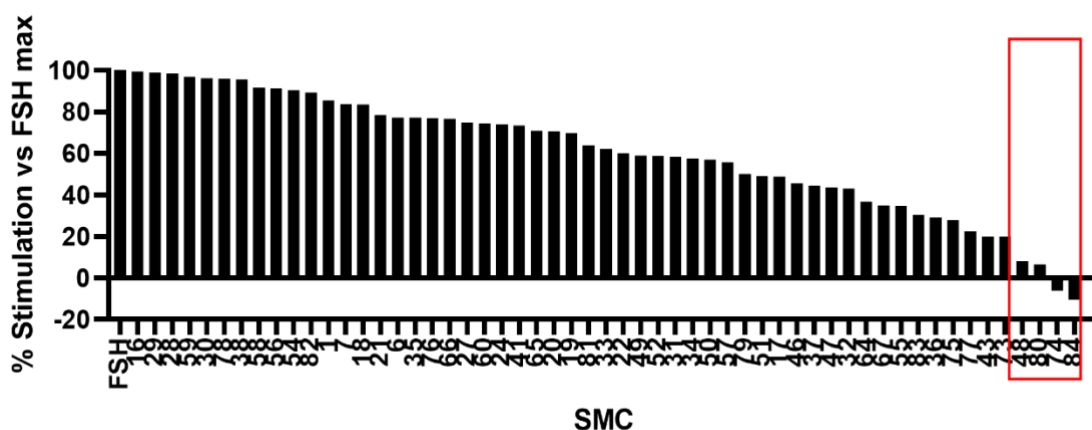


**Figure 6.2: Identification of hit SMCs with the potential to inhibit FSH activity.** Cre-luciferase data was extrapolated from initial small molecule compound (SMC) screen (Figure 6.1) and subtracted from basal activity. Data was presented as percentage of maximal FSH-stimulated cre-luciferase activity. The four SMCs (red box) that displayed >90% ability to inhibit FSH stimulation were taken forward for further analysis. Data points represent the mean from n=1 independent experiment, measured in triplicate.

These SMCs were further profiled to ascertain their ability to inhibit FSH activity by pre-treating cells with increasing concentrations of each compound before stimulation with 100ng/ml FSH (Figure 6.3). The effect of pre-treatment had no effect on FSHR activity in the absence of FSH, suggesting that these hit SMCs did not inhibit basal FSHR cre-luciferase activity. Following FSH stimulation, concentrations lower than 30 $\mu$ M of SMC 48, -74 and -80 were unable to inhibit FSH activity, however, when the maximum concentrations (100 $\mu$ M) were used, there was >90% inhibition of FSH activity observed (Figure 6.3, (a-c)), corroborating with previous results (Figure 6.2). Despite initial inhibition of FSH activity in SMC 84-treated cells during screening, pre-treatment with all concentrations of SMC 84 failed to inhibit FSH activity (Figure 6.3, (d)), and so SMC 84 was omitted from further assessment.

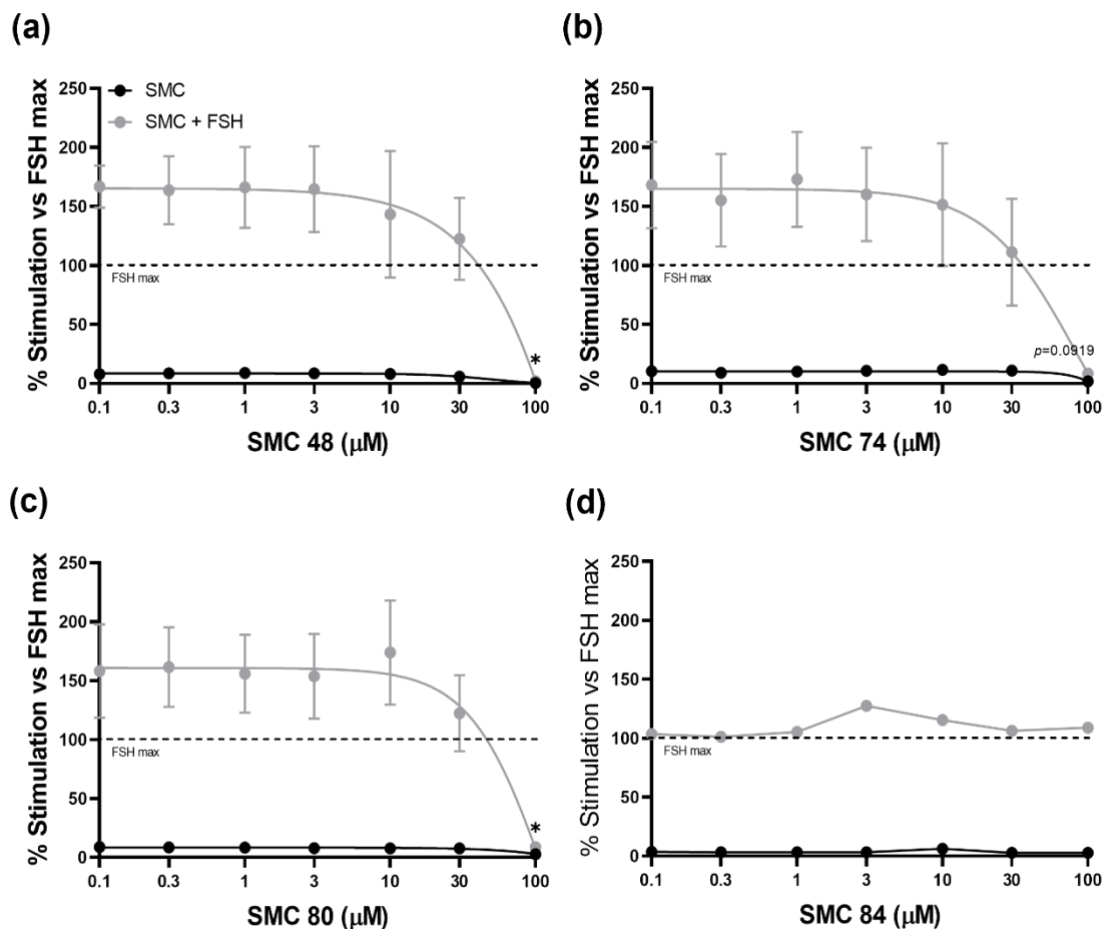


**Figure 6.3: Concentration-dependent effects of FSHR inhibitors on FSH-dependent cre-luciferase activity.** HEK293 cells transiently co-expressing HA-tagged FSHR, and cre-luciferase and *Renilla*-luciferase plasmids were pre-treated in serum-free media with  $\pm$  0-100 $\mu$ M of either **(a)** small molecule compound (SMC) 48, **(b)** SMC 74, **(c)** SMC 80 or **(d)** SMC 84 for 30 minutes. Cells were then stimulated with for 4-6 hours with 100ng/ml of FSH. Cre-luciferase activity was measured and normalised to *Renilla* luminescence for transfection efficiency. Results were recorded as a percentage of maximal FSH-dependent cre-luciferase activity from control cells pre-treated with inhibitor vehicle alone (DMSO) and stimulated with 100ng/ml FSH. Each data point represents mean  $\pm$  SEM from n=3 independent experiments (except for (d), n=1), measured in triplicate. Data analysed using 2-way AVOVA, followed by Dunnett's multiple comparisons test. \*,  $p < 0.05$ .

### 6.2.2 Effect of identified FSHR inhibitors on FSH/FSHR binding using radioligand binding assays

To determine the mechanism of action of the hit SMC 48, -74, and -80 on FSH/FSHR activity, radioligand binding assays were conducted by collaborators (Professor George Bousfield and Dr Viktor Butnev, Wichita State University, Kansas). EpiHEK293 cells transiently expressing the human FSHR were cultured (see chapter 2.10 for details) and cells were pre-treated with  $\pm 100\mu\text{M}$  of each SMC in the presence of a cold tracer  $^{125}\text{I}$ -FSH (AFP7298A). Cells were stimulated with increasing concentrations of FSH (0.1-1000ng) for 3 hours and specific binding of  $^{125}\text{I}$ -FSH to the FSHR was recorded (Figure 6.4).

In control cells that were stimulated with increasing concentrations of FSH, there was a decrease in  $^{125}\text{I}$ -FSH specific binding from  $\sim 8000$  counts per minute (cpm) to  $\sim 400$ cpm, showing that FSH displaced FSHR-bound  $^{125}\text{I}$ -FSH (Figure 6.4). Interestingly, when cells were pre-treated with any of the hit SMCs, there was enhanced  $^{125}\text{I}$ -FSH binding to FSHR, whereby SMC 80 enhanced the binding affinity the most (Figure 6.4). The absence of an evident left/right shift in the binding curves suggest these hit SMCs behave in a non-competitive manner with potential FSHR binding at an allosteric site.

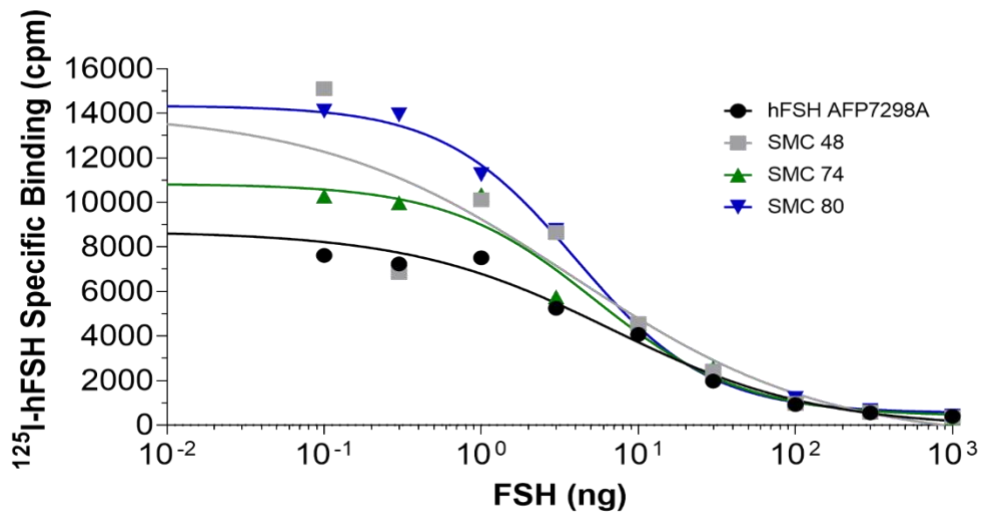


**Figure 6.4: Effect of FSHR inhibitors on the binding affinity of <sup>125</sup>I-FSH to the FSHR.** EpiHEK293 cells transiently expressing the human FSHR were pre-treated with  $\pm 100\mu\text{M}$  either SMC 48, -74 or, -80 in the presence of a cold tracer <sup>125</sup>I-hFSH (AFP7298A). Cells were then stimulated with increasing concentrations of FSH (0.1-1000ng) and incubated for 3 hours at 37°C. Data represents the mean from n=1 independent experiment, measured in duplicate.

### 6.2.3 Concentration-dependent effects of FSH on FSHR activity when inhibited with different concentrations of different FSHR inhibitors

To further profile the identified FSHR inhibitors, the next step was to establish the effect of FSH on FSHR activity when inhibited with different concentrations of the different FSHR inhibitors. Cells transiently expressing FSHR were cultured for cre-luciferase activity analysis (see chapter 2.6 for details). Cells were pre-treated with either DMSO, 1-, 10- or 100 $\mu$ M of SMC 48, -74, or -80 for 30 minutes and stimulated with increasing concentrations of FSH (0-100ng/ml) for 4-6 hours. Lysates were analysed for cre-luciferase luminescence (see chapter 2.6 for details) and cre-luciferase activity recorded as a percentage when compared to maximal cre-luciferase activity from control cells pre-treated with DMSO and stimulated with FSH.

Pre-treatment with 1- and 10 $\mu$ M of SMC 48 had minimal effect on FSH activity when compared to controls cells (Figure 6.5, (a)), however, FSH activity was completely inhibited when cells were pre-treated with 100 $\mu$ M of SMC 48 ( $p < 0.0001$ ) (Figure 6.5, (a)). This suggests a concentration-dependent threshold is required for SMC 48 to inhibit FSH activity. Pre-treatment with all concentrations of SMC 74 induced a modest decrease in FSH activity (~25-33%), however, differences between the concentrations of SMC 74 had little effect of FSH activity (Figure 6.5, (b)), suggesting that low concentrations of SMC 74 is sufficient to inhibit some FSH activity. When cells were pre-treated with all concentrations of SMC 80, maximal FSH activity was unreached when compared to control cells (Figure 6.5, (c)). Upon further analysis, in the presence of 10- and 100 $\mu$ M of SMC 80 there was ~30% ( $p < 0.01$ ) and ~60-80% ( $p < 0.0001$ ) reduction in FSH activity when compared to control cells (Figure 6.5, (d)). This further suggested that SMC 80 may behave as a non-competitive inhibitor.

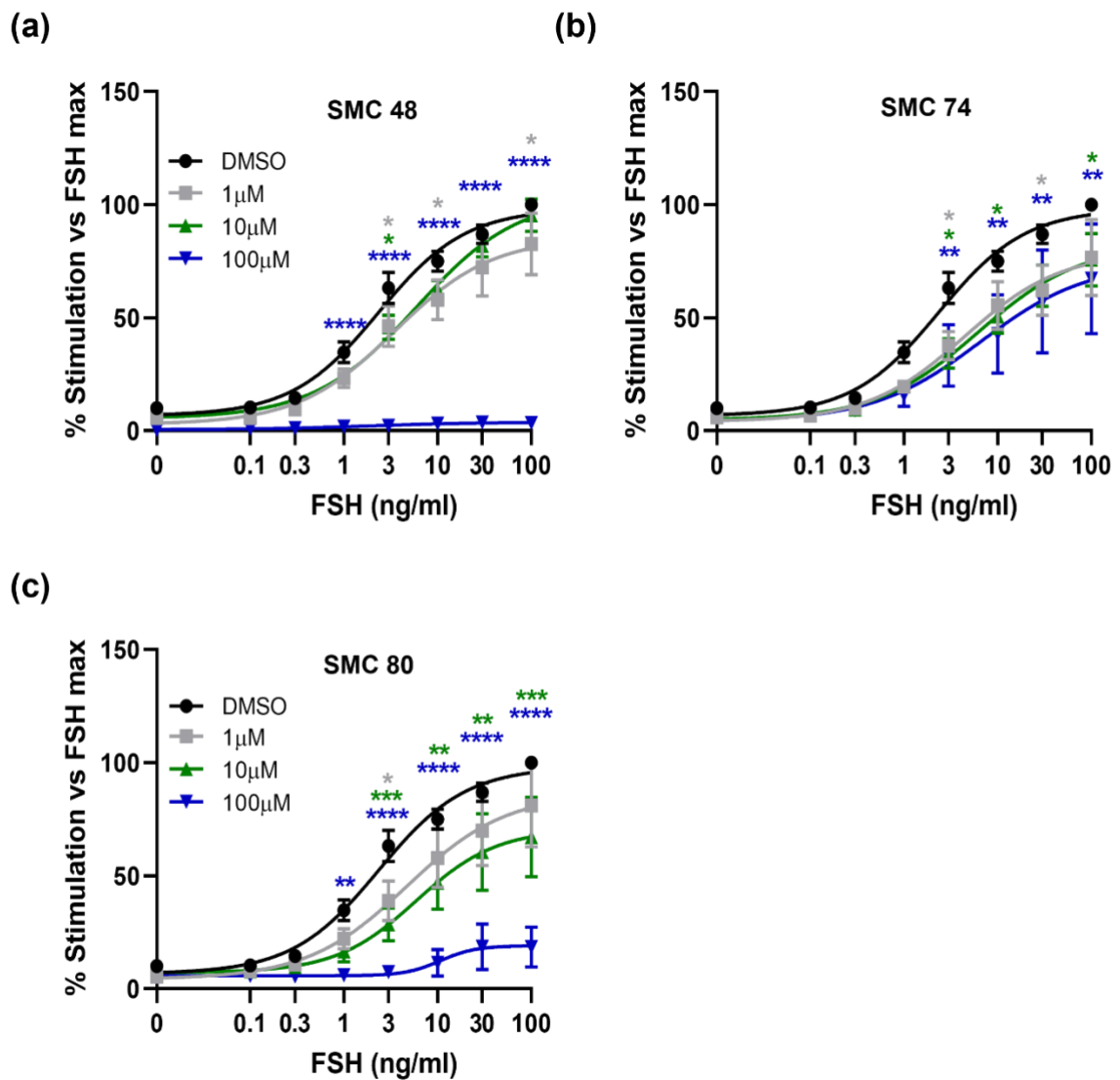


**Figure 6.5: Concentration-dependent effects of FSH on FSHR activity when inhibited with different concentrations of different FSHR inhibitors.** HEK293 cells transiently co-expressing HA-tagged FSHR, and *cre*-luciferase and *Renilla*-luciferase plasmids were pre-treated in serum-free media with DMSO, 1-, 10-, or 100µM of **(a)** small molecule compound (SMC) 48, **(b)** SMC 74, and **(c)** SMC 80 for 30 minutes. Cells were then stimulated with 0-100ng/ml of FSH for 4-6 hours and *cre*-luciferase activity was measured and normalised to *Renilla* luminescence for transfection efficiency. Results were recorded as a percentage when compared to maximal *cre*-luciferase activity from control cells pre-treated with DMSO and stimulated with FSH. Data analysed using two-way ANOVA, followed by Dunnett's multiple comparisons test. All data represent mean  $\pm$  SEM for  $n \geq 5$  independent experiments, measured in triplicate. \*,  $p < 0.05$ ; \*\*,  $p < 0.01$ ; \*\*\*,  $p < 0.001$ ; \*\*\*\*,  $p < 0.0001$ . Asterisks colours represent comparisons between a specific treatment group and DMSO.

#### 6.2.4 Effect of an FSHR inhibitor on FSHR oligomerisation

Since SMC 80 had the greatest effect on FSH binding to FSHR and showed concentration-dependent differences in ability to modulate FSH/FSHR-dependent cre luciferase activity, PD-PALM experiments were conducted in transfected cells to assess how SMC 80 affected FSHR oligomerisation (see chapter 2.4 for details).

When cells were pre-treated with DMSO, ~40% of FSHR molecules were associated (Figure 6.6), and consistent with previous results (see chapter 3 and chapter 5). Stimulation with 30ng/ml of purified pituitary FSH for 2 minutes saw no changes in FSHR association (Figure 6.6, (ai)), nor the type of FSHR oligomers observed (Figure 6.6, (aii)). These results were consistent with previous results observed in FSH24-treated cells (chapter 3) as purified pituitary FSH is largely comprised of fully glycosylated FSH24 (Bousfield et al., 2007). Surprisingly, when cells were pre-treated with 100 $\mu$ M of SMC 80 there appeared to be a decrease in FSHR association arising predominantly from FSHR dimers and tetramers (Figure 6.6). This may suggest that SMC 80 interaction with the FSHR may interfere with FSHR di/oligomerisation interfaces, or it may affect the activation state of the FSHR, and thus disrupting protomer interactions. When SMC 80 pre-treated cells were stimulated with FSH for 2 minutes, FSHR molecules appeared to re-associate into predominantly dimers and trimers and resembled basal configuration (Figure 6.6, (aii)). These results may propose that in the presence of SMC 80, FSH binding induces a conformational change in the FSHR that remodels FSHR oligomerisation. 5-minutes treatment with SMC 80 alone saw FSHR molecules appear to re-associate back to basal configuration (Figure 6.6, (b)), suggesting the actions of SMC 80 at the FSHR may be rapid.

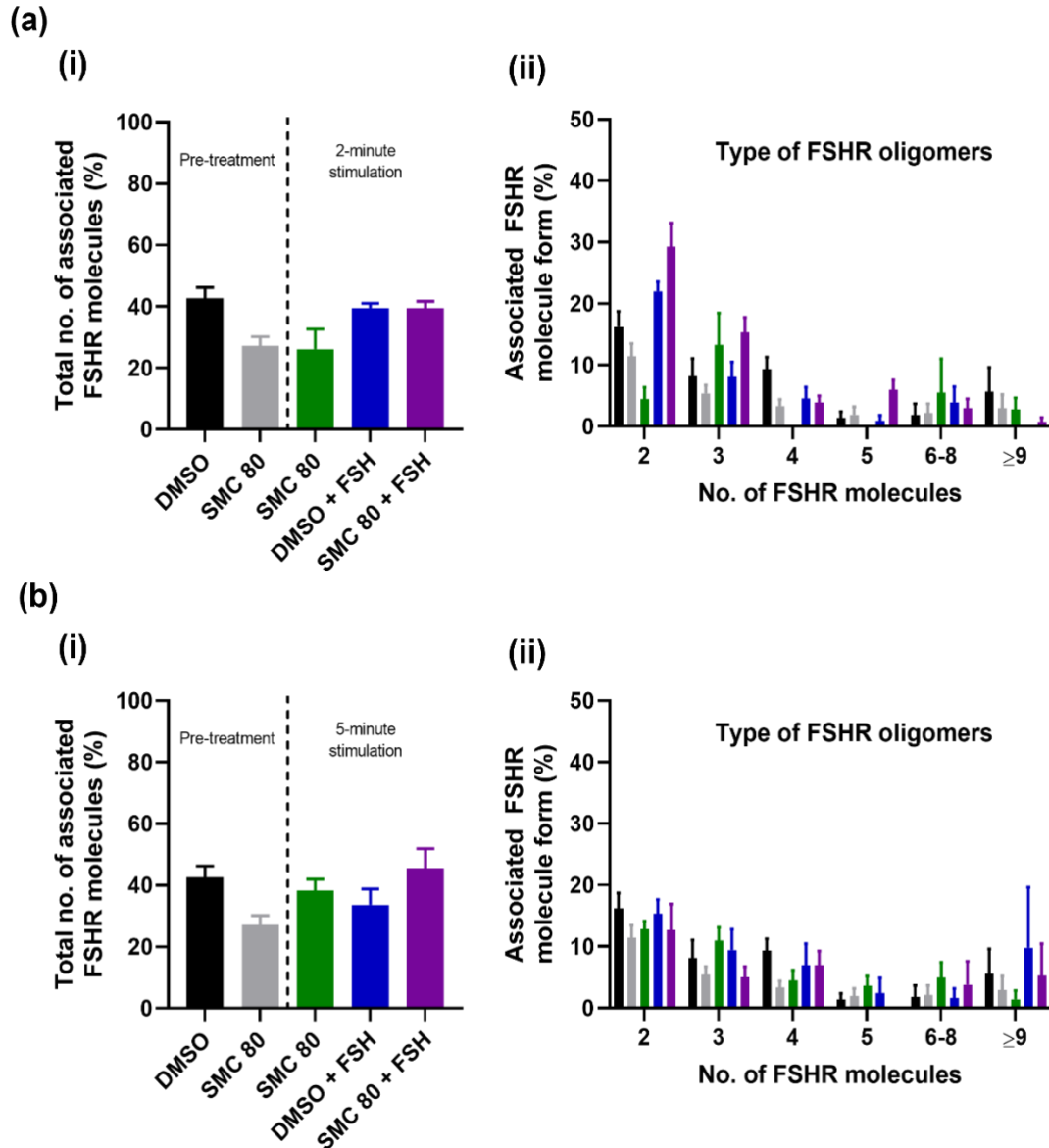


**Figure 6.6: Effect of SMC 80 on FSH-dependent FSHR oligomerisation.** HEK293 cells transiently expressing HA-tagged FSHR were pre-incubated for 30 minutes with CAGE 552-HA antibody and DMSO  $\pm$  100 $\mu$ M small molecule compound (SMC) 80. Cells were stimulated with  $\pm$  30ng/ml of FSH for **(a)** 2- or **(b)** 5 minutes, fixed and imaged via PD-PALM. **(i)** Percentage of the total number of associated FSHR molecules. **(ii)** Percentage of associated FSHR molecule form; 2 (dimer), 3 (trimer), 4 (tetramer), 5 (pentamer), 6-8,  $\geq$ 9. All data represent mean  $\pm$  SEM from n=1 independent experiment with n $\geq$ 3 cells analysed per experiment.



### 6.3 Discussion

Menopause-related increases in FSH has been linked to several pathologies such as bone loss (Ji et al., 2018; Sun et al., 2006; Zhu et al., 2012), increased adiposity (Abildgaard et al., 2021; Liu et al., 2017) ovarian cancer (Song et al., 2020) and Alzheimer's disease (Xiong et al., 2022). Furthermore, there is therapeutic advantage in the development of contraception that is non-steroid hormone-based as current steroid hormone contraceptives have been associated with increased risk of venous and arterial thrombosis (Sech & Mishell, 2015) and cardiovascular disease (Sitruk-Ware & Nath, 2011). Therefore, the aim of this chapter was to screen and identify potential FSHR inhibitors and determine their effect on FSH/FSHR-dependent binding, cAMP-dependent signalling and FSHR oligomerisation. In this study, three SMCs were identified that inhibited FSH-dependent FSHR cre-luciferase activity, whilst enhancing FSH binding affinity to the FSHR. These changes in FSH activity are potentially linked to FSHR oligomerisation at the plasma membrane.

Following the initial screening of the 84 SMCs, SMC 48, -74, -80 and -84 were identified as hit SMCs that inhibited >90% FSH/FSHR cre-luc activity. The structure of the hit SMCs in this study differs from previously identified FSHR inhibitors, such as the Addex compounds (Dias et al., 2011; Dias et al., 2014), given that their chemical structures contained one or more aromatic benzene rings decorated with halogens (bromine and/or chlorine) and/or sulphur atoms (Figure 6.7). Recent studies have suggested that polyaromatic compounds (PACs) behave as endocrine disrupting chemicals (EDCs) and negatively affect mammalian reproductive function (Perono et al., 2022). Acute and chronic exposure to PACs in rats extended the length of their oestrous cycle, significantly

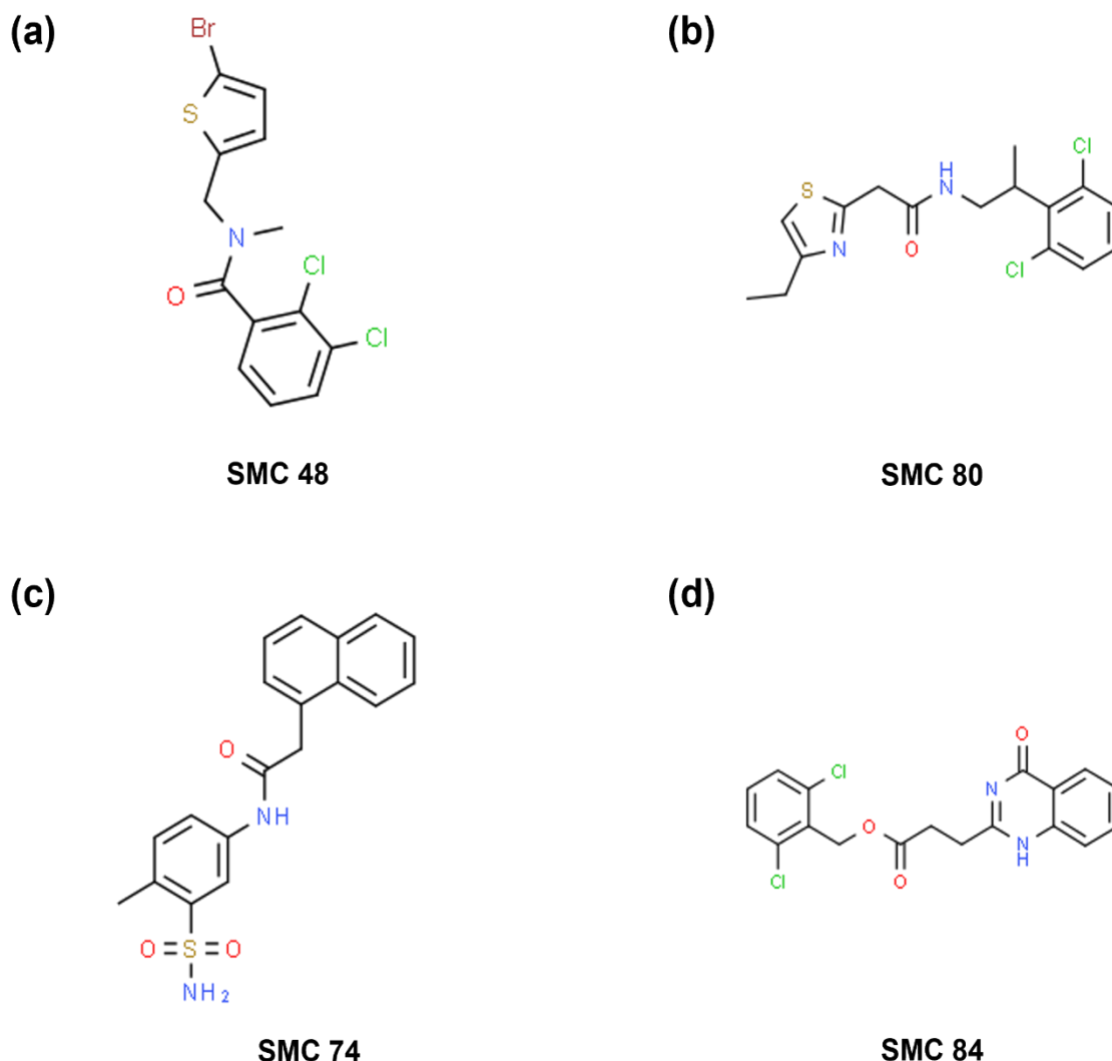


**Figure 6.7: Molecular structure of identified potential FSHR inhibitors.** Molecular structure of small molecule compounds (SMCs) hits identified to inhibit >90% FSH activity following initial SMC screen (Figure 6.2). Subsequent experiments showed maximal concentrations (100 $\mu$ M) of (a) SMC 48, (b) SMC 80, and (c) SMC 74 able to inhibit FSH activity (Figure 6.3). (d) SMC 84 was unable to inhibit FSH activity at all concentrations and was omitted from study. Structures generated using <http://www.chemspider.com/>.

decreased aromatase expression, and decreased oestrogen, LH, and progesterone levels in the serum, with reduction in ovulation and litter sizes (Archibong et al., 2012; Liu et al., 2020; Xu et al., 2010). Furthermore, EDCs containing chlorine atoms, namely *p,p'*-DDT, have also been associated with reduced fertility in women and shortened menstrual cycles

(Jirsová et al., 2010; Windham et al., 2005). Bisphenol A (BPA) has also been linked to reproductive function anomalies (Huo et al., 2015), with the role of BPA in the presence of bromine currently being investigated and proposed to reduce FSH activity by up to 30% in CHO cells stably expressing the human FSHR (Sibilia et al., 2019). This doesn't explain why SMC 84 was initially shown to inhibit FSH activity in earlier experiments, but then failed to inhibit FSH activity in the following concentration-response experiments. It could be associated with the absence of a sulphur atom (Figure 6.7, (d)), although how this is linked to FSHR signalling has not been investigated. Alternatively, this observation may be due to low *n* numbers. Nevertheless, given the presence of benzene rings and halogens atoms in the hit SMCs in this study, it suggests these SMCs contain the ideal chemical properties required for enhanced FSHR inhibition. However, further chemical analysis of these SMCs would need to be investigated to conclude these suggestions.

When cells were stimulated with FSH in the presence of 100µM of SMC 48, -74 and -80 there was enhanced binding of <sup>125</sup>I-hFSH to the FSHR. Interestingly, this correlated with the concentration-response experiments whereby inhibition in FSH activity was observed. Similar findings were reported with the Addex FSHR inhibitor compounds, in which ADX61623 and ADX68692 enhanced FSH binding whilst reducing cAMP production (Dias et al., 2011; Dias et al., 2014). The study suggested that the FSHR may exist in a metastable state, whereby the inactive receptor can be stabilised for ligand binding (Dias et al., 2011). The study further suggested that the metastable state of the FSHR may be similar to what was observed when deglycosylated FSH $\alpha$  at asparagine-52 (N<sup>52</sup>dg- $\alpha$ ) would bind to the FSHR, but failed to activate adenylate cyclase (Butnev et al., 2002; Dias et al., 2011). However, this may differ from the SMCs in this study because N<sup>52</sup>dg- $\alpha$  would bind to the orthosteric site of the FSHR. Indeed, it could be that in this study the SMCs bind to a region

within the TMD of the FSHR, inducing a similar inactive conformational state that was induced by N<sup>52</sup>dg- $\alpha$ , which in turn enhances <sup>125</sup>I-hFSH binding to the FSHR, but fails to activate G $\alpha_s$ -dependent signalling. However, further investigation would be required to confirm this. Furthermore, the ability for the SMC 48, -74, and -80 to enhance FSH binding to the FSHR suggested that the SMCs were non-competitive inhibitors binding to an allosteric region. The FSHR binding site of various other FSHR inhibitors, including ADX61623 and ADX68693, and many FSHR agonists have recently been mapped using molecular docking simulation and shown to predominantly bind within the TMD (Aathi et al., 2022). This suggests that SMC 48, -74 and -80 most likely bind within the TMD, however, future docking experiments or crystallography of the SMCs in complex with FSHR would need to be performed to accurately determine this.

It was surprising to see that pre-treatment with 100 $\mu$ M of SMC 80 mediated decreases in FSHR oligomerisation. Furthermore, upon FSH binding, FSHR monomers re-associated to oligomers. It's possible that SMC 80 induces a conformational change at the FSHR that disrupts FSHR oligomerisation, and upon FSH binding a further conformational change at the FSHR may occur to enhance FSHR association. This lock-in configuration appeared to support basal but not FSH-dependent cre-luciferase activity. However, how this relates to the inhibitory actions of SMC 80 is still unclear. In the presence of SMC 80, the conformational changes in the FSHR may induce coupling to alternative G proteins or recruit  $\beta$ -arrestin to mediate biased signalling (Dias et al., 2014; Landomiel et al., 2019). Therefore, investigations on alternative second messenger signals would be an ideal next step to further understand the implications of the SMCs on FSHR oligomerisation and signalling.

Typical drug screening processes utilise heterologous cells lines to investigate the effect of drugs, however, it makes investigating the physiological relevance challenging in these cell lines. Although not investigated in this chapter, it could be speculated that inhibition of FSH activity in the presence of SMC 48, -74 and -80 may also inhibit cAMP production, progesterone and/or oestrogen, considering that other similar small molecular FSHR inhibitors have been shown to do this in native cells and *in vivo* (Dias et al., 2011; Dias et al., 2014). Furthermore, these SMCs may still pose the same problems as previous FSHR inhibitors such as bioavailability, toxic side effects, off-target effects, and cross-reactivity with other GpHRs (Arey et al., 2002; Dias et al., 2011; Wiedemar et al., 2020), and would need to be tested further in an *in vivo* model to begin to develop potential FSHR inhibitors ideal for commercial use.

AI technology offers a quick and inexpensive way to identify new drugs. Nevertheless, because of the inherent optimisation steps required to identify a drug that is biologically active at its target, has a suitable pharmacokinetic profile, and does not produce toxic side effects *in vivo*, multiple potential compounds are often generated to fit this criterion (Schneider et al., 2020). The initial screening of the potential FSHR inhibitors in this chapter consisted of 84 SMCs, of which many displayed potential FSHR agonist or antagonist characteristics. There are many low molecular weight modulators of the FSHR that currently exist for the development of fertility regulators, of which none are commercially available due to bioavailability and toxicity issues (Aathi et al., 2022; Anderson et al., 2018; Nataraja et al., 2018). Therefore, it's important to not overlook the other SMCs in this chapter that were not investigated to the same extent as SMC 48, 74, 80. Furthermore, since a single-shot approach was taken to identify potential candidate hits, it is possible that other SMCs could have been potential FSHR inhibitor candidates if initial

screening was conducted at different concentrations. Additionally, it is important to reiterate that initial screening to identify hits were screened to n=1. Therefore, further validation through repetition would be necessary to ensure robust identification of candidates and accurately conclude the findings within this chapter.

In conclusion, three novel FSHR targeting SMCs have been identified, which behave as non-competitive inhibitors. Although the mechanisms by which they inhibit the FSHR are not entirely clear, it is suggested that these SMCs may bind to allosteric rather than orthosteric sites. These compounds may provide promising new avenues for treatment of menopausal elevated FSH-related pathologies, and as potential non-steroid hormone-based contraceptives.

**7 Chapter Seven: General Discussion**

## 7.1 Thesis summary

The overall aim of this thesis was to determine the mechanisms by which the FSHR decodes the differential signalling properties displayed by different FSH glycoforms and pharmacological FSHR modulators by assessing how FSHR oligomer reorganisation and internalisation may correlate with FSHR signalling. This thesis has demonstrated that differences in FSH glycosylation modulates FSHR oligomerisation in both a time- and concentration-dependent manner. Higher physiological concentrations of the more biologically active partially glycosylated FSH21/18 rapidly dissociated FSHR oligomers predominantly into more active monomers and dimers, which was associated with increases in cAMP-dependent signalling. This contrasted with the lesser biologically active fully glycosylated FSH24, that induced similar changes but with different kinetics and may be due to differences in FSH/FSHR binding profile (Meher et al., 2015). Furthermore, by using a  $\beta$ -arrestin biased agonist, it was shown that FSHR signal selectivity via  $\beta$ -arrestin may be mediated by increases in FSHR oligomerisation. These results suggest a potential physiological role for FSH glycoforms in fine-tuning FSHR signal specificity and amplitude via FSHR oligomerisation. Moreover, the differences in FSHR-dependent cAMP production that was displayed by FSH21/18 and FSH24 may also be regulated by FSHR endocytosis and differential routing to endosomal compartments, adding additional complexity to current knowledge on FSHR signalling. FSH21/18 may route a small proportion of internalised FSHRs to EEA1-positive EEs, of which their fate is yet to be determined. Whereas FSH24-dependent FSHR-dependent cAMP signalling is negatively regulated by APPL1 and may mediate FSHR recycling. These findings suggest that FSHR trafficking pathway could be targeted to further modulate FSHR signalling.



In addition to endogenous FSH glycoforms, this thesis has shown that small pharmacological FSHR modulators can also regulate FSHR signalling via FSHR oligomerisation and FSHR internalisation. The potent FSHR agonist, C5, was able to rapidly induce FSHR endocytosis-dependent cAMP production and increase FSHR density. Furthermore, three novel small molecule FSHR non-competitive inhibitors have been identified, SMC 48, -74, and -80, that enhance FSH binding to the FSHR, but inhibit >90% of FSH activity and may be mediated by decreases in FSHR oligomerisation. These findings present multiple ways to modulate FSHR signalling, which may have significant therapeutic potential to either enhance or diminish FSHR signalling to improve fertility or treat elevated-related FSH pathologies.

## **7.2 The role cell-surface FSHR oligomerisation plays in modulating FSHR signalling**

The results have shown that different forms of FSHR monomers, dimers and oligomers may propagate FSHR signal amplitude and selectivity. FSH21/18 was faster than FSH24 at mediating different FSHR oligomer arrangements, which correlated with increased cAMP production, CREB phosphorylation and cre-luciferase activity. Conversely, dg-eLHt increased FSHR oligomerisation which supposedly correlates with  $\beta$ -arrestin signalling and low cAMP signalling (Butnev et al., 2002; Wehbi et al., 2010). Furthermore, low concentrations of FSH glycoforms, that correlated with low levels of cAMP and cre-luciferase production, also mediated increases in FSHR oligomerisation, suggesting that FSHR oligomerisation at the cell-surface may play a key role in mediating FSHR signal amplitude and selectivity. On the other hand, the FSHR inhibitor SMC 80 dissociated FSHR oligomer into monomers which correlated with decreases in FSH activity but increased FSHR occupancy. This suggests there could be differences in the threshold for

receptor occupancy for changes in FSHR oligomerisation, especially since FSH glycoforms display different binding affinities at the FSHR (Bousfield et al., 2014a), and the results in this thesis also showed differences in FSH binding at the FSHR in the presence of the different FSHR inhibitors. Additionally, although it's unclear how similar overall FSHR oligomer dissociation into monomers may mediate different FSHR signal responses, the data suggests that there may be micro-regulation of FSHR signalling via changes in FSHR oligomer forms. It is possible that there could be different activation states of the receptor and different conformations that these ligands bring about. For example, FSH21/18 predominantly dissociated FSHR dimers, trimers and 6-8 oligomers into monomers that supposedly regulated increases in FSHR-dependent cAMP production. Whereas SMC 80 predominantly dissociated FSHR tetramers into monomers which supposedly mediated decreases in FSHR signalling. Nevertheless, the low *n* numbers from interrogating the FSHR inhibitor-dependent changes in FSHR oligomerisation make concluding how these FSHR subtypes specifically regulate FSHR signalling difficult and would require further investigation to begin to delineate this.

Alternatively, perhaps FSHR oligomerisation at the plasma membrane plays a lesser role in modulating FSHR signalling than previously assumed. Interestingly, the potent FSHR agonist, C5, mediated FSHR signalling independent of changes in FSHR oligomerisation, despite enhancing FSH glycoform binding and a large enrichment of FSHR at the cell surface. This suggests that, only for some compounds, FSHR oligomerisation is important for mediating FSHR signalling. However, C5 appeared to affect FSHR trafficking, which has been corroborated by published data (Sposini et al., 2020), and may play a key role in mediating FSHR signalling, but whether FSHR oligomer forms act as a signature for internalisation is yet to be determined. Indeed, results reported in this thesis suggest FSH

glycoforms may differentially route the FSHR to possibly different endosomal compartments. FSH21/18 potentially mediates FSHR to EEA1-positive EEs. Although it is not yet clear the fate of these receptors, it is possible that FSHR localised to EEA1-positive EEs facilitate sustained cAMP signalling, as this has been previously observed with the PTHR and LH/CGR localised to EEs (Sposini et al., 2017; Vilardaga et al., 2014). On the other hand, because APPL1 has previously been shown to negatively regulate FSHR-dependent cAMP production to mediate FSHR recycling (Sposini et al., 2020; Sposini et al., 2017), it is possible that from the results presented in this thesis, that FSH24 may possibly mediate FSHR routing to APPL1-positive VEEs, thus causing decreased cAMP production when compared to FSH 21/18 (Bousfield et al., 2014b; Jiang et al., 2015; Wang et al., 2016b), with possible implications on FSHR recycling to the cell surface (Sposini et al., 2020). However, whether FSHR oligomer forms at the plasma membrane determine the FSHR trafficking route is still largely unclear and would be interesting to explore.

Furthermore, this thesis demonstrated that FSH glycoform-dependent FSHR signalling was dependent on FSHR internalisation and may suggest that the FSHR monomers/oligomers observed at the plasma membrane during PD-PALM imaging were, at least, not  $G\alpha_s$ -bound. Maybe FSHR oligomerisation at the plasma membrane plays a predominant role in signal selectivity via regulating differential G protein coupling and  $\beta$ -arrestin recruitment, rather than specific signal amplitude. Besides, previous studies revealed FSHR heterodimerisation with LH/CGR mediated the reduction of LH/hCG- and FSH-dependent  $G\alpha_s$  signalling and enhanced LH/CGR-dependent  $G\alpha_{q/11}$  signalling as a result of distinct FSHR/LH/CGR tetramer rearrangement (Feng et al., 2013; Jonas et al., 2018). Moreover, presumptuous  $G\alpha_s$ -bound FSHR within endosomes may play a key role in specific signal amplitude, regulated by the organisation of distinct scaffolding networks within the cell

mediated by interaction with various proteins, such as APPL1, APPL2, Akt2, FOXO1a, and PKA (Nechamen et al., 2007; Sposini et al., 2017). This may suggest that the differences observed in cAMP production may be predominantly regulated by APPL1 compared to FSHR oligomerisation at the cell-surface. However, to investigate this idea further, FSHR G protein coupling, and other signal pathways, would need to be examined. Moreover, because PD-PALM utilises fixed cells to visualise FSHRs, observation in this thesis only reflected a spatial-temporal snapshot of the FSHR cell-surface landscape. Identifying ways to visualise live FSHR interaction with different G proteins and other cellular proteins will enhance our understanding in the role of FSHR oligomerisation in modulating FSHR signalling. Additionally, this thesis did not explore internalised FSHR interaction with other intracellular proteins associated with FSHR trafficking. Investigating these proteins would be an important next step in order to further understand the role of FSHR oligomerisation and related signalling, and undoubtedly provide an avenue for therapeutic targeting to improve fertility outcomes.

### **7.3 What is the future for FSHR pharmacological modulators?**

Although it's still unclear the direct impact of FSHR oligomers and FSHR trafficking on regulating FSH glycoform-dependent FSHR signalling, this thesis demonstrates a potential role for FSHR pharmacological modulators in further mediating FSHR signalling. With C5 shown to mediate a 3-fold and a 1.5-fold increase in FSHR recycling and cAMP production when compared to FSH treatment, respectively, and to route the FSHR to both APPL1- and EEA1-positive endosomes (Sposini et al., 2020), it poses as a great tool for ART. However, since C5 enhances FSHR density, the effect of chronic FSHR stimulation for folliculogenesis on increased apoptosis-related signalling may need to be considered. Especially since FSHR overexpression in hGL5 cells previously induced pro-apoptotic

activity (Casarini et al., 2016a), and may have detrimental implications on fertility if administered to women undergoing IVF. Furthermore, in older women undergoing IVF, enhancing FSHR activity may increase their susceptibility to early onset of menopausal-dependent elevated FSH-related pathologies, such as bone loss (Ji et al., 2018; Sun et al., 2006; Zhu et al., 2012), increased adiposity (Abildgaard et al., 2021; Liu et al., 2017) ovarian cancer (Song et al., 2020) and Alzheimer's disease (Xiong et al., 2022). Instead, these women may benefit from a combined-oral therapy approach using specific doses of both FSHR agonists and the novel FSHR inhibitors. This approach will be beneficial because it will not only enhance FSHR activity, to potentially increase folliculogenesis, but may simultaneously act as a control to prevent the pathologies associated with elevated FSH. However, like C5, the potential adverse effect of inhibiting FSHR activity in young women on extragonadal FSHR activity may need to be investigated (Chrusciel et al., 2019). Alternatively, deciphering ways to target these FSHR allosteric modulators to the FSHRs localised to the ovaries would be more desirable.

#### **7.4 Limitations**

The studies reported in this thesis utilised the heterologous HEK293 cell line transiently expressing the FSHR to study FSHR oligomerisation and related signalling and trafficking. Although it is a common cell line used for pharmacological-related studies, as it offers a clean read-out of cellular responses with minimal background that can arise from native cells endogenously expressing the protein of interest, it is not physiologically relevant and offers no information on steroid hormone production. Moreover, GCs are steroidogenic cells with a cholesterol-rich plasma membrane environment (Lange et al., 1988). The local membrane environment is increasingly recognised as an important factor regulating GPCR function (Guixà-González et al., 2016; Koldsø & Sansom, 2015; Periole et al., 2007) and

GPCR homomer formation (Prasanna et al., 2016). To begin to understand the physiological context of the findings in this thesis, an important next step is to translate these findings into physiologically relevant cell types.

Another important limitation in this study was the lack of direct evidence that the differences in FSHR-dependent cAMP signalling and related signalling observed were due to changes in FSHR oligomers. To directly investigate these correlations, FSHR oligomerisation would need to be disrupted by site-directed mutagenesis of key residues located within the di/oligomerisation interface, or by small molecule disrupting compounds and/or antibodies that bind within the di/oligomerisation interface. Mutagenesis of important residues in the TMD5/6 dimer interface of the uracil nucleotide/cysteinyll leukotriene receptor, or the G protein-couple receptor 17 (GPR17), homomers disrupted GPR17 homomers into monomers, abrogating  $\text{Ca}^{2+}$  and ERK1/2 signalling, and impairing receptor trafficking (Yang et al., 2020). Likewise, methods involving disruption compounds have been used on the prototypical Class A rhodopsin receptors with dimer disruption having implication on retinal degradation (Kumar et al., 2018; Park, 2019; Zhang et al., 2016). Together, these proof-of-concept tools provide potential avenues for exploring the *in vivo* relevance of FSHR dimerisation.

In addition, other than the canonical  $\text{G}\alpha_s/\text{cAMP}/\text{PKA}$  signalling pathway assessed in this thesis, the FSHR can activate multiple signalling pathways, some via signal pathway crosstalk and G protein-independent  $\beta$ -arrestin signalling (Casarini & Crépieux, 2019). All these signal pathways play a crucial role in regulating folliculogenesis, dominant follicle selection, ovulation, and steroid hormone synthesis (Messinis et al., 2014). Therefore, to

begin to thoroughly understand how FSHR signalling is modulated, and the wider context/implications of the findings within this thesis, these pathways would need to be explored. For example, calcium mobilisation assay is a common method used to measure  $\text{Ca}^{2+}$  influx associated with  $\text{G}\alpha_{q/11}/\text{IP}_3/\text{Ca}^{2+}$  signalling, and BRET or nanoBiT are techniques that can be utilised to measure FSHR interaction with other proteins such as G proteins and (Botta et al., 2019). Furthermore, because FSHR can activate multiple signalling pathways, high-throughput screening assays, such as protein kinase array or ELISA, may be more ideal to thoroughly measure the implications of endogenous FSH glycoforms and FSHR modulators on the vast array of protein abundance.

To conclude, this thesis has demonstrated that the different FSHR signalling elicited by different FSH glycoforms and FSHR pharmacological modulators can be modulated in multiple ways (summarised in Figure 7.1). Such mechanisms may involve FSHR monomer and oligomer rearrangement and/or FSHR internalisation and trafficking to distinct endosomal compartments. These findings open potential avenues for therapeutic targeting with the prospect to improve fertility outcomes in patients undergoing IVF, as alternative non-steroid hormone-based contraception, and to potentially treat menopausal-elevated FSH-related pathologies.

1

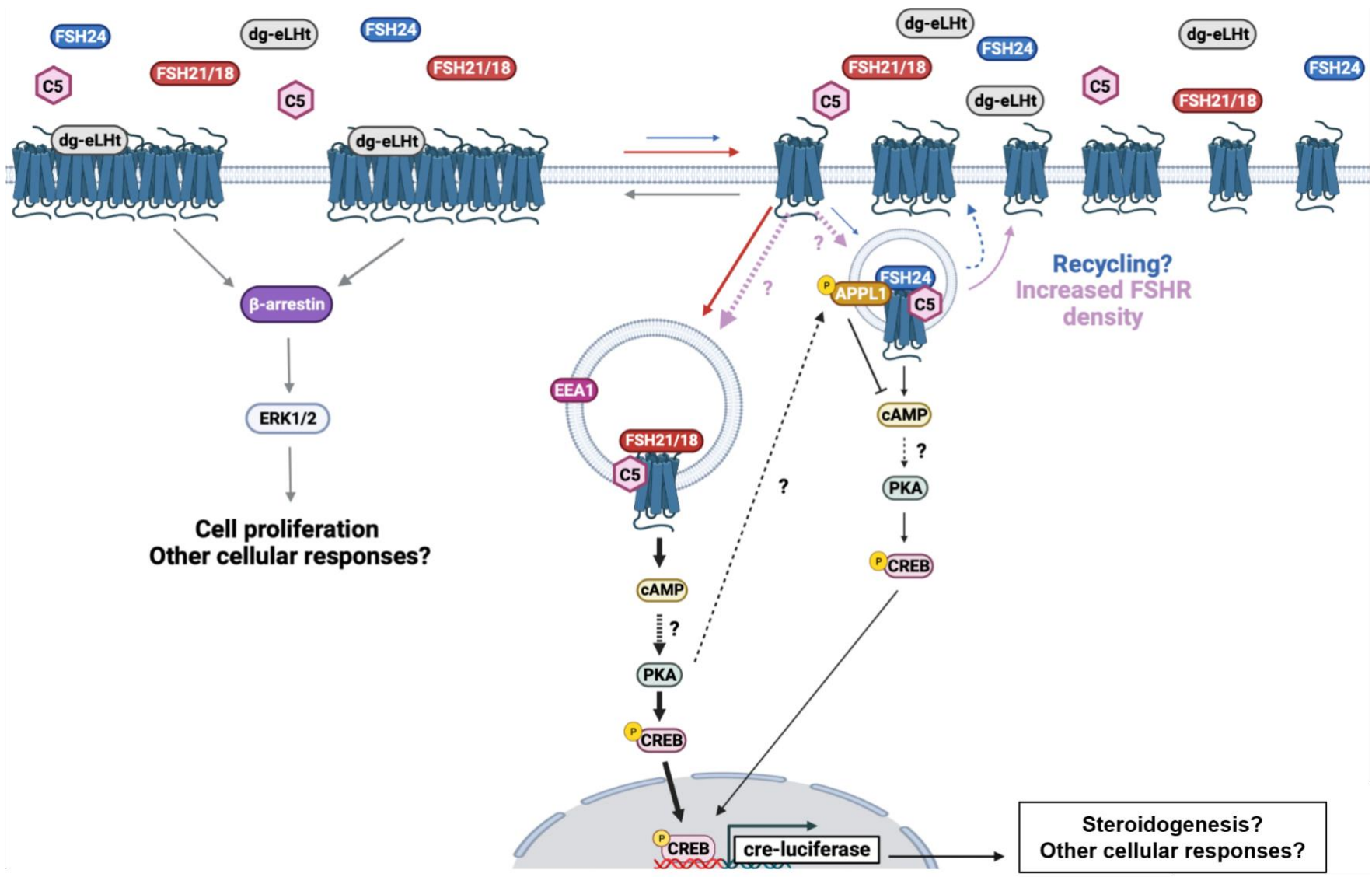




**Figure 7.1: Simplified schematic diagram of the effect of different FSH glycoforms and an FSHR pharmacological modulator on FSHR oligomerisation, trafficking, and signalling.** The  $\beta$ -arrestin biased agonist (dg-eLHt) increases FSHR oligomerisation to mediate  $\beta$ -arrestin/ERK1/2 signalling (grey arrows). FSH21/18 rapidly mediates FSHR oligomer rearrangement into monomers and smaller FSHR oligomers (red thick/long arrows). This may correlate with increases in cAMP signalling and CREB-phosphorylation from internalised FSHRs routed to EEA1-positive early endosomes (EEs). FSH24 also mediates FSHR oligomer rearrangement into monomers and smaller FSHR oligomers, but via slower kinetics (thin/small blue arrows). This may correlate with lower increases in cAMP signalling and CREB-phosphorylation negatively regulated by APPL1 from internalised FSHRs routed to APPL1-positive very early endosomes (VEEs). This may have implications on FSHR recycling. The FSHR pharmacological modulator, C5- a potent FSHR agonist, enhances both cAMP signalling and FSHR cell-surface density independent of FSHR oligomerisation and possibly by routing the FSHR to EEs and VEEs (thick pink arrows). The action of C5 can occur in the absence and presence of FSH glycoforms. Dashed arrows represent pathways not yet investigated. *Figure created using BioRender.com.*

## 7.5 Future directions

To further build on the findings from this thesis, the next steps would be to:

- Identify ways to disrupt FSHR oligomerisation to determine the effects on FSHR signalling, as this will provide direct evidence for the role of FSHR oligomers and its impact on FSHR signalling. To begin to explore this, first the residues involved in FSHR di/oligomer formation would need to be determined using structure-based methods such as x-ray crystallography or cryo-EM. Once determined, disruptive compounds or antibodies complimentary to the residues of the di/oligomer interface can be designed. Their ability to disrupt FSHR di/oligomerisation can then be tested using various biophysical and/or physiological methods such as BRET and/or PD-PALM.
- Understand the effect of FSH glycoform occupancy within FSHR monomer/oligomers in determining FSHR activation state and related signalling. This will delineate the role that different FSHR complexes play in mediating FSH binding and subsequent signalling. To investigate this, each FSH glycoform would need to be labelled with a CAGE<sup>TM</sup> dye that emits at a different wavelength than the FSHR-bound HA.11-CAGE<sup>TM</sup> 552 antibody. Once achieved, each of the FSH glycoforms and FSHR can be dual-imaged using the Zeiss Elyra PS.1 super resolution microscope.
- Determine the effect of FSH glycoforms and pharmacological modulators on FSHR routing to APPL1-positive VEEs, EEA1-positive EEs, and the effect on the rate of FSHR recycling. Exploring this will help thoroughly depict how different ligands mediate FSHR trafficking and the impact on FSHR signalling. Further immunocytochemistry immunofluorescence will be able to determine the spatial localisation of FSHR within cells. Likewise, nanobodies are ideal tools that have

been used to study GPCR dynamics and can be used to potentially examine FSHR recycling.

- Further screen and identify potential novel FSHR agonists/inhibitors and their effect on FSH-dependent cAMP production. This is important because in addition to the three novel FSHR inhibitors identified in this thesis, under alternative experimental conditions, the remaining 81 compounds may display agonist/antagonist characteristics and have therapeutic potential. Furthermore, unlike the experiments in this thesis, assessing real-time cAMP production may show different signalling profiles than cre-luciferase assays.
- Explore the effect of pharmacological FSHR modulators on cell-based assays to measure the effect of these compounds on cell proliferation, viability, apoptosis, and necrosis. This will determine whether identified FSHR agonists or inhibitors have the potential to produce *in vitro* and *in vivo* adverse side-effects. Many techniques and kit are available to measure these different parameters. Such techniques involve colorimetric, dye exclusion, and flow cytometric assays to measure cell viability and q-PCR to measure gene expression.
- Study the effect of FSH glycoforms and pharmacological FSHR modulators on G protein coupling,  $\beta$ -arrestin recruitment and other related signalling pathways. This will provide more information on how FSH glycoforms and pharmacological FSHR modulators can mediate FSHR signal diversification. Many techniques can measure different aspects of the FSHR signalling pathway, such as FRET/BRET or nanoBiT to measure protein interaction and calcium mobilisation assays to measure  $\text{Ca}^{2+}$  influx associated with  $G\alpha_{q/11}/\text{IP}_3/\text{Ca}^{2+}$  signalling.
- Recapitulate the findings within this thesis in a native cell line, such as KGN cells endogenously expressing the FSHR, and/or in an *in vivo* model such as transgenic

mice expressing tagged FSHR, so that their GCs can be isolated and experimented on. Furthermore, the effects the FSHR pharmacological modulators on steroidogenesis, the ovulation of oocytes *in vivo*, and extragonadal cells/tissue expressing the FSHR could be determined in this model. Ultimately, findings could then be compared to FSHR oligomerisation, trafficking, and related signalling in women with fertility issues undergoing IVF to understand FSHR functioning in a pathological context.

## 8 References

- Aathi, M. S., Kumar, C., Prabhudesai, K. S., Shanmugarajan, D., & Idicula-Thomas, S. (2022). Mapping of FSHR agonists and antagonists binding sites to identify potential peptidomimetic modulators. *Biochim Biophys Acta Biomembr*, 1864(4), 183842. <https://doi.org/10.1016/j.bbamem.2021.183842>
- Abel, M. H., Wootton, A. N., Wilkins, V., Huhtaniemi, I., Knight, P. G., & Charlton, H. M. (2000). The effect of a null mutation in the follicle-stimulating hormone receptor gene on mouse reproduction. *Endocrinology*, 141(5), 1795-1803. <https://doi.org/10.1210/endo.141.5.7456>
- Abildgaard, J., Ploug, T., Al-Saoudi, E., Wagner, T., Thomsen, C., Ewertsen, C., Bzorek, M., Pedersen, B. K., Pedersen, A. T., & Lindegaard, B. (2021). Changes in abdominal subcutaneous adipose tissue phenotype following menopause is associated with increased visceral fat mass. *Sci Rep*, 11(1), 14750. <https://doi.org/10.1038/s41598-021-94189-2>
- Adashi, E. Y. (1994). Endocrinology of the ovary. *Hum Reprod*, 9(5), 815-827. <https://doi.org/10.1093/oxfordjournals.humrep.a138602>
- Agrawal, G., & Dighe, R. R. (2009). Critical involvement of the hinge region of the follicle-stimulating hormone receptor in the activation of the receptor. *J Biol Chem*, 284(5), 2636-2647. <https://doi.org/10.1074/jbc.M808199200>
- Aittomäki, K., Lucena, J. L., Pakarinen, P., Sistonen, P., Tapanainen, J., Gromoll, J., Kaskikari, R., Sankila, E. M., Lehvälaiho, H., Engel, A. R., Nieschlag, E., Huhtaniemi, I., & de la Chapelle, A. (1995). Mutation in the follicle-stimulating hormone receptor gene causes hereditary hypergonadotropic ovarian failure. *Cell*, 82(6), 959-968. [https://doi.org/10.1016/0092-8674\(95\)90275-9](https://doi.org/10.1016/0092-8674(95)90275-9)
- Allan, C. M., Kalak, R., Dunstan, C. R., McTavish, K. J., Zhou, H., Handelsman, D. J., & Seibel, M. J. (2010). Follicle-stimulating hormone increases bone mass in female mice. *Proc Natl Acad Sci U S A*, 107(52), 22629-22634. <https://doi.org/10.1073/pnas.1012141108>
- Altschul, S. F., Madden, T. L., Schäffer, A. A., Zhang, J., Zhang, Z., Miller, W., & Lipman, D. J. (1997). Gapped BLAST and PSI-BLAST: a new generation of protein database search programs. *Nucleic Acids Res*, 25(17), 3389-3402. <https://doi.org/10.1093/nar/25.17.3389>
- Ambao, V., Rulli, S. B., Carino, M. H., Cónsole, G., Ulloa-Aguirre, A., Calandra, R. S., & Campo, S. (2009). Hormonal regulation of pituitary FSH sialylation in male rats. *Mol Cell Endocrinol*, 309(1-2), 39-47. <https://doi.org/10.1016/j.mce.2009.05.002>
- Amsterdam, A., Hanoch, T., Dantes, A., Tajima, K., Strauss, J. F., & Seger, R. (2002). Mechanisms of gonadotropin desensitization. *Mol Cell Endocrinol*, 187(1-2), 69-74. [https://doi.org/10.1016/s0303-7207\(01\)00701-8](https://doi.org/10.1016/s0303-7207(01)00701-8)
- Anderson, R. C., Newton, C. L., & Millar, R. P. (2018). Small Molecule Follicle-Stimulating Hormone Receptor Agonists and Antagonists. *Front Endocrinol (Lausanne)*, 9, 757. <https://doi.org/10.3389/fendo.2018.00757>
- Annibale, P., Vanni, S., Scarselli, M., Rothlisberger, U., & Radenovic, A. (2011a). Identification of clustering artifacts in photoactivated localization microscopy. *Nat Methods*, 8(7), 527-528. <https://doi.org/10.1038/nmeth.1627>
- Annibale, P., Vanni, S., Scarselli, M., Rothlisberger, U., & Radenovic, A. (2011b). Quantitative photo activated localization microscopy: unraveling the effects of photoblinking. *PLoS One*, 6(7), e22678. <https://doi.org/10.1371/journal.pone.0022678>
- Archibong, A. E., Ramesh, A., Inyang, F., Niaz, M. S., Hood, D. B., & Kopsombut, P. (2012). Endocrine disruptive actions of inhaled benzo(a)pyrene on ovarian function and fetal survival in fisher F-344 adult rats. *Reprod Toxicol*, 34(4), 635-643. <https://doi.org/10.1016/j.reprotox.2012.09.003>
- Arey, B. J., Deecher, D. C., Shen, E. S., Stevis, P. E., Meade, E. H., Wrobel, J., Frail, D. E., & López, F. J. (2002). Identification and characterization of a selective, nonpeptide follicle-stimulating

- hormone receptor antagonist. *Endocrinology*, 143(10), 3822-3829. <https://doi.org/10.1210/en.2002-220372>
- Arey, B. J., Yanofsky, S. D., Claudia Pérez, M., Holmes, C. P., Wrobel, J., Gopalsamy, A., Stevis, P. E., López, F. J., & Winneker, R. C. (2008). Differing pharmacological activities of thiazolidinone analogs at the FSH receptor. *Biochem Biophys Res Commun*, 368(3), 723-728. <https://doi.org/10.1016/j.bbrc.2008.01.119>
- Ascoli, M., Fanelli, F., & Segaloff, D. L. (2002). The lutropin/choriogonadotropin receptor, a 2002 perspective. *Endocr Rev*, 23(2), 141-174. <https://doi.org/10.1210/edrv.23.2.0462>
- Attwood, T. K., & Findlay, J. B. (1994). Fingerprinting G-protein-coupled receptors. *Protein Eng*, 7(2), 195-203. <https://doi.org/10.1093/protein/7.2.195>
- Baenziger, J. U., & Green, E. D. (1988). Pituitary glycoprotein hormone oligosaccharides: structure, synthesis and function of the asparagine-linked oligosaccharides on lutropin, follitropin and thyrotropin. *Biochim Biophys Acta*, 947(2), 287-306. [https://doi.org/10.1016/0304-4157\(88\)90012-3](https://doi.org/10.1016/0304-4157(88)90012-3)
- Baltoumas, F. A., Theodoropoulou, M. C., & Hamodrakas, S. J. (2016). Molecular dynamics simulations and structure-based network analysis reveal structural and functional aspects of G-protein coupled receptor dimer interactions. *J Comput Aided Mol Des*, 30(6), 489-512. <https://doi.org/10.1007/s10822-016-9919-y>
- Baumgarten, S. C., Convissar, S. M., Fierro, M. A., Winston, N. J., Scoccia, B., & Stocco, C. (2014). IGF1R signaling is necessary for FSH-induced activation of AKT and differentiation of human Cumulus granulosa cells. *J Clin Endocrinol Metab*, 99(8), 2995-3004. <https://doi.org/10.1210/jc.2014-1139>
- Bhartiya, D., & Patel, H. (2021). An overview of FSH-FSHR biology and explaining the existing conundrums. *J Ovarian Res*, 14(1), 144. <https://doi.org/10.1186/s13048-021-00880-3>
- Bhaskaran, R. S., Min, L., Krishnamurthy, H., & Ascoli, M. (2003). Studies with chimeras of the gonadotropin receptors reveal the importance of third intracellular loop threonines on the formation of the receptor/nonvisual arrestin complex. *Biochemistry*, 42(47), 13950-13959. <https://doi.org/10.1021/bi034907w>
- Bhowmick, N., Huang, J., Puett, D., Isaacs, N. W., & Laphorn, A. J. (1996). Determination of residues important in hormone binding to the extracellular domain of the luteinizing hormone/chorionic gonadotropin receptor by site-directed mutagenesis and modeling. *Mol Endocrinol*, 10(9), 1147-1159. <https://doi.org/10.1210/mend.10.9.8885249>
- Biebermann, H., Schöneberg, T., Krude, H., Schultz, G., Gudermann, T., & Grüters, A. (1997). Mutations of the human thyrotropin receptor gene causing thyroid hypoplasia and persistent congenital hypothyroidism. *J Clin Endocrinol Metab*, 82(10), 3471-3480. <https://doi.org/10.1210/jcem.82.10.4286>
- BioSpace. (2021). *IVF Services Market Size on Target to Reach \$25.6 Billion by 2026, at a CAGR of 9.3% | AMR*. <https://www.biospace.com/article/ivf-services-market-size-on-target-to-reach-25-6-billion-by-2026-at-a-cagr-of-9-3-percent-amr/>
- Bishop, L. A., Nguyen, T. V., & Schofield, P. R. (1995). Both of the beta-subunit carbohydrate residues of follicle-stimulating hormone determine the metabolic clearance rate and in vivo potency. *Endocrinology*, 136(6), 2635-2640. <https://doi.org/10.1210/endo.136.6.7750487>
- Bishop, L. A., Robertson, D. M., Cahir, N., & Schofield, P. R. (1994). Specific roles for the asparagine-linked carbohydrate residues of recombinant human follicle stimulating hormone in receptor binding and signal transduction. *Mol Endocrinol*, 8(6), 722-731. <https://doi.org/10.1210/mend.8.6.7935488>
- Bonomi, M., Busnelli, M., Persani, L., Vassart, G., & Costagliola, S. (2006). Structural differences in the hinge region of the glycoprotein hormone receptors: evidence from the sulfated tyrosine residues. *Mol Endocrinol*, 20(12), 3351-3363. <https://doi.org/10.1210/me.2005-0521>

- Bonomi, M., & Persani, L. (2013). Modern methods to investigate the oligomerization of glycoprotein hormone receptors (TSHR, LHR, FSHR). *Methods Enzymol*, 521, 367-383. <https://doi.org/10.1016/B978-0-12-391862-8.00020-X>
- Botta, J., Bibic, L., Killoran, P., McCormick, P. J., & Howell, L. A. (2019). Design and development of stapled transmembrane peptides that disrupt the activity of G-protein-coupled receptor oligomers. *J Biol Chem*, 294(45), 16587-16603. <https://doi.org/10.1074/jbc.RA119.009160>
- Bousfield, G. R., Butnev, V. Y., Hiromasa, Y., Harvey, D. J., & May, J. V. (2014a). Hypo-glycosylated human follicle-stimulating hormone (hFSH(21/18)) is much more active in vitro than fully-glycosylated hFSH (hFSH(24)). *Mol Cell Endocrinol*, 382(2), 989-997. <https://doi.org/10.1016/j.mce.2013.11.008>
- Bousfield, G. R., Butnev, V. Y., Rueda-Santos, M. A., Brown, A., Hall, A. S., & Harvey, D. J. (2014b). Macro- and Micro-heterogeneity in Pituitary and Urinary Follicle-Stimulating Hormone Glycosylation. *J Glycomics Lipidomics*, 4. <https://doi.org/10.4172/2153-0637.1000125>
- Bousfield, G. R., Butnev, V. Y., Walton, W. J., Nguyen, V. T., Huneidi, J., Singh, V., Kolli, V. S., Harvey, D. J., & Rance, N. E. (2007). All-or-none N-glycosylation in primate follicle-stimulating hormone beta-subunits. *Mol Cell Endocrinol*, 260-262, 40-48. <https://doi.org/10.1016/j.mce.2006.02.017>
- Bousfield, G. R., May, J. V., Davis, J. S., Dias, J. A., & Kumar, T. R. (2018). In Vivo and In Vitro Impact of Carbohydrate Variation on Human Follicle-Stimulating Hormone Function. *Front Endocrinol (Lausanne)*, 9, 216. <https://doi.org/10.3389/fendo.2018.00216>
- Braun, T., Schofield, P. R., & Sprengel, R. (1991). Amino-terminal leucine-rich repeats in gonadotropin receptors determine hormone selectivity. *EMBO J*, 10(7), 1885-1890. <https://www.ncbi.nlm.nih.gov/pubmed/2050124>
- Brink, C. B., Harvey, B. H., Bodenstein, J., Venter, D. P., & Oliver, D. W. (2004). Recent advances in drug action and therapeutics: relevance of novel concepts in G-protein-coupled receptor and signal transduction pharmacology. *Br J Clin Pharmacol*, 57(4), 373-387. <https://doi.org/10.1111/j.1365-2125.2003.02046.x>
- Bruysters, M., Verhoef-Post, M., & Themmen, A. P. (2008). Asp330 and Tyr331 in the C-terminal cysteine-rich region of the luteinizing hormone receptor are key residues in hormone-induced receptor activation. *J Biol Chem*, 283(38), 25821-25828. <https://doi.org/10.1074/jbc.M804395200>
- Butnev, V. Y., May, J. V., Shuai, B., Tran, P., White, W. K., Brown, A., Smalter Hall, A., Harvey, D. J., & Bousfield, G. R. (2015). Production, purification, and characterization of recombinant hFSH glycoforms for functional studies. *Mol Cell Endocrinol*, 405, 42-51. <https://doi.org/10.1016/j.mce.2015.01.026>
- Butnev, V. Y., Singh, V., Nguyen, V. T., & Bousfield, G. R. (2002). Truncated equine LH beta and asparagine(56)-deglycosylated equine LH alpha combine to produce a potent FSH antagonist. *J Endocrinol*, 172(3), 545-555. <https://doi.org/10.1677/joe.0.1720545>
- Calebiro, D., Nikolaev, V. O., Gagliani, M. C., de Filippis, T., Dees, C., Tacchetti, C., Persani, L., & Lohse, M. J. (2009). Persistent cAMP-signals triggered by internalized G-protein-coupled receptors. *PLoS Biol*, 7(8), e1000172. <https://doi.org/10.1371/journal.pbio.1000172>
- Calebiro, D., Rieken, F., Wagner, J., Sungkaworn, T., Zabel, U., Borzi, A., Cocucci, E., Zürn, A., & Lohse, M. J. (2013). Single-molecule analysis of fluorescently labeled G-protein-coupled receptors reveals complexes with distinct dynamics and organization. *Proc Natl Acad Sci U S A*, 110(2), 743-748. <https://doi.org/10.1073/pnas.1205798110>
- Campo, S., Andreone, L., Ambao, V., Urrutia, M., Calandra, R. S., & Rulli, S. B. (2019). Hormonal Regulation of Follicle-Stimulating Hormone Glycosylation in Males. *Front Endocrinol (Lausanne)*, 10, 17. <https://doi.org/10.3389/fendo.2019.00017>
- Candelaria, J. I., Rabaglino, M. B., & Denicol, A. C. (2020). Ovarian preantral follicles are responsive to FSH as early as the primary stage of development. *J Endocrinol*, 247(2), 153-168. <https://doi.org/10.1530/JOE-20-0126>

- Carr, D. W., DeManno, D. A., Atwood, A., Hunzicker-Dunn, M., & Scott, J. D. (1993). Follicle-stimulating hormone regulation of A-kinase anchoring proteins in granulosa cells. *J Biol Chem*, 268(28), 20729-20732. <https://www.ncbi.nlm.nih.gov/pubmed/8407895>
- Casarini, L., & Crépieux, P. (2019). Molecular Mechanisms of Action of FSH. *Front Endocrinol (Lausanne)*, 10, 305. <https://doi.org/10.3389/fendo.2019.00305>
- Casarini, L., Lazzaretti, C., Paradiso, E., Limoncella, S., Riccetti, L., Sperduti, S., Melli, B., Marcozzi, S., Anzivino, C., Sayers, N. S., Czapinski, J., Brigante, G., Potì, F., La Marca, A., De Pascali, F., Reiter, E., Falbo, A., Daolio, J., Villani, M. T., . . . Simoni, M. (2020). Membrane Estrogen Receptor (GPER) and Follicle-Stimulating Hormone Receptor (FSHR) Heteromeric Complexes Promote Human Ovarian Follicle Survival. *iScience*, 23(12), 101812. <https://doi.org/10.1016/j.isci.2020.101812>
- Casarini, L., Lispi, M., Longobardi, S., Milosa, F., La Marca, A., Tagliasacchi, D., Pignatti, E., & Simoni, M. (2012). LH and hCG action on the same receptor results in quantitatively and qualitatively different intracellular signalling. *PLoS One*, 7(10), e46682. <https://doi.org/10.1371/journal.pone.0046682>
- Casarini, L., Moriondo, V., Marino, M., Adversi, F., Capodanno, F., Grisolia, C., La Marca, A., La Sala, G. B., & Simoni, M. (2014). FSHR polymorphism p.N680S mediates different responses to FSH in vitro. *Mol Cell Endocrinol*, 393(1-2), 83-91. <https://doi.org/10.1016/j.mce.2014.06.013>
- Casarini, L., Reiter, E., & Simoni, M. (2016a).  $\beta$ -arrestins regulate gonadotropin receptor-mediated cell proliferation and apoptosis by controlling different FSHR or LHCGR intracellular signaling in the hGL5 cell line. *Mol Cell Endocrinol*, 437, 11-21. <https://doi.org/10.1016/j.mce.2016.08.005>
- Casarini, L., Riccetti, L., De Pascali, F., Nicoli, A., Tagliavini, S., Trenti, T., La Sala, G. B., & Simoni, M. (2016b). Follicle-stimulating hormone potentiates the steroidogenic activity of chorionic gonadotropin and the anti-apoptotic activity of luteinizing hormone in human granulosa-lutein cells in vitro. *Mol Cell Endocrinol*, 422, 103-114. <https://doi.org/10.1016/j.mce.2015.12.008>
- Cerpa-Poljak, A., Bishop, L. A., Hort, Y. J., Chin, C. K., DeKroon, R., Mahler, S. M., Smith, G. M., Stuart, M. C., & Schofield, P. R. (1993). Isoelectric charge of recombinant human follicle-stimulating hormone isoforms determines receptor affinity and in vitro bioactivity. *Endocrinology*, 132(1), 351-356. <https://doi.org/10.1210/endo.132.1.8419133>
- Chan, W. K., & Tan, C. H. (1987). Induction of aromatase activity in porcine granulosa cells by FSH and cyclic AMP. *Endocr Res*, 13(3), 285-299. <https://www.ncbi.nlm.nih.gov/pubmed/2448135>
- Chang, R., Zhang, X., Qiao, A., Dai, A., Belousoff, M. J., Tan, Q., Shao, L., Zhong, L., Lin, G., Liang, Y. L., Ma, L., Han, S., Yang, D., Danev, R., Wang, M. W., Wootten, D., Wu, B., & Sexton, P. M. (2020). Cryo-electron microscopy structure of the glucagon receptor with a dual-agonist peptide. *J Biol Chem*, 295(28), 9313-9325. <https://doi.org/10.1074/jbc.RA120.013793>
- Chrusciel, M., Ponikwicka-Tyszko, D., Wolczynski, S., Huhtaniemi, I., & Rahman, N. A. (2019). Extragonadal FSHR Expression and Function-Is It Real? *Front Endocrinol (Lausanne)*, 10, 32. <https://doi.org/10.3389/fendo.2019.00032>
- Clarke, I. J., & Cummins, J. T. (1982). The temporal relationship between gonadotropin releasing hormone (GnRH) and luteinizing hormone (LH) secretion in ovariectomized ewes. *Endocrinology*, 111(5), 1737-1739. <https://doi.org/10.1210/endo-111-5-1737>
- Conti, M., Kasson, B. G., & Hsueh, A. J. (1984). Hormonal regulation of 3',5'-adenosine monophosphate phosphodiesterases in cultured rat granulosa cells. *Endocrinology*, 114(6), 2361-2368. <https://doi.org/10.1210/endo-114-6-2361>
- Cornelis, S., Uttenweiler-Joseph, S., Panneels, V., Vassart, G., & Costagliola, S. (2001). Purification and characterization of a soluble bioactive amino-terminal extracellular domain of the human thyrotropin receptor. *Biochemistry*, 40(33), 9860-9869. <https://doi.org/10.1021/bi0107389>
- Coss, D. (2018). Regulation of reproduction via tight control of gonadotropin hormone levels. *Mol Cell Endocrinol*, 463, 116-130. <https://doi.org/10.1016/j.mce.2017.03.022>



- Costagliola, S., Panneels, V., Bonomi, M., Koch, J., Many, M. C., Smits, G., & Vassart, G. (2002). Tyrosine sulfation is required for agonist recognition by glycoprotein hormone receptors. *EMBO J*, *21*(4), 504-513. <https://doi.org/10.1093/emboj/21.4.504>
- Cottet, M., Albizu, L., Perkovska, S., Jean-Alphonse, F., Rahmeh, R., Orcel, H., Méjean, C., Granier, S., Mendre, C., Mouillac, B., & Durroux, T. (2010). Past, present and future of vasopressin and oxytocin receptor oligomers, prototypical GPCR models to study dimerization processes. *Curr Opin Pharmacol*, *10*(1), 59-66. <https://doi.org/10.1016/j.coph.2009.10.003>
- Cottom, J., Salvador, L. M., Maizels, E. T., Reierstad, S., Park, Y., Carr, D. W., Davare, M. A., Hell, J. W., Palmer, S. S., Dent, P., Kawakatsu, H., Ogata, M., & Hunzicker-Dunn, M. (2003). Follicle-stimulating hormone activates extracellular signal-regulated kinase but not extracellular signal-regulated kinase kinase through a 100-kDa phosphotyrosine phosphatase. *J Biol Chem*, *278*(9), 7167-7179. <https://doi.org/10.1074/jbc.M203901200>
- Crépieux, P., Marion, S., Martinat, N., Fafeur, V., Vern, Y. L., Kerboeuf, D., Guillou, F., & Reiter, E. (2001). The ERK-dependent signalling is stage-specifically modulated by FSH, during primary Sertoli cell maturation. *Oncogene*, *20*(34), 4696-4709. <https://doi.org/10.1038/sj.onc.1204632>
- Creus, S., Pellizzari, E., Cigorraga, S. B., & Campo, S. (1996). FSH isoforms: bio and immuno-activities in post-menopausal and normal menstruating women. *Clin Endocrinol (Oxf)*, *44*(2), 181-189. <https://doi.org/10.1046/j.1365-2265.1996.646467.x>
- Cui, H., Zhao, G., Liu, R., Zheng, M., Chen, J., & Wen, J. (2012). FSH stimulates lipid biosynthesis in chicken adipose tissue by upregulating the expression of its receptor FSHR. *J Lipid Res*, *53*(5), 909-917. <https://doi.org/10.1194/jlr.M025403>
- Dalpathado, D. S., Irungu, J., Go, E. P., Butnev, V. Y., Norton, K., Bousfield, G. R., & Desaire, H. (2006). Comparative glycomics of the glycoprotein follicle stimulating hormone: glycopeptide analysis of isolates from two mammalian species. *Biochemistry*, *45*(28), 8665-8673. <https://doi.org/10.1021/bi060435k>
- Damián-Matsumura, P., Zaga, V., Maldonado, A., Sánchez-Hernández, C., Timossi, C., & Ulloa-Aguirre, A. (1999). Oestrogens regulate pituitary alpha2,3-sialyltransferase messenger ribonucleic acid levels in the female rat. *J Mol Endocrinol*, *23*(2), 153-165. <https://www.ncbi.nlm.nih.gov/pubmed/10514553>
- Danesi, R., La Rocca, R. V., Cooper, M. R., Ricciardi, M. P., Pellegrini, A., Soldani, P., Kragel, P. J., Paparelli, A., Del Tacca, M., & Myers, C. E. (1996). Clinical and experimental evidence of inhibition of testosterone production by suramin. *J Clin Endocrinol Metab*, *81*(6), 2238-2246. <https://doi.org/10.1210/jcem.81.6.8964858>
- Das, N., & Kumar, T. R. (2018). Molecular regulation of follicle-stimulating hormone synthesis, secretion and action. *J Mol Endocrinol*, *60*(3), R131-R155. <https://doi.org/10.1530/JME-17-0308>
- Davis, D., Liu, X., & Segaloff, D. L. (1995). Identification of the sites of N-linked glycosylation on the follicle-stimulating hormone (FSH) receptor and assessment of their role in FSH receptor function. *Mol Endocrinol*, *9*(2), 159-170. <https://doi.org/10.1210/mend.9.2.7776966>
- Davis, J. S., Kumar, T. R., May, J. V., & Bousfield, G. R. (2014). Naturally Occurring Follicle-Stimulating Hormone Glycosylation Variants. *J Glycomics Lipidomics*, *4*(1), e117. <https://doi.org/10.4172/2153-0637.1000e117>
- Daya, S., & Gunby, J. (2000). Recombinant versus urinary follicle stimulating hormone for ovarian stimulation in assisted reproduction cycles. *Cochrane Database Syst Rev*(4), CD002810. <https://doi.org/10.1002/14651858.CD002810>
- De Pascali, F., Ayoub, M. A., Benevelli, R., Sposini, S., Lehoux, J., Gallay, N., Raynaud, P., Landomiel, F., Jean-Alphonse, F., Gauthier, C., Pellissier, L. P., Crépieux, P., Poupon, A., Inoue, A., Joubert, N., Viaud-Massuard, M. C., Casarini, L., Simoni, M., Hanyaloglu, A. C., . . . Reiter, E. (2021). Pharmacological Characterization of Low Molecular Weight Biased Agonists at the Follicle Stimulating Hormone Receptor. *Int J Mol Sci*, *22*(18). <https://doi.org/10.3390/ijms22189850>

- De Pascali, F., & Reiter, E. (2018).  $\beta$ -arrestins and biased signaling in gonadotropin receptors. *Minerva Ginecol*, 70(5), 525-538. <https://doi.org/10.23736/S0026-4784.18.04272-7>
- DeManno, D. A., Cottom, J. E., Kline, M. P., Peters, C. A., Maizels, E. T., & Hunzicker-Dunn, M. (1999). Follicle-stimulating hormone promotes histone H3 phosphorylation on serine-10. *Mol Endocrinol*, 13(1), 91-105. <https://doi.org/10.1210/mend.13.1.0222>
- Dias, J. A., Bonnet, B., Weaver, B. A., Watts, J., Kluetzman, K., Thomas, R. M., Poli, S., Mutel, V., & Campo, B. (2011). A negative allosteric modulator demonstrates biased antagonism of the follicle stimulating hormone receptor. *Mol Cell Endocrinol*, 333(2), 143-150. <https://doi.org/10.1016/j.mce.2010.12.023>
- Dias, J. A., Campo, B., Weaver, B. A., Watts, J., Kluetzman, K., Thomas, R. M., Bonnet, B., Mutel, V., & Poli, S. M. (2014). Inhibition of follicle-stimulating hormone-induced preovulatory follicles in rats treated with a nonsteroidal negative allosteric modulator of follicle-stimulating hormone receptor. *Biol Reprod*, 90(1), 19. <https://doi.org/10.1095/biolreprod.113.109397>
- Dias, J. A., Cohen, B. D., Lindau-Shepard, B., Nechamen, C. A., Peterson, A. J., & Schmidt, A. (2002). Molecular, structural, and cellular biology of follitropin and follitropin receptor. *Vitam Horm*, 64, 249-322. <https://www.ncbi.nlm.nih.gov/pubmed/11898394>
- Dias, J. A., & Van Roey, P. (2001). Structural biology of human follitropin and its receptor. *Arch Med Res*, 32(6), 510-519. [https://doi.org/10.1016/s0188-4409\(01\)00333-2](https://doi.org/10.1016/s0188-4409(01)00333-2)
- Dias, J. A., Zhang, Y., & Liu, X. (1994). Receptor binding and functional properties of chimeric human follitropin prepared by an exchange between a small hydrophilic intercysteine loop of human follitropin and human lutropin. *J Biol Chem*, 269(41), 25289-25294. <https://www.ncbi.nlm.nih.gov/pubmed/7929221>
- Dierich, A., Sairam, M. R., Monaco, L., Fimia, G. M., Gansmuller, A., LeMeur, M., & Sassone-Corsi, P. (1998). Impairing follicle-stimulating hormone (FSH) signaling in vivo: targeted disruption of the FSH receptor leads to aberrant gametogenesis and hormonal imbalance. *Proc Natl Acad Sci U S A*, 95(23), 13612-13617. <https://doi.org/10.1073/pnas.95.23.13612>
- Driancourt, M. A. (2001). Regulation of ovarian follicular dynamics in farm animals. Implications for manipulation of reproduction. *Theriogenology*, 55(6), 1211-1239. [https://doi.org/10.1016/s0093-691x\(01\)00479-4](https://doi.org/10.1016/s0093-691x(01)00479-4)
- Dror, R. O., Arlow, D. H., Maragakis, P., Mildorf, T. J., Pan, A. C., Xu, H., Borhani, D. W., & Shaw, D. E. (2011). Activation mechanism of the  $\beta$ 2-adrenergic receptor. *Proc Natl Acad Sci U S A*, 108(46), 18684-18689. <https://doi.org/10.1073/pnas.1110499108>
- Dungan, H. M., Clifton, D. K., & Steiner, R. A. (2006). Minireview: kisspeptin neurons as central processors in the regulation of gonadotropin-releasing hormone secretion. *Endocrinology*, 147(3), 1154-1158. <https://doi.org/10.1210/en.2005-1282>
- Duprez, L., Parma, J., Costagliola, S., Hermans, J., Van Sande, J., Dumont, J. E., & Vassart, G. (1997). Constitutive activation of the TSH receptor by spontaneous mutations affecting the N-terminal extracellular domain. *FEBS Lett*, 409(3), 469-474. [https://doi.org/10.1016/s0014-5793\(97\)00532-2](https://doi.org/10.1016/s0014-5793(97)00532-2)
- Duvernay, M. T., Zhou, F., & Wu, G. (2004). A conserved motif for the transport of G protein-coupled receptors from the endoplasmic reticulum to the cell surface. *J Biol Chem*, 279(29), 30741-30750. <https://doi.org/10.1074/jbc.M313881200>
- Dwivedi-Agnihotri, H., Chaturvedi, M., Baidya, M., Stepniowski, T. M., Pandey, S., Maharana, J., Srivastava, A., Caengprasath, N., Hanyaloglu, A. C., Selent, J., & Shukla, A. K. (2020). Distinct phosphorylation sites in a prototypical GPCR differently orchestrate  $\beta$ -arrestin interaction, trafficking, and signaling. *Sci Adv*, 6(37). <https://doi.org/10.1126/sciadv.abb8368>
- Fan, Q. R., & Hendrickson, W. A. (2005). Structure of human follicle-stimulating hormone in complex with its receptor. *Nature*, 433(7023), 269-277. <https://doi.org/10.1038/nature03206>
- Feng, X., Zhang, M., Guan, R., & Segaloff, D. L. (2013). Heterodimerization between the lutropin and follitropin receptors is associated with an attenuation of hormone-dependent signaling. *Endocrinology*, 154(10), 3925-3930. <https://doi.org/10.1210/en.2013-1407>

- Ferrandon, S., Feinstein, T. N., Castro, M., Wang, B., Bouley, R., Potts, J. T., Gardella, T. J., & Villardaga, J. P. (2009). Sustained cyclic AMP production by parathyroid hormone receptor endocytosis. *Nat Chem Biol*, *5*(10), 734-742. <https://doi.org/10.1038/nchembio.206>
- Flack, M. R., Froehlich, J., Bennet, A. P., Anasti, J., & Nisula, B. C. (1994). Site-directed mutagenesis defines the individual roles of the glycosylation sites on follicle-stimulating hormone. *J Biol Chem*, *269*(19), 14015-14020. <https://www.ncbi.nlm.nih.gov/pubmed/8188681>
- Flores, J. A., Leong, D. A., & Veldhuis, J. D. (1992). Is the calcium signal induced by follicle-stimulating hormone in swine granulosa cells mediated by adenosine cyclic 3',5'-monophosphate-dependent protein kinase? *Endocrinology*, *130*(4), 1862-1866. <https://doi.org/10.1210/endo.130.4.1547716>
- Flores, J. A., Veldhuis, J. D., & Leong, D. A. (1990). Follicle-stimulating hormone evokes an increase in intracellular free calcium ion concentrations in single ovarian (granulosa) cells. *Endocrinology*, *127*(6), 3172-3179. <https://doi.org/10.1210/endo-127-6-3172>
- Flower, D. R. (1999). Modelling G-protein-coupled receptors for drug design. *Biochim Biophys Acta*, *1422*(3), 207-234. [https://doi.org/10.1016/s0304-4157\(99\)00006-4](https://doi.org/10.1016/s0304-4157(99)00006-4)
- Fox, K. M., Dias, J. A., & Van Roey, P. (2001). Three-dimensional structure of human follicle-stimulating hormone. *Mol Endocrinol*, *15*(3), 378-389. <https://doi.org/10.1210/mend.15.3.0603>
- Fredriksson, R., Lagerström, M. C., Lundin, L. G., & Schiöth, H. B. (2003). The G-protein-coupled receptors in the human genome form five main families. Phylogenetic analysis, paralogon groups, and fingerprints. *Mol Pharmacol*, *63*(6), 1256-1272. <https://doi.org/10.1124/mol.63.6.1256>
- García-Nafria, J., Lee, Y., Bai, X., Carpenter, B., & Tate, C. G. (2018). Cryo-EM structure of the adenosine A. *Elife*, *7*. <https://doi.org/10.7554/eLife.35946>
- Gera, S., Sant, D., Haider, S., Korkmaz, F., Kuo, T. C., Mathew, M., Perez-Pena, H., Xie, H., Chen, H., Batista, R., Ma, K., Cheng, Z., Hadelia, E., Robinson, C., Macdonald, A., Miyashita, S., Williams, A., Jebian, G., Miyashita, H., . . . Zaidi, M. (2020). First-in-class humanized FSH blocking antibody targets bone and fat. *Proc Natl Acad Sci U S A*, *117*(46), 28971-28979. <https://doi.org/10.1073/pnas.2014588117>
- Getter, T., Gulati, S., Zimmerman, R., Chen, Y., Vinberg, F., & Palczewski, K. (2019). Stereospecific modulation of dimeric rhodopsin. *FASEB J*, *33*(8), 9526-9539. <https://doi.org/10.1096/fj.201900443RR>
- Gloaguen, P., Crépieux, P., Heitzler, D., Poupon, A., & Reiter, E. (2011). Mapping the follicle-stimulating hormone-induced signaling networks. *Front Endocrinol (Lausanne)*, *2*, 45. <https://doi.org/10.3389/fendo.2011.00045>
- Gorczyńska, E., Spaliviero, J., & Handelsman, D. J. (1994). The relationship between 3',5'-cyclic adenosine monophosphate and calcium in mediating follicle-stimulating hormone signal transduction in Sertoli cells. *Endocrinology*, *134*(1), 293-300. <https://doi.org/10.1210/endo.134.1.8275946>
- Gotschall, R. R., & Bousfield, G. R. (1996). Oligosaccharide mapping reveals hormone-specific glycosylation patterns on equine gonadotropin alpha-subunit Asn56. *Endocrinology*, *137*(6), 2543-2557. <https://doi.org/10.1210/endo.137.6.8641208>
- Gougeon, A. (2010). Human ovarian follicular development: from activation of resting follicles to preovulatory maturation. *Ann Endocrinol (Paris)*, *71*(3), 132-143. <https://doi.org/10.1016/j.ando.2010.02.021>
- Gromoll, J., Pekel, E., & Nieschlag, E. (1996). The structure and organization of the human follicle-stimulating hormone receptor (FSHR) gene. *Genomics*, *35*(2), 308-311. <https://doi.org/10.1006/geno.1996.0361>
- Grüters, A., Schöneberg, T., Biebermann, H., Krude, H., Krohn, H. P., Dralle, H., & Gudermann, T. (1998). Severe congenital hyperthyroidism caused by a germ-line neo mutation in the extracellular portion of the thyrotropin receptor. *J Clin Endocrinol Metab*, *83*(5), 1431-1436. <https://doi.org/10.1210/jcem.83.5.4776>

- Guan, R., Wu, X., Feng, X., Zhang, M., Hébert, T. E., & Segaloff, D. L. (2010). Structural determinants underlying constitutive dimerization of unoccupied human follitropin receptors. *Cell Signal*, *22*(2), 247-256. <https://doi.org/10.1016/j.cellsig.2009.09.023>
- Guixà-González, R., Javanainen, M., Gómez-Soler, M., Cordobilla, B., Domingo, J. C., Sanz, F., Pastor, M., Ciruela, F., Martínez-Seara, H., & Selent, J. (2016). Membrane omega-3 fatty acids modulate the oligomerisation kinetics of adenosine A2A and dopamine D2 receptors. *Sci Rep*, *6*, 19839. <https://doi.org/10.1038/srep19839>
- Guo, H., An, S., Ward, R., Yang, Y., Liu, Y., Guo, X. X., Hao, Q., & Xu, T. R. (2017). Methods used to study the oligomeric structure of G-protein-coupled receptors. *Biosci Rep*, *37*(2). <https://doi.org/10.1042/BSR20160547>
- Guo, W., Shi, L., Filizola, M., Weinstein, H., & Javitch, J. A. (2005). Crosstalk in G protein-coupled receptors: changes at the transmembrane homodimer interface determine activation. *Proc Natl Acad Sci U S A*, *102*(48), 17495-17500. <https://doi.org/10.1073/pnas.0508950102>
- Ha, S. H., & Ferrell, J. E. (2016). Thresholds and ultrasensitivity from negative cooperativity. *Science*, *352*(6288), 990-993. <https://doi.org/10.1126/science.aad5937>
- Han, H. (2018). RNA Interference to Knock Down Gene Expression. *Methods Mol Biol*, *1706*, 293-302. [https://doi.org/10.1007/978-1-4939-7471-9\\_16](https://doi.org/10.1007/978-1-4939-7471-9_16)
- Hansen, R. B., & Kavanaugh, A. (2014). Novel treatments with small molecules in psoriatic arthritis. *Curr Rheumatol Rep*, *16*(9), 443. <https://doi.org/10.1007/s11926-014-0443-6>
- Hanyaloglu, A. C. (2018). Advances in Membrane Trafficking and Endosomal Signaling of G Protein-Coupled Receptors. *Int Rev Cell Mol Biol*, *339*, 93-131. <https://doi.org/10.1016/bs.ircmb.2018.03.001>
- Hardy, K., Fenwick, M., Mora, J., Laird, M., Thomson, K., & Franks, S. (2017). Onset and Heterogeneity of Responsiveness to FSH in Mouse Preantral Follicles in Culture. *Endocrinology*, *158*(1), 134-147. <https://doi.org/10.1210/en.2016-1435>
- Hausch, F. (2017). Cryo-EM Structures of Class B GPCR Reveal the Activation Mechanism. *Angew Chem Int Ed Engl*, *56*(41), 12412-12414. <https://doi.org/10.1002/anie.201707200>
- Hauser, A. S., Chavali, S., Masuho, I., Jahn, L. J., Martemyanov, K. A., Gloriam, D. E., & Babu, M. M. (2018). Pharmacogenomics of GPCR Drug Targets. *Cell*, *172*(1-2), 41-54.e19. <https://doi.org/10.1016/j.cell.2017.11.033>
- Hauser, A. S., Kooistra, A. J., Munk, C., Heydenreich, F. M., Veprintsev, D. B., Bouvier, M., Babu, M. M., & Gloriam, D. E. (2021). GPCR activation mechanisms across classes and macro/microscales. *Nat Struct Mol Biol*, *28*(11), 879-888. <https://doi.org/10.1038/s41594-021-00674-7>
- Heckert, L. L., Daggett, M. A., & Chen, J. (1998). Multiple promoter elements contribute to activity of the follicle-stimulating hormone receptor (FSHR) gene in testicular Sertoli cells. *Mol Endocrinol*, *12*(10), 1499-1512. <https://doi.org/10.1210/mend.12.10.0183>
- Heckert, L. L., Sawadogo, M., Daggett, M. A., & Chen, J. K. (2000). The USF proteins regulate transcription of the follicle-stimulating hormone receptor but are insufficient for cell-specific expression. *Mol Endocrinol*, *14*(11), 1836-1848. <https://doi.org/10.1210/mend.14.11.0557>
- Hermann, B. P., & Heckert, L. L. (2007). Transcriptional regulation of the FSH receptor: new perspectives. *Mol Cell Endocrinol*, *260-262*, 100-108. <https://doi.org/10.1016/j.mce.2006.09.005>
- Hern, J. A., Baig, A. H., Mashanov, G. I., Birdsall, B., Corrie, J. E., Lazareno, S., Molloy, J. E., & Birdsall, N. J. (2010). Formation and dissociation of M1 muscarinic receptor dimers seen by total internal reflection fluorescence imaging of single molecules. *Proc Natl Acad Sci U S A*, *107*(6), 2693-2698. <https://doi.org/10.1073/pnas.0907915107>
- Hernanz-Falcón, P., Rodríguez-Frade, J. M., Serrano, A., Juan, D., del Sol, A., Soriano, S. F., Roncal, F., Gómez, L., Valencia, A., Martínez-A, C., & Mellado, M. (2004). Identification of amino acid residues crucial for chemokine receptor dimerization. *Nat Immunol*, *5*(2), 216-223. <https://doi.org/10.1038/ni1027>

- Herrick-Davis, K., Grinde, E., Lindsley, T., Teitler, M., Mancina, F., Cowan, A., & Mazurkiewicz, J. E. (2015). Native serotonin 5-HT<sub>2C</sub> receptors are expressed as homodimers on the apical surface of choroid plexus epithelial cells. *Mol Pharmacol*, *87*(4), 660-673. <https://doi.org/10.1124/mol.114.096636>
- HFEA. (2021). *Fertility treatment 2019: trends and figures*. <https://www.hfea.gov.uk/about-us/publications/research-and-data/fertility-treatment-2019-trends-and-figures/>
- Hillier, S. G., Whitelaw, P. F., & Smyth, C. D. (1994). Follicular oestrogen synthesis: the 'two-cell, two-gonadotrophin' model revisited. *Mol Cell Endocrinol*, *100*(1-2), 51-54. [https://doi.org/10.1016/0303-7207\(94\)90278-x](https://doi.org/10.1016/0303-7207(94)90278-x)
- Hirakawa, T., Galet, C., Kishi, M., & Ascoli, M. (2003). GIPC binds to the human lutropin receptor (hLHR) through an unusual PDZ domain binding motif, and it regulates the sorting of the internalized human choriogonadotropin and the density of cell surface hLHR. *J Biol Chem*, *278*(49), 49348-49357. <https://doi.org/10.1074/jbc.M306557200>
- Hollenstein, K., Kean, J., Bortolato, A., Cheng, R. K., Doré, A. S., Jazayeri, A., Cooke, R. M., Weir, M., & Marshall, F. H. (2013). Structure of class B GPCR corticotropin-releasing factor receptor 1. *Nature*, *499*(7459), 438-443. <https://doi.org/10.1038/nature12357>
- Hu, C. L., Cowan, R. G., Harman, R. M., & Quirk, S. M. (2004). Cell cycle progression and activation of Akt kinase are required for insulin-like growth factor I-mediated suppression of apoptosis in granulosa cells. *Mol Endocrinol*, *18*(2), 326-338. <https://doi.org/10.1210/me.2003-0178>
- Hua, G., George, J. W., Clark, K. L., Jonas, K. C., Johnson, G. P., Southehal, S., Guda, C., Hou, X., Blum, H. R., Eudy, J., Butnev, V. Y., Brown, A. R., Katta, S., May, J. V., Bousfield, G. R., & Davis, J. S. (2021). Hypo-glycosylated hFSH drives ovarian follicular development more efficiently than fully-glycosylated hFSH: enhanced transcription and PI3K and MAPK signaling. *Hum Reprod*, *36*(7), 1891-1906. <https://doi.org/10.1093/humrep/deab135>
- Huang, J., Chen, S., Zhang, J. J., & Huang, X. Y. (2013). Crystal structure of oligomeric  $\beta$ 1-adrenergic G protein-coupled receptors in ligand-free basal state. *Nat Struct Mol Biol*, *20*(4), 419-425. <https://doi.org/10.1038/nsmb.2504>
- Hunzicker-Dunn, M. E., Lopez-Biladeau, B., Law, N. C., Fiedler, S. E., Carr, D. W., & Maizels, E. T. (2012). PKA and GAB2 play central roles in the FSH signaling pathway to PI3K and AKT in ovarian granulosa cells. *Proc Natl Acad Sci U S A*, *109*(44), E2979-2988. <https://doi.org/10.1073/pnas.1205661109>
- Huo, X., Chen, D., He, Y., Zhu, W., Zhou, W., & Zhang, J. (2015). Bisphenol-A and Female Infertility: A Possible Role of Gene-Environment Interactions. *Int J Environ Res Public Health*, *12*(9), 11101-11116. <https://doi.org/10.3390/ijerph120911101>
- Irannejad, R., Tomshine, J. C., Tomshine, J. R., Chevalier, M., Mahoney, J. P., Steyaert, J., Rasmussen, S. G., Sunahara, R. K., El-Samad, H., Huang, B., & von Zastrow, M. (2013). Conformational biosensors reveal GPCR signalling from endosomes. *Nature*, *495*(7442), 534-538. <https://doi.org/10.1038/nature12000>
- Jaeschke, H., Schaarschmidt, J., Günther, R., & Mueller, S. (2011). The hinge region of the TSH receptor stabilizes ligand binding and determines different signaling profiles of human and bovine TSH. *Endocrinology*, *152*(10), 3986-3996. <https://doi.org/10.1210/en.2011-1389>
- Janovick, J. A., Maya-Núñez, G., Ulloa-Aguirre, A., Huhtaniemi, I. T., Dias, J. A., Verboost, P., & Conn, P. M. (2009). Increased plasma membrane expression of human follicle-stimulating hormone receptor by a small molecule thienopyr(im)idine. *Mol Cell Endocrinol*, *298*(1-2), 84-88. <https://doi.org/10.1016/j.mce.2008.09.015>
- Jayes, F. C., Britt, J. H., & Esbenshade, K. L. (1997). Role of gonadotropin-releasing hormone pulse frequency in differential regulation of gonadotropins in the gilt. *Biol Reprod*, *56*(4), 1012-1019. <https://doi.org/10.1095/biolreprod56.4.1012>
- Jean-Alphonse, F., Bowersox, S., Chen, S., Beard, G., Puthenveedu, M. A., & Hanyaloglu, A. C. (2014). Spatially restricted G protein-coupled receptor activity via divergent endocytic compartments. *J Biol Chem*, *289*(7), 3960-3977. <https://doi.org/10.1074/jbc.M113.526350>

- Jeoung, M., Lee, C., Ji, I., & Ji, T. H. (2007). Trans-activation, cis-activation and signal selection of gonadotropin receptors. *Mol Cell Endocrinol*, 260-262, 137-143. <https://doi.org/10.1016/j.mce.2005.09.015>
- Ji, I., Lee, C., Jeoung, M., Koo, Y., Sievert, G. A., & Ji, T. H. (2004). Trans-activation of mutant follicle-stimulating hormone receptors selectively generates only one of two hormone signals. *Mol Endocrinol*, 18(4), 968-978. <https://doi.org/10.1210/me.2003-0443>
- Ji, Y., Liu, P., Yuen, T., Haider, S., He, J., Romero, R., Chen, H., Bloch, M., Kim, S. M., Lizneva, D., Munshi, L., Zhou, C., Lu, P., Iqbal, J., Cheng, Z., New, M. I., Hsueh, A. J., Bian, Z., Rosen, C. J., . . . Zaidi, M. (2018). Epitope-specific monoclonal antibodies to FSH $\beta$  increase bone mass. *Proc Natl Acad Sci U S A*, 115(9), 2192-2197. <https://doi.org/10.1073/pnas.1718144115>
- Jiang, C., Hou, X., Wang, C., May, J. V., Butnev, V. Y., Bousfield, G. R., & Davis, J. S. (2015). Hypoglycosylated hFSH Has Greater Bioactivity Than Fully Glycosylated Recombinant hFSH in Human Granulosa Cells. *J Clin Endocrinol Metab*, 100(6), E852-860. <https://doi.org/10.1210/jc.2015-1317>
- Jiang, X., Dias, J. A., & He, X. (2014a). Structural biology of glycoprotein hormones and their receptors: insights to signaling. *Mol Cell Endocrinol*, 382(1), 424-451. <https://doi.org/10.1016/j.mce.2013.08.021>
- Jiang, X., Dreano, M., Buckler, D. R., Cheng, S., Ythier, A., Wu, H., Hendrickson, W. A., & el Tayar, N. (1995). Structural predictions for the ligand-binding region of glycoprotein hormone receptors and the nature of hormone-receptor interactions. *Structure*, 3(12), 1341-1353. [https://doi.org/10.1016/s0969-2126\(01\)00272-6](https://doi.org/10.1016/s0969-2126(01)00272-6)
- Jiang, X., Fischer, D., Chen, X., McKenna, S. D., Liu, H., Sriraman, V., Yu, H. N., Goutopoulos, A., Arkinstall, S., & He, X. (2014b). Evidence for Follicle-stimulating Hormone Receptor as a Functional Trimer. *J Biol Chem*, 289(20), 14273-14282. <https://doi.org/10.1074/jbc.M114.549592>
- Jiang, X., Liu, H., Chen, X., Chen, P. H., Fischer, D., Sriraman, V., Yu, H. N., Arkinstall, S., & He, X. (2012). Structure of follicle-stimulating hormone in complex with the entire ectodomain of its receptor. *Proc Natl Acad Sci U S A*, 109(31), 12491-12496. <https://doi.org/10.1073/pnas.1206643109>
- Jirsová, S., Masata, J., Jech, L., & Zvárová, J. (2010). Effect of polychlorinated biphenyls (PCBs) and 1,1,1-trichloro-2,2-bis (4-chlorophenyl)-ethane (DDT) in follicular fluid on the results of in vitro fertilization-embryo transfer (IVF-ET) programs. *Fertil Steril*, 93(6), 1831-1836. <https://doi.org/10.1016/j.fertnstert.2008.12.063>
- Johnson, G. P., Onabanjo, C. G. A., Hardy, K., Butnev, V. Y., Bousfield, G. R., & Jonas, K. C. (2022). Follicle-Stimulating Hormone Glycosylation Variants Distinctly Modulate Pre-antral Follicle Growth and Survival. *Endocrinology*, 163(12). <https://doi.org/10.1210/endocr/bqac161>
- Jonas, K. C., Chen, S., Virta, M., Mora, J., Franks, S., Huhtaniemi, I., & Hanyaloglu, A. C. (2018). Temporal reprogramming of calcium signalling via crosstalk of gonadotrophin receptors that associate as functionally asymmetric heteromers. *Sci Rep*, 8(1), 2239. <https://doi.org/10.1038/s41598-018-20722-5>
- Jonas, K. C., Fanelli, F., Huhtaniemi, I. T., & Hanyaloglu, A. C. (2015). Single molecule analysis of functionally asymmetric G protein-coupled receptor (GPCR) oligomers reveals diverse spatial and structural assemblies. *J Biol Chem*, 290(7), 3875-3892. <https://doi.org/10.1074/jbc.M114.622498>
- Jonas, K. C., & Hanyaloglu, A. C. (2019). Analysis of Spatial Assembly of GPCRs Using Photoactivatable Dyes and Localization Microscopy. *Methods Mol Biol*, 1947, 337-348. [https://doi.org/10.1007/978-1-4939-9121-1\\_19](https://doi.org/10.1007/978-1-4939-9121-1_19)
- Jonas, K. C., Huhtaniemi, I., & Hanyaloglu, A. C. (2016). Single-molecule resolution of G protein-coupled receptor (GPCR) complexes. *Methods Cell Biol*, 132, 55-72. <https://doi.org/10.1016/bs.mcb.2015.11.005>

- Juengel, J. L., & McNatty, K. P. (2005). The role of proteins of the transforming growth factor-beta superfamily in the intraovarian regulation of follicular development. *Hum Reprod Update*, *11*(2), 143-160. <https://doi.org/10.1093/humupd/dmh061>
- Kaiser, U. B., Jakubowiak, A., Steinberger, A., & Chin, W. W. (1997). Differential effects of gonadotropin-releasing hormone (GnRH) pulse frequency on gonadotropin subunit and GnRH receptor messenger ribonucleic acid levels in vitro. *Endocrinology*, *138*(3), 1224-1231. <https://doi.org/10.1210/endo.138.3.4968>
- Kajava, A. V., Vassart, G., & Wodak, S. J. (1995). Modeling of the three-dimensional structure of proteins with the typical leucine-rich repeats. *Structure*, *3*(9), 867-877. [https://doi.org/10.1016/S0969-2126\(01\)00222-2](https://doi.org/10.1016/S0969-2126(01)00222-2)
- Kanaya, M., Baba, T., Kitajima, Y., Ikeda, K., Shimizu, A., Morishita, M., Honnma, H., Endo, T., & Saito, T. (2012). Continuous follicle-stimulating hormone exposure from pituitary adenoma causes periodic follicle recruitment and atresia, which mimics ovarian hyperstimulation syndrome. *Int J Womens Health*, *4*, 427-431. <https://doi.org/10.2147/IJWH.S33386>
- Kara, E., Crépieux, P., Gauthier, C., Martinat, N., Piketty, V., Guillou, F., & Reiter, E. (2006). A phosphorylation cluster of five serine and threonine residues in the C-terminus of the follicle-stimulating hormone receptor is important for desensitization but not for beta-arrestin-mediated ERK activation. *Mol Endocrinol*, *20*(11), 3014-3026. <https://doi.org/10.1210/me.2006-0098>
- Kasai, R. S., Suzuki, K. G., Prossnitz, E. R., Koyama-Honda, I., Nakada, C., Fujiwara, T. K., & Kusumi, A. (2011). Full characterization of GPCR monomer-dimer dynamic equilibrium by single molecule imaging. *J Cell Biol*, *192*(3), 463-480. <https://doi.org/10.1083/jcb.201009128>
- Kaur, G., & Lakkaraju, A. (2018). Early Endosome Morphology in Health and Disease. *Adv Exp Med Biol*, *1074*, 335-343. [https://doi.org/10.1007/978-3-319-75402-4\\_41](https://doi.org/10.1007/978-3-319-75402-4_41)
- Kim, J., Ahn, S., Ren, X. R., Whalen, E. J., Reiter, E., Wei, H., & Lefkowitz, R. J. (2005). Functional antagonism of different G protein-coupled receptor kinases for beta-arrestin-mediated angiotensin II receptor signaling. *Proc Natl Acad Sci U S A*, *102*(5), 1442-1447. <https://doi.org/10.1073/pnas.0409532102>
- Kobe, B., & Deisenhofer, J. (1993). Crystal structure of porcine ribonuclease inhibitor, a protein with leucine-rich repeats. *Nature*, *366*(6457), 751-756. <https://doi.org/10.1038/366751a0>
- Koldsø, H., & Sansom, M. S. (2015). Organization and Dynamics of Receptor Proteins in a Plasma Membrane. *J Am Chem Soc*, *137*(46), 14694-14704. <https://doi.org/10.1021/jacs.5b08048>
- Kopp, P., Muirhead, S., Jourdain, N., Gu, W. X., Jameson, J. L., & Rodd, C. (1997). Congenital hyperthyroidism caused by a solitary toxic adenoma harboring a novel somatic mutation (serine281-->isoleucine) in the extracellular domain of the thyrotropin receptor. *J Clin Invest*, *100*(6), 1634-1639. <https://doi.org/10.1172/JCI119687>
- Krause, G., Kreuchwig, A., & Kleinau, G. (2012). Extended and structurally supported insights into extracellular hormone binding, signal transduction and organization of the thyrotropin receptor. *PLoS One*, *7*(12), e52920. <https://doi.org/10.1371/journal.pone.0052920>
- Krishnamurthy, H., Kishi, H., Shi, M., Galet, C., Bhaskaran, R. S., Hirakawa, T., & Ascoli, M. (2003). Postendocytotic trafficking of the follicle-stimulating hormone (FSH)-FSH receptor complex. *Mol Endocrinol*, *17*(11), 2162-2176. <https://doi.org/10.1210/me.2003-0118>
- Kumar, S., Lambert, A., Rainier, J., & Fu, Y. (2018). Disruption of Rhodopsin Dimerization in Mouse Rod Photoreceptors by Synthetic Peptides Targeting Dimer Interface. *Methods Mol Biol*, *1753*, 115-128. [https://doi.org/10.1007/978-1-4939-7720-8\\_8](https://doi.org/10.1007/978-1-4939-7720-8_8)
- Kumar, T. R. (2018). Extragonadal Actions of FSH: A Critical Need for Novel Genetic Models. *Endocrinology*, *159*(1), 2-8. <https://doi.org/10.1210/en.2017-03118>
- Kumar, T. R., Wang, Y., Lu, N., & Matzuk, M. M. (1997). Follicle stimulating hormone is required for ovarian follicle maturation but not male fertility. *Nat Genet*, *15*(2), 201-204. <https://doi.org/10.1038/ng0297-201>

- Lander, E. S., Linton, L. M., Birren, B., Nusbaum, C., Zody, M. C., Baldwin, J., Devon, K., Dewar, K., Doyle, M., FitzHugh, W., Funke, R., Gage, D., Harris, K., Heaford, A., Howland, J., Kann, L., Lehoczky, J., LeVine, R., McEwan, P., . . . Consortium, I. H. G. S. (2001). Initial sequencing and analysis of the human genome. *Nature*, *409*(6822), 860-921. <https://doi.org/10.1038/35057062>
- Landomiel, F., De Pascali, F., Raynaud, P., Jean-Alphonse, F., Yvinec, R., Pellissier, L. P., Bozon, V., Bruneau, G., Crépieux, P., Poupon, A., & Reiter, E. (2019). Biased Signaling and Allosteric Modulation at the FSHR. *Front Endocrinol (Lausanne)*, *10*, 148. <https://doi.org/10.3389/fendo.2019.00148>
- Lange, Y., Schmit, V. M., & Schreiber, J. R. (1988). Localization and movement of newly synthesized cholesterol in rat ovarian granulosa cells. *Endocrinology*, *123*(1), 81-86. <https://doi.org/10.1210/endo-123-1-81>
- Laphorn, A. J., Harris, D. C., Littlejohn, A., Lustbader, J. W., Canfield, R. E., Machin, K. J., Morgan, F. J., & Isaacs, N. W. (1994). Crystal structure of human chorionic gonadotropin. *Nature*, *369*(6480), 455-461. <https://doi.org/10.1038/369455a0>
- Latif, R., Graves, P., & Davies, T. F. (2002). Ligand-dependent inhibition of oligomerization at the human thyrotropin receptor. *J Biol Chem*, *277*(47), 45059-45067. <https://doi.org/10.1074/jbc.M206693200>
- Lazari, M. F., Liu, X., Nakamura, K., Benovic, J. L., & Ascoli, M. (1999). Role of G protein-coupled receptor kinases on the agonist-induced phosphorylation and internalization of the follitropin receptor. *Mol Endocrinol*, *13*(6), 866-878. <https://doi.org/10.1210/mend.13.6.0289>
- Lebon, G., Warne, T., Edwards, P. C., Bennett, K., Langmead, C. J., Leslie, A. G., & Tate, C. G. (2011). Agonist-bound adenosine A2A receptor structures reveal common features of GPCR activation. *Nature*, *474*(7352), 521-525. <https://doi.org/10.1038/nature10136>
- Lee, J. H., de Val, N., Lyumkis, D., & Ward, A. B. (2015). Model Building and Refinement of a Natively Glycosylated HIV-1 Env Protein by High-Resolution Cryoelectron Microscopy. *Structure*, *23*(10), 1943-1951. <https://doi.org/10.1016/j.str.2015.07.020>
- Lefkowitz, R. J., & Shenoy, S. K. (2005). Transduction of receptor signals by beta-arrestins. *Science*, *308*(5721), 512-517. <https://doi.org/10.1126/science.1109237>
- Li, Y., Heng, J., Sun, D., Zhang, B., Zhang, X., Zheng, Y., Shi, W. W., Wang, T. Y., Li, J. Y., Sun, X., Liu, X., Zheng, J. S., Kobilka, B. K., & Liu, L. (2021). Chemical Synthesis of a Full-Length G-Protein-Coupled Receptor  $\beta$ . *J Am Chem Soc*, *143*(42), 17566-17576. <https://doi.org/10.1021/jacs.1c07369>
- Li, Z., Zhang, P., Zhang, Z., Pan, B., Chao, H., Li, L., Pan, Q., & Shen, W. (2011). A co-culture system with preantral follicular granulosa cells in vitro induces meiotic maturation of immature oocytes. *Histochem Cell Biol*, *135*(5), 513-522. <https://doi.org/10.1007/s00418-011-0812-4>
- Liang, A., Plewes, M. R., Hua, G., Hou, X., Blum, H. R., Przygodzka, E., George, J. W., Clark, K. L., Bousfield, G. R., Butnev, V. Y., May, J. V., & Davis, J. S. (2020). Bioactivity of recombinant hFSH glycosylation variants in primary cultures of porcine granulosa cells. *Mol Cell Endocrinol*, *514*, 110911. <https://doi.org/10.1016/j.mce.2020.110911>
- Liu, M., Deng, T., He, J., Ding, Y., Liu, X., Xu, H., Gao, R., Mu, X., Geng, Y., Liu, T., Wang, Y., & Chen, X. (2020). Exposure to Benzo[a]pyrene impairs the corpus luteum vascular network in rats during early pregnancy. *Environ Pollut*, *259*, 113915. <https://doi.org/10.1016/j.envpol.2020.113915>
- Liu, P., Ji, Y., Yuen, T., Rendina-Ruedy, E., DeMambro, V. E., Dhawan, S., Abu-Amer, W., Izadmehr, S., Zhou, B., Shin, A. C., Latif, R., Thangeswaran, P., Gupta, A., Li, J., Shnyder, V., Robinson, S. T., Yu, Y. E., Zhang, X., Yang, F., . . . Zaidi, M. (2017). Blocking FSH induces thermogenic adipose tissue and reduces body fat. *Nature*, *546*(7656), 107-112. <https://doi.org/10.1038/nature22342>
- Liu, X. M., Chan, H. C., Ding, G. L., Cai, J., Song, Y., Wang, T. T., Zhang, D., Chen, H., Yu, M. K., Wu, Y. T., Qu, F., Liu, Y., Lu, Y. C., Adashi, E. Y., Sheng, J. Z., & Huang, H. F. (2015). FSH regulates fat accumulation and redistribution in aging through the Gai/Ca(2+)/CREB pathway. *Aging Cell*, *14*(3), 409-420. <https://doi.org/10.1111/acel.12331>



- Lopez-Gimenez, J. F., Canals, M., Pediani, J. D., & Milligan, G. (2007). The alpha1b-adrenoceptor exists as a higher-order oligomer: effective oligomerization is required for receptor maturation, surface delivery, and function. *Mol Pharmacol*, *71*(4), 1015-1029. <https://doi.org/10.1124/mol.106.033035>
- Lundquist, L. M., Cole, S. W., & Sikes, M. L. (2014). Efficacy and safety of tofacitinib for treatment of rheumatoid arthritis. *World J Orthop*, *5*(4), 504-511. <https://doi.org/10.5312/wjo.v5.i4.504>
- Lyga, S., Volpe, S., Werthmann, R. C., Götz, K., Sungkaworn, T., Lohse, M. J., & Calebiro, D. (2016). Persistent cAMP Signaling by Internalized LH Receptors in Ovarian Follicles. *Endocrinology*, *157*(4), 1613-1621. <https://doi.org/10.1210/en.2015-1945>
- Maclean, D., Holden, F., Davis, A. M., Scheuerman, R. A., Yanofsky, S., Holmes, C. P., Fitch, W. L., Tsutsui, K., Barrett, R. W., & Gallop, M. A. (2004). Agonists of the follicle stimulating hormone receptor from an encoded thiazolidinone library. *J Comb Chem*, *6*(2), 196-206. <https://doi.org/10.1021/cc0300154>
- Manna, P. R., Chandrala, S. P., Jo, Y., & Stocco, D. M. (2006). cAMP-independent signaling regulates steroidogenesis in mouse Leydig cells in the absence of StAR phosphorylation. *J Mol Endocrinol*, *37*(1), 81-95. <https://doi.org/10.1677/jme.1.02065>
- Mao, C., Shen, C., Li, C., Shen, D. D., Xu, C., Zhang, S., Zhou, R., Shen, Q., Chen, L. N., Jiang, Z., Liu, J., & Zhang, Y. (2020). Cryo-EM structures of inactive and active GABA. *Cell Res*. <https://doi.org/10.1038/s41422-020-0350-5>
- Marion, S., Kara, E., Crepieux, P., Piketty, V., Martinat, N., Guillou, F., & Reiter, E. (2006). G protein-coupled receptor kinase 2 and beta-arrestins are recruited to FSH receptor in stimulated rat primary Sertoli cells. *J Endocrinol*, *190*(2), 341-350. <https://doi.org/10.1677/joe.1.06857>
- Martens, J. W., Lumbroso, S., Verhoef-Post, M., Georget, V., Richter-Unruh, A., Szarras-Czapnik, M., Romer, T. E., Brunner, H. G., Themmen, A. P., & Sultan, C. (2002). Mutant luteinizing hormone receptors in a compound heterozygous patient with complete Leydig cell hypoplasia: abnormal processing causes signaling deficiency. *J Clin Endocrinol Metab*, *87*(6), 2506-2513. <https://doi.org/10.1210/jcem.87.6.8523>
- Matzuk, M. M., & Boime, I. (1988). The role of the asparagine-linked oligosaccharides of the alpha subunit in the secretion and assembly of human chorionic gonadotrophin. *J Cell Biol*, *106*(4), 1049-1059. <https://doi.org/10.1083/jcb.106.4.1049>
- Matzuk, M. M., & Boime, I. (1989). Mutagenesis and gene transfer define site-specific roles of the gonadotropin oligosaccharides. *Biol Reprod*, *40*(1), 48-53. <https://doi.org/10.1095/biolreprod40.1.48>
- Maudsley, S., Martin, B., & Luttrell, L. M. (2005). The origins of diversity and specificity in g protein-coupled receptor signaling. *J Pharmacol Exp Ther*, *314*(2), 485-494. <https://doi.org/10.1124/jpet.105.083121>
- Mazurkiewicz, J. E., Herrick-Davis, K., Barroso, M., Ulloa-Aguirre, A., Lindau-Shepard, B., Thomas, R. M., & Dias, J. A. (2015). Single-molecule analyses of fully functional fluorescent protein-tagged follitropin receptor reveal homodimerization and specific heterodimerization with lutropin receptor. *Biol Reprod*, *92*(4), 100. <https://doi.org/10.1095/biolreprod.114.125781>
- McCluskey, A., Daniel, J. A., Hadzic, G., Chau, N., Clayton, E. L., Mariana, A., Whiting, A., Gorgani, N. N., Lloyd, J., Quan, A., Moshkanbaryans, L., Krishnan, S., Perera, S., Chircop, M., von Kleist, L., McGeachie, A. B., Howes, M. T., Parton, R. G., Campbell, M., . . . Robinson, P. J. (2013). Building a better dynasore: the dyngo compounds potently inhibit dynamin and endocytosis. *Traffic*, *14*(12), 1272-1289. <https://doi.org/10.1111/tra.12119>
- McDonald, P. H., Chow, C. W., Miller, W. E., Laporte, S. A., Field, M. E., Lin, F. T., Davis, R. J., & Lefkowitz, R. J. (2000). Beta-arrestin 2: a receptor-regulated MAPK scaffold for the activation of JNK3. *Science*, *290*(5496), 1574-1577. <https://doi.org/10.1126/science.290.5496.1574>
- McGee, E. A., Perlas, E., LaPolta, P. S., Tsafiriri, A., & Hsueh, A. J. (1997). Follicle-stimulating hormone enhances the development of preantral follicles in juvenile rats. *Biol Reprod*, *57*(5), 990-998. <https://doi.org/10.1095/biolreprod57.5.990>

- Meher, B. R., Dixit, A., Bousfield, G. R., & Lushington, G. H. (2015). Glycosylation Effects on FSH-FSHR Interaction Dynamics: A Case Study of Different FSH Glycoforms by Molecular Dynamics Simulations. *PLoS One*, *10*(9), e0137897. <https://doi.org/10.1371/journal.pone.0137897>
- Melo-Nava, B., Casas-González, P., Pérez-Solís, M. A., Castillo-Badillo, J., Maravillas-Montero, J. L., Jardón-Valadez, E., Zariñán, T., Aguilar-Rojas, A., Gallay, N., Reiter, E., & Ulloa-Aguirre, A. (2016). Role of Cysteine Residues in the Carboxyl-Terminus of the Follicle-Stimulating Hormone Receptor in Intracellular Traffic and Postendocytic Processing. *Front Cell Dev Biol*, *4*, 76. <https://doi.org/10.3389/fcell.2016.00076>
- Messinis, I. E., Messini, C. I., & Dafopoulos, K. (2014). Novel aspects of the endocrinology of the menstrual cycle. *Reprod Biomed Online*, *28*(6), 714-722. <https://doi.org/10.1016/j.rbmo.2014.02.003>
- Miao, Y., & McCammon, J. A. (2016). G-protein coupled receptors: advances in simulation and drug discovery. *Curr Opin Struct Biol*, *41*, 83-89. <https://doi.org/10.1016/j.sbi.2016.06.008>
- Milligan, G., Ward, R. J., & Marsango, S. (2019). GPCR homo-oligomerization. *Curr Opin Cell Biol*, *57*, 40-47. <https://doi.org/10.1016/j.ceb.2018.10.007>
- Mizrachi, D., & Segaloff, D. L. (2004). Intracellularly located misfolded glycoprotein hormone receptors associate with different chaperone proteins than their cognate wild-type receptors. *Mol Endocrinol*, *18*(7), 1768-1777. <https://doi.org/10.1210/me.2003-0406>
- Moeker, N., Peters, S., Rauchenberger, R., Ghinea, N., & Kunz, C. (2017). Antibody Selection for Cancer Target Validation of FSH-Receptor in Immunohistochemical Settings. *Antibodies (Basel)*, *6*(4). <https://doi.org/10.3390/antib6040015>
- Montanelli, L., Van Durme, J. J., Smits, G., Bonomi, M., Rodien, P., Devor, E. J., Moffat-Wilson, K., Pardo, L., Vassart, G., & Costagliola, S. (2004). Modulation of ligand selectivity associated with activation of the transmembrane region of the human follitropin receptor. *Mol Endocrinol*, *18*(8), 2061-2073. <https://doi.org/10.1210/me.2004-0036>
- Moore, R. K., Otsuka, F., & Shimasaki, S. (2003). Molecular basis of bone morphogenetic protein-15 signaling in granulosa cells. *J Biol Chem*, *278*(1), 304-310. <https://doi.org/10.1074/jbc.M207362200>
- Mueller, S., Jaeschke, H., Günther, R., & Paschke, R. (2010). The hinge region: an important receptor component for GPHR function. *Trends Endocrinol Metab*, *21*(2), 111-122. <https://doi.org/10.1016/j.tem.2009.09.001>
- Mueller, S., Szkudlinski, M. W., Schaarschmidt, J., Günther, R., Paschke, R., & Jaeschke, H. (2011). Identification of novel TSH interaction sites by systematic binding analysis of the TSHR hinge region. *Endocrinology*, *152*(8), 3268-3278. <https://doi.org/10.1210/en.2011-0153>
- Nakamura, M., Minegishi, T., Hasegawa, Y., Nakamura, K., Igarashi, S., Ito, I., Shinozaki, H., Miyamoto, K., Eto, Y., & Ibuki, Y. (1993). Effect of an activin A on follicle-stimulating hormone (FSH) receptor messenger ribonucleic acid levels and FSH receptor expressions in cultured rat granulosa cells. *Endocrinology*, *133*(2), 538-544. <https://doi.org/10.1210/endo.133.2.8393766>
- Nataraja, S., Sriraman, V., & Palmer, S. (2018). Allosteric Regulation of the Follicle-Stimulating Hormone Receptor. *Endocrinology*, *159*(7), 2704-2716. <https://doi.org/10.1210/en.2018-00317>
- Nechamen, C. A., & Dias, J. A. (2000). Human follicle stimulating hormone receptor trafficking and hormone binding sites in the amino terminus. *Mol Cell Endocrinol*, *166*(2), 101-110. [https://doi.org/10.1016/s0303-7207\(00\)00281-1](https://doi.org/10.1016/s0303-7207(00)00281-1)
- Nechamen, C. A., Thomas, R. M., Cohen, B. D., Acevedo, G., Poulikakos, P. I., Testa, J. R., & Dias, J. A. (2004). Human follicle-stimulating hormone (FSH) receptor interacts with the adaptor protein APPL1 in HEK 293 cells: potential involvement of the PI3K pathway in FSH signaling. *Biol Reprod*, *71*(2), 629-636. <https://doi.org/10.1095/biolreprod.103.025833>

- Nechamen, C. A., Thomas, R. M., & Dias, J. A. (2007). APPL1, APPL2, Akt2 and FOXO1a interact with FSHR in a potential signaling complex. *Mol Cell Endocrinol*, 260-262, 93-99. <https://doi.org/10.1016/j.mce.2006.08.014>
- Newton, C. L., Anderson, R. C., Kreuchwig, A., Krause, G., Katz, A. A., & Millar, R. P. (2021). Rescue of Function of Mutant Luteinising Hormone Receptors with Deficiencies in Cell Surface Expression, Hormone Binding, and Hormone Signalling. *Neuroendocrinology*, 111(5), 451-464. <https://doi.org/10.1159/000508000>
- Newton, C. L., Whay, A. M., McArdle, C. A., Zhang, M., van Koppen, C. J., van de Lagemaat, R., Segaloff, D. L., & Millar, R. P. (2011). Rescue of expression and signaling of human luteinizing hormone G protein-coupled receptor mutants with an allosterically binding small-molecule agonist. *Proc Natl Acad Sci U S A*, 108(17), 7172-7176. <https://doi.org/10.1073/pnas.1015723108>
- Nöth, U., Tuli, R., Seghatoleslami, R., Howard, M., Shah, A., Hall, D. J., Hickok, N. J., & Tuan, R. S. (2003). Activation of p38 and Smads mediates BMP-2 effects on human trabecular bone-derived osteoblasts. *Exp Cell Res*, 291(1), 201-211. [https://doi.org/10.1016/s0014-4827\(03\)00386-0](https://doi.org/10.1016/s0014-4827(03)00386-0)
- Nygaard, R., Zou, Y., Dror, R. O., Mildorf, T. J., Arlow, D. H., Manglik, A., Pan, A. C., Liu, C. W., Fung, J. J., Bokoch, M. P., Thian, F. S., Kobilka, T. S., Shaw, D. E., Mueller, L., Prosser, R. S., & Kobilka, B. K. (2013). The dynamic process of  $\beta(2)$ -adrenergic receptor activation. *Cell*, 152(3), 532-542. <https://doi.org/10.1016/j.cell.2013.01.008>
- Park, P. S. (2019). Rhodopsin Oligomerization and Aggregation. *J Membr Biol*, 252(4-5), 413-423. <https://doi.org/10.1007/s00232-019-00078-1>
- Pavlos, N. J., & Friedman, P. A. (2017). GPCR Signaling and Trafficking: The Long and Short of It. *Trends Endocrinol Metab*, 28(3), 213-226. <https://doi.org/10.1016/j.tem.2016.10.007>
- Periole, X., Huber, T., Marrink, S. J., & Sakmar, T. P. (2007). G protein-coupled receptors self-assemble in dynamics simulations of model bilayers. *J Am Chem Soc*, 129(33), 10126-10132. <https://doi.org/10.1021/ja0706246>
- Perono, G. A., Petrik, J. J., Thomas, P. J., & Holloway, A. C. (2022). The effects of polycyclic aromatic compounds (PACs) on mammalian ovarian function. *Curr Res Toxicol*, 3, 100070. <https://doi.org/10.1016/j.crttox.2022.100070>
- Persani, L., Rossetti, R., Di Pasquale, E., Cacciatore, C., & Fabre, S. (2014). The fundamental role of bone morphogenetic protein 15 in ovarian function and its involvement in female fertility disorders. *Hum Reprod Update*, 20(6), 869-883. <https://doi.org/10.1093/humupd/dmu036>
- Pin, J. P., Kniazeff, J., Liu, J., Binet, V., Goudet, C., Rondard, P., & Prézeau, L. (2005). Allosteric functioning of dimeric class C G-protein-coupled receptors. *FEBS J*, 272(12), 2947-2955. <https://doi.org/10.1111/j.1742-4658.2005.04728.x>
- Plant, T. M. (2015). 60 YEARS OF NEUROENDOCRINOLOGY: The hypothalamo-pituitary-gonadal axis. *J Endocrinol*, 226(2), T41-54. <https://doi.org/10.1530/JOE-15-0113>
- Ponikwicka-Tyszko, D., Chrusciel, M., Stelmaszewska, J., Bernaczyk, P., Sztachelska, M., Sidorkiewicz, I., Doroszko, M., Tomaszewski, J., Tapanainen, J. S., Huhtaniemi, I., Wolczynski, S., & Rahman, N. A. (2016). Functional Expression of FSH Receptor in Endometriotic Lesions. *J Clin Endocrinol Metab*, 101(7), 2905-2914. <https://doi.org/10.1210/jc.2016-1014>
- Prasanna, X., Sengupta, D., & Chattopadhyay, A. (2016). Cholesterol-dependent Conformational Plasticity in GPCR Dimers. *Sci Rep*, 6, 31858. <https://doi.org/10.1038/srep31858>
- Querat, B. (2021). Unconventional Actions of Glycoprotein Hormone Subunits: A Comprehensive Review. *Front Endocrinol (Lausanne)*, 12, 731966. <https://doi.org/10.3389/fendo.2021.731966>
- Rannikko, A., Pakarinen, P., Manna, P. R., Beau, I., Misrahi, M., Aittomäki, K., & Huhtaniemi, I. (2002). Functional characterization of the human FSH receptor with an inactivating Ala189Val mutation. *Mol Hum Reprod*, 8(4), 311-317. <https://doi.org/10.1093/molehr/8.4.311>
- Rasmussen, S. G., Choi, H. J., Fung, J. J., Pardon, E., Casarosa, P., Chae, P. S., Devree, B. T., Rosenbaum, D. M., Thian, F. S., Kobilka, T. S., Schnapp, A., Konetzki, I., Sunahara, R. K., Gellman, S. H., Pautsch, A., Steyaert, J., Weis, W. I., & Kobilka, B. K. (2011). Structure of a nanobody-stabilized

- active state of the  $\beta(2)$  adrenoceptor. *Nature*, 469(7329), 175-180. <https://doi.org/10.1038/nature09648>
- Reiter, E., & Lefkowitz, R. J. (2006). GRKs and beta-arrestins: roles in receptor silencing, trafficking and signaling. *Trends Endocrinol Metab*, 17(4), 159-165. <https://doi.org/10.1016/j.tem.2006.03.008>
- Remy, J. J., Nespoulous, C., Grosclaude, J., Grébert, D., Couture, L., Pajot, E., & Salesse, R. (2001). Purification and structural analysis of a soluble human choriongonadotropin hormone-receptor complex. *J Biol Chem*, 276(3), 1681-1687. <https://doi.org/10.1074/jbc.M005206200>
- Richards, J. S., & Pangas, S. A. (2010). The ovary: basic biology and clinical implications. *J Clin Invest*, 120(4), 963-972. <https://doi.org/10.1172/JCI41350>
- Rivero-Müller, A., Chou, Y. Y., Ji, I., Lajic, S., Hanyaloglu, A. C., Jonas, K., Rahman, N., Ji, T. H., & Huhtaniemi, I. (2010). Rescue of defective G protein-coupled receptor function in vivo by intermolecular cooperation. *Proc Natl Acad Sci U S A*, 107(5), 2319-2324. <https://doi.org/10.1073/pnas.0906695106>
- Rivero-Müller, A., Jonas, K. C., Hanyaloglu, A. C., & Huhtaniemi, I. (2013). Di/oligomerization of GPCRs-mechanisms and functional significance. *Prog Mol Biol Transl Sci*, 117, 163-185. <https://doi.org/10.1016/B978-0-12-386931-9.00007-6>
- Robinson, L. J., Tourkova, I., Wang, Y., Sharrow, A. C., Landau, M. S., Yaroslavskiy, B. B., Sun, L., Zaidi, M., & Blair, H. C. (2010). FSH-receptor isoforms and FSH-dependent gene transcription in human monocytes and osteoclasts. *Biochem Biophys Res Commun*, 394(1), 12-17. <https://doi.org/10.1016/j.bbrc.2010.02.112>
- Rosenbaum, D. M., Cherezov, V., Hanson, M. A., Rasmussen, S. G., Thian, F. S., Kobilka, T. S., Choi, H. J., Yao, X. J., Weis, W. I., Stevens, R. C., & Kobilka, B. K. (2007). GPCR engineering yields high-resolution structural insights into beta2-adrenergic receptor function. *Science*, 318(5854), 1266-1273. <https://doi.org/10.1126/science.1150609>
- Rovati, G. E., Capra, V., & Neubig, R. R. (2007). The highly conserved DRY motif of class A G protein-coupled receptors: beyond the ground state. *Mol Pharmacol*, 71(4), 959-964. <https://doi.org/10.1124/mol.106.029470>
- Rozell, T. G., Davis, D. P., Chai, Y., & Segaloff, D. L. (1998). Association of gonadotropin receptor precursors with the protein folding chaperone calnexin. *Endocrinology*, 139(4), 1588-1593. <https://doi.org/10.1210/endo.139.4.5881>
- Safavi, M., Nikfar, S., & Abdollahi, M. (2015). A systematic review of drugs in late-stage development for the treatment of multiple sclerosis: a focus on oral synthetic drugs. *Inflamm Allergy Drug Targets*, 13(6), 351-366. <https://doi.org/10.2174/1871528114666150529102613>
- Sairam, M. R., & Babu, P. S. (2007). The tale of follitropin receptor diversity: a recipe for fine tuning gonadal responses? *Mol Cell Endocrinol*, 260-262, 163-171. <https://doi.org/10.1016/j.mce.2005.11.052>
- Salvador, L. M., Park, Y., Cottom, J., Maizels, E. T., Jones, J. C., Schillace, R. V., Carr, D. W., Cheung, P., Allis, C. D., Jameson, J. L., & Hunzicker-Dunn, M. (2001). Follicle-stimulating hormone stimulates protein kinase A-mediated histone H3 phosphorylation and acetylation leading to select gene activation in ovarian granulosa cells. *J Biol Chem*, 276(43), 40146-40155. <https://doi.org/10.1074/jbc.M106710200>
- Sanders, J., Chirgadze, D. Y., Sanders, P., Baker, S., Sullivan, A., Bhardwaja, A., Bolton, J., Reeve, M., Nakatake, N., Evans, M., Richards, T., Powell, M., Miguel, R. N., Blundell, T. L., Furmaniak, J., & Smith, B. R. (2007). Crystal structure of the TSH receptor in complex with a thyroid-stimulating autoantibody. *Thyroid*, 17(5), 395-410. <https://doi.org/10.1089/thy.2007.0034>
- Sayers, N., & Hanyaloglu, A. C. (2018). Intracellular Follicle-Stimulating Hormone Receptor Trafficking and Signaling. *Front Endocrinol (Lausanne)*, 9, 653. <https://doi.org/10.3389/fendo.2018.00653>
- Schmidt, A., MacColl, R., Lindau-Shepard, B., Buckler, D. R., & Dias, J. A. (2001). Hormone-induced conformational change of the purified soluble hormone binding domain of follitropin receptor

- complexed with single chain follitropin. *J Biol Chem*, 276(26), 23373-23381. <https://doi.org/10.1074/jbc.M100057200>
- Schmidt, M., Dekker, F. J., & Maarsingh, H. (2013). Exchange protein directly activated by cAMP (epac): a multidomain cAMP mediator in the regulation of diverse biological functions. *Pharmacol Rev*, 65(2), 670-709. <https://doi.org/10.1124/pr.110.003707>
- Schneider, P., Walters, W. P., Plowright, A. T., Sieroka, N., Listgarten, J., Goodnow, R. A., Fisher, J., Jansen, J. M., Duca, J. S., Rush, T. S., Zentgraf, M., Hill, J. E., Krutoholow, E., Kohler, M., Blaney, J., Funatsu, K., Luebke, C., & Schneider, G. (2020). Rethinking drug design in the artificial intelligence era. *Nat Rev Drug Discov*, 19(5), 353-364. <https://doi.org/10.1038/s41573-019-0050-3>
- Sech, L. A., & Mishell, D. R. (2015). Oral steroid contraception. *Womens Health (Lond)*, 11(6), 743-748. <https://doi.org/10.2217/whe.15.82>
- Shaye, H., Ishchenko, A., Lam, J. H., Han, G. W., Xue, L., Rondard, P., Pin, J. P., Katritch, V., Gati, C., & Cherezov, V. (2020). Structural basis of the activation of a metabotropic GABA receptor. *Nature*. <https://doi.org/10.1038/s41586-020-2408-4>
- Shimada, I., Ueda, T., Kofuku, Y., Eddy, M. T., & Wüthrich, K. (2019). GPCR drug discovery: integrating solution NMR data with crystal and cryo-EM structures. *Nat Rev Drug Discov*, 18(1), 59-82. <https://doi.org/10.1038/nrd.2018.180>
- Shimizu, K., Nakamura, T., Bayasula, Nakanishi, N., Kasahara, Y., Nagai, T., Murase, T., Osuka, S., Goto, M., Iwase, A., & Kikkawa, F. (2019). Molecular mechanism of FSHR expression induced by BMP15 in human granulosa cells. *J Assist Reprod Genet*, 36(6), 1185-1194. <https://doi.org/10.1007/s10815-019-01469-y>
- Sibilia, P., Doumas, M., Gourdin, L., Briet, C., Carato, P., Rodien, P., & Munier, M. (2019). *Halogenous derivatives of Bisphenol A inhibit the human FSH receptor activity* (63)[Poster presentation].
- Silverman, E., Eimerl, S., & Orly, J. (1999). CCAAT enhancer-binding protein beta and GATA-4 binding regions within the promoter of the steroidogenic acute regulatory protein (StAR) gene are required for transcription in rat ovarian cells. *J Biol Chem*, 274(25), 17987-17996. <https://doi.org/10.1074/jbc.274.25.17987>
- Simoni, M., Gromoll, J., & Nieschlag, E. (1997). The follicle-stimulating hormone receptor: biochemistry, molecular biology, physiology, and pathophysiology. *Endocr Rev*, 18(6), 739-773. <https://doi.org/10.1210/edrv.18.6.0320>
- Simoni, M., Nieschlag, E., & Gromoll, J. (2002). Isoforms and single nucleotide polymorphisms of the FSH receptor gene: implications for human reproduction. *Hum Reprod Update*, 8(5), 413-421. <https://doi.org/10.1093/humupd/8.5.413>
- Sites, C. K., Patterson, K., Jamison, C. S., Degen, S. J., & LaBarbera, A. R. (1994). Follicle-stimulating hormone (FSH) increases FSH receptor messenger ribonucleic acid while decreasing FSH binding in cultured porcine granulosa cells. *Endocrinology*, 134(1), 411-417. <https://doi.org/10.1210/endo.134.1.8275955>
- Sitruk-Ware, R., & Nath, A. (2011). Metabolic effects of contraceptive steroids. *Rev Endocr Metab Disord*, 12(2), 63-75. <https://doi.org/10.1007/s11154-011-9182-4>
- Sleno, R., & Hébert, T. E. (2018). The Dynamics of GPCR Oligomerization and Their Functional Consequences. *Int Rev Cell Mol Biol*, 338, 141-171. <https://doi.org/10.1016/bs.ircmb.2018.02.005>
- Smits, G., Campillo, M., Govaerts, C., Janssens, V., Richter, C., Vassart, G., Pardo, L., & Costagliola, S. (2003). Glycoprotein hormone receptors: determinants in leucine-rich repeats responsible for ligand specificity. *EMBO J*, 22(11), 2692-2703. <https://doi.org/10.1093/emboj/cdg260>
- Son, W. Y., Das, M., Shalom-Paz, E., & Holzer, H. (2011). Mechanisms of follicle selection and development. *Minerva Ginecol*, 63(2), 89-102. <https://www.ncbi.nlm.nih.gov/pubmed/21508900>

- Song, K., Dai, L., Long, X., Wang, W., & Di, W. (2020). Follicle-stimulating hormone promotes the proliferation of epithelial ovarian cancer cells by activating sphingosine kinase. *Sci Rep*, *10*(1), 13834. <https://doi.org/10.1038/s41598-020-70896-0>
- Soto-Velasquez, M., Hayes, M. P., Alpsy, A., Dykhuizen, E. C., & Watts, V. J. (2018). A Novel CRISPR/Cas9-Based Cellular Model to Explore Adenylyl Cyclase and cAMP Signaling. *Mol Pharmacol*, *94*(3), 963-972. <https://doi.org/10.1124/mol.118.111849>
- Soudan, B., & Pigny, P. (2017). LH and FSH isoforms: clinical and therapeutical significance.
- Sposini, S., De Pascali, F., Richardson, R., Sayers, N. S., Perrais, D., Yu, H. N., Palmer, S., Nataraja, S., Reiter, E., & Hanyaloglu, A. C. (2020). Pharmacological Programming of Endosomal Signaling Activated by Small Molecule Ligands of the Follicle Stimulating Hormone Receptor. *Front Pharmacol*, *11*, 593492. <https://doi.org/10.3389/fphar.2020.593492>
- Sposini, S., Jean-Alphonse, F. G., Ayoub, M. A., Oqua, A., West, C., Lavery, S., Brosens, J. J., Reiter, E., & Hanyaloglu, A. C. (2017). Integration of GPCR Signaling and Sorting from Very Early Endosomes via Opposing APPL1 Mechanisms. *Cell Rep*, *21*(10), 2855-2867. <https://doi.org/10.1016/j.celrep.2017.11.023>
- Sriraman, V., Denis, D., de Matos, D., Yu, H., Palmer, S., & Nataraja, S. (2014). Investigation of a thiazolidinone derivative as an allosteric modulator of follicle stimulating hormone receptor: evidence for its ability to support follicular development and ovulation. *Biochem Pharmacol*, *89*(2), 266-275. <https://doi.org/10.1016/j.bcp.2014.02.023>
- Stelmaszewska, J., Chrusciel, M., Doroszko, M., Akerfelt, M., Ponikwicka-Tyszko, D., Nees, M., Frentsch, M., Li, X., Kero, J., Huhtaniemi, I., Wolczynski, S., & Rahman, N. A. (2016). Revisiting the expression and function of follicle-stimulation hormone receptor in human umbilical vein endothelial cells. *Sci Rep*, *6*, 37095. <https://doi.org/10.1038/srep37095>
- Stevens, R. C., Cherezov, V., Katritch, V., Abagyan, R., Kuhn, P., Rosen, H., & Wüthrich, K. (2013). The GPCR Network: a large-scale collaboration to determine human GPCR structure and function. *Nat Rev Drug Discov*, *12*(1), 25-34. <https://doi.org/10.1038/nrd3859>
- Stilley, J. A., Guan, R., Duffy, D. M., & Segaloff, D. L. (2014). Signaling through FSH receptors on human umbilical vein endothelial cells promotes angiogenesis. *J Clin Endocrinol Metab*, *99*(5), E813-820. <https://doi.org/10.1210/jc.2013-3186>
- Stilley, J. A. W., & Segaloff, D. L. (2018). FSH Actions and Pregnancy: Looking Beyond Ovarian FSH Receptors. *Endocrinology*, *159*(12), 4033-4042. <https://doi.org/10.1210/en.2018-00497>
- Stocco, D. M. (2000). The role of the StAR protein in steroidogenesis: challenges for the future. *J Endocrinol*, *164*(3), 247-253. <https://doi.org/10.1677/joe.0.1640247>
- Sun, G. W., Kobayashi, H., Suzuki, M., Kanayama, N., & Terao, T. (2003). Follicle-stimulating hormone and insulin-like growth factor I synergistically induce up-regulation of cartilage link protein (Crtl1) via activation of phosphatidylinositol-dependent kinase/Akt in rat granulosa cells. *Endocrinology*, *144*(3), 793-801. <https://doi.org/10.1210/en.2002-220900>
- Sun, L., Peng, Y., Sharrow, A. C., Iqbal, J., Zhang, Z., Papachristou, D. J., Zaidi, S., Zhu, L. L., Yaroslavskiy, B. B., Zhou, H., Zallone, A., Sairam, M. R., Kumar, T. R., Bo, W., Braun, J., Cardoso-Landa, L., Schaffler, M. B., Moonga, B. S., Blair, H. C., & Zaidi, M. (2006). FSH directly regulates bone mass. *Cell*, *125*(2), 247-260. <https://doi.org/10.1016/j.cell.2006.01.051>
- Syrovatkina, V., Alegre, K. O., Dey, R., & Huang, X. Y. (2016). Regulation, Signaling, and Physiological Functions of G-Proteins. *J Mol Biol*, *428*(19), 3850-3868. <https://doi.org/10.1016/j.jmb.2016.08.002>
- Szkudlinski, M. W., Fremont, V., Ronin, C., & Weintraub, B. D. (2002). Thyroid-stimulating hormone and thyroid-stimulating hormone receptor structure-function relationships. *Physiol Rev*, *82*(2), 473-502. <https://doi.org/10.1152/physrev.00031.2001>
- Tabor, A., Weisenburger, S., Banerjee, A., Purkayastha, N., Kaindl, J. M., Hübner, H., Wei, L., Grömer, T. W., Kornhuber, J., Tschammer, N., Birdsall, N. J., Mashanov, G. I., Sandoghdar, V., & Gmeiner, P. (2016). Visualization and ligand-induced modulation of dopamine receptor

- dimerization at the single molecule level. *Sci Rep*, 6, 33233. <https://doi.org/10.1038/srep33233>
- Tanaka, K. A., Suzuki, K. G., Shirai, Y. M., Shibutani, S. T., Miyahara, M. S., Tsuboi, H., Yahara, M., Yoshimura, A., Mayor, S., Fujiwara, T. K., & Kusumi, A. (2010). Membrane molecules mobile even after chemical fixation. *Nat Methods*, 7(11), 865-866. <https://doi.org/10.1038/nmeth.f.314>
- Tano, M., Minegishi, T., Nakamura, K., Nakamura, M., Karino, S., Miyamoto, K., & Ibuki, Y. (1995). Regulation of follistatin messenger ribonucleic acid in cultured rat granulosa cells. *Mol Cell Endocrinol*, 109(2), 167-174. [https://doi.org/10.1016/0303-7207\(95\)03499-w](https://doi.org/10.1016/0303-7207(95)03499-w)
- Tao, Y. X., & Segaloff, D. L. (2009). Follicle stimulating hormone receptor mutations and reproductive disorders. *Prog Mol Biol Transl Sci*, 89, 115-131. [https://doi.org/10.1016/S1877-1173\(09\)89005-4](https://doi.org/10.1016/S1877-1173(09)89005-4)
- Tapanainen, J. S., Vaskivuo, T., Aittomäki, K., & Huhtaniemi, I. T. (1998). Inactivating FSH receptor mutations and gonadal dysfunction. *Mol Cell Endocrinol*, 145(1-2), 129-135. <https://www.ncbi.nlm.nih.gov/pubmed/9922109>
- Terrillon, S., & Bouvier, M. (2004). Receptor activity-independent recruitment of betaarrestin2 reveals specific signalling modes. *EMBO J*, 23(20), 3950-3961. <https://doi.org/10.1038/sj.emboj.7600387>
- Thackray, V. G., Mellon, P. L., & Coss, D. (2010). Hormones in synergy: regulation of the pituitary gonadotropin genes. *Mol Cell Endocrinol*, 314(2), 192-203. <https://doi.org/10.1016/j.mce.2009.09.003>
- Thomas, R. M., Nechamen, C. A., Mazurkiewicz, J. E., Muda, M., Palmer, S., & Dias, J. A. (2007). Follicle-stimulating hormone receptor forms oligomers and shows evidence of carboxyl-terminal proteolytic processing. *Endocrinology*, 148(5), 1987-1995. <https://doi.org/10.1210/en.2006-1672>
- Thomas, R. M., Nechamen, C. A., Mazurkiewicz, J. E., Ulloa-Aguirre, A., & Dias, J. A. (2011). The adapter protein APPL1 links FSH receptor to inositol 1,4,5-trisphosphate production and is implicated in intracellular Ca(2+) mobilization. *Endocrinology*, 152(4), 1691-1701. <https://doi.org/10.1210/en.2010-1353>
- Timossi, C., Damian-Matsumura, P., Dominguez-Gonzalez, A., & Ulloa-Aguirre, A. (1998). A less acidic human follicle-stimulating hormone preparation induces tissue-type plasminogen activator enzyme activity earlier than a predominantly acidic analogue in phenobarbital-blocked pro-oestrous rats. *Mol Hum Reprod*, 4(11), 1032-1038.
- Timossi, C., Ortiz-Elizondo, C., Pineda, D. B., Dias, J. A., Conn, P. M., & Ulloa-Aguirre, A. (2004). Functional significance of the BBXXB motif reversed present in the cytoplasmic domains of the human follicle-stimulating hormone receptor. *Mol Cell Endocrinol*, 223(1-2), 17-26. <https://doi.org/10.1016/j.mce.2004.06.004>
- Timossi, C. M., Barrios-de-Tomasi, J., González-Suárez, R., Arranz, M. C., Padmanabhan, V., Conn, P. M., & Ulloa-Aguirre, A. (2000). Differential effects of the charge variants of human follicle-stimulating hormone. *J Endocrinol*, 165(2), 193-205. <https://doi.org/10.1677/joe.0.1650193>
- Tranchant, T., Durand, G., Gauthier, C., Crépieux, P., Ulloa-Aguirre, A., Royère, D., & Reiter, E. (2011). Preferential  $\beta$ -arrestin signalling at low receptor density revealed by functional characterization of the human FSH receptor A189 V mutation. *Mol Cell Endocrinol*, 331(1), 109-118. <https://doi.org/10.1016/j.mce.2010.08.016>
- Troispoux, C., Guillou, F., Elalouf, J. M., Firsov, D., Iacovelli, L., De Blasi, A., Combarnous, Y., & Reiter, E. (1999). Involvement of G protein-coupled receptor kinases and arrestins in desensitization to follicle-stimulating hormone action. *Mol Endocrinol*, 13(9), 1599-1614. <https://doi.org/10.1210/mend.13.9.0342>
- Ulloa-Aguirre, A., Dias, J. A., Bousfield, G., Huhtaniemi, I., & Reiter, E. (2013). Trafficking of the follitropin receptor. *Methods Enzymol*, 521, 17-45. <https://doi.org/10.1016/B978-0-12-391862-8.00002-8>

- Ulloa-Aguirre, A., Mejia, J. J., Dominguez, R., Guevara-Aguirre, J., Diaz-Sánchez, V., & Larrea, F. (1986). Microheterogeneity of anterior pituitary FSH in the male rat: isoelectric focusing pattern throughout sexual maturation. *J Endocrinol*, *110*(3), 539-549. <https://doi.org/10.1677/joe.0.1100539>
- Ulloa-Aguirre, A., Midgley, A. R., Beitins, I. Z., & Padmanabhan, V. (1995). Follicle-stimulating isohormones: characterization and physiological relevance. *Endocr Rev*, *16*(6), 765-787. <https://doi.org/10.1210/edrv-16-6-765>
- Ulloa-Aguirre, A., Reiter, E., & Crépieux, P. (2018). FSH Receptor Signaling: Complexity of Interactions and Signal Diversity. *Endocrinology*, *159*(8), 3020-3035. <https://doi.org/10.1210/en.2018-00452>
- Ulloa-Aguirre, A., Timossi, C., Damian-Matsumura, P., & Dias, J. A. (1999). Role of glycosylation in function of follicle-stimulating hormone. *Endocrine*, *11*(3), 205-215. <https://doi.org/10.1385/endo:11:3:205>
- Ulloa-Aguirre, A., Zariñán, T., Jardón-Valadez, E., Gutiérrez-Sagal, R., & Dias, J. A. (2018). Structure-Function Relationships of the Follicle-Stimulating Hormone Receptor. *Front Endocrinol (Lausanne)*, *9*, 707. <https://doi.org/10.3389/fendo.2018.00707>
- Uribe, A., Zariñán, T., Pérez-Solis, M. A., Gutiérrez-Sagal, R., Jardón-Valadez, E., Piñeiro, A., Dias, J. A., & Ulloa-Aguirre, A. (2008). Functional and structural roles of conserved cysteine residues in the carboxyl-terminal domain of the follicle-stimulating hormone receptor in human embryonic kidney 293 cells. *Biol Reprod*, *78*(5), 869-882. <https://doi.org/10.1095/biolreprod.107.063925>
- Urizar, E., Montanelli, L., Loy, T., Bonomi, M., Swillens, S., Gales, C., Bouvier, M., Smits, G., Vassart, G., & Costagliola, S. (2005). Glycoprotein hormone receptors: link between receptor homodimerization and negative cooperativity. *EMBO J*, *24*(11), 1954-1964. <https://doi.org/10.1038/sj.emboj.7600686>
- van Straten, N. C., van Berkel, T. H., Demont, D. R., Karstens, W. J., Merckx, R., Oosterom, J., Schulz, J., van Someren, R. G., Timmers, C. M., & van Zandvoort, P. M. (2005). Identification of substituted 6-amino-4-phenyltetrahydroquinoline derivatives: potent antagonists for the follicle-stimulating hormone receptor. *J Med Chem*, *48*(6), 1697-1700. <https://doi.org/10.1021/jm049676l>
- van Zuylen, C. W., Kamerling, J. P., & Vliegthart, J. F. (1997). Glycosylation beyond the Asn78-linked GlcNAc residue has a significant enhancing effect on the stability of the alpha subunit of human chorionic gonadotropin. *Biochem Biophys Res Commun*, *232*(1), 117-120. <https://doi.org/10.1006/bbrc.1997.6241>
- Vassart, G., Pardo, L., & Costagliola, S. (2004). A molecular dissection of the glycoprotein hormone receptors. *Trends Biochem Sci*, *29*(3), 119-126. <https://doi.org/10.1016/j.tibs.2004.01.006>
- Venkatakrishnan, A. J., Deupi, X., Lebon, G., Tate, C. G., Schertler, G. F., & Babu, M. M. (2013). Molecular signatures of G-protein-coupled receptors. *Nature*, *494*(7436), 185-194. <https://doi.org/10.1038/nature11896>
- Venter, J. C., Adams, M. D., Myers, E. W., Li, P. W., Mural, R. J., Sutton, G. G., Smith, H. O., Yandell, M., Evans, C. A., Holt, R. A., Gocayne, J. D., Amanatides, P., Ballew, R. M., Huson, D. H., Wortman, J. R., Zhang, Q., Kodira, C. D., Zheng, X. H., Chen, L., . . . Zhu, X. (2001). The sequence of the human genome. *Science*, *291*(5507), 1304-1351. <https://doi.org/10.1126/science.1058040>
- Verma, A., & Saraf, S. K. (2008). 4-thiazolidinone--a biologically active scaffold. *Eur J Med Chem*, *43*(5), 897-905. <https://doi.org/10.1016/j.ejmech.2007.07.017>
- Villardaga, J. P., Jean-Alphonse, F. G., & Gardella, T. J. (2014). Endosomal generation of cAMP in GPCR signaling. *Nat Chem Biol*, *10*(9), 700-706. <https://doi.org/10.1038/nchembio.1611>
- Vogel, R., Mahalingam, M., Lüdeke, S., Huber, T., Siebert, F., & Sakmar, T. P. (2008). Functional role of the "ionic lock"--an interhelical hydrogen-bond network in family A heptahelical receptors. *J Mol Biol*, *380*(4), 648-655. <https://doi.org/10.1016/j.jmb.2008.05.022>



- von Beek, C., Alriksson, L., Palle, J., Gustafson, A. M., Grujic, M., Melo, F. R., Sellin, M. E., & Pejler, G. (2021). Dynamin inhibition causes context-dependent cell death of leukemia and lymphoma cells. *PLoS One*, *16*(9), e0256708. <https://doi.org/10.1371/journal.pone.0256708>
- Wang, C., Prossnitz, E. R., & Roy, S. K. (2007). Expression of G protein-coupled receptor 30 in the hamster ovary: differential regulation by gonadotropins and steroid hormones. *Endocrinology*, *148*(10), 4853-4864. <https://doi.org/10.1210/en.2007-0727>
- Wang, F. I., Ding, G., Ng, G. S., Dixon, S. J., & Chidiac, P. (2022). Luciferase-based GloSensor™ cAMP assay: Temperature optimization and application to cell-based kinetic studies. *Methods*, *203*, 249-258. <https://doi.org/10.1016/j.ymeth.2021.10.009>
- Wang, H., Butnev, V., Bousfield, G. R., & Kumar, T. R. (2016a). A human FSHB transgene encoding the double N-glycosylation mutant (Asn(7Δ) Asn(24Δ)) FSHβ subunit fails to rescue Fshb null mice. *Mol Cell Endocrinol*, *426*, 113-124. <https://doi.org/10.1016/j.mce.2016.02.015>
- Wang, H., May, J., Butnev, V., Shuai, B., May, J. V., Bousfield, G. R., & Kumar, T. R. (2016b). Evaluation of in vivo bioactivities of recombinant hypo- (FSH. *Mol Cell Endocrinol*, *437*, 224-236. <https://doi.org/10.1016/j.mce.2016.08.031>
- Wayne, C. M., Fan, H. Y., Cheng, X., & Richards, J. S. (2007). Follicle-stimulating hormone induces multiple signaling cascades: evidence that activation of Rous sarcoma oncogene, RAS, and the epidermal growth factor receptor are critical for granulosa cell differentiation. *Mol Endocrinol*, *21*(8), 1940-1957. <https://doi.org/10.1210/me.2007-0020>
- Wehbi, V., Tranchant, T., Durand, G., Musnier, A., Decourtye, J., Piketty, V., Butnev, V. Y., Bousfield, G. R., Crépieux, P., Maurel, M. C., & Reiter, E. (2010). Partially deglycosylated equine LH preferentially activates beta-arrestin-dependent signaling at the follicle-stimulating hormone receptor. *Mol Endocrinol*, *24*(3), 561-573. <https://doi.org/10.1210/me.2009-0347>
- Wettschureck, N., & Offermanns, S. (2005). Mammalian G proteins and their cell type specific functions. *Physiol Rev*, *85*(4), 1159-1204. <https://doi.org/10.1152/physrev.00003.2005>
- Wide, L. (1989). Follicle-stimulating hormones in anterior pituitary glands from children and adults differ in relation to sex and age. *J Endocrinol*, *123*(3), 519-529. <https://doi.org/10.1677/joe.0.1230519>
- Wide, L., & Eriksson, K. (2013). Dynamic changes in glycosylation and glycan composition of serum FSH and LH during natural ovarian stimulation. *Ups J Med Sci*, *118*(3), 153-164. <https://doi.org/10.3109/03009734.2013.782081>
- Wide, L., & Eriksson, K. (2018). Low-glycosylated forms of both FSH and LH play major roles in the natural ovarian stimulation. *Ups J Med Sci*, *123*(2), 100-108. <https://doi.org/10.1080/03009734.2018.1467983>
- Wide, L., & Naessén, T. (1994). 17 beta-oestradiol counteracts the formation of the more acidic isoforms of follicle-stimulating hormone and luteinizing hormone after menopause. *Clin Endocrinol (Oxf)*, *40*(6), 783-789. <https://doi.org/10.1111/j.1365-2265.1994.tb02513.x>
- Wiedemar, N., Hauser, D. A., & Mäser, P. (2020). 100 Years of Suramin. *Antimicrob Agents Chemother*, *64*(3). <https://doi.org/10.1128/AAC.01168-19>
- Windham, G. C., Lee, D., Mitchell, P., Anderson, M., Petreas, M., & Lasley, B. (2005). Exposure to organochlorine compounds and effects on ovarian function. *Epidemiology*, *16*(2), 182-190. <https://doi.org/10.1097/01.ede.0000152527.24339.17>
- Wrobel, J., Jetter, J., Kao, W., Rogers, J., Di, L., Chi, J., Pérez, M. C., Chen, G. C., & Shen, E. S. (2006). 5-Alkylated thiazolidinones as follicle-stimulating hormone (FSH) receptor agonists. *Bioorg Med Chem*, *14*(16), 5729-5741. <https://doi.org/10.1016/j.bmc.2006.04.012>
- Wu, X., Spiro, C., Owen, W. G., & McMurray, C. T. (1998). cAMP response element-binding protein monomers cooperatively assemble to form dimers on DNA. *J Biol Chem*, *273*(33), 20820-20827. <https://doi.org/10.1074/jbc.273.33.20820>
- Xing, W., & Sairam, M. R. (2001). Characterization of regulatory elements of ovine follicle-stimulating hormone (FSH) receptor gene: the role of E-box in the regulation of ovine FSH receptor expression. *Biol Reprod*, *64*(2), 579-589. <https://doi.org/10.1095/biolreprod64.2.579>

- Xing, Y., Myers, R. V., Cao, D., Lin, W., Jiang, M., Bernard, M. P., & Moyle, W. R. (2004). Glycoprotein hormone assembly in the endoplasmic reticulum: III. The seatbelt and its latch site determine the assembly pathway. *J Biol Chem*, 279(34), 35449-35457. <https://doi.org/10.1074/jbc.M403054200>
- Xiong, J., Kang, S. S., Wang, Z., Liu, X., Kuo, T. C., Korkmaz, F., Padilla, A., Miyashita, S., Chan, P., Zhang, Z., Katsel, P., Burgess, J., Gumerova, A., Ilevleva, K., Sant, D., Yu, S. P., Muradova, V., Frolinger, T., Lizneva, D., . . . Ye, K. (2022). FSH blockade improves cognition in mice with Alzheimer's disease. *Nature*, 603(7901), 470-476. <https://doi.org/10.1038/s41586-022-04463-0>
- Xu, C., Chen, J. A., Qiu, Z., Zhao, Q., Luo, J., Yang, L., Zeng, H., Huang, Y., Zhang, L., Cao, J., & Shu, W. (2010). Ovotoxicity and PPAR-mediated aromatase downregulation in female Sprague-Dawley rats following combined oral exposure to benzo[a]pyrene and di-(2-ethylhexyl) phthalate. *Toxicol Lett*, 199(3), 323-332. <https://doi.org/10.1016/j.toxlet.2010.09.015>
- Yang, J., Gong, Z., Lu, Y. B., Xu, C. J., Wei, T. F., Yang, M. S., Zhan, T. W., Yang, Y. H., Lin, L., Liu, J., Tang, C., & Zhang, W. P. (2020). FLIM-FRET-Based Structural Characterization of a Class-A GPCR Dimer in the Cell Membrane. *J Mol Biol*. <https://doi.org/10.1016/j.jmb.2020.06.009>
- Yanofsky, S. D., Shen, E. S., Holden, F., Whitehorn, E., Aguilar, B., Tate, E., Holmes, C. P., Scheuerman, R., MacLean, D., Wu, M. M., Frail, D. E., López, F. J., Winneker, R., Arey, B. J., & Barrett, R. W. (2006). Allosteric activation of the follicle-stimulating hormone (FSH) receptor by selective, nonpeptide agonists. *J Biol Chem*, 281(19), 13226-13233. <https://doi.org/10.1074/jbc.M600601200>
- Yding Andersen, C. (2002). Effect of FSH and its different isoforms on maturation of oocytes from pre-ovulatory follicles. *Reprod Biomed Online*, 5(3), 232-239. [https://doi.org/10.1016/s1472-6483\(10\)61826-3](https://doi.org/10.1016/s1472-6483(10)61826-3)
- Ye, L., Van Eps, N., Zimmer, M., Ernst, O. P., & Prosser, R. S. (2016). Activation of the A2A adenosine G-protein-coupled receptor by conformational selection. *Nature*, 533(7602), 265-268. <https://doi.org/10.1038/nature17668>
- Zariñán, T., Butnev, V. Y., Gutiérrez-Sagal, R., Maravillas-Montero, J. L., Martínez-Luis, I., Mejía-Domínguez, N. R., Juárez-Vega, G., Bousfield, G. R., & Ulloa-Aguirre, A. (2020). In Vitro Impact of FSH Glycosylation Variants on FSH Receptor-stimulated Signal Transduction and Functional Selectivity. *J Endocr Soc*, 4(5), bvaa019. <https://doi.org/10.1210/jendso/bvaa019>
- Zariñán, T., Perez-Solís, M. A., Maya-Núñez, G., Casas-González, P., Conn, P. M., Dias, J. A., & Ulloa-Aguirre, A. (2010). Dominant negative effects of human follicle-stimulating hormone receptor expression-deficient mutants on wild-type receptor cell surface expression. Rescue of oligomerization-dependent defective receptor expression by using cognate decoys. *Mol Cell Endocrinol*, 321(2), 112-122. <https://doi.org/10.1016/j.mce.2010.02.027>
- Zeleznik, A. J. (2004). The physiology of follicle selection. *Reprod Biol Endocrinol*, 2, 31. <https://doi.org/10.1186/1477-7827-2-31>
- Zhang, T., Cao, L. H., Kumar, S., Enemchukwu, N. O., Zhang, N., Lambert, A., Zhao, X., Jones, A., Wang, S., Dennis, E. M., Fnu, A., Ham, S., Rainier, J., Yau, K. W., & Fu, Y. (2016). Dimerization of visual pigments in vivo. *Proc Natl Acad Sci U S A*, 113(32), 9093-9098. <https://doi.org/10.1073/pnas.1609018113>
- Zhao, D. Y., Pöge, M., Morizumi, T., Gulati, S., Van Eps, N., Zhang, J., Miszta, P., Filipek, S., Mahamid, J., Plitzko, J. M., Baumeister, W., Ernst, O. P., & Palczewski, K. (2019). Cryo-EM structure of the native rhodopsin dimer in nanodiscs. *J Biol Chem*, 294(39), 14215-14230. <https://doi.org/10.1074/jbc.RA119.010089>
- Zhu, L. L., Blair, H., Cao, J., Yuen, T., Latif, R., Guo, L., Tourkova, I. L., Li, J., Davies, T. F., Sun, L., Bian, Z., Rosen, C., Zallone, A., New, M. I., & Zaidi, M. (2012). Blocking antibody to the  $\beta$ -subunit of FSH prevents bone loss by inhibiting bone resorption and stimulating bone synthesis. *Proc Natl Acad Sci U S A*, 109(36), 14574-14579. <https://doi.org/10.1073/pnas.1212806109>

## **9 Appendix I**

A. Volume of 0.1% (v/v) gelatine

Size of TC well/dish	Volume per TC well/dish
96-well plate	100µl
12-well plate	1ml
6-well plate	2ml
10cm dish	15ml

B. Transient transfection mix

Reagent/Solution	Volume/amount per well (6-well plate)		Volume/amount per well (10cm dish)	
	Tube 1	Tube 2	Tube 1	Tube 2
Opti-MEM™	250µl	250µl	1.5ml	1.5ml
Lipofectamine 2000™	8µl	-	60µl	-
HA-FSHR plasmid DNA	-	3µg	-	24µg
GloSensor™-20F plasmid DNA	-	1.02µg	-	-
Cre-luciferase plasmid DNA	-	800ng	-	-
<i>Renilla</i> -luciferase plasmid DNA	-	150ng	-	-
siRNA APPL1	-	0.8µM	-	-

### C. Antibodies

<b>Antibody</b>	<b>Species</b>	<b>Stock concentration</b>	<b>Final assay concentration (Dilution)</b>	<b>Product code</b>	<b>Product code/ Manufacturer</b>
HA.11-CAGE™ 552	Mouse	445nM	1.78nM (1:250)	-	BioLegend®  London, UK
Phospho- ERK1/2	Mouse	1mg/ml	1µg/ml (1:1000)	89967	Cell Signalling Technology  London, England
Total- ERK	Mouse	251µg/ml	251ng/ml (1:1000)	4696	Cell Signalling Technology  London, England
Phospho- CREB	Rabbit	58µg/ml	58ng/ml (1:1000)	9198S	Cell Signalling Technology London, England
Total- CREB	Rabbit	114µg/ml	114ng/ml (1:1000)	9197S	Cell Signalling Technology London, England
β-tubulin	Mouse	25µg/ml	25ng/ml (1:1000)	86298	Cell Signalling Technology London, England
FLAG, M1	Mouse	4.0mg/ml	8.0µg.ml (1:500)	F3040	Sigma Darmstadt, Germany
EEA1	Rabbit	44µg/ml	88ng/ml (1:500)	3288	Cell Signalling Technology London, England
Anti- mouse HRP	Goat	1.0g/L	100ng/ml (1:10,000)	P0447	DAKO London, England

secondary antibody					
Anti-rabbit HRP secondary antibody	Goat	0.25g/L	25ng/ml (1:10,000)	P0448	DAKO London, England
Anti-mouse AlexFluor 488 secondary antibody	Goat	2mg/ml	2µg/ml (1:1000)	A-11001	Thermo Fisher Scientific Dartford, England
Anti-rabbit AlexFluor 555 secondary antibody	Goat	2mg/ml	2µg/ml (1:1000)	A-21428	Thermo Fisher Scientific Dartford, England

#### D. 1X Lysis buffer

Reagent/Solution	Amount per 1ml
10X RIPA buffer	100µl
100X Phosphatase inhibitor	10µl
25X Protease inhibitor	40µl
Distilled H <sub>2</sub> O	850µl

#### E. 1X Loading dye

Reagent/Solution	Amount per 50µl
4X LDS sample buffer	45µl
10X Bolt™ sample reducing agent	5µl

F. Polyacrylamide gel

<b>Reagent/Solution</b>	<b>Amount per 10% resolving gel</b>	<b>Amount per 4% stacking gel</b>
Distilled H <sub>2</sub> O	3.3ml	3.1ml
30% (w/v) Protogel <sup>®</sup>	2.8ml	650μl
1.5M Tris-HCl (pH 8.4)	2.1ml	-
0.5M Tris-HCl (pH 6.8)	-	1.25ml
10% (w/v) SDS	83.3μl	50μl
10% (w/v) 2-acrylamido-2-methylpropane sulfonic acid	83.3μl	31.3μl
TEMED	3.3μl	6.25μl

G. 1X TBST

<b>Reagent/Solution</b>	<b>Amount per 1 litre</b>
10X TBS	100ml
Tween <sup>®</sup> 20	1ml
Distilled H <sub>2</sub> O	899ml

#### H. 1X Stripping buffer

<b>Reagent/Solution</b>	<b>Amount per 50ml</b>
1M Tris-HCl (pH 6.8)	3.125ml
2-mercaptoethanol	350µl
20% (w/v) SDS	5ml
Distilled H <sub>2</sub> O	41.525ml



**10 Appendix II**

Sea Blue Plus 2 protein greyscale protein ladder.

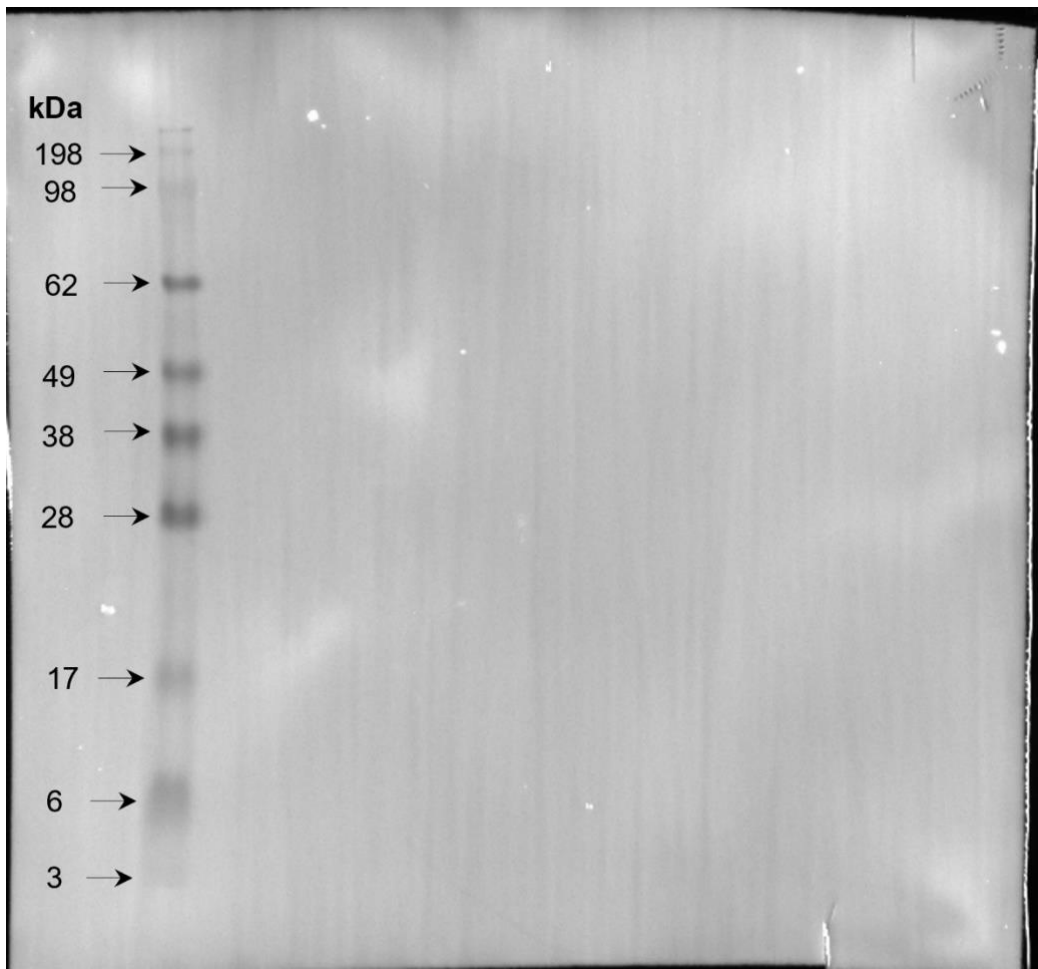


Figure 3.10, a: Uncropped blots following FSH21/18 and FSH24 treatment.

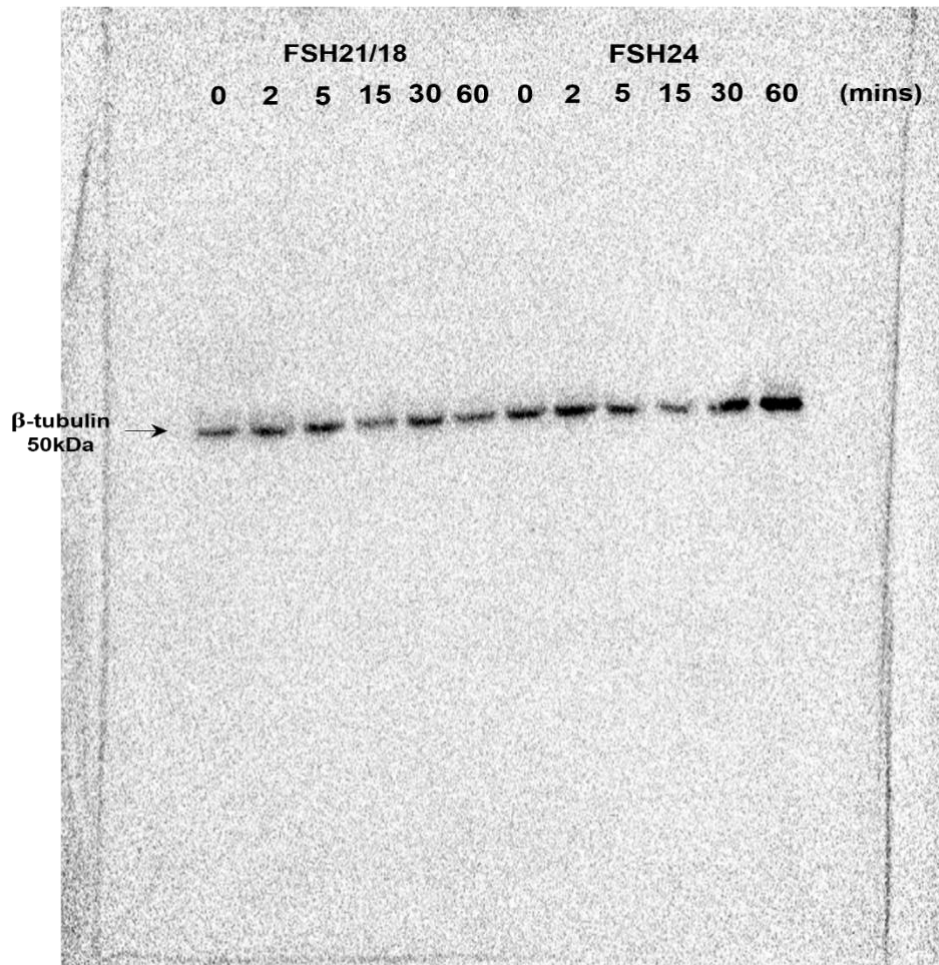
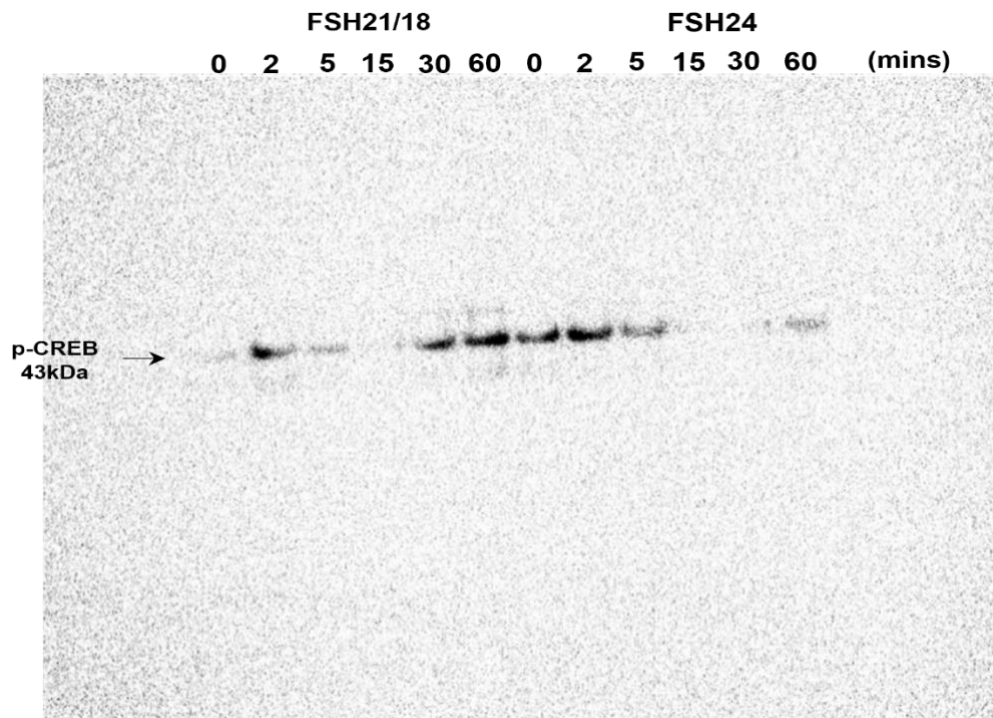


Figure 3.12, a: Uncropped blots following FSH21/18 and FSH24 treatment.

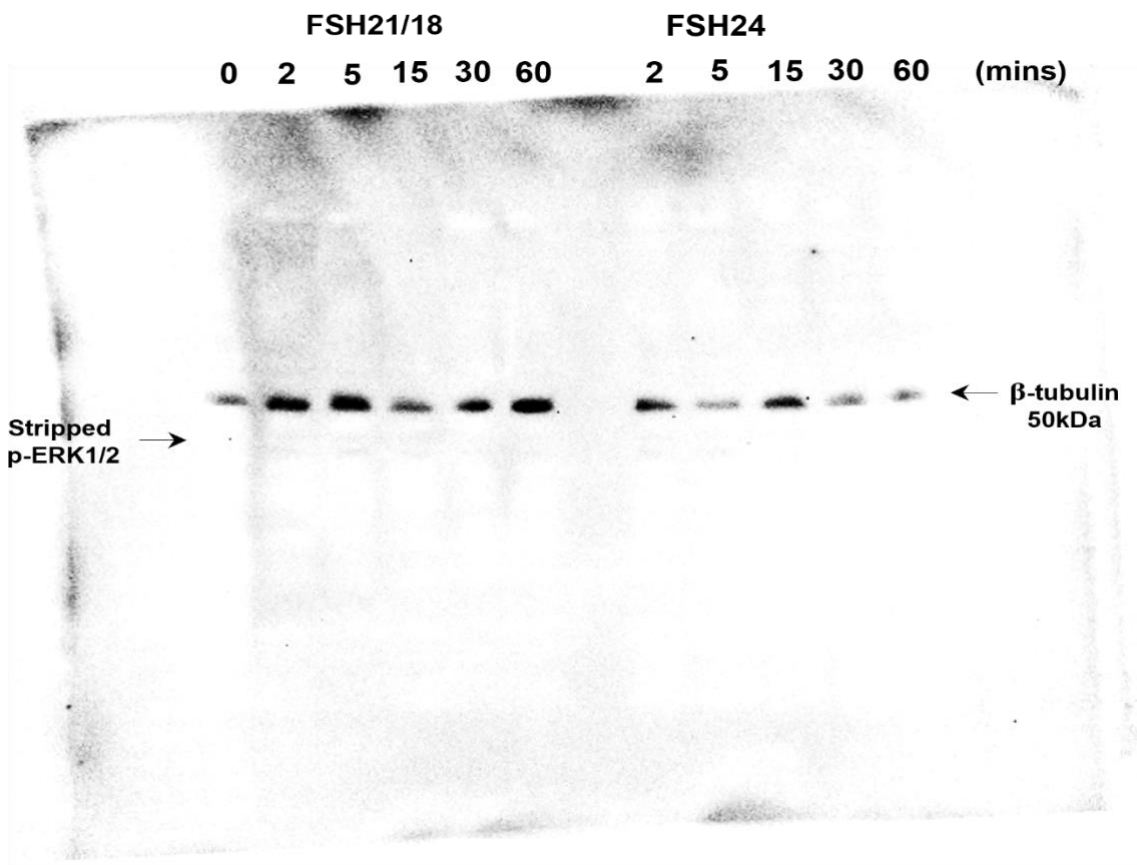
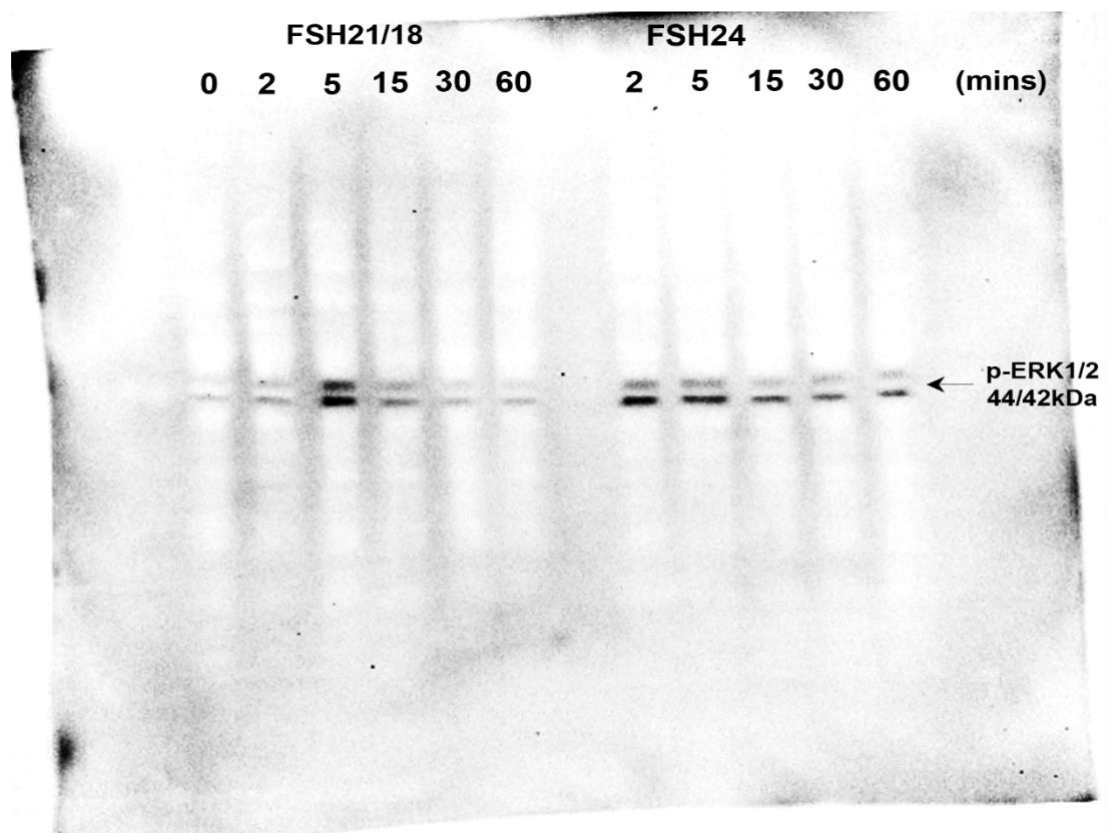
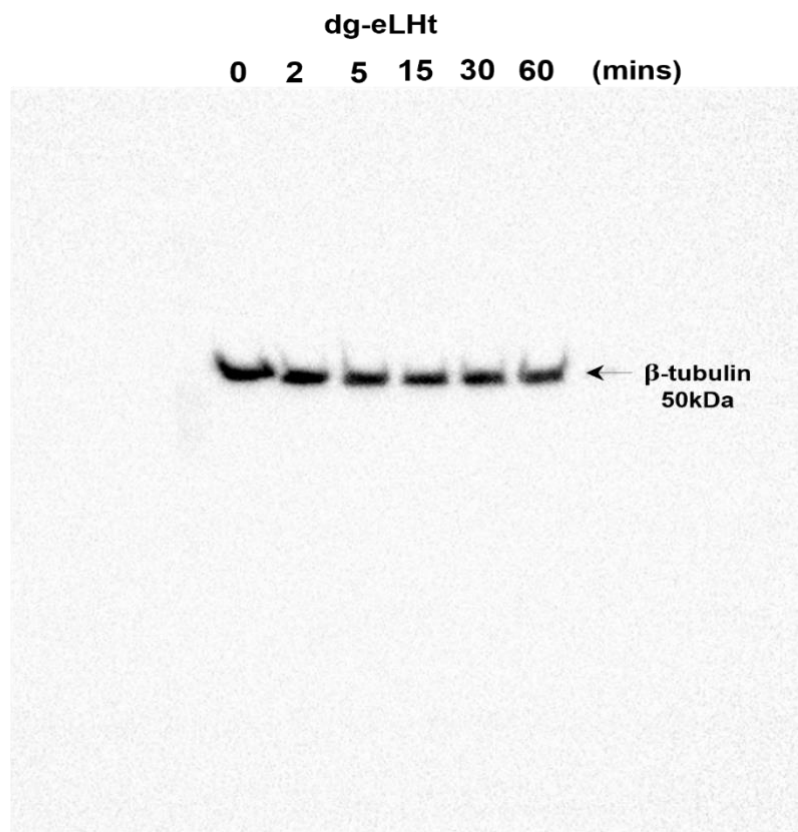
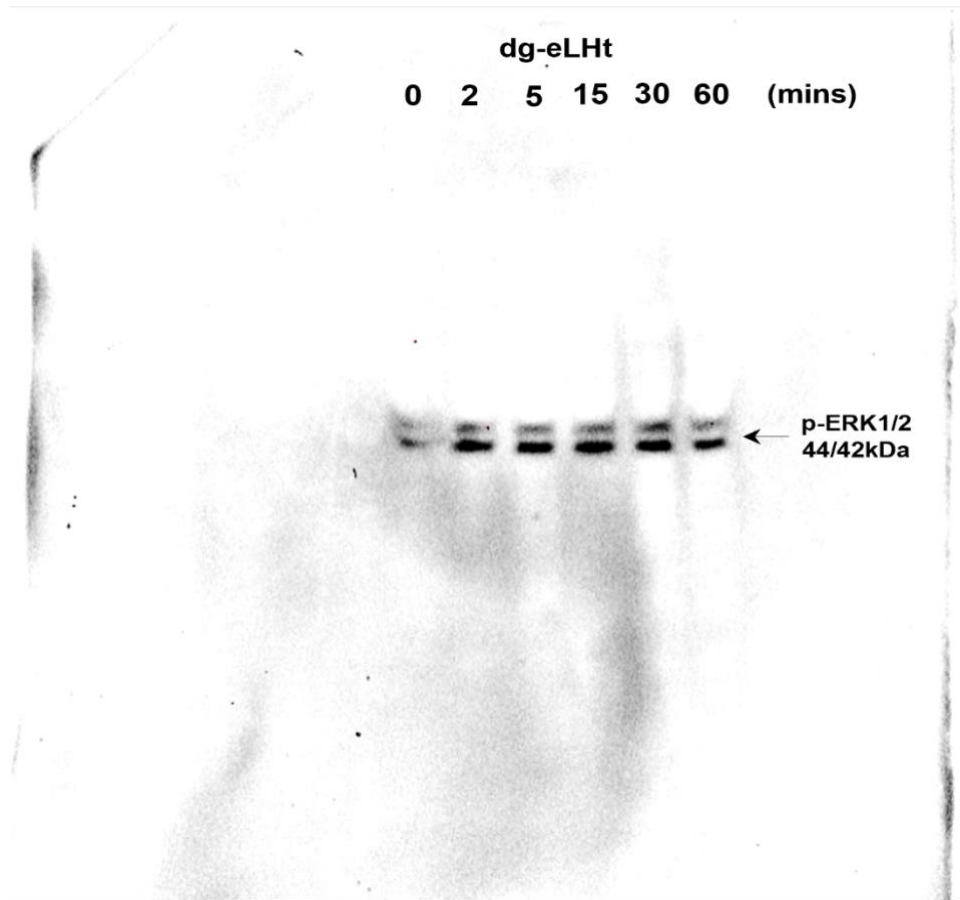


Figure 3.12, a: Uncropped blots following dg-eLHt treatment.



## **11 Appendix III**



# Differential FSH Glycosylation Modulates FSHR Oligomerization and Subsequent cAMP Signaling

Uchechukwu T. Agwuegbo<sup>1</sup>, Emily Colley<sup>2</sup>, Anthony P. Albert<sup>3</sup>, Viktor Y. Butnev<sup>4</sup>, George R. Bousfield<sup>4</sup> and Kim C. Jonas<sup>1\*</sup>

<sup>1</sup> School of Life Course and Population Sciences, Department of Women and Children's Health, Guy's Campus, King's College London, London, United Kingdom, <sup>2</sup> Institute of Reproductive and Developmental Biology, Imperial College London, London, United Kingdom, <sup>3</sup> Vascular Biology Research Centre, Molecular & Clinical Science Research Centre, St George's University of London, London, United Kingdom, <sup>4</sup> Department of Biological Sciences, Wichita State University, Wichita, KS, United States

## OPEN ACCESS

### Edited by:

Livio Casarini,  
University of Modena and Reggio  
Emilia, Italy

### Reviewed by:

Mohammed Aki AYOUB,  
United Arab Emirates University,  
United Arab Emirates  
Francesco Poli,  
University of Parma, Italy

### \*Correspondence:

Kim C. Jonas  
kim.jonas@kcl.ac.uk

### Specialty section:

This article was submitted to  
Reproduction,  
a section of the journal  
Frontiers in Endocrinology

Received: 27 August 2021

Accepted: 02 November 2021

Published: 03 December 2021

### Citation:

Agwuegbo UT, Colley E,  
Albert AP, Butnev VY,  
Bousfield GR and Jonas KC (2021)  
Differential FSH Glycosylation  
Modulates FSHR Oligomerization  
and Subsequent cAMP Signaling.  
Front. Endocrinol. 12:765727.  
doi: 10.3389/fendo.2021.765727

Follicle-stimulating hormone (FSH) and its target G protein-coupled receptor (FSHR) are essential for reproduction. Recent studies have established that the hypo-glycosylated pituitary FSH glycoform (FSH21/18), is more bioactive *in vitro* and *in vivo* than the fully-glycosylated variant (FSH24). FSH21/18 predominates in women of reproductive prime and FSH24 in peri-post-menopausal women, suggesting distinct functional roles of these FSH glycoforms. The aim of this study was to determine if differential FSH glycosylation modulated FSHR oligomerization and resulting impact on cAMP signaling. Using a modified super-resolution imaging technique (PD-PALM) to assess FSHR complexes in HEK293 cells expressing FSHR, we observed time and concentration-dependent modulation of FSHR oligomerization by FSH glycoforms. High eFSH and FSH21/18 concentrations rapidly dissociated FSHR oligomers into monomers, whereas FSH24 displayed slower kinetics. The FSHR  $\beta$ -arrestin biased agonist, truncated eLH $\beta$  ( $\Delta$ 121-149) combined with asparagine56-deglycosylated eLH $\alpha$  (dg-eLH $\alpha$ ), increased FSHR homomerization. In contrast, low FSH21/18 and FSH24 concentrations promoted FSHR association into oligomers. Dissociation of FSHR oligomers correlated with time points where higher cAMP production was observed. Taken together, these data suggest that FSH glycosylation may modulate the kinetics and amplitude of cAMP production, in part, by forming distinct FSHR complexes, highlighting potential avenues for novel therapeutic targeting of the FSHR to improve IVF outcomes.

**Keywords:** follicle-stimulating hormone receptor, follicle-stimulating hormone, gonadotropic hormones, G protein-coupled receptors (GPCR), oligomers, oligomerization

## INTRODUCTION

The actions of follicle-stimulating hormone (FSH) and its receptor (FSHR) are essential for reproduction (1–5). With critical roles in follicle maturation, recruitment, and dominant follicle selection, FSH/FSHR are pivotal for granulosa cell (GC) proliferation and estradiol production (6, 7). Consequently, FSHR is a key therapeutic target of assisted reproductive technologies (ART), where supraphysiological concentrations of recombinant and urinary FSH preparations are utilized



during the ovarian stimulation phase of *in vitro* fertilization (IVF) to facilitate the recruitment and maturation of multiple antral follicles (8–10). Despite technological advances in IVF, there has been little change in the success rates (11), which are highest in women <35 and decline thereafter, highlighting the need for novel therapeutic FSH/FSHR targeting strategies to advance IVF success rates.

FSH is a complex heterodimeric glycoprotein hormone, comprised of an alpha subunit, that is common to other glycoprotein hormone family members such as thyroid-stimulating hormone (TSH), luteinizing hormone (LH) and human chorionic gonadotropin hormone (hCG), along with a hormone specific beta subunit (FSH $\beta$ ). FSH $\beta$  differs in amino acid sequence and glycosylation pattern to other glycoprotein hormone beta subunits, conferring biological specificity and selectivity of FSH to FSHR (12). FSH possesses 4 Asn-linked glycosylation sites, with two sites on the alpha subunit (Asn52 and Asn78) and two sites on the beta subunit (Asn7 and Asn24). Naturally occurring differences in the macro-glycosylation pattern of FSH have been previously reported in human pituitary extracts (13), with modification of the FSH $\beta$  subunit glycosylation pattern resulting in the identification of three FSH glycoforms; partially glycosylated FSH (FSH21/18, as purified preparations possess both variants) with a single glycosylated site at either Asn7 (FSH21) or Asn24 (FSH18) and fully glycosylated FSH (FSH24) with both FSH $\beta$  subunit Asn residues glycosylated. Interestingly, age-dependent differences in pituitary expression levels of FSH21/18 and FSH24 have been reported. FSH21/18 has been shown to be predominant in pituitary extracts from women in their 20's, decreasing thereafter, with a concomitant increase in FSH24 expression, resulting in FSH24 predominating in menopausal-aged women (13). Functional analysis has shown that this difference in glycosylation pattern results in modulation of binding to the FSHR (14) and the amplitude of the canonical FSHR signaling pathway, the G $\alpha$ s/cAMP/PKA signaling, with FSH21/18 displaying faster binding kinetics and more potent activation of G $\alpha$ s signaling (15–17). Recent studies suggest that FSH glycoforms may display distinct signaling profiles, or signal bias (18) in activation of AKT (19, 20),  $\beta$ -arrestin (17) and calcium signaling (17, 21). Important functional differences have also been observed, with differences in ovarian and testicular gene expression in mice injected with either FSH21/18 or FSH24 (19). However, how these differences in the signaling properties of FSH21/18 and FSH24 are interpreted by FSHR remain unknown.

FSHR is a Class A G protein-coupled receptor (GPCR). An increasingly important way that GPCRs have been shown to regulate ligand specificity and signal amplitude is via association and formation of dimers/oligomers (22–25). FSHR has been demonstrated to self-associate and homomerize (26–30), which is thought to underpin the inherent negative cooperativity displayed by FSHR (26). The FSHR has also been shown to heteromerize with the LHR (30–32) and membrane-bound estrogen receptor (GPER) (33), resulting in modulation of signal selectivity (31, 32). However, the functional role of FSHR homomerization remains to be demonstrated, and how

different FSH ligands may impact FSHR homomerization to mediate their differences in signal specificity and selectivity remains unknown.

With advances in single molecule imaging technology, we are now in the position to investigate the molecular mechanisms underpinning how FSH glycoforms specify the differences observed in the kinetics and amplitude of cAMP signaling, with single molecule precision and at physiological levels of receptor density. Using a combination of the single molecule imaging technique, photoactivated dye-localization microscopy (PD-PALM) (34, 35), and differential FSH glycosylation variants- FSH21/18, FSH24, a potent FSHR stimulator- equine FSH (eFSH) and a FSHR  $\beta$ -arrestin biased agonist with diminished ability to activate cAMP - truncated eLH $\beta$  ( $\Delta$ 121–149) combined with asparagine56-deglycosylated eLH $\alpha$ , designated dg-eLHt (36), we have determined that FSH glycoforms differentially modulate FSHR oligomerization in both a temporal and concentration-dependent manner. These differences observed in FSHR oligomerization correlated with temporal and magnitude differences observed in cAMP production and cre-luciferase activity. These data suggest a novel mechanism by which different FSH ligands may modulate the magnitude of cAMP signal through differential regulation of FSHR oligomerization.

## MATERIAL AND METHODS

### Materials

Purified pituitary FSH21/18 and FSH24 (17), equine FSH (eFSH) and dg-eLHt (37) were kindly supplied by Professor George Bousfield, Wichita State University, Wichita, KS, USA. CAGE 552 fluorophore dye was purchased from Abberior. N-terminally hemagglutinin-tagged FSHR (HA-FSHR) encoded plasmid DNA were constructed as previously described (32). Primary antibody HA.11 was purchased from BioLegend<sup>®</sup>. Plasmid DNA encoding GloSensor<sup>™</sup>-20F, cAMP-response element-luciferase reporter gene (cre-luciferase), *Renilla* luciferase reporter gene (*R*-luciferase), GloSensor<sup>™</sup> reagent stock and Dual-Luciferase<sup>®</sup> Reporter Assay System were purchased from Promega.

### Cell Culture and Transient Transfections

HEK293 cells were maintained and cultured in 5% CO<sub>2</sub> in air at 37°C in Dulbecco's Modified Eagle's Medium (DMEM-6429, Sigma-Aldrich) supplemented with 10% Fetal Bovine Serum (FBS-F9665, Sigma-Aldrich), and 1% Antibiotic-Antimycotic (15240062, ThermoFisher). For PD-PALM experiments, cells were transiently transfected with 3  $\mu$ g HA-FSHR, and then replated 24 hours later onto 8-well 1.5 glass-bottomed chamber slides. For cAMP GloSensor<sup>™</sup> and cre-luciferase activity assays, HEK293 cells were co-transiently co-transfected with 3  $\mu$ g of HA-FSHR and either 1  $\mu$ g GloSensor<sup>™</sup>-20F DNA plasmid or 800 ng cre-luciferase and 150 ng *R*-luciferase DNA plasmids, and cells replated the following day onto white clear-bottomed 96-well plates (50,000 cells/well). All transient transfections were carried out in tissue culture-treated 6-well plates (600,000 cells/well)



using Lipofectamine 2000<sup>®</sup> (Invitrogen) as per manufacturer's instructions. Cells were assayed 48 hours post-transfection.

### PD-PALM

To assess FSHR monomer, dimer and oligomer populations at the plasma membrane, PD-PALM experiments were performed as previously described (32, 34, 35). Briefly, HEK293 cells expressing HA-FSHR were pre-incubated for 30 minutes with CAGE 552-labeled HA.11 antibody at 37°C, protected from light. HA.11 primary antibodies were labeled with CAGE 552 photoswitchable dyes at a 1:1 ratio, as previously described (34, 35) and following manufacturer's protocols (Abberior). At the end of the pre-incubation, antibodies were removed, and cells were treated with 0 (control), or either 30 or 1 ng/ml of eFSH, FSH21/18, FSH24 or dg-eLHt for 0, 2-, 5- or 15 minutes. Cells were washed with PBS and fixed for 30 minutes with 0.2% glutaraldehyde in 4% PFA at room temperature. Following fixation, cells were subsequently washed, stored and imaged in PBS using an inverted Zeiss Elyra PS.1 microscope with a 100x 1.45 NA objective lens in TIRF-mode at a rate of 10 frames/second over a total of 31,500 frames.

### Localization Analysis

Individual FSHR molecules were resolved as previously described (32, 34, 35). To summarize, cropped non-overlapping 5 x 5  $\mu\text{m}$  areas, within cell boundaries, of fluorescent intensity image frames were analyzed using the QuickPALM Fiji plug-in, generating x-y coordinates of each FSHR molecule. The range of FSHR density basally observed at the cell surface was 10–80 FSHR/ $\mu\text{m}^2$  across all experiments. For standardization of data analysis and to eliminate receptor density as a variable factor, cells with FSHR expression levels of ~10–40 FSHR/ $\mu\text{m}^2$  were selected for analysis, as this was the physiological receptor density range previously reported for the FSHR (30) and other native GPCRs (38). To prevent the overestimation of FSHR association, coordinates localized within 15 nm of 15 consecutive frames were filtered using an add-on algorithm JAVA program. To determine the number of associated FSHRs and type of associated forms, from the localized and filtered x-y coordinates, a PD-interpreter JAVA program was employed to perform Getis-Franklin neighborhood analysis with a search radius of 50 nm. Reconstructed heat maps representing the different numbers of associated FSHRs were produced as a result.

### GloSensor<sup>™</sup> cAMP Assay

Post-transfection, cells were pre-equilibrated for 2 hours at 37°C in 88% CO<sub>2</sub>-independent media (18045, Gibco) supplemented with 10% FBS and 2% GloSensor<sup>™</sup> cAMP reagent stock, as per manufacturer's instructions. Following this, cells were treated for 30 minutes at 37°C with 0–100 ng/ml of eFSH, FSH21/18, FSH24 or dg-eLHt. Real-time cAMP fluorescence was measured using a multi-mode plate reader (PHERAstar<sup>®</sup> FS, BMG Labtech) using the parameter of 100 flashes per well, with a cycle time of 36 seconds.

### Cre-Luciferase Assay

Post-transfection, cells were stimulated in serum-free DMEM supplemented and treated with 0–100 ng/ml eFSH, FSH21/18,

FSH24 or dg-eLHt for 4–6 hours at 37°C. As an early-response gene, we expected this length of treatment to be sufficient for rapid gene expression induction in concordance with previous work (15). At the end of the incubation period, cells were lysed and treated with the Dual-Luciferase<sup>®</sup> Reporter Assay System, as per manufacturer's instructions. Lysate preps were measured for cre-luciferase and R-luciferase (for internal transfection control) luminescence levels using a multi-mode plate reader (PHERAstar<sup>®</sup> FS, BMG Labtech).

### Statistical Analysis

For PD-PALM studies, to compare the effect of FSHR ligands on the percentage of total FSHR homomers, ordinary one-way ANOVA, followed by Tukey's multiple comparisons test were conducted. To compare the effect of different FSHR ligands on the percentage of FSHR homomer subtypes, we performed multiple unpaired t-tests followed by Holm-Sidak's multiple comparisons. For each experiment a total of 3 individual sections/well were imaged containing 3–4 cells. For each section typically 15 ROIs, within cell borders, were analyzed as previously described (34). For GloSensor<sup>™</sup> assays, a baseline read of each well was performed for 10 read cycles prior to FSHR ligand treatment. The average baseline value of each cell was subtracted from its respective FSHR ligand-treatment, from the same wells. The mean cAMP response was plotted over 30 minutes and second order smoothed graph with 10 neighbors was performed. The area under the curve (AUC) measurements at 2-, 5- and 15-minutes were determined by measuring the total area from the number of peaks. All GloSensor<sup>™</sup> data were represented as fold change/basal. Comparisons of the AUC between FSHR ligands were carried out using one-way ANOVA, followed by Tukey's multiple comparisons test. Cre-luciferase luminescence readings were normalized to R-luciferase luminescence readings from the same well, to control for transfection efficiency. All data were represented as fold change/basal. Analysis of concentration-response curve were made using two-way ANOVA, followed by Dunnett's multiple comparisons test. Comparisons between FSHR ligands at specific concentrations were performed using two-way ANOVA, followed by Dunnett's multiple comparisons test. For PD-PALM, a minimum of 3 independent experiments were performed, for GloSensor<sup>™</sup> and cre-luciferase assays, a minimum of 3 independent experiments in triplicate were conducted. All data presented represent the mean  $\pm$  SEM. All statistical evaluations were performed using GraphPad Prism V9, and significance was determined as a probability value of  $p < 0.05$ .

## RESULTS

### FSH Ligands Differentially Modulate FSHR Monomer and Homomer Complex Formation in a Temporal and Concentration-Dependent Manner

To determine the effects of differentially glycosylated FSHR ligands on cell surface FSHR oligomerization, we utilized the

previously described single molecule imaging technique, PD-PALM, which afforded imaging of individual FSHR molecules to <10nm resolution (34). Two concentrations of FSH glycoforms were utilized, based on previous reports showing differential cAMP production evoked by FSH21/18 and FSH24, with ~50% of maximal cAMP production at 30 ng/ml in the concentration ranges assessed, and low-level cAMP production at 1 ng/ml (15).

HEK293 cells transiently expressing HA-FSHR were treated  $\pm$  30 ng/ml of FSH21/18 and FSH24 for 2-, 5- and 15 minutes. As a positive control, cells were also stimulated with the potent FSHR activator, eFSH, which is a naturally occurring analog of hypoglycosylated FSH21/18. Conversely, as a negative control for cAMP activation, we utilized the FSHR  $\beta$ -arrestin biased agonist, dg-eLHt, which has been previously shown to display minimal cAMP production, with biased activation of  $\beta$ -arrestin (36, 37). Representative images (top panels) and heat maps depicting the number of associated molecules (bottom panels) were generated. Analysis of the basal number of associated FSHR showed that  $30.2 \pm 1.8\%$  of FSHR were associated as dimers and oligomers (Figure 1), with ~70% as FSHR monomers. Analysis of the basal composition of associated cell surface FSHR showed  $15.5 \pm 0.8\%$  resided as dimers and  $5.5 \pm 0.5\%$  as trimers (Figure 1), suggesting that basally the majority of FSHR reside as lower-order homomers and monomers. Acute 2-minute treatment of HEK293 cells expressing FSHR with either eFSH or FSH21/18 significantly decreased the overall percentage of associated FSHR, with  $20.0 \pm 1.3\%$  and  $17.5 \pm 1.6\%$  associated as dimers and oligomers, respectively (Figure 1Aii). A decrease was observed in almost all FSHR homomeric subtypes (dimers, trimers, pentamers and 6-8 oligomers) (Figure 1Aiii). In contrast, treatment with FSH24 had no effect on the total percentage of associated FSHR, however modulation in the type of FSHR homomeric complexes was observed with a modest increase in  $\geq 9$  complexes and a decrease in dimers. Surprisingly, 2-minute treatment with dg-eLHt showed a trend for increasing FSHR association with  $38.7 \pm 3.8\%$  of FSHR molecules associated (Figure 1Aii), with  $15.9 \pm 2.9\%$  FSHR as trimers (Figure 1Aiii).

A 5-minute stimulation with eFSH treatment showed the percentage of FSHR associations to resemble basal (Figure 1Bi), suggesting a rapid re-organization of FSHR monomers into FSHR homomers. The documented fast binding kinetics of eFSH may explain this (17). FSH21/18, however, maintained a sustained reduction in FSHR homomers (Figure 1Bi). Interestingly, 5-minute treatment with FSH24 resulted in FSHR dissociation (Figure 1Bi), with a decrease in dimeric and trimeric FSHR homomers ( $p < 0.001$ ) (Figure 1Bii). A 5-minute dg-eLHt treatment sustained the increase in FSHR association observed at 2 minute-treatment (Figure 1Bi), suggesting that different FSH ligands have distinct effects on FSHR oligomerization.

A more chronic 15-minute treatment with either eFSH, FSH21/18 or FSH24 resulted in FSHR total homomeric complex percentages resembling those of basal levels (Figure 1Ci). However, dg-eLHt-treated cells continued to

show increased FSHR association ( $49.7 \pm 6.4\%$ ) with increases observed in trimers, tetramers to  $\geq 9$  complexes (Figure 1Cii), further supporting the proposition that different FSH ligands can differentially modulate FSHR association.

Since FSH concentrations and glycosylation patterns are differentially regulated across the menstrual cycle (39) and have also been shown to change with age (13), we sought to determine the effects of FSH ligand concentration on FSHR association. As previously, HEK293 cells expressing FSHR were treated  $\pm$  eFSH, FSH21/18, FSH24 or dg-eLHt for 2-, 5- or 15-minutes, but using 1 ng/ml of each. Representative reconstructed images of FSHR localizations and heat maps showing associated molecules following 2-minute treatment were generated (Figure 2Ai). Assessment of FSHR association following 2-minute treatment with all ligands revealed no significant changes in the total percentage of FSHR homomers (Figure 2Aii), nor the type of FSHR homomeric complexes observed (Figure 2Aiii), suggesting that lower concentrations of FSHR ligands had little effect on FSHR association at this acute time-point.

Similarly, 5-minute treatment with 1 ng/ml eFSH, FSH21/18 and dg-eLHt had no effect on FSHR association (Figure 2Bi). Interestingly, FSH24 induced a significant increase in FSHR association, with an increase in the formation of pentamers ( $6.1 \pm 2.6\%$ ) (Figure 2Bii), contrasting to the dissociation of FSHR homomers observed with 30 ng/ml FSH24 shown above. Intriguingly, 15-minute treatment with FSH21/18 also induced FSHR association (Figure 2Ci), with an increase in FSHR tetramers ( $9.0 \pm 1.8\%$ ) and  $\geq 9$  oligomers ( $18.2 \pm 4.1\%$ ) (Figure 2Cii). FSH24-treated cells appeared to show FSHRs return to basal configuration (Figure 2C). Taken together, these data suggest that different FSHR ligands specify distinct re-organization of FSHR monomer, dimer, and oligomer populations in both a concentration- and time-dependent manner.

## FSHR Ligands Differentially Modulate cAMP Production

Ligand-dependent modulation of the related luteinizing hormone receptor homomers and LHR/FSHR and FSH/GPER heteromers has been shown to regulate signal amplitude and specificity (32–34). To investigate if the time- and concentration-dependent changes in FSHR monomers and homomers observed at the plasma membrane correlated with modulation in cAMP signals in our cell system, we employed the cAMP GloSensor™ reporter, which afforded real-time monitoring of cAMP production. HEK293 cells expressing FSHR were treated  $\pm$  0–100 ng/ml of eFSH, FSH21/18, FSH24 or dg-eLHt. Full cAMP concentration-response curves showing the AUC and maximal response of cAMP accumulation were recorded (Supplementary Figure S1), and the 30- and 1 ng/ml data extrapolated for further analysis at the 2-, 5-, and 15-minute time points, for correlation with the time points utilized for PD-PALM experiments. The mean cAMP accumulated over 30 minutes following a 30 ng/ml treatment with all ligands were plotted (Figure 3Ai). A 2-minute treatment with either eFSH and FSH21/18 induced a significant



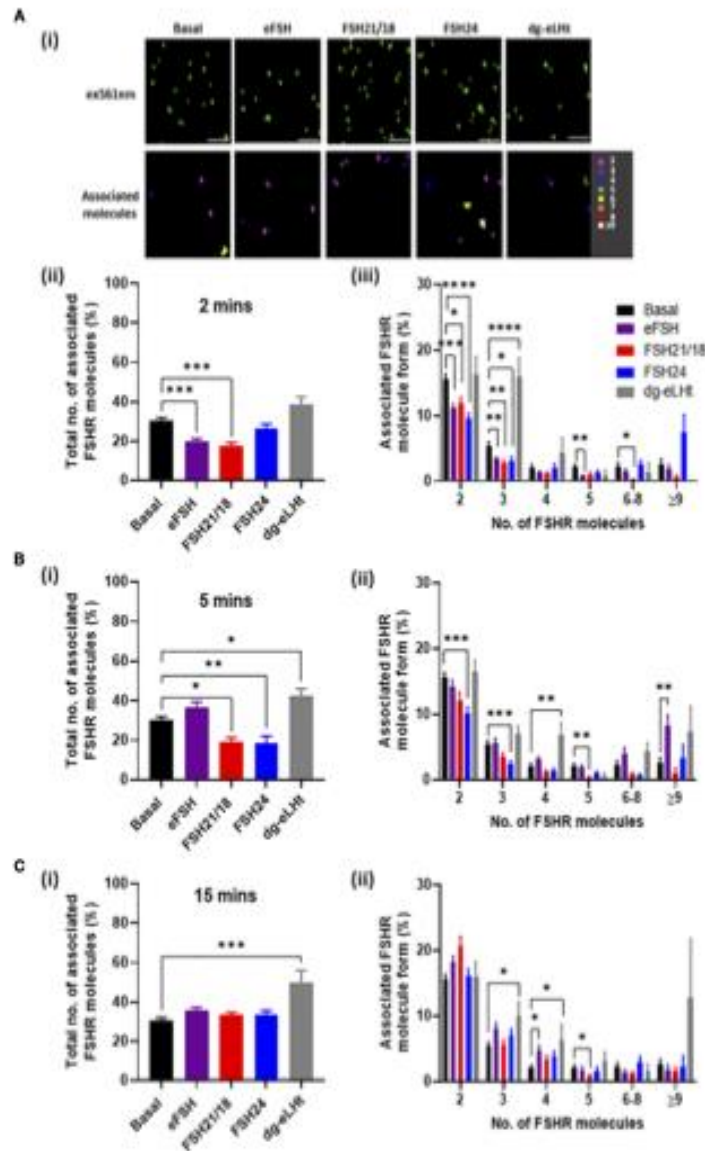
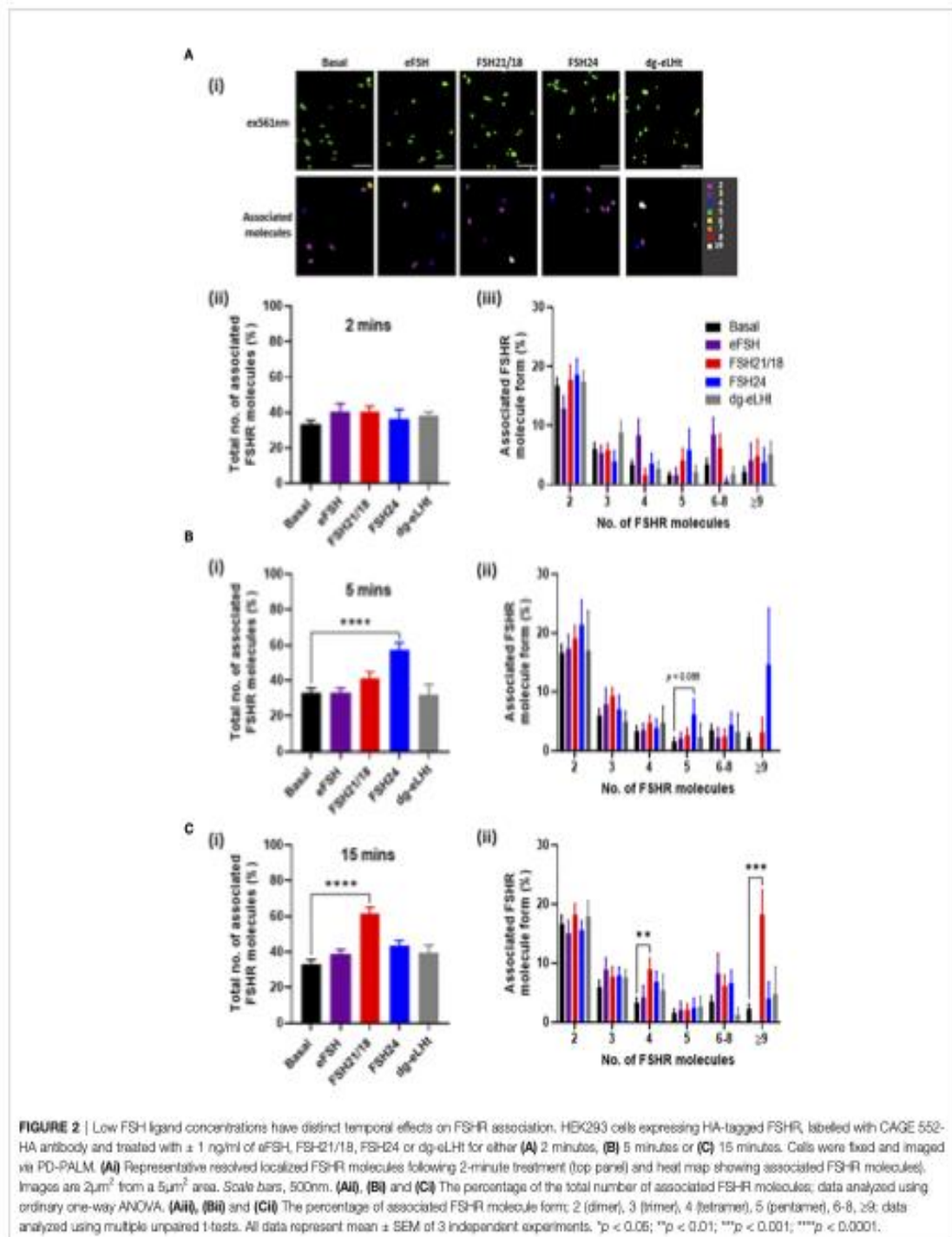


**FIGURE 1** | FSH ligands differentially modulate FSHR association. HEK293 cells transiently expressing HA-tagged FSHR were pre-incubated for 30 minutes with CAGE 5S2-HA antibody and treated with  $\pm$  30 ng/ml of eFSH, FSH21/18, FSH24 or dg-eLHt for either **(A)** 2 minutes, **(B)** 5 minutes or **(C)** 15 minutes, fixed for 30 minutes and imaged via PD-PALM. **(A)** Representative x-y coordinate plots of resolved FSHR molecules (upper panel) and reconstructed heat map of FSHR molecules following 2-minute treatment (lower panel). Images are  $2\mu\text{m}^2$  from a  $5\mu\text{m}^2$  area. Scale bars, 500nm. **(Aii)**, **(Bii)** and **(Cii)** Show the percentage of the total number of associated FSHR molecules; data analyzed using ordinary one-way ANOVA. **(Aii)**, **(Bii)** and **(Cii)** Shows the percentage of associated FSHR molecule form: 2 (dimer), 3 (trimer), 4 (tetramer), 5 (pentamer), 6-8,  $\geq 9$ , with data analyzed using multiple unpaired t-tests. All data represent mean  $\pm$  SEM of 3 independent experiments. \* $p < 0.05$ ; \*\* $p < 0.01$ ; \*\*\* $p < 0.001$ ; \*\*\*\* $p < 0.0001$ .

increase in cAMP production of  $8.6 \pm 2.6$ - and  $6.7 \pm 0.8$ -fold change/basal, respectively (Figure 3Aii). There were no significant effects of either FSH24 or dg-eLHt, on cAMP production at this time point (Figure 3Aii). When compared and correlated with PD-PALM data, a trend was observed for 2-

minute 30 ng/ml eFSH and FSH21/18 promoting dissociation of FSHR homomers into predominantly monomers (Figures 1Aii, iii), suggesting that dissociation of FSHR oligomers into monomers and re-organization of FSHR oligomeric complexes may, at least in part, promote acute cAMP production.



Moreover, that no change or enhancement of FSHR oligomerization may facilitate low level production of cAMP.

Treatment for 5-minutes with FSH24 significantly increased cAMP (**Figure 3Aiii**). When compared to observations with PD-

PALM data, a decrease in FSHR association at 5-minutes FSH24 treatment was observed (**Figure 1B**). This provided further support that FSHR dissociation into monomers may promote cAMP production. Differences in the magnitude of cAMP

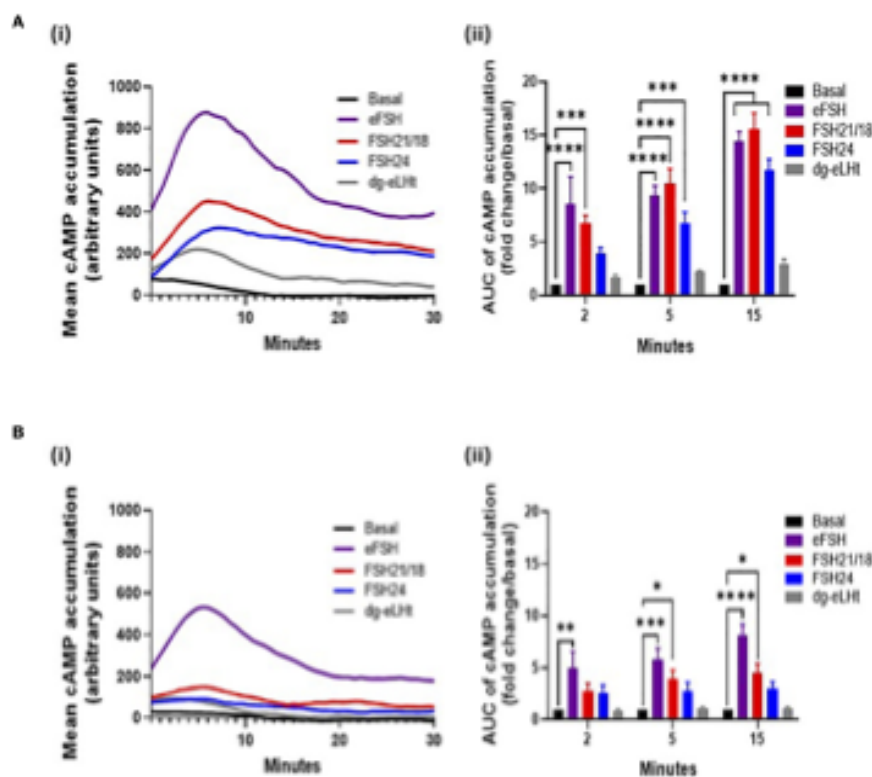


**FIGURE 3** | Different concentrations of FSH ligands differentially modulate cAMP production in a temporal manner. HEK293 cells expressing the HA-tagged FSHR and pGloSensor™<sub>2DF</sub> plasmid to assess live GloSensor™ cAMP kinetics. Cells were stimulated with either (A) ± 30 ng/ml or (B) ± 1 ng/ml of eFSH, FSH21/18, FSH24 or dg-eLHt. (i) Smoothed curve of the mean cAMP accumulation following treatment over 30 minutes (no error bars). (ii) AUC of the mean ligand-dependent cAMP accumulation at 2-, 5- and 15 minutes. AUC data was baseline subtracted and represented as fold change/basal. Data analyzed using two-way ANOVA. All data represent mean ± SEM of 3-5 independent experiments, measured in triplicate. \**p* < 0.05; \*\**p* < 0.01; \*\*\**p* < 0.001; \*\*\*\**p* < 0.0001.

accumulation between eFSH, FSH21/18 and FSH24 were observed (Supplementary Figure S1) and may result from the temporal differences in the kinetics of FSHR homomeric complex dissociation and profile of FSHR homomers favored by different FSHR ligands. We observed predominantly eFSH- and FSH21/18-dependent pentamer dissociation with acute treatment (Figures 1Aiii, Bii) compared to FSH24-dependent FSHR dimer and trimer dissociation (Figure 1Bii). The dg-eLHt preparation failed to significantly stimulate cAMP production (Figure 3Aii), as compared to PD-PALM data, which showed increased FSHR oligomerization (Figure 1).

A 15-minute stimulation with either eFSH, FSH21/18 or FSH24 continued to significantly increase cAMP production (Figure 3Aii). However, from the maximal cAMP concentration-response curves (Supplementary Figure S1Cii), steady-state levels appeared to have been reached. Interestingly, at this time point, FSHR homomer arrangements predominantly resembled basal conditions in all treatment groups (Figure 1C), suggesting that this receptor configuration may be important in initiating FSHR signal activation, with other mechanisms such as

receptor internalization important in maintaining cAMP production thereafter. As anticipated, dg-eLHt was unable to induce significant cAMP production at any time point analyzed (Figure 3Aii). PD-PALM data at the corresponding time point showing preferential re-arrangement of FSHR into higher order oligomers (Figure 1), suggesting that low level cAMP production (and potential β-arrestin recruitment and subsequent signaling) may be mediated, at least in part, by FSHR oligomer formation.

Next, we determined the effects of lower FSHR ligand concentrations that differentially modulated FSHR homomerization, on cAMP production. As with our previous PD-PALM experiments, we utilized 1 ng/ml of eFSH, FSH21/18, FSH24 or dg-eLHt and measured the mean cAMP accumulated over 30 minutes (Figure 3Bi). An acute, 2-minute treatment with all ligands, except eFSH, showed minimal increases in cAMP production in comparison to basal (Figure 3Bii). When compared to the PD-PALM data (Figure 2), these data correlated with a lack of effect on FSHR oligomerization at 2 minutes, following 1 ng/ml treatment with any FSHR ligand (Figures 2Aii, iii).



At 5- and 15 minutes, although we observed an eFSH-dependent increase in cAMP production of  $5.8 \pm 1.1$ - and  $8.1 \pm 1.1$ -fold, respectively (Figure 3Bii), when correlated to the PD-PALM data at these time points, no changes in the total percentage of FSHR homomers at the plasma membrane were observed (Figure 2). This suggests that there may be a dose-dependent threshold for different FSH glycosylated ligands to modulate FSHR homomerization. Small changes were observed in FSHR homomer subtypes, which may be important for modulating the magnitude of cAMP signaling, however this remains to be demonstrated. In contrast, FSH24 treatment at 5- and 15-minutes had no significant effect on cAMP production (Figure 3Bii). Interestingly, when correlating PD-PALM analysis, an increase in FSHR oligomerization was observed, predominately from enhanced formation of pentamers (Figure 2Bii), which may indicate that low level cAMP production may favor FSHR association. Supporting this observation, we observed increases in the total percentage of FSHR homomers with FSH21/18 treatment at 15 minutes (Figure 2Ci), correlating with low level cAMP production at the same time (Figure 3Bii). As anticipated, no significant changes in cAMP were observed following 2-, 5-, or 15-minute treatment with dg-eLHt (Figure 3Bii).

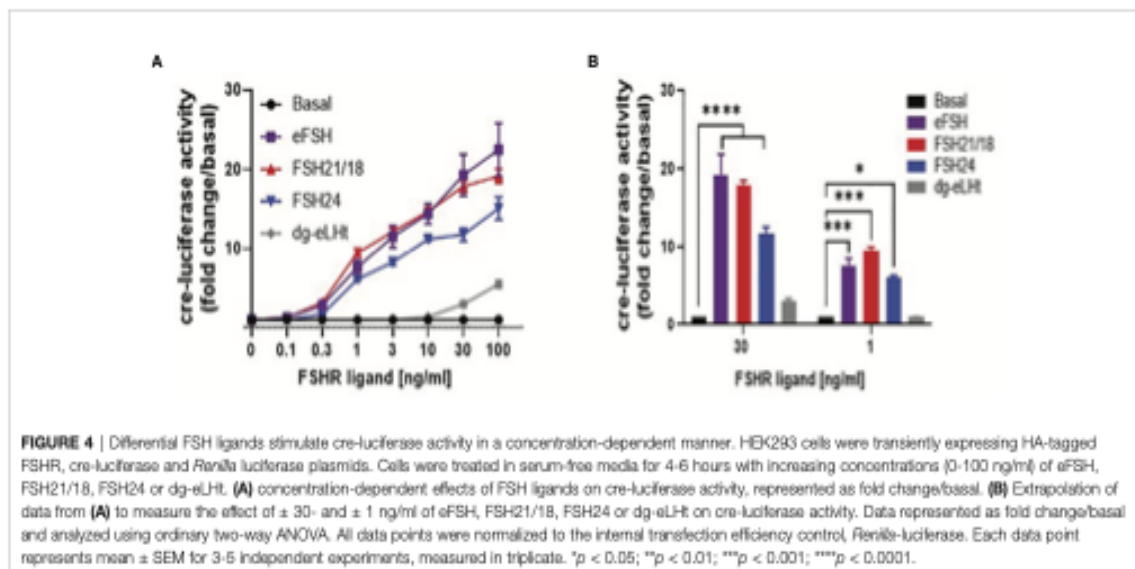
### FSHR Ligands Differentially Modulate Cre-Luciferase Activity

As the principal pathway activated by FSH/FSHR is *G $\alpha$ s*/cAMP/PKA, which is physiologically important for regulating the expression of cre-response genes, including CYP19 essential for estradiol production (16, 19, 40–42), we went on to determine the effects of FSHR ligands on cre-luciferase reporter gene activity. HEK293 cells transiently expressing the HA-FSHR were co-transfected with cre-luciferase and *R*-luciferase

(transfection efficiency control) and treated with  $\pm$  0–100 ng/ml of eFSH, FSH21/18, FSH24 and dg-eLHt for 4–6 hours. In line with the GloSensor™ data, eFSH and FSH21/18 were most potent at activating cre-luciferase for all concentrations  $\geq$  1 ng/ml when compared to basal in contrast to FSH24-treated cells (Figure 4A). As anticipated, dg-eLHt was unable to induce any changes in cre-luciferase activity at lower concentrations. However, at the higher concentrations of 30- and 100 ng/ml, dg-eLHt appeared to act as a weak agonist at the FSHR (Figure 4A), in corroboration with previous reports (36).

Comparison of 30 ng/ml treatments with FSHR ligands showed ligand-dependent differences in cre-luciferase activation, with eFSH and FSH21/18 significantly stimulating cre-luciferase activity by  $19.3 \pm 2.6$ - and  $17.8 \pm 0.7$ -fold increase over basal, respectively, in comparison to an  $11.8 \pm 0.8$ -fold increase for FSH24-treated cells ( $p < 0.0001$ ) (Figure 4B). This reflects similar differences observed between eFSH, FSH21/18 and FSH24 in 30 ng/ml GloSensor™ cAMP data (Figure 3Aii). Furthermore, when compared to FSH ligands eliciting changes in FSHR homomerization, it suggests that the changes observed in FSHR complexes at the plasma membrane may contribute to modulating the magnitude of cre-responsive gene activation.

Comparison of cre-luciferase responses following 1 ng/ml treatment with eFSH, FSH21/18, FSH24 and dg-eLHt revealed both eFSH and FSH21/18 induced 7-fold increases in cre-luciferase activation ( $p < 0.001$ ) (Figure 4B). Additionally, FSH24 induced a comparable increase ( $6.1 \pm 0.2$ -fold over basal) in cre-luciferase activity. This was interesting as differential regulation of FSHR homomeric forms and cAMP production was observed at this concentration. As predicted, dg-eLHt failed to significantly induce any increase in cre-luciferase activity (Figure 4B), further supporting its  $\beta$ -arrestin biased agonist activity.



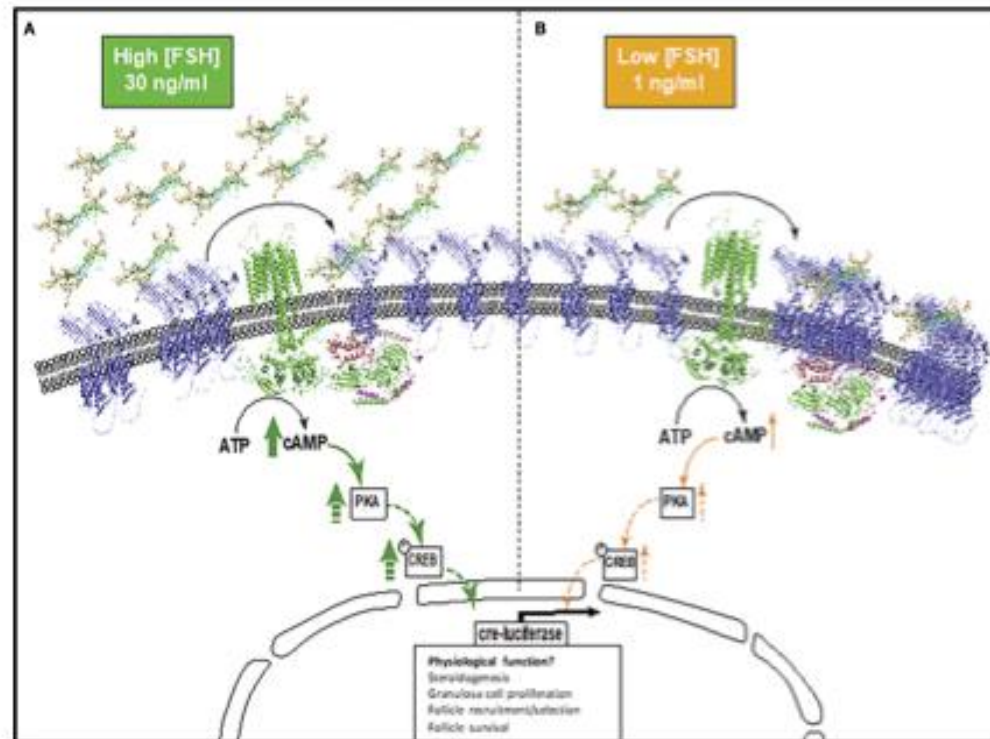


**FIGURE 5** | Schematic depicting the proposed model of FSHR monomer/oligomer-dependent modulation of cAMP signaling. **(A)** Higher physiological concentrations of FSH glycoforms (30 ng/ml), mediates the re-organization of FSHR oligomers into monomers at the plasma membrane, activating the G $\alpha$ s-adenylyl cyclase-cAMP-PKA-CREB pathway and resulting in high cre-responsive gene activation. **(B)** Lower physiological concentrations of FSH glycoforms (1 ng/ml), FSHR monomer-homomer populations remain quiescent or further associate to promote FSHR oligomerization. This results in lower levels of cAMP and cre-responsive gene activation. This may have implications on granulosa cell functions including steroidogenesis, granulosa cell proliferation, follicle recruitment and selection, and follicle survival. Dashed arrows indicate proteins in the cAMP pathway that were not investigated, but are concordant with published literature. FSH glycoforms are modeled, FSHR is represented by an alpha-fold model (blue) and structural depiction of adenylyl cyclase (green).

## DISCUSSION

FSH glycosylation variants have been previously shown to display differences in the magnitude and specificity of pathways activated (15, 17, 19, 43). Yet how FSHR decodes and propagates such signal diversity and differences in signal amplitude and duration remains unknown. GPCR homomerization is a well-recognized mechanism for modulating functional diversity and specifying signal responses (44, 45). Here we propose a mechanism for FSH glycoform-specific temporal and concentration-dependent regulation of FSHR homomerization, which correlates modulation of the amplitude and temporal activation of cAMP signaling (Figure 5).

We have shown that pituitary FSH glycoforms regulate FSHR homomerization in a time- and concentration-dependent manner. At higher physiological concentrations, eFSH and FSH21/18 rapidly dissociated FSHR homomers predominantly into monomers, correlating with significant increases in eFSH and FSH21/18-dependent cAMP production (Figure 5A). Interestingly FSH24 displayed slower temporal kinetics of

modulating FSHR homomerization, but dissociated FSHR homomers into predominantly monomers at time points when cAMP production was significantly increased. These data are in concordance with early studies of the related glycoprotein hormone receptor, TSHR, where FRET and co-immunoprecipitation analysis revealed less active dimer and oligomer conformations dissociated into monomers upon TSH stimulation (46). Conversely, at high concentrations of the  $\beta$ -arrestin biased agonist, dg-eLHt, a rapid increase in FSHR homomerization was observed. For the purpose of this study, this FSHR biased agonist was used as a negative control for cAMP production, and this increase in FSHR oligomerization correlated with a limited ability to activate cAMP, consistent with previous reports (36). These data suggest that defined FSHR monomer, dimer and oligomeric forms may at least in part, modulate the magnitude of cAMP production. This proposition is interesting as FSH glycoforms have been demonstrated to be dynamically regulated during ageing, with modulation in the ratio of FSH21/18 and FSH24 and overall circulating levels of FSH as ovarian ageing proceeds (13), and reported changes in secretion across the menstrual cycle (13, 39). It



is tempting to speculate that modulation of FSH glycoform and concentrations during these physiological processes may modulate FSHR homomer subtype and the dynamic shift between monomer-dimer-oligomer forms. This in turn may specify the amplitude and duration of cAMP signaling, with potential for signal specific physiological outcomes. Such FSH glycoform specific modulation of FSHR complexes and tempering of cAMP production may present ways for therapeutic exploitation in assisted reproduction. However, further research is required to understand the molecular detail and physiological control of this. These data also have implication for other GPCRs reported to homomerize/heteromerize, as ligand concentration is often overlooked and is particularly important for receptors with endogenous ligands that have diurnal/circadian/cyclical changes in secretion.

The glycoprotein hormone receptors have been previously reported to display inherent negative cooperativity, or functional asymmetry (26). This has been described for homomers for many GPCRs (47, 48) and has been proposed as a mechanism for mediating more graded responses. It has additionally been suggested that negative cooperativity may play an important role in many biological responses as it can cause marked threshold and ultra-sensitivity, allowing a biological system to filter out small stimuli and respond decisively to suprathreshold stimuli (48). Our observations of FSHR dissociation at high ligand concentrations and FSHR association/no change with low ligand concentrations support this idea, whereby FSHR oligomerization decodes the ligand threshold to regulate signal activation. In a physiological context within the ovary, such regulation may help prevent mass activation of FSHR, and fine-tune FSHR function during the fluctuations in FSH concentrations that are observed in different phases of folliculogenesis such as follicle recruitment, selection and ovulation (6, 49, 50).

Differences in binding affinity and the number of FSHR sites occupied by FSH21/18 and FSH24 have previously been reported, with FSH21 displaying a higher binding affinity to FSHR and occupying more FSHR (51, 52). Additionally, competition binding assays have shown that unlabeled eFSH and FSH21/18 was more efficacious at displacing <sup>125</sup>I-FSH24 and <sup>125</sup>I-FSH21/18 at lower concentrations than unlabeled hFSH24 (14), supporting the differences in FSHR binding affinities. In the context of this study, it is possible that these reported differences in the binding properties of the FSH glycoforms may have implications for the temporal differences observed in FSHR oligomer re-arrangement and dissociation into monomers observed with eFSH and FSH21/18 versus FSH24. However, future studies are required to determine how FSH glycoform-dependent differences in FSHR binding affinity and kinetics may drive changes in FSHR oligomerization.

We utilized the FSHR biased agonist, dg-eLHt, with known preferential  $\beta$ -arrestin signaling at lower concentrations ( $\leq 1$ nM) and weak cAMP activation (36), and observed concentration dependent modulation of FSHR oligomerization, with enhanced association at high concentrations. For other GPCRs, agonist dependent induction of homomerization has also been observed,

including the dopamine D2 receptor homodimers (53). As dg-eLHt is a preferentially recruits  $\beta$ -arrestin, which has well established roles in receptor desensitization and internalization, we can't rule out the induction of FSHR clustering, rather than FSHR oligomerization for initiation of FSHR internalization, particularly at high ligand concentrations. Indeed, interesting next steps will be to explore the effects of FSH glycoforms on the desensitization, internalization and trafficking of FSHR. It will be interesting to unpick how these observed differences in FSHR organization at the plasma membrane may direct FSHR internalization and trafficking, and understand the relationship between canonical G $\alpha$ s coupling and  $\beta$ -arrestin recruitment and signaling. The association of FSHR and  $\beta$ -arrestin has long been established, with roles of this molecular scaffold in ERK phosphorylation (18, 54–56), with ligand activation rapidly phosphorylating a cluster of residues within the C terminus of FSHR to facilitate  $\beta$ -arrestin recruitment and receptor internalization (57). Interestingly, a recent study has suggesting FSH glycoform-specific differences in the dependency of  $\beta$ -arrestin for ERK activation (17). With the recently reported roles of ligand-dependent differences in regulatory 'phosphorylation barcodes' for other Class A GPCRs (58), it may be that FSH ligands generate differential phosphorylation barcodes resulting in ligand-specific modulation of FSHR trafficking and signal propagation. Recent reports have suggested that internalization of FSHR is required for initiation of FSH-dependent cAMP production (59), with low molecular weight FSHR agonists reported to differentially modulate FSHR exocytosis (59), which may explain differential profiles for activating cAMP. How FSH glycoforms direct FSHR internalization and trafficking, remains to be determined. However, the use of single molecule imaging and single particle tracking presents exciting opportunities to determine the spatial-temporal regulation of these processes and uncover how/if different FSHR complexes are routed through the endosomal machinery to modulate FSH ligand-dependent signaling.

FSH glycoforms have been demonstrated to activate additional non-canonical G protein-signaling including G $\alpha_q$  and G $\alpha_i$  linked pathways (56, 60, 61). It will be interesting to determine if FSHR oligomerization contributes to determining and specifying G protein-coupling within a FSHR oligomeric/monomer complex. Indeed, observations with LHR/FSHR heteromers support this idea, whereby an increase in heterotetramers was reported to drive the enhanced LH/LHR-dependent G $\alpha_q$ /11 signaling (32). Interestingly, the formation of FSHR and membrane bound estrogen receptors (GPER) heteromers (FSHR-GPER) have been recently reported (33), with a proposed role in reprogramming FSHR-related death signals into life signals, as a result of high density FSHRs (62) and/or too high cAMP (63). These data support the physiological roles of FSHR homomers and heteromers with potentially distinct biological functions. This may be important for extragonadal FSHR functions where FSH/FSHR has been shown to activate G $\alpha_i$ -dependent MEK/ERK NF- $\kappa$ B, and Akt signaling to enhance osteoclast formation (64–66) and G $\alpha_i$ -



dependent induction of uncoupling protein-1 expression for FSH-dependent regulation of adipocytes (65, 67). However, this remains to be determined.

This study highlighted that ~70% of FSHR basally resided as monomers. This is in concordance with previous studies with the gonadotrophin hormone receptors, where the LHR was reported to reside as ~60% as monomers (34). Earlier studies into the Class A rhodopsin GPCR revealed that the majority of these receptors function as monomers despite their high concentrations within the plasma membrane (68). An important next step is to understand the role of FSHR monomers, and how they regulate the functionality and physiological responses of FSHR.

One of the limitations of this study is the utilization of HEK293 cells to study FSHR oligomerization, with transfected FSHR expression. A primary function of ovarian granulosa cells, in which FSHR are endogenously expressed, is to produce estrogen via aromatase expression. As a steroidogenic cell, the granulosa cell plasma membrane environment is cholesterol rich (69). The local membrane environment is increasingly recognized as an important factor regulating GPCR function (70–72) and GPCR homomer formation (73). To begin to understand the physiological context of this study findings, an important next step is to translate these findings into physiologically relevant cell types.

In conclusion, we have demonstrated that differential FSHR ligands modulate FSHR homomerization in a concentration and time-dependent manner. These data suggest that modulation of FSHR homomerization may provide a mechanism to fine-tune signal specificity and amplitude. This may be important means to decode the occurring cyclical and age-dependent changes in FSH concentration and glycosylation patterns in both a physiological and pathophysiological context. Moreover, modulation of FSHR homomerization may provide potential novel therapeutic avenues for targeting FSHR to improve IVF outcomes.

## REFERENCES

1. Chu L, Li J, Liu Y, Cheng CH. Gonadotropin Signaling in Zebrafish Ovary and Testis Development: Insights From Gene Knockout Study. *Mol Endocrinol* (2015) 29(12):1743–58. doi: 10.1210/me.2015-1126
2. Kumar TR, Wang Y, Lu N, Matzuk MM. Follicle Stimulating Hormone is Required for Ovarian Follicle Maturation But Not Male Fertility. *Nat Genet* (1997) 15(2):201–4. doi: 10.1038/ng0297-201
3. Kumar TR. Fshb Knockout Mouse Model, Two Decades Later and Into the Future. *Endocrinology* (2018) 159(5):1941–9. doi: 10.1210/en.2018-00072
4. Stille JAW, Segaloff DL. FSH Actions and Pregnancy: Looking Beyond Ovarian FSH Receptors. *Endocrinology* (2018) 159(12):4033–42. doi: 10.1210/en.2018-00497
5. Zhang Z, Lau SW, Zhang L, Ge W. Disruption of Zebrafish Follicle-Stimulating Hormone Receptor (*Fshr*) But Not Luteinizing Hormone Receptor (*Lhr*) Gene by TALEN Leads to Failed Follicle Activation in Females Followed by Sexual Reversal to Males. *Endocrinology* (2015) 156(10):3747–62. doi: 10.1210/en.2015-1039
6. Son WY, Das M, Shalom-Paz E, Holzer H. Mechanisms of Follicle Selection and Development. *Minerva Ginecol* (2011) 63(2):89–102.
7. Messinis IE, Messini CI, Dafopoulos K. Novel Aspects of the Endocrinology of the Menstrual Cycle. *Reprod BioMed Online* (2014) 28(6):714–22. doi: 10.1016/j.rbmo.2014.02.003

## DATA AVAILABILITY STATEMENT

The original contributions presented in the study are included in the article/Supplementary Material. Further inquiries can be directed to the corresponding author.

## AUTHOR CONTRIBUTIONS

KJ and GB conceived the study. KJ, GB, and AA supervised the study. UA, EC, and KJ carried out experiments. UA, EC, and KJ analyzed data. UA, KJ, AA, VB, and GB wrote and revised the manuscript. All authors contributed to the article and approved the submitted version.

## FUNDING

This work was supported by National Institutes of Health (P01AG029531), BBSRC grant (BB/R015961/1 and BB/R015961/2), and Society for Reproduction and Fertility Covid-19 support scheme for PhD Students 2021.

## ACKNOWLEDGMENTS

We thank the Facility for Imaging of Light Microscopy at Imperial College London for technical support in PD-PALM imaging.

## SUPPLEMENTARY MATERIAL

The Supplementary Material for this article can be found online at: <https://www.frontiersin.org/articles/10.3389/fendo.2021.765727/full#supplementary-material>

8. Baker VL, Fujimoto VY, Kettel LM, Adamson GD, Hoehler F, Jones CE, et al. Clinical Efficacy of Highly Purified Urinary FSH Versus Recombinant FSH in Volunteers Undergoing Controlled Ovarian Stimulation for *In Vitro* Fertilization: A Randomized, Multicenter, Investigator-Blind Trial. *Fertil Steril* (2009) 91(4):1005–11. doi: 10.1016/j.fertnstert.2008.01.064
9. Cheon KW, Byun HK, Yang KM, Song IO, Choi KH, Yoo KJ. Efficacy of Recombinant Human Follicle-Stimulating Hormone in Improving Oocyte Quality in Assisted Reproductive Techniques. *J Reprod Med* (2004) 49(9):733–8.
10. Palagiano A, Nesti E, Pace L. FSH: Urinary and Recombinant. *Eur J Obstet Gynecol Reprod Biol* (2004) 115(Suppl 1):S30–3. doi: 10.1016/j.ejogrb.2004.01.023
11. Gleicher N, Kushnir VA, Barad DH. Worldwide Decline of IVF Birth Rates and Its Probable Causes. *Hum Reprod Open* (2019) 2019(3):hoz017. doi: 10.1093/hropen/hoz017
12. Bousfield GR, Harvey DJ. Follicle-Stimulating Hormone Glycobiology. *Endocrinology* (2019) 160(6):1515–35. doi: 10.1210/en.2019-00001
13. Bousfield GR, Butnev VY, Rueda-Santos MA, Brown A, Hall AS, Harvey DJ. Macro- and Micro-Heterogeneity in Pituitary and Urinary Follicle-Stimulating Hormone Glycosylation. *J Glycomics Lipidomics* (2014) 4:1000124. doi: 10.4172/2153-0637.1000125
14. Bousfield GR, Butnev VY, Hiromasa Y, Harvey DJ, May JV. Hypo-Glycosylated Human Follicle-Stimulating Hormone (hFSH(21/18)) is Much

- More Active *In Vitro* Than Fully-Glycosylated hFSH (hFSH(24)). *Mol Cell Endocrinol* (2014) 382(2):989–97. doi: 10.1016/j.mce.2013.11.008
15. Jiang C, Hou X, Wang C, May JV, Butnev VY, Bousfield GR, et al. Hypoglycosylated hFSH Has Greater Bioactivity Than Fully Glycosylated Recombinant hFSH in Human Granulosa Cells. *J Clin Endocrinol Metab* (2015) 100(6):E852–60. doi: 10.1210/jc.2015-1317
  16. Simon LE, Liu Z, Bousfield GR, Kumar TR, Duncan FE. Recombinant FSH Glycoforms Are Bioactive in Mouse Preantral Ovarian Follicles. *Reproduction* (2019) 158(6):517–27. doi: 10.1530/REP-19-0392
  17. Zariwán T, Butnev VY, Gutiérrez-Sagal R, Maravillas-Montero JL, Martínez-Luis I, Mejía-Domínguez NR, et al. *In Vitro* Impact of FSH Glycosylation Variants on FSH Receptor-Stimulated Signal Transduction and Functional Selectivity. *J Endocr Soc* (2020) 4(5):bvaa019. doi: 10.1210/endo/bvaa019
  18. Landomiel F, De Pascali F, Raynaud P, Jean-Alphonse F, Yvinec R, Pellissier LP, et al. Biased Signaling and Allosteric Modulation at the FSHR. *Front Endocrinol (Lausanne)* (2019) 10:148. doi: 10.3389/fendo.2019.00148
  19. Wang H, May J, Butnev V, Shuai B, May JV, Bousfield GR, et al. Evaluation of *In Vivo* Bioactivities of Recombinant Hypo- (FSH). *Mol Cell Endocrinol* (2016) 437:224–36. doi: 10.1016/j.mce.2016.08.031
  20. Hua G, George JW, Clark KL, Jonas KC, Johnson GP, Southekal S, et al. Hypo-Glycosylated hFSH Drives Ovarian Follicular Development More Efficiently Than Fully-Glycosylated hFSH: Enhanced Transcription and PI3K and MAPK Signaling. *Hum Reprod* (2021) 36(7):1891–906. doi: 10.1093/humrep/deab135
  21. Lai TH, Lin YF, Wu FC, Tsai YH. Follicle-Stimulating Hormone-Induced Galphah/phospholipase C-Delta1 Signaling Mediating a Noncapacitative Ca2+ Influx Through T-Type Ca2+ Channels in Rat Sertoli Cells. *Endocrinology* (2008) 149(3):1031–7. doi: 10.1210/en.2007-1244
  22. Sleno R, Hébert TE. The Dynamics of GPCR Oligomerization and Their Functional Consequences. *Int Rev Cell Mol Biol* (2018) 338:141–71. doi: 10.1016/b9c.2018.02.005
  23. Wang W, Qiao Y, Li Z. New Insights Into Modes of GPCR Activation. *Trends Pharmacol Sci* (2018) 39(4):367–86. doi: 10.1016/j.tips.2018.01.001
  24. Breitwieser GE. G Protein-Coupled Receptor Oligomerization: Implications for G Protein Activation and Cell Signaling. *Circ Res* (2004) 94(1):17–27. doi: 10.1161/01.RES.0000110420.68526.19
  25. Rios CD, Jordan BA, Gomes I, Devi LA. G-Protein-Coupled Receptor Dimerization: Modulation of Receptor Function. *Pharmacol Ther* (2001) 92(2-3):71–87. doi: 10.1016/S0163-7258(01)00160-7
  26. Urizar E, Montanelli L, Loy T, Bonomi M, Swillens S, Gales C, et al. Glycoprotein Hormone Receptors: Link Between Receptor Homodimerization and Negative Cooperativity. *EMBO J* (2005) 24(11):1954–64. doi: 10.1038/sj.emboj.7600686
  27. Thomas RM, Nechamen CA, Mazurkiewicz JE, Muda M, Palmer S, Dias JA. Follicle-Stimulating Hormone Receptor Forms Oligomers and Shows Evidence of Carboxyl-Terminal Proteolytic Processing. *Endocrinology* (2007) 148(5):1987–95. doi: 10.1210/en.2006-1672
  28. Guan R, Wu X, Feng X, Zhang M, Hébert TE, Segaloff DL. Structural Determinants Underlying Constitutive Dimerization of Unoccupied Human Follicle-Stimulating Receptors. *Cell Signal* (2010) 22(2):247–56. doi: 10.1016/j.cellsig.2009.09.023
  29. Jiang X, Fischer D, Chen X, McKenna SD, Liu H, Sriraman V, et al. Evidence for Follicle-Stimulating Hormone Receptor as a Functional Trimer. *J Biol Chem* (2014) 289(20):14273–82. doi: 10.1074/jbc.M114.549592
  30. Mazurkiewicz JE, Herrick-Davis K, Barroso M, Ulloa-Aguirre A, Lindau-Shepard B, Thomas RM, et al. Single-Molecule Analyses of Fully Functional Fluorescent Protein-Tagged Follicle-Stimulating Receptor Reveal Homodimerization and Specific Heterodimerization With Lutropin Receptor. *Biol Reprod* (2015) 92(4):100. doi: 10.1095/biolreprod.114.125781
  31. Feng X, Zhang M, Guan R, Segaloff DL. Heterodimerization Between the Lutropin and Follicle-Stimulating Receptors is Associated With an Attenuation of Hormone-Dependent Signaling. *Endocrinology* (2013) 154(10):3925–30. doi: 10.1210/en.2013-1407
  32. Jonas KC, Chen S, Virta M, Mora J, Franks S, Huhtaniemi I, et al. Temporal Reprogramming of Calcium Signaling via Crosstalk of Gonadotrophin Receptors That Associate as Functionally Asymmetric Heteromers. *Sci Rep* (2018) 8(1):2239. doi: 10.1038/s41598-018-20722-5
  33. Casarini L, Lazzaretti C, Paradiso E, Limoncella S, Riccetti L, Sperduti S, et al. Membrane Estrogen Receptor (GPER) and Follicle-Stimulating Hormone Receptor (FSHR) Heteromeric Complexes Promote Human Ovarian Follicle Survival. *iScience* (2020) 23(12):101812. doi: 10.1016/j.isci.2020.101812
  34. Jonas KC, Fanelli F, Huhtaniemi IT, Hanyaloglu AC. Single Molecule Analysis of Functionally Asymmetric G Protein-Coupled Receptor (GPCR) Oligomers Reveals Diverse Spatial and Structural Assemblies. *J Biol Chem* (2015) 290(7):3875–92. doi: 10.1074/jbc.M114.622498
  35. Jonas KC, Hanyaloglu AC. Analysis of Spatial Assembly of GPCRs Using Photoactivatable Dyes and Localization Microscopy. *Methods Mol Biol* (2019) 1947:337–48. doi: 10.1007/978-1-4939-9121-1\_19
  36. Webbi V, Tranchant T, Durand G, Musnier A, Decourtye J, Piketty V, et al. Partially Deglycosylated Equine LH Preferentially Activates Beta-Arrestin-Dependent Signaling at the Follicle-Stimulating Hormone Receptor. *Mol Endocrinol* (2010) 24(3):561–73. doi: 10.1210/me.2009-0347
  37. Butnev VY, Singh V, Nguyen VT, Bousfield GR. Truncated Equine LH Beta and Asparagine(56)-Deglycosylated Equine LH Alpha Combine to Produce a Potent FSH Antagonist. *J Endocrinol* (2002) 172(3):545–55. doi: 10.1677/joe.0.1720545
  38. Herrick-Davis K, Grinde E, Lindsley T, Tettler M, Mancía F, Cowan A, et al. Native Serotonin 5-HT2C Receptors Are Expressed as Homodimers on the Apical Surface of Choroid Plexus Epithelial Cells. *Mol Pharmacol* (2015) 87(4):660–73. doi: 10.1124/mol.114.096636
  39. Wide L, Eriksson K. Low-Glycosylated Forms of Both FSH and LH Play Major Roles in the Natural Ovarian Stimulation. *Ups J Med Sci* (2018) 123(2):100–8. doi: 10.1080/03009734.2018.1467983
  40. Parakh TN, Hernandez JA, Grammer JC, Weck J, Hunzicker-Dunn M, Zeleznik AJ, et al. Follicle-Stimulating Hormone/cAMP Regulation of Aromatase Gene Expression Requires Beta-Catenin. *Proc Natl Acad Sci USA* (2006) 103(33):12435–40. doi: 10.1073/pnas.0603006103
  41. Stocco C. Aromatase Expression in the Ovary: Hormonal and Molecular Regulation. *Steroids* (2008) 73(5):473–87. doi: 10.1016/j.steroids.2008.01.017
  42. Reichert LE, Dattatreyaumurthy B. The Follicle-Stimulating Hormone (FSH) Impact on Testis Interaction With FSH: Mechanism of Signal Transduction, and Properties of the Purified Receptor. *Biol Reprod* (1989) 40(1):13–26. doi: 10.1095/biolreprod40.1.13
  43. Bousfield GR, May JV, Davis JS, Dias JA, Kumar TR. *In Vivo* and *In Vitro* Impact of Carbohydrate Variation on Human Follicle-Stimulating Hormone Function. *Front Endocrinol (Lausanne)* (2018) 9:216. doi: 10.3389/fendo.2018.00216
  44. Agwuogbo UC, Jonas KC. Molecular and Functional Insights Into Gonadotropin Hormone Receptor Dimerization and Oligomerization. *Minerva Ginecol* (2018) 70(5):539–48. doi: 10.23736/S0026-4784.18.04287-9
  45. Casarini L, Crépeux P. Molecular Mechanisms of Action of FSH. *Front Endocrinol (Lausanne)* (2019) 10:305. doi: 10.3389/fendo.2019.00305
  46. Latif R, Graves P, Davies TF. Ligand-Dependent Inhibition of Oligomerization at the Human Thyrotropin Receptor. *J Biol Chem* (2002) 277(47):45059–67. doi: 10.1074/jbc.M206693200
  47. Rivero-Müller A, Jonas KC, Hanyaloglu AC, Huhtaniemi I. Di/oligomerization of GPCRs—Mechanisms and Functional Significance. *Prog Mol Biol Transl Sci* (2013) 117:163–85. doi: 10.1016/B978-0-12-386931-9.00007-6
  48. Ha SH, Ferrell JE. Thresholds and Ultrasensitivity From Negative Cooperativity. *Science* (2016) 352(6288):990–3. doi: 10.1126/science.1259577
  49. Driancourt MA. Regulation of Ovarian Follicular Dynamics in Farm Animals. Implications for Manipulation of Reproduction. *Theriogenology* (2001) 55(6):1211–39. doi: 10.1016/S0093-691X(01)00479-4
  50. Gougeon A. Human Ovarian Follicular Development: From Activation of Resting Follicles to Preovulatory Maturation. *Ann Endocrinol (Paris)* (2010) 71(3):132–43. doi: 10.1016/j.ando.2010.02.021
  51. Butnev VY, May JV, Shuai B, Tran P, White WK, Brown A, et al. Production, Purification, and Characterization of Recombinant hFSH Glycoforms for Functional Studies. *Mol Cell Endocrinol* (2015) 405:42–51. doi: 10.1016/j.mce.2015.01.026
  52. Davis JS, Kumar TR, May JV, Bousfield GR. Naturally Occurring Follicle-Stimulating Hormone Glycosylation Variants. *J Glycomics Lipidomics* (2014) 4(1):e117. doi: 10.4172/2153-0637.1000e117
  53. Tabor A, Weisenburger S, Bamerjee A, Parkayastha N, Kaindl JM, Hübner H, et al. Visualization and Ligand-Induced Modulation of Dopamine Receptor



- Dimerization at the Single Molecule Level. *Sci Rep* (2016) 6:33233. doi: 10.1038/srep33233
54. De Pascali F, Reiter E.  $\beta$ -Arrestins and Biased Signaling in Gonadotropin Receptors. *Minerva Ginecol* (2018) 70(5):525–38. doi: 10.23736/S0026-4784.18.04272-7
  55. Lefkowitz RJ, Shenoy SK. Transduction of Receptor Signals by Beta-Arrestins. *Science* (2005) 308(5721):512–7. doi: 10.1126/science.1109237
  56. Gloaguen P, Crépieux P, Heitzler D, Poupon A, Reiter E. Mapping the Follicle-Stimulating Hormone-Induced Signaling Networks. *Front Endocrinol (Lausanne)* (2011) 2:45. doi: 10.3389/fendo.2011.00045
  57. Kara E, Crépieux P, Gauthier C, Martinat N, Piketty V, Guillouf P, et al. A Phosphorylation Cluster of Five Serine and Threonine Residues in the C-Terminus of the Follicle-Stimulating Hormone Receptor is Important for Desensitization But Not for Beta-Arrestin-Mediated ERK Activation. *Mol Endocrinol* (2006) 20(11):3014–26. doi: 10.1210/me.2006-0098
  58. Dwevedi-Agnihotri H, Chaturvedi M, Baidya M, Stepniwski TM, Pandey S, Maharana J, et al. Distinct Phosphorylation Sites in a Prototypical GPCR Differently Orchestrate  $\beta$ -Arrestin Interaction, Trafficking, and Signaling. *Sci Adv* (2020) 6(37):eabb8368. doi: 10.1126/sciadv.abb8368
  59. Sposini S, De Pascali F, Richardson R, Sayers NS, Perrais D, Yu HN, et al. Pharmacological Programming of Endosomal Signaling Activated by Small Molecule Ligands of the Follicle Stimulating Hormone Receptor. *Front Pharmacol* (2020) 11:593492. doi: 10.3389/fphar.2020.593492
  60. Stille JA, Guan R, Santillan DA, Mitchell BF, Lamping KG, Segaloff DL. Differential Regulation of Human and Mouse Myometrial Contractile Activity by FSH as a Function of FSH Receptor Density. *Biol Reprod* (2016) 95(2):36. doi: 10.1095/biolreprod.116.141648
  61. Crépieux P, Marion S, Martinat N, Fafeur V, Vern YL, Kerboeuf D, et al. The ERK-Dependent Signaling Is Stage-Specifically Modulated by FSH, During Primary Sertoli Cell Maturation. *Oncogene* (2001) 20(34):4696–709. doi: 10.1038/sj.onc.1204632
  62. Casarini L, Reiter E, Simoni M.  $\beta$ -Arrestins Regulate Gonadotropin Receptor-Mediated Cell Proliferation and Apoptosis by Controlling Different FSHR or LHCGR Intracellular Signaling in the Hg15 Cell Line. *Mol Cell Endocrinol* (2016) 437:11–21. doi: 10.1016/j.mce.2016.08.005
  63. Aharoni D, Dantes A, Oren M, Amsterdam A. cAMP-Mediated Signals as Determinants for Apoptosis in Primary Granulosa Cells. *Exp Cell Res* (1995) 218(1):271–82. doi: 10.1006/excr.1995.1156
  64. Sun L, Peng Y, Sharrow AC, Iqbal J, Zhang Z, Papachristou D, et al. FSH Directly Regulates Bone Mass. *Cell* (2006) 125(2):247–60. doi: 10.1016/j.cell.2006.01.051
  65. Liu P, Ji Y, Yuen T, Rendina-Ruedy E, DeMambro VE, Dhawan S, et al. Blocking FSH Induces Thermogenic Adipose Tissue and Reduces Body Fat. *Nature* (2017) 546(7656):107–12. doi: 10.1038/nature22342
  66. Zhu LL, Blair H, Cao J, Yuen T, Latif R, Guo L, et al. Blocking Antibody to the  $\beta$ -Subunit of FSH Prevents Bone Loss by Inhibiting Bone Resorption and Stimulating Bone Synthesis. *Proc Natl Acad Sci USA* (2012) 109(36):14574–9. doi: 10.1073/pnas.1212806109
  67. Liu XM, Chan HC, Ding GL, Cai J, Song Y, Wang TT, et al. FSH Regulates Fat Accumulation and Redistribution in Aging Through the Gai/Ca(2+)/CREB Pathway. *Aging Cell* (2015) 14(3):409–20. doi: 10.1111/acel.12331
  68. Park PS, Filipek S, Wells JW, Palczewski K. Oligomerization of G Protein-Coupled Receptors: Past, Present, and Future. *Biochemistry* (2004) 43(50):15643–56. doi: 10.1021/bi047907k
  69. Lange Y, Schmit VM, Schreiber JR. Localization and Movement of Newly Synthesized Cholesterol in Rat Ovarian Granulosa Cells. *Endocrinology* (1988) 123(1):81–6. doi: 10.1210/endo-123-1-81
  70. Periole X, Huber T, Marrink SJ, Sakmar TP. G Protein-Coupled Receptors Self-Assemble in Dynamics Simulations of Model Bilayers. *J Am Chem Soc* (2007) 129(33):10126–32. doi: 10.1021/ja0706246
  71. Koldse H, Sansom MS. Organization and Dynamics of Receptor Proteins in a Plasma Membrane. *J Am Chem Soc* (2015) 137(46):14694–704. doi: 10.1021/jacs.5b08048
  72. Guixá-González R, Javanainen M, Gómez-Soler M, Coedobilla B, Domingo JC, Sanz F, et al. Membrane Omega-3 Fatty Acids Modulate the Oligomerisation Kinetics of Adenosine A2A and Dopamine D2 Receptors. *Sci Rep* (2016) 6:19839. doi: 10.1038/srep19839
  73. Prasanna X, Sengupta D, Chattopadhyay A. Cholesterol-Dependent Conformational Plasticity in GPCR Dimers. *Sci Rep* (2016) 6:31858. doi: 10.1038/srep31858

**Conflict of Interest:** The authors declare that the research was conducted in the absence of any commercial or financial relationships that could be construed as a potential conflict of interest.

**Publisher's Note:** All claims expressed in this article are solely those of the authors and do not necessarily represent those of their affiliated organizations, or those of the publisher, the editors and the reviewers. Any product that may be evaluated in this article, or claim that may be made by its manufacturer, is not guaranteed or endorsed by the publisher.

Copyright © 2021 Agwuagbo, Colley, Albert, Butnev, Bougfield and Jonas. This is an open-access article distributed under the terms of the Creative Commons Attribution License (CC BY). The use, distribution or reproduction in other forums is permitted, provided the original author(s) and the copyright owner(s) are credited and that the original publication in this journal is cited, in accordance with accepted academic practice. No use, distribution or reproduction is permitted which does not comply with these terms.